

Performance evaluation of real time control in urban wastewater systems

van Daal-Rombouts, Petra

DOI

[10.4233/uuid:b1d5d733-b271-474f-ad32-b5fdde257161](https://doi.org/10.4233/uuid:b1d5d733-b271-474f-ad32-b5fdde257161)

Publication date

2017

Document Version

Final published version

Citation (APA)

van Daal-Rombouts, P. (2017). *Performance evaluation of real time control in urban wastewater systems*. [Dissertation (TU Delft), Delft University of Technology]. <https://doi.org/10.4233/uuid:b1d5d733-b271-474f-ad32-b5fdde257161>

Important note


To cite this publication, please use the final published version (if applicable). Please check the document version above.

Copyright

Other than for strictly personal use, it is not permitted to download, forward or distribute the text or part of it, without the consent of the author(s) and/or copyright holder(s), unless the work is under an open content license such as Creative Commons.

Takedown policy

Please contact us and provide details if you believe this document breaches copyrights. We will remove access to the work immediately and investigate your claim.



Performance evaluation of
real time control in urban
wastewater systems

Petra van Daal-Rombouts

Propositions

accompanying the dissertation

Performance evaluation of real time control in urban wastewater systems

by

Petronella Martina Maria van Daal-Rombouts

1. Proposition 1. If PhD students would first gain work experience, the Graduate School would be superfluous, their research more successful and the translation into practice better secured.
2. Proposition 2. The structure of the financing of scientific research goes against the integrity that is pointed out to Doctors when obtaining their degree.
3. Proposition 3. Unlike in top sports, in science there is too little attention for the balance between effort and relaxation.
4. Proposition 4. Scientific research on RTC in wastewater systems was obscured by the non-reproducibility of the weather for too long (*this thesis*).
5. Proposition 5. Research into control without applying measurements is like driving with your eyes closed.
6. Proposition 6. It is technically and organizationally feasible to indisputably determine the effect of RTC in wastewater systems (*this thesis*).
7. Proposition 7. The emphasis on achieving the highest possible degree limits the freedom of the individual and the entrepreneurial strength of society.
8. Proposition 8. If politicians would exchange their spin doctors for a Super Nanny, the world would be a better place.
9. Proposition 9. The severity of some pregnancy disorders revive a critical attitude towards evolution.
10. Proposition 10. Best intentions and ambition in the wastewater sector are not sufficient to compensate for a lack of knowledge and skills.

These propositions are regarded as opposable and defensible, and have been approved as such by the promotor prof. dr. ir. F.L.H.R. Clemens and the co-promotor dr. ir. J.G. Langeveld.

Stellingen

behorende bij het proefschrift

Performance evaluation of real time control in urban wastewater systems

door

Petronella Martina Maria van Daal-Rombouts

1. Stelling 1. Door promovendi eerst werkervaring te laten opdoen wordt de Graduate School overbodig, loopt promotieonderzoek voorspoediger en is de vertaling naar de praktijk beter geborgd.
2. Stelling 2. De opzet van de financiering van wetenschappelijk onderzoek druist in tegen de integriteit waarop bij het behalen van de doctorstitel wordt gewezen.
3. Stelling 3. In tegenstelling tot in de topsport is er in de wetenschap te weinig aandacht voor het evenwicht tussen inspanning en ontspanning.
4. Stelling 4. Wetenschappelijk onderzoek naar RTC in afvalwatersystemen heeft zich te lang verscholen achter de niet-reproduceerbaarheid van het weer (*dit proefschrift*).
5. Stelling 5. Onderzoek naar sturing zonder metingen toe te passen is als autorijden met je ogen dicht.
6. Stelling 6. Het onomstotelijk vaststellen van het effect van RTC in afvalwatersystemen in de praktijk is technisch en organisatorisch haalbaar (*dit proefschrift*).
7. Stelling 7. De nadruk op het behalen van het hoogst haalbare diploma beperkt de keuzevrijheid van het individu en de ondernemingskracht van de samenleving.
8. Stelling 8. Als politici hun spindokters zouden inruilen voor een Super Nanny zou de wereld een stuk opknappen.
9. Stelling 9. De ernst van sommige zwangerschapskwalen zet aan tot twijfel over de evolutietheorie.
10. Stelling 10. Goede wil en ambitie in de afvalwatersector zijn onvoldoende compensatie voor gebrek aan kennis en kunde.

Deze stellingen worden oponeerbaar en verdedigbaar geacht en zijn als zodanig goedgekeurd door de promotor prof. dr. ir. F.L.H.R. Clemens en de co-promotor dr. ir. J.G. Langeveld.

Performance evaluation of real time control in urban wastewater systems

Performance evaluation of real time control in urban wastewater systems

Proefschrift

ter verkrijging van de graad van doctor
aan de Technische Universiteit Delft,
op gezag van de Rector Magnificus prof. ir. K.C.A.M. Luyben,
voorzitter van het College van Promoties
in het openbaar te verdedigen op
vrijdag 22 september 2017 om 10.00 uur

door

Petronella Martina Maria VAN DAAL-ROMBOUTS

Natuurkundig Ingenieur, Technische Universiteit Eindhoven
geboren te Waalwijk, Nederland

Dit proefschrift is goedgekeurd door:

promotor prof. dr. ir. F.H.L.R. Clemens
copromotor dr. ir. J.G. Langeveld

Samenstelling promotiecommissie:

Rector Magnificus	voorzitter
Prof. dr. ir. F.H.L.R. Clemens	Technische Universiteit Delft, promotor
Dr. ir. J.G. Langeveld	Technische Universiteit Delft, copromotor

Onafhankelijke leden:

Prof. dr. P.S. Mikkelsen	Danmarks Tekniske Universitet, Denemarken
Prof. dr. ir. P. Willems	Katholieke Universiteit Leuven, België
Prof. dr. ir. N.C. van de Giesen	Technische Universiteit Delft
Dr. ir. A.N.A. Schellart	The University Of Scheffield, Verenigd Koninkrijk
Prof. dr. ir. L.C. Rietveld	Technische Universiteit Delft, reservelid

Overige leden:

Univ.-Prof. Dr.-Ing. D. Muschalla	Technische Universität Graz, Duitsland
-----------------------------------	--

Dit proefschrift is tot stand gekomen met ondersteuning van het Kennisprogramma Urban Drainage. De betrokken partijen zijn: ARCADIS, Deltares, Evides, Gemeente Almere, Gemeente Arnhem, Gemeente Breda, Gemeente 's-Gravenhage, Gemeentewerken Rotterdam, Gemeente Utrecht, GMB Rioleringsstechniek, KWR Watercycle Research Institute, Royal HaskoningDHV, Stichting RIONED, STOWA, Sweco, Tauw, vandervalk+degroot, Waterschap De Dommel, Waternet en Witteveen+Bos.

© 2017 by P.M.M. van Daal-Rombouts

ISBN: 978-94-6233-707-7

Printed by: Gildeprint, Enschede

Cover design by: A. Graat

An electronic version of this document is available free of charge in the Delft University Repository at <http://repository.tudelft.nl/>.

*“It is much better to do a little with certainty and leave the rest
for others that come after, than to explain all things by
conjecture without making sure of anything.”*

Isaac Newton

Voorwoord

Het proefschrift dat hier voor jullie ligt is onder wat ongebruikelijke omstandigheden tot stand gekomen. Ik ben gedurende het onderzoek en de afronding ervan in dienst geweest van Witteveen+Bos, maar heb vrijwel fulltime aan mijn onderzoek aan de TU Delft en een casus bij waterschap De Dommel gewerkt. Deze vorm heeft voor mij vrijwel alleen voordelen gehad. Ik noemde, en noem nog steeds, het onderzoek zelf en de inrichting er van niet voor niets mijn lotje uit de loterij. Ik heb hier met heel veel plezier zo'n vijf jaar aan besteed en wil graag mijn dank uitspreken aan iedereen die dit mee mogelijk heeft gemaakt. Mocht je jezelf niet terugvinden: het was onmogelijk om iedereen persoonlijk op te nemen.

Als eerste hoort François te worden genoemd. Jij stond aan de start van mijn carrière in de afvalwatersector en aan de start van dit onderzoek, zowel wat betreft de inhoud als de praktische inrichting. Aan jou, en Rémy Schilperoort, dank ik het feit dat ik überhaupt aan een promotieonderzoek ben begonnen. Daarnaast waardeer ik je inhoudelijke en kritische blik en het feit dat je er op de momenten dat het nodig was altijd was. Een goede tweede eerste is Jeroen. Je bent een bijzonder betrouwbare en geïnterseerde begeleider geweest. Je hebt me geholpen met een onuitputtelijke kennis over de het afvalwatersysteem van Eindhoven, snelle inzichten en een gave de juiste toon aan te slaan.

Verder wil ik wat betreft TU Delft het Kennisprogramma Urban Drainage bedanken. Dit programma heeft niet alleen mijn onderzoek grotendeels gefinancierd, maar was ook inhoudelijk betrokken. De discussies met de vakwereld leveren een mooie aanvulling op de academische insteek van een promotieonderzoek. En tot slot alle collega's van de sectie Gezondheidstechniek met wie ik naast het alledaagse werk ook avonturen heb beleefd tijdens congressen, uitjes en excursies.

Bij Witteveen+Bos wil ik iedereen bedanken die zich heeft ingespannen mij de mogelijkheid te geven aan mijn onderzoek te beginnen en af te ronden. De afspraken zijn niet alleen naar de letter maar ook naar de intentie door de hele organisatie gedragen. Dat is meer dan ik had durven vragen. In deze context wil ik in ieder geval Rina en Stephan noemen. En natuurlijk ook Erik, Erwin, Jitte Jan en mijn groepsgenoten in Breda voor de zachte landing terug in de advieswereld.

Waterschap De Dommel gaf de mogelijkheid mijn onderzoek een praktische invalshoek te geven. Dit was bijzonder waardevol en vond ik erg leuk om te doen. Stefan en Jarno: het is prettig werken met jullie als betrokken, maar ruimte gevende leidinggevend. Victor, Han en Paul: jullie kennis, ervaring en rust zijn één van de succesfactoren van de Slimme Buffers. Het verzamelen van hoge kwaliteit data in afvalwater blijft een uitdaging, bedankt aan iedereen die hier met mij in heeft willen leren. Ik hoop jullie nog veel tegen te komen.

Verder heb ik samengewerkt met een diverse groep mensen binnen en buiten de academische wereld. Siao, Jean-Luc, Femke, Aldo, Tommaso, Luc, Ger, Johan, Roel, Lorenzo, Dirk en Günter van harte bedankt voor alle discussies en hulp.

Dit alles was nooit mogelijk geweest zonder de steun van het thuisfront in de breedste zin van het woord. Een groot deel van het hier beschreven werk valt in de categorie wat bij ons thuis wordt omschreven als ‘gezond verstand’. Zoals je ziet kun je er een heel eind mee komen. Papa en mama, Christian en Tessa, Trudy, Marjolein en Sabine, SicK, Loes, DT6 en alle andere vrienden: dank jullie wel voor een luisterend oor, afleiding en de broodnodige lichaamsbeweging.

En als laatste natuurlijk Leon. Mijn rustpunt. Mijn thuis. We hebben het toch maar mooi gedaan samen. We gaan nog veel mooie jaren tegemoet met onze prachtige zoon Brian, die nu al vraagt waar het water in een rioolbuis naartoe gaat.

Petra van Daal
Augustus 2017

Abstract

Introduction

This thesis deals with real time control (RTC) in urban wastewater systems, where urban wastewater systems are defined as a combination of combined sewer systems and wastewater treatment plants (WWTPs). Urban wastewater systems discharge, through combined sewer overflows (CSOs) and WWTP effluent, onto the receiving waters. Receiving waters are thus closely linked to urban wastewater systems but are not a part of it.

RTC is about the continuous adjustment of the operation of a system with respect to a predefined goal based on real time measurements. The application of RTC in urban wastewater management is interesting, since the urban infrastructure is rigid (long life span, high cost for replacement), but the circumstances in which the system is operated (aims and loading) vary.

At a small scale, RTC is frequently applied in urban wastewater systems: from local controls to operate pumps to optimisation of the treatment process at WWTPs. System wide control, optimisation of sewer systems and WWTP together, is much less common. Literature on system wide control displays a wide conviction in the possibility to optimise the functioning of urban wastewater systems through RTC. This conviction, however, seems unfounded as no convincing evidence is presented in literature so far that application of RTC can realize a significant improvement in the functioning of urban wastewater systems. Furthermore, no unambiguous methodology is available to determine the effect of RTC.

Therefore, the research question at the heart of this thesis is: How can the effectiveness of RTC in urban wastewater systems be determined? Topics that are covered answering this question are: i) the instruments needed, ii) the key elements of a methodology for such an evaluation, and iii) how to apply such a methodology in practice.

Results

With respect to the tools needed for an evaluation, it was decided to investigate models that describe interactions between sewer systems and WWTPs and/or receiving waters.

In investigation I the applicability of unverified computational fluid dynamics (CFD) simulations to derive accurate discharge relationships for weirs with deviating weir chamber geometries was researched. It was shown that the derived discharge relationships, if the weir chamber geometry was not limiting the flow, describe the discharging flows equally well as the standard weir equation in case of free outflow. If the chamber geometry does limit the flow, the derived discharge relationships describe the flow with an deviation $<10\%$ and the standard equation is no longer applicable.

Investigation II examined the design and performance of simplified sewer models for determining CSO activity (number of discharges and total discharged volume) for looped, pumped sewer systems. It was shown that calibrated simplified sewer models outperform uncalibrated full hydrodynamic models with respect to CSO activity. Furthermore, the simplified models simulate >1000 times faster. Whether a ‘standard’ or more detailed ‘dynamic’ simplified model should be applied, depends on the the quality of the information available for the simplified model design and calibration.

In investigation III a model was designed to determine WWTP influent quality parameters based on influent quantity measurements. For the calibration of this empirical model, which is based on processes such as dilution, recovery and resuspension, high-frequency measurements are needed of the influent quality and quantity. The model results in high-frequency quality series containing both dry and wet weather conditions. For ammonium and total chemical oxygen demand the model was shown to describe the quality parameters with a deviation of $<25\%$ of the average dry weather flow concentration.

Regarding the methodology for evaluating RTC in urban wastewater systems, a methodology is proposed for determining the effectiveness of RTC. The methodology can be applied based on measurements or model simulations. The key elements of the methodology are the inclusion of uncertainty analysis and the application of an appropriate evaluation period. For both elements the importance is demonstrated through a case study.

Finally, the practical applicability of the methodology is demonstrated for two integrated, impact based RTC scenarios at WWTP Eindhoven. It was demonstrated that a significant improvement can be achieved through the application of RTC in practice taking uncertainties into account and using representative evaluation periods. The Storm Tank Control aims to prevent unnecessary discharges from the storm water settling tank that cause dissolved oxygen depletion in the receiving waters. It is evaluated based on measurements. The control reduced the tank discharges by 44% in number and an estimated 33% in volume. The Primary Clarifier Control aims to reduce ammonium peak loading of the activated sludge tanks, as they cause ammonium peaks in the effluent and receiving waters. It was evaluated based on model simulations. The control reduced the maximum event ammonium concentration in the effluent on average 19% for large events, while the load reduced 20%. Including small and medium events the reductions are 11 and 4% respectively.

Recommendations

For the further development of RTC in urban wastewater systems it is of importance that evaluations of the functioning of RTC in practice are performed with a more critical attitude, and are shared. Furthermore, no performance evaluations for the functioning of RTC in the long-term are available at this time, but would be desirable.

Scientific research should focus more on the requirements for the application of different RTC strategies: volume, impact and quality based RTC. Is more knowledge needed about certain measurements, systems or model descriptions to make application feasible? And is it possible to develop a tool to determine which strategy should be applied for a certain case?

For the practical application of RTC, the proposed evaluation methodology can serve in several respects. The methodology can be applied in the decision-making process to quantify the expected effect of the control, to execute a thorough system analysis, and to gain early insight in the possibilities and/or demands for a successful evaluation once a control is implemented.

Samenvatting

Introductie

Dit proefschrift gaat over realtime control (RTC) in stedelijke afvalwatersystemen. Onder het stedelijke afvalwatersysteem wordt hier de combinatie van gemengde rioolstelsels en rioolwaterzuiveringsinstallaties (rwzi's) verstaan. Lozingen vanuit het afvalwatersysteem (overstorting van de riolering en effluent van de rwzi), komen terecht op het ontvangende water, dat hierdoor nauw verbonden is met het stedelijke afvalwatersysteem maar er geen direct onderdeel van uitmaakt.

RTC gaat over het continu aanpassen van de aansturing van een systeem ten opzichte van een vooraf gedefinieerd doel op basis van realtime metingen. Het toepassen van RTC in stedelijke afvalwatersystemen is interessant omdat de stedelijke infrastructuur erg rigide is (lange levensduur, hoge kosten voor vervanging), maar de omstandigheden waarin het systeem functioneert (doelstellingen en belasting) wisselen.

Lokaal wordt RTC veelvuldig toegepast in stedelijke afvalwatersystemen: van regelingen om pompen aan te sturen tot het optimaliseren van het zuiveringsproces op rwzi's. Systeembrede sturing, optimalisatie van riolering en rwzi samen, komt veel minder vaak voor. Uit wetenschappelijke literatuur naar systeembrede sturing blijkt dat er een groot vertrouwen bestaat in het vermogen om met RTC het functioneren van het stedelijke afvalwatersysteem te verbeteren. Dit vertrouwen lijkt echter ongegrond omdat in de literatuur tot nu toe geen overtuigend bewijs is geleverd dat RTC in de praktijk een significante verbetering van het functioneren van stedelijke afvalwatersystemen heeft bewerkstelligd. Daarnaast ontbreekt een eenduidige methode om het effect van RTC vast te stellen.

De onderzoeksvraag die centraal staat in dit proefschrift is daarom: Hoe kan de effectiviteit van RTC in stedelijke afvalwatersystemen worden bepaald? Onderwerpen, die aan de orde komen bij het beantwoorden van deze vraag, omvatten: i) de instrumenten die hiervoor nodig zijn, ii) de belangrijkste elementen in een methode voor een dergelijke evaluatie, en iii) hoe een evaluatie methode in de praktijk kan worden toegepast.

Resultaten

Met betrekking tot de instrumenten die nodig zijn voor een evaluatie, is ervoor gekozen om enkele modellen, die de interacties tussen de riolering en de rwzi en/of het ontvangende water beschrijven, nader te onderzoeken.

Deelonderzoek I onderzoekt de vraag of ongeverifieerde computational fluid dynamics (CFD) berekeningen kunnen worden toegepast voor het afleiden van nauwkeurige overstortrelaties voor overstorten met een afwijkende keldergerometrie. Hieruit blijkt dat de afgeleide overstortrelaties, in de situatie dat de keldergerometrie geen bepalende rol speelt, het overstortende debiet net zo goed bepaalt als de standaard overstortvergelijking voor vrije uitstroom. Voor de situatie dat de keldergerometrie wel een bepalende rol speelt, beschrijft de afgeleide relatie het overstortende debiet met een afwijking van <10%. De standaard overstortvergelijking is hier niet van toepassing.

Deelonderzoek II gaat in op het ontwerp en de prestatie van eenvoudige bakmodellen voor het beschrijven van het overstortgedrag (aantal overstortingen en totale overstortende volume) van vermaasde rioolstelsels. Er is aangetoond dat gekalibreerde eenvoudige bakmodellen beter in staat zijn het overstortgedrag te beschrijven dan ongekalibreerde volledig hydrodynamische modellen. Bovendien rekenen de bakmodellen >1000 maal zo snel. Tevens is gedemonstreerd dat het ontwerpen van een heel gedetailleerd bakmodel alleen zinnig is als de kwaliteit van de beschikbare gegevens voor het ontwerp en de kalibratie van het bakmodel hoog is.

Deelonderzoek III gaat over het ontwerp van een model dat de kwaliteit van het rwzi influent bepaalt aan de hand van influent kwantiteitsmetingen. Voor de kalibratie van dit empirische model, dat is gebaseerd op processen als verdunning, herstel en opwoeling, zijn hoogfrequente metingen van zowel de influentkwaliteit als de -kwantiteit gebruikt. Het resulteert in hoogfrequente kwaliteitsreeksen die zowel droogweer- als regenweersituaties omvatten. Voor ammonium en totaal chemisch zuurstofverbruik is aangetoond dat de kwaliteitsparameters met een nauwkeurigheid van <25% van de gemiddelde droogweerconcentratie kan worden bepaald.

Wat betreft de methodologie voor het evalueren van RTC in stedelijke afvalwatersystemen is een voorstel gedaan waarmee de effectiviteit van RTC kan worden vastgesteld. De methodologie kan worden toegepast op basis van metingen en modelberekeningen. De belangrijkste elementen in de methodologie zijn het uitvoeren van een onzekerheidsanalyse en het toepassen van een geschikte evaluatieperiode. In een simpel voorbeeld is voor beide elementen laten zien dat ze van groot belang zijn voor het trekken van betrouwbare conclusies over de effectiviteit van RTC.

Tot slot is de praktische toepasbaarheid van de methodologie gedemonstreerd voor twee integrale, op impact gebaseerde regelingen op rwzi Eindhoven. Er is aangetoond dat door toepassing van RTC in de praktijk, een significante verbetering van het functioneren van een afvalwatersysteem kan worden bereikt, ook als onzekerheden worden meegenomen en een representatieve evaluatieperiode wordt toegepast. De zogenaamde RBT-regeling is geëvalueerd op basis van metingen en beoogt onnodige overstortingen uit de regenweerbezinktank, die zorgen voor zuurstofdips in het ontvangende water, te voorkomen. De regeling beperkt het aantal overstortingen van de regenweerbezinktank met 44% en het overstortende volume met een geschatte 33%. De zogenaamde VBT-regeling is geëvalueerd op basis van modelberekeningen. Deze regeling beoogt ammonium piekvrachten naar de biologische zuivering af te zwakken omdat deze resulteren in ammoniumpieken in het effluent en ontvangende water. De regeling beperkt de maximale concentratie van ammoniumpieken in het effluent van de rwzi met gemiddeld 19% voor grote buien. Tegelijkertijd wordt de ammoniumvracht met 20% gereduceerd. Als naar alle buien wordt gekeken bedraagt de reductie van de piekconcentratie en totale vracht 11% en 4% respectievelijk.

Aanbevelingen

Voor de verdere ontwikkeling van RTC in stedelijke afvalwatersystemen is het van belang dat evaluaties van het functioneren van RTC in de praktijk kritischer worden uitgevoerd en met anderen gedeeld. Daarnaast zijn nog geen evaluaties beschikbaar van het functioneren van RTC op de lange termijn, maar zijn deze wel wenselijk.

Wetenschappelijk onderzoek zou zich meer moeten richten op de behoeften voor het toepassen van verschillende RTC strategieën: volume, impact en kwaliteit gebaseerde RTC. Is er meer kennis nodig over bepaalde metingen, systemen of modelbeschrijvingen om toepassing mogelijk te maken? En is het mogelijk een instrument te ontwikkelen waarmee kan worden bepaald welke strategie voor een bepaald systeem het beste kan worden toegepast?

Voor de praktische toepassing van RTC biedt de voorgestelde methodologie diverse handvatten. De methodologie kan worden gebruikt in het besluitvormingsproces om het verwachte resultaat van sturing te kwantificeren, een grondige systeemanalyse uit te voeren, maar ook om vooraf inzicht te krijgen in de mogelijkheden en/of eisen voor de succesvolle evaluatie van een regeling.

Contents

Voorwoord	vii
Abstract	ix
Samenvatting	xiii
1 Introduction	1
1.1 Urban wastewater systems	1
1.2 Real Time Control	5
1.3 Goal	9
1.4 Case: the wastewater system of Eindhoven	10
1.5 Outline	14
2 Weir discharge relationships	15
2.1 Introduction	15
2.2 Materials and method	18
2.3 Results	26
2.4 Discussion	35
2.5 Conclusions and recommendations	37
3 Design and performance evaluation of simplified sewer models	39
3.1 Introduction	39
3.2 Materials and method	42
3.3 Results	61
3.4 Discussion	71
3.5 Conclusions and recommendations	72
4 Empirical influent water quality model	75
4.1 Introduction	75
4.2 Materials and method	77

4.3	Results and discussion	87
4.4	Conclusions and recommendations	101
5	A methodology for the performance evaluation of RTC	103
5.1	Introduction	103
5.2	Problem statement	104
5.3	Methodology	107
5.4	Case study	113
5.5	Discussion	123
5.6	Conclusions and recommendations	128
6	Application of the methodology on the wastewater system of Eindhoven	129
6.1	Introduction	129
6.2	Materials and method	131
6.3	Results	146
6.4	Discussion	154
6.5	Conclusions	156
7	Concluding remarks	157
7.1	Results summary	157
7.2	Recommendations	160
	Bibliography	165
A	CSO pollution analysis	181
B	Data requirements for quality based RTC	195
C	Monitoring network description	207
D	Implementation of Smart Buffer controls	223
E	Primary clarifier field test	229
	List of publications	231
	About the author	235

1 Introduction

1.1 Urban wastewater systems

1.1.1 Components and interactions

Urban wastewater systems are designed to collect, transport and treat wastewater before discharging the treated water into the receiving waters. They consist of different components such as sewer systems and treatment facilities. This thesis deals with a common form of urban wastewater system: combined sewer systems and a wastewater treatment plant (WWTP) discharging to a river. In combined sewer systems, household and industrial wastewater and rainfall runoff from streets and roofs are collected in one system and transported to a WWTP.

Figure 1.1 shows the components of an urban wastewater system as defined in this thesis and indicates interactions between these components and the receiving water. The first interaction takes place between the sewer system and the WWTP, at the WWTP influent. The second interaction takes place between the WWTP and river, where WWTP effluent is discharged. Wastewater can also be discharged directly from the sewer system into the river through combined sewer overflows (CSOs), which are the final point of interaction. CSOs were introduced for situations where the capacity of the sewer system and WWTP is insufficient to collect, transport and treat all wastewater (e.g. during heavy rainfall or due to technical failures). To prevent flooding of the public area or buildings, the CSOs provide additional outflow locations.

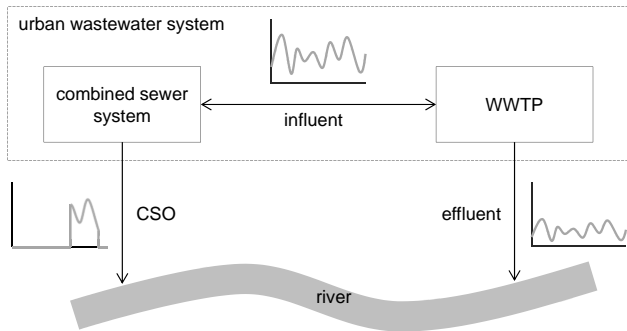


Figure 1.1: Schematic representation of an urban wastewater system as defined in this thesis. Influences between its components and the river are indicated through arrows. The graphs represent the dynamics of the resulting flows between the components.

The wastewater flows at the points of interaction vary in some respects. Influent and effluent are continuous flows, although the amounts and constituents change over time. CSO discharges are discontinuous. Another difference is the direction of the interactions as indicated by the arrows in figure 1.1. Through the influent the sewer system affects the WWTP operation, e.g. by the amount or quality of the wastewater. At the WWTP the amount of influent can be restricted, causing storage of wastewater in the sewer system. For CSO discharges and effluent the influence is normally unidirectional: the river receives both flows without possibility to interfere with the operation of the sewer system and/or WWTP. Situations where the receiving waters are elevated to the extent that negative overflows (inflow of surface water into the sewer system) or hampered WWTP outflow occurs, are considered beyond the scope of this thesis.

A more detailed introduction in the field of urban wastewater system components and interactions can be found in e.g. (Lijklema et al., 1993; Butler and Davies, 2004)

1.1.2 Management

Historically, sewer systems were introduced for the protection of the public health (Van Zon, 1986). By transporting wastewater out of densely populated areas, contact between people and faecal waste was decimated as well as the chance of contamination. Currently, protection of society from waterborne diseases is still the most important aim of urban wastewater management. Other aims such as the prevention of flooding (rainwater transport) and protection of the environment (wastewater treatment) now also apply. Naturally, the aims should be accomplished at minimum cost (RIONED Foundation, 2016).

Legislation regarding urban wastewater management developed from rules on maximum allowed discharge quantities and frequencies (emission based) to guidelines for minimal impact on the quality of the receiving waters (immission based) (Zabel et al., 2001). Another development regards the size of the system under consideration: from evaluation of one component (local) to one or multiple wastewater systems (basin wide) (Harremoës, 2002). Current legislation in Europe (WFD, 2000) dictates a good ecological status of the surface waters at basin level.

Legislation reflects the public opinion of what is or is not acceptable, e.g. with respect to pollution. As the public opinion evolved, the legislation did as well and will continue to do so. Therefore, the aims of urban wastewater management have changed accordingly (Tyson et al., 1993; Butler and Davies, 2004). For the Netherlands the changing aims are graphically displayed in figure 1.2. Wastewater systems should be capable of dealing with these changes.

Apart from changes in public opinion, another challenge for urban wastewater systems lies ahead that likely calls for system adaptation: climate change (IPCC, 2014). Rainfall is one of the main drivers for the functioning of urban wastewater systems and is greatly influenced by climate change. The Royal Netherlands Meteorological Institute released climate scenarios in 2014 (KNMI, 2015) that demonstrate the likely effect of climate change on the Dutch weather. The scenarios indicate more rainfall in winter, more extreme rainfall in summer and a higher probability of long dry periods. Extreme rain events cause CSO discharges, one of the major negative impacts of urban wastewater systems on the river ecology, while long dry periods only increase these impacts (Langeveld et al., 2012).

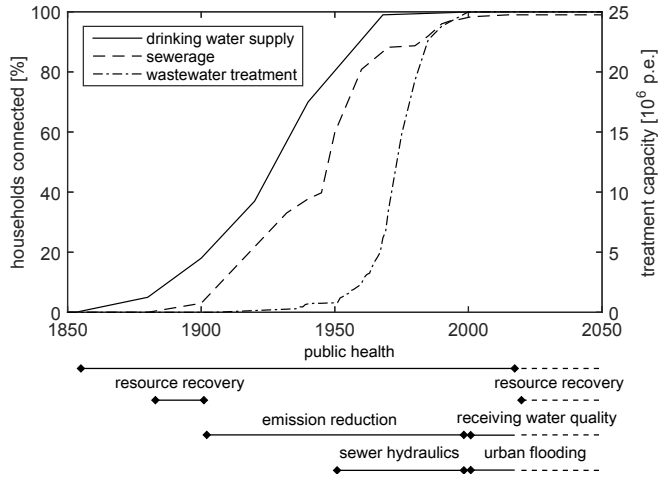


Figure 1.2: Historic overview of the development of urban (waste)water management and its evolving aims in the Netherlands. Adapted with permission from (Langeveld, 2004).

1.1.3 Adaptation

Evolving aims for urban wastewater management and climate change ask for flexibility in wastewater management. Urban wastewater systems, however, are far from flexible. Extensive infrastructure was built over decades, see figure 1.2, most of which is below ground level and thus hard to access. The investments involved are enormous. In the Netherlands, sewer systems consist of 150,000 km of conduits with an expected lifetime of 64 and an average age of 31 years. In 2015 only, 1.54 billion Euro was spent on sewer system construction, maintenance, renovation and replacement. The replacement value of the Dutch sewer systems equals 87 billion Euro (RIONED Foundation, 2016). These numbers demonstrate the economic rigidity of the system. Rigorous adaptation is economically unfeasible.

At the short term, major adaptation of urban wastewater system functioning should therefore be achieved through using the system differently. This could be accomplished by application of real time control (RTC). Applying RTC could also settle the other outstanding issue, namely the unidirectional influence of CSOs and effluent on the river. By taking into account river (quality) measurements in the operation of the urban wastewater system, the interactions at the CSOs and the effluent could possibly be reversed.

1.2 Real Time Control

1.2.1 Definition

RTC deals with the continuous optimisation of a system with respect to a certain goal based on real time measurements. Or in terminology: A control algorithm sets the systems actuators (for wastewater systems e.g. pumps, valves, movable weirs, etc.) to their optimal values based on real time input from process variables (e.g. water levels, flow capacities, rainfall, etc.) that reflect the current systems functioning.

An overview of the research dedicated to RTC in urban wastewater systems over the past decades can be found in several review papers: (Schilling, 1989) describes some of the first steps, (Schütze et al., 2004) present uniform definitions and give a state of the art in the following years, and a recent survey can be found in (Garcia et al., 2015).

In this thesis RTC in urban wastewater systems is defined by: *“An urban wastewater system is controlled in real time if process variables are monitored in the system and (almost) immediately used to decide on the status of the actuators.”* This definition deviates from the definition by (Schütze et al., 2004), who state that *“an urban wastewater system is controlled in real time if process variables are monitored in the system and, (almost) at the same time, used to operate actuators.”* The definition of this thesis distinguishes between the moment of decision making based on the monitoring data and the moment of taking action, which facilitates delayed action or taking no action at all.

1.2.2 Requirements

For the application of RTC several requirements have to be fulfilled:

- A goal for the functioning of the system should be determined;
- The system should contain actuators;
- The systems functioning with respect to the goal should be sensitive for actuator operation;
- Real time measurements representative for the systems functioning should be available;

- A communication system to transfer measurements and actuator settings has to be operational;
- A model describing the systems functioning should be available for the design, and possibly implementation, of the control algorithm.

Numerous RTC applications in urban wastewater management show that it is possible to meet these requirements. These applications range from very basic local control (e.g. sewer pump switches based on a water level measurement in a pump sump) to system wide control (e.g. adjusting WWTP influent capacities on anticipated flows based on rainfall measurements in a contributing catchment).

When aspiring towards the application of RTC, the strategy and implementation level constrain the above requirements. In urban wastewater management most RTC goals can be categorised in one of these strategies:

- Volume based, making optimal use of the available system capacity. See e.g. (Weyand, 2002; Dirckx et al., 2011);
- Quality based, exploiting differences in pollution level of the wastewater. See e.g. (Lacour et al., 2011; Vezzaro et al., 2014);
- Impact based, taking differences in vulnerability of the environment (receiving waters, atmosphere) into account. See e.g. (Risholt et al., 2002; Erbe and Schütze, 2005).

Each strategy sets its own demands on the information required for the development, implementation and operation of the control. Any strategy has a need for information on water quantities (water level measurements and possibly flows), as quantities are ultimately controlled. For quality based control additional quality measurements of the wastewater are needed. Impact based control demands knowledge about the response of the environmental parameters of interest on actuator operation.

Optimising the performance of an urban wastewater system through RTC can be implemented at very different levels of complexity, ranging from local control to model predictive control. Each level is defined by several characteristics, such as local or system wide optimisation, how measurements are applied and how models are used. Table 1.1 gives a non-exhaustive list of possible implementation levels, together with their characteristics.

Table 1.1: Non-exhaustive list of possible RTC implementation levels with characteristics in increasing order of complexity.

implementa- tion level	optimisa- tion	actuator settings	need for measurements	use of models		
				purpose	modus	
local	local	individual	compare to set points	determine actuator settings	actuator	off-line
system wide - one set	system wide	optimised set	compare to set points	determine actuator settings	actuator	off-line
system wide - more sets	system wide	choose optimised set	determine sys- tem state, compare to set points	define system state, determine actuator settings	actuator	off-line
model predictive control	system wide	individual	input for algo- rithm	determine actuator settings	actuator	on-line

The selected implementation level determines to a large extent the allowed simulation speed of the model used in the optimisation, the reliability of the required measurements and the complexity of the resulting control.

Combining possible strategies and implementation levels in one matrix, as depicted in figure 1.3, results in a kind of landscape. Moving from the top left to bottom right increases the demands put on measurements, models, communication systems and algorithms. For the application of RTC, ideally, for each case the optimal location in the landscape would be selected, weighing the cost of increased demands against the expected benefits.

1.2.3 Performance evaluation

Scientific research on RTC in urban wastewater management has mostly dealt with modelling exercises, for both hypothetical systems and case studies such as described in (Nelen, 1992; Erbe et al., 2002; Puig et al., 2009). Simultaneously, publications appeared about RTC applied in practice, see e.g. (Hoppe et al., 2011; Seggelke et al., 2013). The essence of these publications, which location in the RTC landscape is displayed in figure 1.3, and other publications elaborated on in chapter 5, is positive: RTC has great potential to reduce the impact of sewer systems and WWTPs on receiving waters, to improve the operation of urban wastewater systems and to help adapt the systems to changing conditions.

		implementation level				
		local	system wide – one optimal set	system wide – choose between sets	model predictive control	...
strategy ↓	volume based		Nelen, 1992		Puig et al., 2009	
	quality based			Hoppe et al., 2011		
	impact based			Seggelke et al., 2013		
	...		Erbe et al., 2002			

Figure 1.3: Application of RTC can follow different strategies and implementation levels. In the resulting landscape, demands increase from the top left to bottom right.

Looking in more detail to the results on which the supposed RTC potential is based, the validity of this conviction could be questioned on multiple grounds:

- Results based on simulations only do not guarantee a similar outcome in practical situations;
- In practical cases only a few events or short periods are considered in a performance evaluation, thus only a limited range of conditions under which urban wastewater systems operate have been considered;
- Uncertainties in measurements and models are generally not accounted for in a performance evaluation, resulting in a lack of certainty on the significance of the outcome;
- In some cases results are attributed to RTC, while careful reading reveals that additional changes to the infrastructure were made such as increasing storage volume or discharge capacities. When evaluating the effect of RTC only minor adaptation of infrastructure is allowed, such as the introduction of valves to make better use of the existing systems storage capacity.

For above reasons the effectiveness of RTC in urban wastewater management is not yet established. Moreover, no methodology was found to determine whether the application of RTC in practice is effective. A more detailed problem statement on this issue will be presented in chapter 5.

1.3 Goal

This thesis is part of a continuous research line about RTC in urban wastewater systems at Delft University of Technology. The thesis of Langeveld (Langeveld, 2004) mainly dealt with a literature review of the state of the art at that time and explorations to exploit dynamics in urban wastewater system operation through field measurements and modelling exercises. Schilperoort (Schilperoort, 2011) scrutinised on-line water quality monitoring techniques for wastewater as well as the resulting data. During his work a fruitful cooperation with water board De Dommel began. Simultaneously, for the wastewater system of Eindhoven, the research project KALLISTO (Langeveld et al., 2013) indicated a potential for RTC to reduce the impact of the sewer system and WWTP on the river Dommel. The work presented in this thesis started when implementation of RTC for this purpose was initiated.

Having dealt with important requirements for RTC in previous theses, namely models and measurements, the research line continued with RTC itself. The cooperation with water board De Dommel provided the opportunity to work on RTC in the real world, i.e. actually applying RTC on a real system and following its operation. Combined with a lack of a methodology to evaluate the actual operation of a RTC system, this leads to the following main research question:

How can the effectiveness of real time control in urban wastewater systems be determined?

The main question is further specified in three sub questions:

- What tools are needed for an evaluation?
- What are the key elements of an evaluation methodology?
- How can such a methodology be applied in practice?

The research thus combines theoretical work on instruments and a methodology for the evaluation of effectiveness of RTC in wastewater systems with a practical application of this methodology on a case study.

A mind map displaying the main features associated with RTC is shown in figure 1.4. It indicates what topics have previously been contributed to by Langeveld, Schilperoord and water board De Dommel, as well as the additions described in this thesis.

1.4 Case: the wastewater system of Eindhoven

Throughout this thesis the wastewater system of Eindhoven, located in the south of the Netherlands, has served as a case study. The entire system, individual elements, or measurements in the system have been applied whenever possible for consistency and convenience. Alternatives could have been used everywhere except for chapter 6 which is case specific. This section provides a general overview of the system. Some aspects will be recalled, or further details will be supplied, in the respective chapters when appropriate.

1.4.1 Layout and characteristics

A geographical overview of the wastewater system of Eindhoven is shown in figure 1.5. It consists of the WWTP of Eindhoven and three contributing sewer catchments, and it discharges to the river Dommel as main receiving water body:

- The WWTP is one of the largest plants in the Netherlands. It is designed for 750,000 population equivalent, has a maximum hydraulic capacity of 35,000 m^3/h and an average dry weather flow of $\sim 4,500 m^3/h$;
- The three sewer catchments are all equipped with combined sewer systems. Nuenen-Son serves two municipalities and presents less than 10% of the total WWTP inflow. Eindhoven Stad serves the city of Eindhoven only and constitutes $\sim 45\%$ of the influent. Riool Zuid collects wastewater from seven municipalities through a 31 km transport sewer and makes up $\sim 45\%$ of the total WWTP influent. More than 200 CSOs are present in the three sewer catchments;
- The Dommel is a typical small lowland river. It originates in Belgium and flows north until it reaches the river Meuse. It has a base flow of 2 to 4 m^3/s that goes down to 1 m^3/s during dry summer periods.

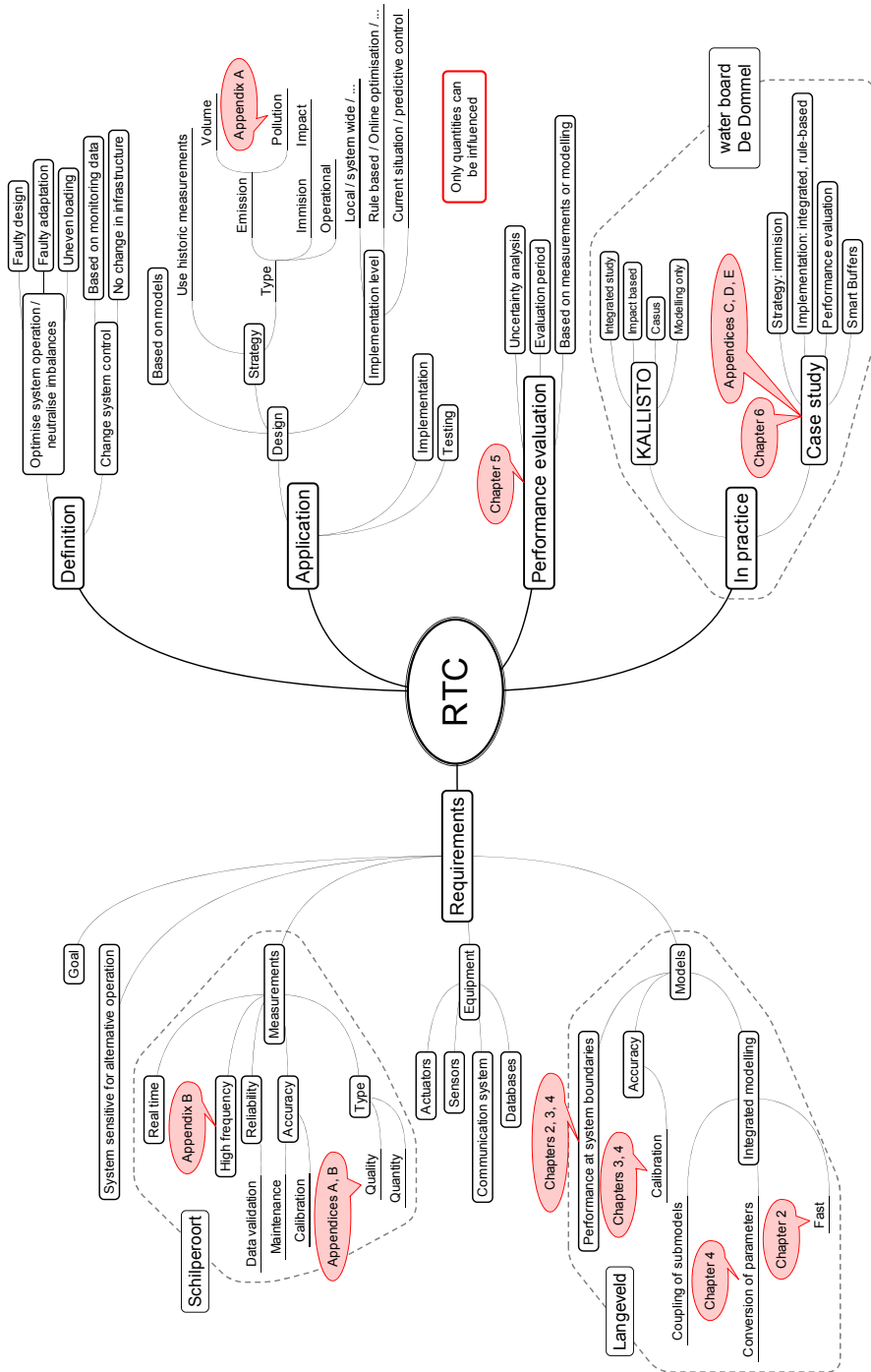


Figure 1.4: Mind map displaying the main features of RTC. Call out balloons point out to which features this thesis contributes. In dashed circles features previously covered in the research line are indicated.

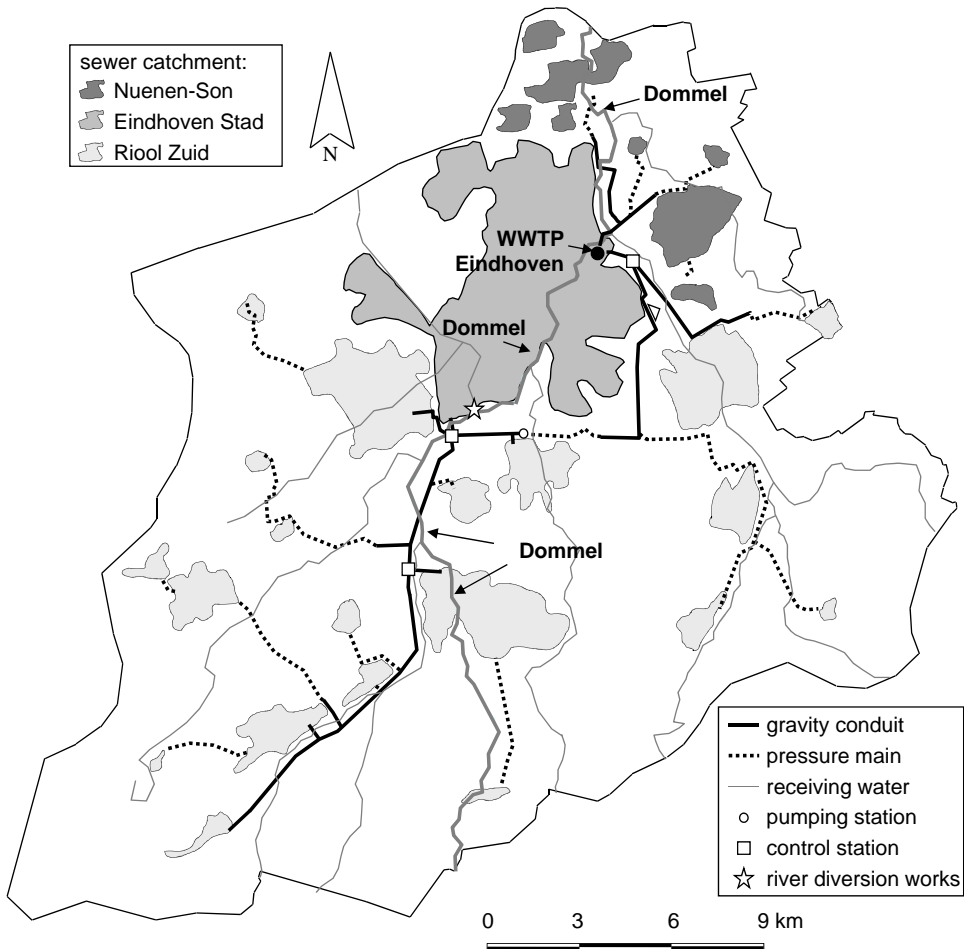


Figure 1.5: Geographical overview of the wastewater system of Eindhoven. Adapted with permission from (Schilperoort, 2011).

The size of the wastewater system compared to the river is illustrated by the ratio between the WWTP effluent and the river base flow. During a dry day in a dry summer period this ratio is approximately 1:1, indicating that the river downstream of the WWTP consists of as much treated wastewater as original river water. During a big rain event in a dry period the ratio turns into 9:1, meaning that 90% of the river water downstream of the WWTP consists of effluent. Due to these ratios, the river is particularly vulnerable for malfunctioning of the WWTP or sewer systems. Acute water quality problems in the Dommel occur in the form of dissolved oxygen depletion due to CSO activity and WWTP effluent, and toxic ammonium peaks due to the WWTP effluent.

1.4.2 Available materials

Water quality problems in the river Dommel gave rise to research project KALLISTO (Weijers et al., 2012) and implementation project POLARIS, both carried out by water board De Dommel. For this purpose an extensive monitoring and modelling program was set up. Rainfall, water quantity and water quality measurements have been performed at high frequency (one-minute to ten-minute interval) in the sewer systems, at the WWTP and in the river. A description of the monitoring network is presented in appendix C.

Detailed models were constructed for all municipal sewer systems, the transport sewers, WWTP and river. The models were verified with field measurements and packed together in a (partly lumped) integrated model. Also an evaluation framework was developed to determine the impact of investigated measures on the river water quality. For more details on the models and the evaluation framework the reader is referred to (Langeveld et al., 2013).

1.4.3 Possibilities for RTC

The wastewater system of Eindhoven is an interesting case for the application of RTC for several reasons, see also figure 1.5:

1. Total area of $\sim 600 \text{ km}^2$;
2. WWTP influent from three separate sewer catchments;
3. Transport sewer Riool Zuid is equipped with one pumping station and three control stations;

4. A diversion works in the river Dommel just south of Eindhoven.

Reason number 1 indicates that severe storms are likely to pass over parts of the total area only. Combined with number 2 this means that the maximum WWTP inflow for such storms is likely to arrive at different times for the sewer catchments. Reason 3 gives further possibilities to delay or level out high inflows from Riool Zuid. Number 4 finally creates the possibility to divert (or not) river water around Eindhoven. All present possibilities to interfere with the operation of the wastewater system or its impact on the river through RTC. This agrees with the outcome of the PASST planning tool (Schütze et al., 2008) as described in (Langeveld et al., 2013), which revealed the system was ‘suited for control’.

1.5 Outline

The outline of this thesis follows the defined research questions in section 1.3. The first sub question, on the tools needed for a RTC performance evaluation, can encompass a multitude of topics. In this work it was decided to focus on enhancing the models that describe the interactions at the boundaries of the sewer system: with the WWTP and the receiving water. Chapter 2 deals with quantity aspects between sewer systems and receiving water, i.e. determining discharge characteristics for CSO locations through computational fluid dynamics simulations. Chapter 3 also looks into CSO discharge quantities, but now from the point of (rapid) model simulations. Chapter 4 deals with water quality aspects between sewer systems and WWTP. It describes a novel influent model for deriving influent quality parameters from influent quantity measurements.

The second sub question, on the key elements of an evaluation methodology, is treated in chapter 5. It proposes a methodology for determining the effect of RTC in urban wastewater systems in practice and supplies a simplified case study to show the importance of several elements of the methodology. Chapter 6 deals with the final sub question about the practical applicability of an evaluation methodology. It demonstrates a practical application of the proposed methodology for the wastewater system of Eindhoven.

Finally in chapter 7 concluding remarks and recommendations for further research and application of the results are presented.

2 Weir discharge relationships

2.1 Introduction

Combined sewer overflow (CSO) discharges are one of the most important interactions of an urban wastewater system: from a combined sewer system to the receiving water. The discharge of (diluted) sewage to prevent flooding of urban areas or downstream overloading of the system has a negative impact on the ecological status of these waters through for example dissolved oxygen depletion. Application of real time control (RTC) therefore often (in-)directly aims at preventing or reducing CSO discharges. The design and assessment of control scenarios that interfere with CSO discharges, or more generally weir discharges, require accurate knowledge on these discharges and hence the hydraulic performance of weirs in sewer systems.

Weir discharges can be determined in various ways:

- Flow measurements. Direct measurement of the flow rate. Expensive, difficult to install in existing situations, inaccurate in partly filled pipes (Mignot et al., 2012; Campisano et al., 2013; Lepot et al., 2014);
- Local calibration. Derive a unique relationship between flow rate and water level measurements from on-site experiments. Expensive, causes inconvenience for surroundings, laborious (Ruban et al., 2002; Soulis and Dercas, 2012);

This chapter is an adapted version of: Van Daal-Rombouts, P.M.M., Tralli, A., Verhaart, F., Langeveld, J.G., Clemens, F.H.L.R., (*submitted*). Validation of computational fluid dynamics for deriving weir discharge relationships with scale model experiments and prototype measurements. *Flow Measurement & Instrumentation*.

- Model experiments. Derive a unique relationship between flow rate and water level measurements from lab measurements on scaled or full scale models. Expensive, laborious (Bettez et al., 2001; Bos and Kruger-Van der Griendt, 2007; Campisano et al., 2009).

All methods are expensive and most are laborious. Weir discharges are therefore most often estimated by application of a standard weir equation and local water level measurements, which are more affordable and easier to install in existing situations than direct flow rate measurements.

The standard equation for the discharge of frontal weirs under free outflow conditions is

$$Q = a_1 h^{a_2}, \quad (2.1)$$

with Q [m^3/s] the flow rate, h [m] the water level above the weir crest, a_1 [$m^{1.5}/s$] and a_2 [-] constants generally taken to be 1.36 times the weir length in meters and 1.5, respectively. The conditions for application of this equation, such as a sharp and horizontal weir crest, flow perpendicular to the weir, one in- and one outflow and a horizontal water level above the weir crest, are hardly ever met in practice. This may lead to errors of up to 50% in the determined discharged volumes, see e.g. (Fach et al., 2009). The main error sources originate from the shape of the weir crest at low water levels and the geometry of the weir chamber that dominates the water flow at high water levels. Applying a more ideal crest shape can mitigate the impact of the first source of error (Brombach and Weiss, 2005), or a specifically derived set of constants matching the implemented weir can be applied (Johnson, 2000; Azimi and Rajaratnam, 2009; Hoseini, 2014). In a similar fashion it is not possible to account for the effect the chamber geometry has on the discharge relationship.

A survey of the weir and weir chamber details for nine CSO locations in the sewer system of Eindhoven, which are equipped with water level sensors to determine their discharges, has been carried out. It revealed that only one of these locations meets the conditions required for the application of the standard equation. All other locations have additional in- or outflows, no sharp weir crest, weirs with an angular shape, or erratic weir chamber geometries. Application of the standard equation will most likely lead to substantial errors depending on for example the moment backwater effects start to emerge. An appropriate method to derive a local relationship with a quantified uncertainty between flow rate and water level, for weirs where the chamber geometry is the dominant source of deviation from the standard equation, is therefore required.

Several computational fluid dynamics (CFD) studies show promising results in modelling complex hydraulic behaviour, see e.g. (He et al., 2006; Zhao et al., 2008). (Fach et al., 2009; Lipeme Kouyi et al., 2011) deal with CFD for the derivation of weir discharge relationships for odd shaped weirs and weir chambers. In these studies, however, models are calibrated on literature values and results remain unchecked due to a lack of monitoring data. Only (Isel et al., 2014) report on an attempt to validate the methodology described in (Isel et al., 2013), but refrain to validate the derived relationships by measurements.

Little research is documented on the validation of CFD results. (Lipeme Kouyi et al., 2003), for example, use a weir situated in a conduit and focus on the validation of a novel technique for determining the free water surface, with modelling and validation of CFD receiving little attention. (Mignot et al., 2012) validate the flow velocity in a 90 degree bend and (Larrarte, 2006) investigates the velocity fields within sewers. Validation of CFD results for the specific conditions required (odd weir or weir chamber geometries, water level verification) was not found in literature.

This chapter investigates the applicability of CFD to determine discharge relationships with known uncertainty for weirs where the chamber geometry dominates the hydraulic regime. For this purpose one of nine surveyed CSO locations was taken as a case study. A unique combination of field measurements, lab experiments on a scale model, and CFD simulations for the scale model and prototype CSO are used. The pictures taken and data sets gathered during the experiments and simulations will be used to i) determine whether CFD simulations can correctly describe the hydraulic behaviour (validate CFD results), and ii) derive and compare the discharge relationships between the measurements and CFD results mutually and with the standard equation, equation 2.1, for the scale model and prototype (validate discharge relationships derived from CFD results).

The CFD simulations performed for this study are ‘unverified’. This means that the CFD models are not calibrated and that a blind approach was taken in the set-up of the CFD models, i.e. no a priori knowledge on the functioning of the weir and weir chamber was applied. These choices mimic the practical engineering situation, where the weir has to be designed and the discharge relationship has to be known prior to construction. By doing so it is aimed to validate the application of CFD for both scientific and engineering purposes, where in the latter case generally fewer resources (time, budget) are available.

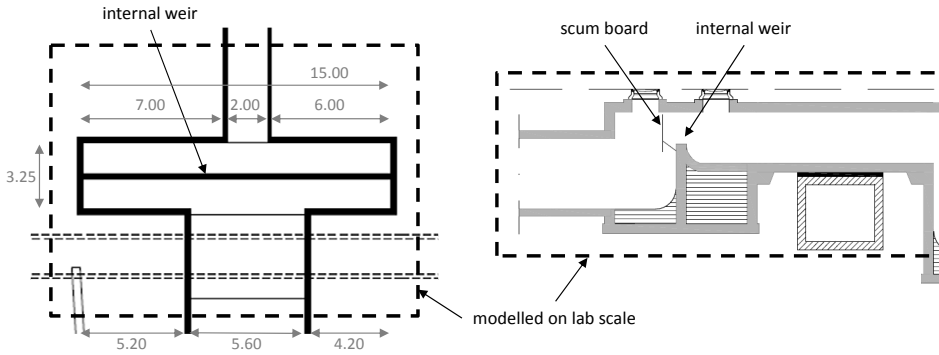


Figure 2.1: Top view (left) and side view (right) of the designed weir and weir chamber. Flow direction is from top to bottom (left) and left to right (right). At the weir the downstream invert is much higher than the upstream invert to cross a transport sewer. All dimensions are given in meters.

This chapter is organised as follows. Section 2.2 introduces the case study, the acquisition of the data sets, the derivation of the discharge relationships from these sets and the analysis procedure. Section 2.3 describes the results for the scale model and the prototype, followed by a discussion on the results in section 2.4. Finally, conclusions and recommendations are presented in section 2.5.

2.2 Materials and method

2.2.1 Prototype

The case study selected for this research is the internal weir of a storm water settling tank (SST) in the city of Eindhoven, the Netherlands. Figure 2.1 displays a top and side view of the design drawings of the weir and weir chamber. The weir chamber measures 15×3.25 m with one inflow and one outflow that are symmetrical with respect to each other but not to the weir chamber itself. The weir crest consists of a 0.25 m thick concrete wall with a metal rounded downstream edge and is equipped with a scum board to prevent floating debris from entering the SST.

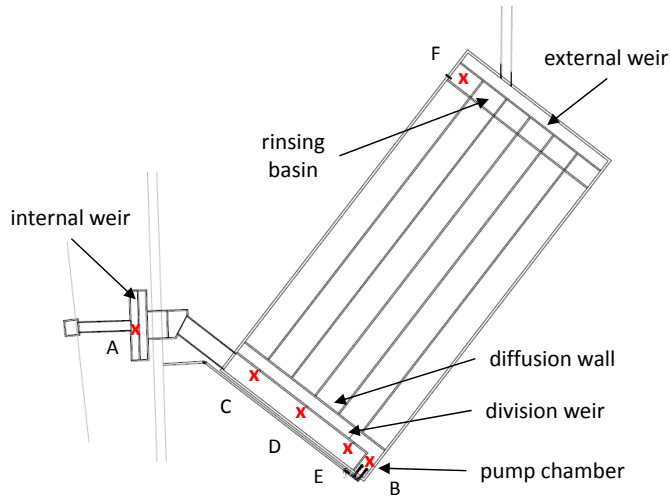


Figure 2.2: Layout of the SST. The internal weir is displayed in detail in figure 2.1. Water level sensor locations are indicated by crosses and labelled A to F.

A site inspection revealed some minor differences between the designed and the as-built weir chamber. In the as-built situation the inflow is located approximately 0.25 m more off centre with respect to the weir chamber while the outflow moved approximately 0.35 m towards the centre. The thickness of the weir crest is 0.30 m and the upstream and downstream side of the weir chamber are provided with flow profiles. The downstream flow profile was surveyed, which was not feasible for the upstream profile.

2.2.2 Field measurements

2.2.2.1 Monitoring setup

The layout of the entire SST is shown in figure 2.2. From upstream to downstream the SST consists of the internal weir and weir chamber, a series of constructions to guide and divide the wastewater into six identical chambers for storage and settling, and the external weir and outflow. Rinsing basins and a pump provide emptying of the SST and cleaning facilities for settled debris. The chambers divided by the division weir are connected through three openings at the bottom of this weir.

Water level measurements (Vega, Vegawell 52) are performed as part of regular monitoring at locations A to F as indicated in figure 2.2. The monitoring data applied in this study runs from February 2012 to November 2015. The water levels are stored in a central database with a resolution of 1 *cm*. The registration takes place on change only, at a frequency of 1 *s* which is approximately the response time of the sensor. Consequently, no uniform time axis is available. A uniform one-minute time axis is constructed by linear interpolation of each data series.

2.2.2.2 Data quality

Validation of the field measurements revealed several irregularities in the registered levels, e.g. steps in the base level and registered levels in a full basin at different heights. Inquiry and the site visit learned that the sensor installation, calibration and maintenance are not ideal or have not taken place at all. Data validation and correction were performed to overcome these irregularities:

- Sensors B to F in figure 2.2. In the period between a discharge of the external weir and the emptying of the SST, the water level in the SST is stable at the crest level of the lowest weir for a certain period of time. Measurements were corrected to match this crest level, averaged over all events registered. This resulted in adjustments of -5 to +8 *cm*;
- Sensor A in figure 2.2. The measurement series for sensor A could not be corrected in the same manner as it fluctuates with the water level in the sewer system. Therefore, a different approach was adopted. Logically, the SST can only fill once the internal weir overflows. This is visible some time later in a change in water level in the SST, starting at location B (the lowest point). Depending on the filling rate, the corrected water level was made to match the internal weir crest level 2, 5 or 8 *min* before the onset of the filling of the SST. Averaged over all events no correction had to be performed, but all events between October and December 2013 were excluded as a temporary systematic error in the sensor readings of approximately 30 *cm* occurred.

The water level sensor uncertainty was found to be 1.3 *cm* (2σ) from a field test where the sensor was placed in a bucket of water. This uncertainty is used while comparing two values within one series, assuming this uncertainty does not change over the measuring range. When applying data (derived) from multiple sensors a higher uncertainty of 2.0 *cm* (2σ) is assumed, as this is also influenced by factors such as installation, maintenance, data resolution, and subsequent corrections.

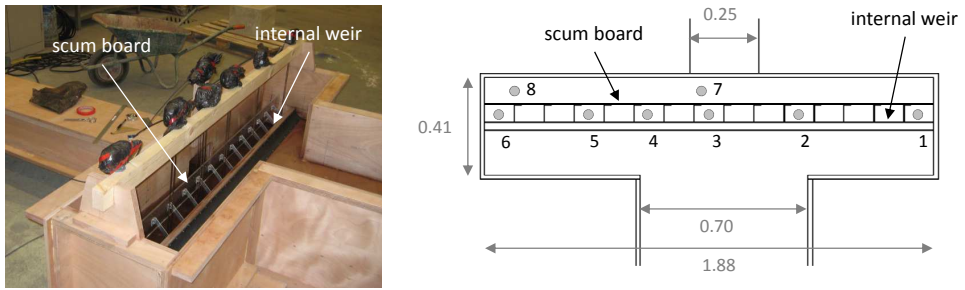


Figure 2.3: Picture of the lab scale model (left) and schematic top view of the lab scale weir chamber with dimensions and numbered sensor locations (right). All dimensions are given in meters.

2.2.2.3 Flow rate determination

Based on the rate of water level change in the SST and the area of the SST at the corresponding water level, the volume discharged over the internal weir for each time step was determined. Combining the water level measurement upstream from the weir (sensor A in figure 2.2) with this discharge creates a data set that was used to derive the discharge relationship from the field measurements. For this purpose the surface area of the SST has been determined from the CAD design drawings for each millimetre height. Only free outflow conditions are considered, i.e. only periods with rising water levels in the SST and a maximum water level below the crest level of the division weir of 10 *cm* are taken into account. As the openings in the bottom of the division weir present a hydraulic resistance, different water levels before (sensor D) and after (sensor B) the division weir were applied. A time shift of 3 *min* was adopted between the water level at the internal weir and the discharge, as the water level correction for sensor A revealed a time shift between the start of overflow and response in the SST of 2 to 5 *min*.

2.2.3 Lab experiments

A scale model of the internal weir and weir chamber, as indicated in the dashed outline in figure 2.1, was built in the lab based on the design drawings. The scale factor is 1:8. A picture of the resulting scale model (left) and a schematic top view with dimensions (right) are shown in figure 2.3. The scale model is situated above a large water basin. At the inlet water is pumped into the model, at the outlet the water is discharged back into the basin.

The scale model was equipped with 8 water level sensors (Deltares, 2016) to determine the water level before the weir at imposed flows rates of 0.004 to 0.030 m^3/s . The sensor locations are indicated in figure 2.3 (right). Locations 1 to 6 are in between the weir and the scum board. Locations 7 and 8 are situated before the scum board. Location 7 is fitted to the side of the inlet, which corresponds to the field measurement location. All sensors were calibrated for this specific setup. Measurements were performed in two sessions, at a frequency of 1 kHz for 5 to 10 min , after the water level reached equilibrium. Additionally, pictures were taken and movie clips recorded.

Because the dimensionless Froude number is equal for the scale model and prototype, Froude scaling applies. When up-scaling the scale model results, lengths should be multiplied by the scale factor (8), velocities by $8^{1/2}$ and flow rates by $8^{5/2}$.

The influence of the performed scaling was checked following (Heller, 2011). Appropriate for the applied scaling are the dimensionless numbers Froude ($\frac{v}{\sqrt{gh}}$), Reynolds ($\frac{\rho vl}{\mu}$) and Weber ($\frac{\rho v^2 l}{\sigma}$), where v [m/s] is the water velocity, g the gravitational constant of 9.8 m/s^2 , h [m] the thickness of the water layer, l [m] the hydraulic radius of the structure, ρ the density of 1000 kg/m^3 , μ the dynamic viscosity of 0.001 $Pa\cdot s$ and σ the surface tension of 0.073 N/m (all for water at 20 °C). The standard weir equation (equation 2.1) was used to determine the flow rate and flow velocities for the prototype and scale model.

The Froude number is equal for the scale model and prototype. The Reynolds number in the inflow and above the weir crest are approximately 23 times smaller for the scale model compared to the prototype, but remain $>2,000$ for all flows ensuring turbulent flow in all situations. The Weber number above the weir crest is 64 times smaller for the scale model compared to the prototype, indicating a stronger influence of the surface tension resulting in higher water levels due to the stronger curvature of the water surface.

2.2.4 Computational fluid dynamics

2.2.4.1 Models

Two CFD models have been built to simulate the hydraulic behaviour of the weir and weir chamber. The first model, M1, corresponds to the lab experiments and is scale model sized following the design drawings. Model M2 is prototype sized, follows the as-built situation and corresponds to the field measurements.

In the CFD models the (up-scaled) sensor locations in the lab experiments are replicated to extract the simulated water levels. For model M1 steady flow rates of 0.004 to 0.030 m^3/s have been applied as in the lab experiments. For model M2 the applied flow rates range from 0.035 to 5.43 m^3/s , which correspond to the up-scaled flow rates for the scale model and additional values at low flow rates.

2.2.4.2 Simulations

The CFD models are implemented in the commercial software StarCCM+[®] v10 with a blind approach to mimic the practical engineering setting: i) it was assumed no information was available of the actual functioning of the CSO, ii) no attempt has been made at calibrating the models (use of commonly available numerical schemes, no tuning of parameters in the numerical schemes, etc.), iii) only one mesh was created and used for all flow regimes, and iv) the overall complexity of the models was tuned to run on a commonly available desktop computer. By doing so the results should comply with the engineering practice and help advance that field.

Transient simulations are performed with a constant prescribed water discharge at the inlet. In the models, water and air are included as continuous phases and treated by means of the volume-of-fluid (VOF) method (Hirt and Nichols, 1981). Both phases are treated as isothermal and incompressible, at 25 °C and at a reference pressure of 1 *bar*. Buoyancy effects are taken into account by adding a gravity term. The inner surface of the structures walls is defined as hydraulically smooth with a non-slip boundary condition. The channel outlet is modelled with a pressure controlled outlet boundary condition, roughly representing a free fall.

In the VOF method, the evolution of the water within the domain is tracked by computing the advection of its volume fraction: the water level is computed as the locus where the volume fraction of water is 0.5. The mean water level and 2σ model fluctuations were determined over 300 time steps after a stabilisation period.

Test runs with model M1 were performed to check the influence of the simulation time step and cell type on the simulated water levels:

- Time step. The model was simulated with time steps of 1, 10 and 100 *ms* to investigate the impact on the simulated water levels. They revealed that a changing time step does not lead to a significant change in the mean water levels; it does lead to smaller model fluctuations at lower time steps due to the spectral content of the simulated levels;
- Cell type. A polyhedral mesh was found to better approximate the free surface in zones of highly three-dimensional flow than a mesh based on hexahedral elements. The enhanced predictive capability comes at the price of increased computational cost.

The reported simulations have been performed with a time step of 7.5 *ms* (M1) and 15 *ms* (M2). For the grid a polyhedral grid of approximately 7 million cells with a size of 3 *mm* (M1) and 8x3=24 *mm* (M2) around the weir has been judged to provide acceptable results.

2.2.5 Derivation of discharge relationships

Irrespective of their origin (measured, calculated or simulated) all data sets consist of multiple water level-flow rate combinations with uncertainties in both parameters. For each data set the discharge relationship was derived by application of a constrained nonlinear multi variable fitting function to minimise the sum of squared errors between the data set and the resulting fit. The standard equation for frontal weirs, equation (2.1), was applied as the basic curve, since a power function describes the data sets well. Constants a_1 and a_2 were adjusted in the minimisation.

Uncertainties in the input water level and flow rate were incorporated through Monte Carlo simulations. N fits were determined for N replicates of the data set. The replicates consist of random values selected for each level-flow rate combination that served as the mean value with a given standard deviation in both directions based on the normal distribution. From the resulting N values for a_1 and a_2 , their mean value, standard deviation and mutual correlation (ρ) were calculated. The (1σ) uncertainty in the fitted flow rates were subsequently calculated through

$$\sigma_Q^2 = \left(a_1 a_2 h^{(a_2-1)} \right)^2 \sigma_h^2 + \left(h^{2a_2} \right)^2 \sigma_{a_1}^2 + \left(a_1 h^{a_2} \ln h \right)^2 \sigma_{a_2}^2 + 2 \left(a_1 h^{2a_2} \ln h \right)^2 \rho \quad (2.2)$$

with x the mean value and σ_x the (1σ) uncertainties in a_1 , a_2 and h .

In case application of the normal distribution led to negative water levels in the Monte Carlo simulation data sets, the tail of the distribution that fell below zero was added to the distribution between zero and the mean to remove the negative values while conserving the median value of the distribution. In all Monte Carlo simulations $N=10,000$ was applied, except in case of the lab experiments where due to the lower uncertainty in the input parameters and large number of available measurements $N=1,000$ was deemed sufficient.

2.2.6 Analysis steps

As the most detailed measurements are available for the lab experiments, these are used in the first evaluation of the CFD simulation results (model M1). The ability of the CFD simulations to describe the hydraulic behaviour of the lab experiments is investigated based on a qualitative comparison of the simulated free surface level images and pictures taken during the lab experiments. Quantitatively, the water levels for the different sensor locations and flow rates are compared. Discharge relationships are derived and compared mutually and with the standard equation.

The second evaluation of the CFD simulation results (model M2) is based on the field measurements, for which the discharge relationships are again compared mutually and with the standard equation.

2.3 Results

2.3.1 Lab experiments vs CFD (scale model)

2.3.1.1 Hydraulic behaviour

The lab experiments give much insight into the hydraulic behaviour of the weir and weir chamber. At low flow rates, see figure 2.4 (left), the water level upstream from the weir is stable. Free outflow occurs along the full length of the weir. At high flow rates, see figure 2.4 (right), the water level upstream from the weir is unstable and mostly convex, downstream it is unstable and mostly concave. This is due to the elongated shape of the weir chamber and the sharp corners of the in- and outflow. It causes free outflow to occur centrally over the weir, while to the sides submerged outflow takes place. The scum board further adds to the complexity of the flow. The CFD simulations for model M1 exhibit the same behaviour in a qualitative sense. Figure 2.5 displays the free surface level for a flow rate of $0.024 \text{ m}^3/\text{s}$. It is very similar to the corresponding water surface in the right of figure 2.4.

Quantitatively, the measured and simulated water levels were compared. Figure 2.6 shows the mean water levels above the weir crest for locations 1, 3, 7 and 8. For the lab experiments 2σ error bars are included, for the model simulations the 2σ fluctuations in the transient simulations are shown. The fluctuation of the water level at the different locations (locations 1 and 8 are stable, locations 3 and 7 are unstable) and for different flow rates (low flow rates are stable, high flow rates are unstable) visible during the experiments is well represented by the widths of the error bars/model fluctuations. For locations 1, 3 and 8 the error bars and model fluctuations overlap for all flow rates. For location 7 the error bars and model fluctuations do not overlap, with increasing deviations for flow rates $>0.016 \text{ m}^3/\text{s}$. As location 7 is most unstable, it is not surprising that the free surface level in the CFD model is less well resolved than for the other locations. This is likely due to a combination of factors ranging from the selected grid to limitations of the software/algorithms applied.

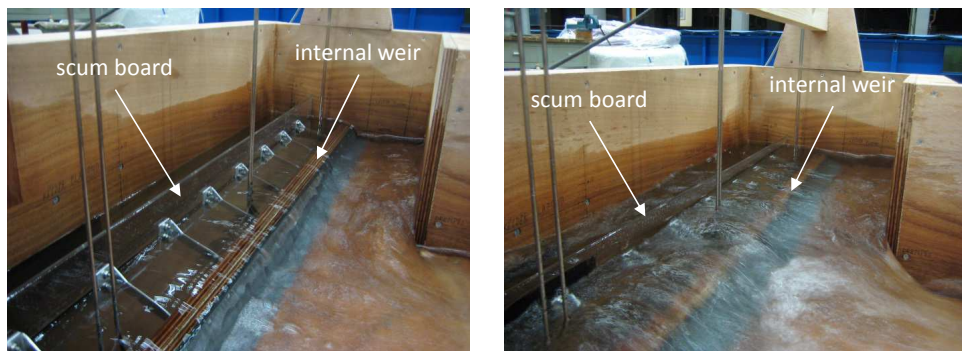


Figure 2.4: Pictures of the water surface at flow rates of 0.008 (left) and 0.024 m^3/s (right) for the lab experiments.

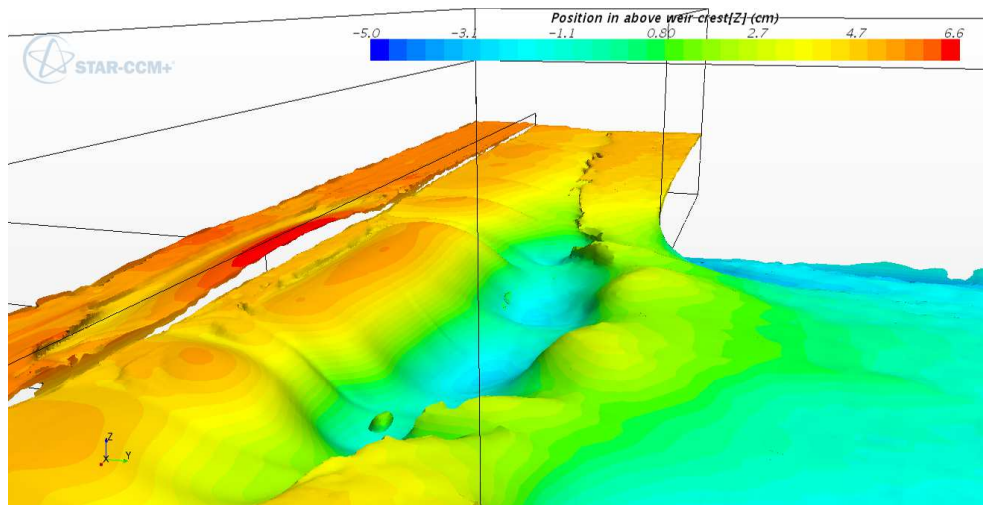


Figure 2.5: Free surface level from CFD simulations with model M1 at a flow rate of 0.024 m^3/s .

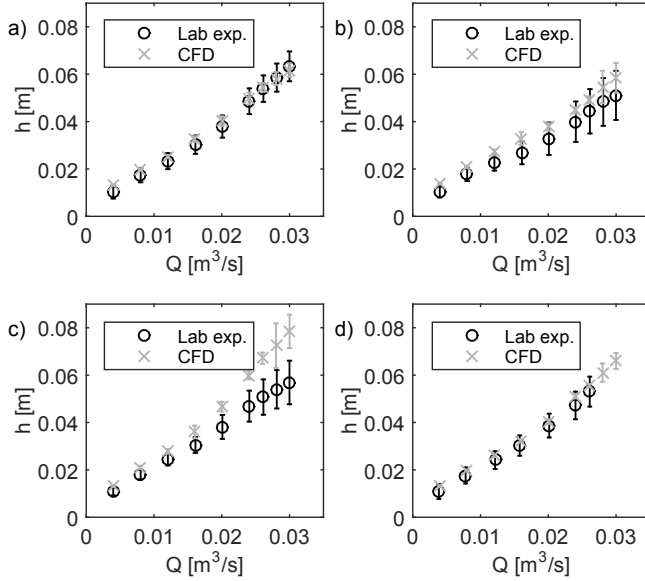


Figure 2.6: Measured and simulated water levels above the weir crest for the lab experiments and model M1 for sensor locations 1 (a), 3 (b), 7 (c) and 8 (d). Mean values and 2σ error bars/model fluctuations are displayed.

In hindsight, a systematic error is observed in the simulated water levels which are consistently higher than the measured water levels. This likely has two causes: i) the lab experiments were performed with increasing flow rate while in the simulations the flow rate was decreased, perhaps leading to an overestimation of the water level due to hysteresis in the experiments/simulations, and ii) insufficient convergence of the VOF transient solver, leading to numerical diffusion of the water phase into the air phase. This leads to a higher measured water level, while the total water mass is conserved. This could also justify the larger deviation of the CFD results from the measurements in the locations where the fluctuation of the water level is larger (sensor 7 and to a smaller extent sensor 3). In order to improve the convergence, simulations should have been run with a smaller time step.

2.3.1.2 Determining sensor locations

Despite the systematic error, the overall hydraulic behaviour of the scale model is well described by the CFD simulations: the model fluctuations of the simulated water levels evolve in the same way as the error bars of the water levels in the lab experiments, and the sensitivity of the water level for a change in discharge at a certain location is evident. The CFD simulations can therefore be used to decide on the optimal sensor location for determining the weir discharge. From CFD simulations the mean water levels and model fluctuations in a transient simulation for several practically feasible sensor locations could be determined. The optimal location would be selected based on small model fluctuations (stable water level) and high sensitivity of the water level for discharge changes. For the sensor locations applied in the scale model this would result in placing a water level sensor at the side of the weir chamber: location 1 or 6. The current location (7), selected by the sewer operator for practical considerations, is likely the worst possible location that could have been selected.

2.3.1.3 Flow regime change

The lab experiment indicates a flow regime change: below a certain threshold the flow is undisturbed; above it backwater effects occur due to the geometry of the weir chamber leading to more diverse flow behaviour. In figure 2.7 the measured water levels along the length of the weir in the scale model experiments are displayed for all applied flow rates. The mean water levels are similar for water levels above the weir crest $<2.5\text{ cm}$ (or flow rates $<0.012\text{ m}^3/\text{s}$) and will be referred to as the ‘undisturbed’ flow regime. For mean water levels above the weir crest $>2.5\text{ cm}$ (or flow rates $>0.012\text{ m}^3/\text{s}$) the water levels start to deviate due to backwater effects and will be referred to as the ‘disturbed’ flow regime.

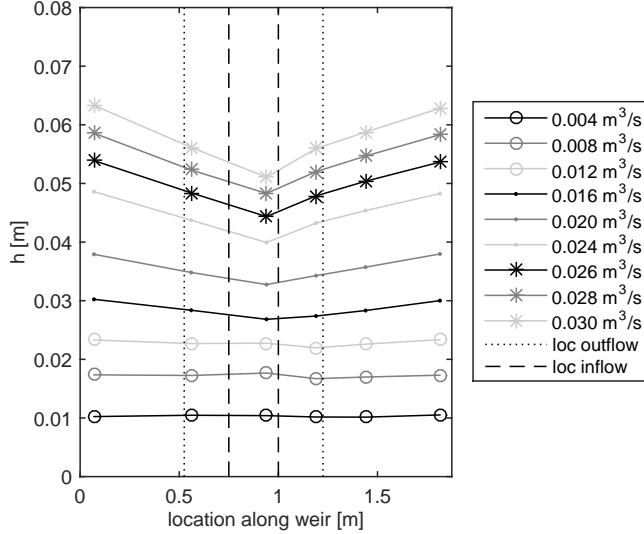


Figure 2.7: Mean water levels above the weir crest along the length of the weir for different flows based on the lab experiments. Markers indicate sensor locations: 1 (left) to 6 (right). In dashed lines the location of the inflow is indicated, in dotted lines the outflow.

2.3.1.4 Discharge relationships

In figures 2.8 and 2.9 the data points, fitted discharge relationships and 2σ uncertainty bands for sensors locations 1 and 3 based on the lab experiments (left) and the CFD simulations for model M1 (right) are shown. As described in section 2.2.5 the discharge relationships are determined by fitting the constants a_1 and a_2 from the standard equation (equation 2.1). The resulting values are added to the legend of the figures. The flow regime change is also evident from the derived discharge relationships: in the undisturbed regime the data points display the behaviour of a power function with $a_2 > 1$, while in the disturbed regime $a_2 < 1$. Therefore, two discharge relationships have been fitted joining at $h=2.5$ cm with uncertainty bands for each relationship.

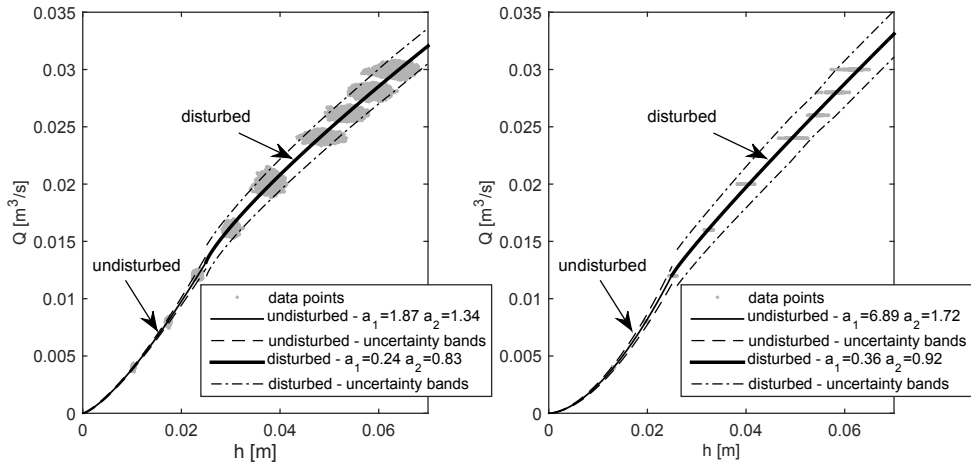


Figure 2.8: Discharge relationships with 2σ uncertainty bands for location 1 derived from the lab experiments (left) and CFD simulations with model M1 (right).

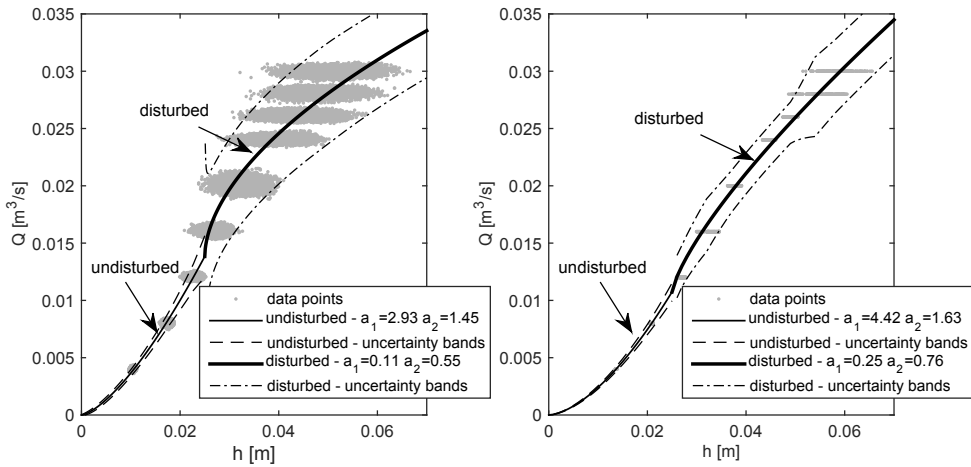


Figure 2.9: Discharge relationships with 2σ uncertainty bands for location 3 derived from the lab experiments (left) and CFD simulations with model M1 (right). The uncertainty bands in the disturbed regime run to infinity at the start of the regime due to the fitting procedure.

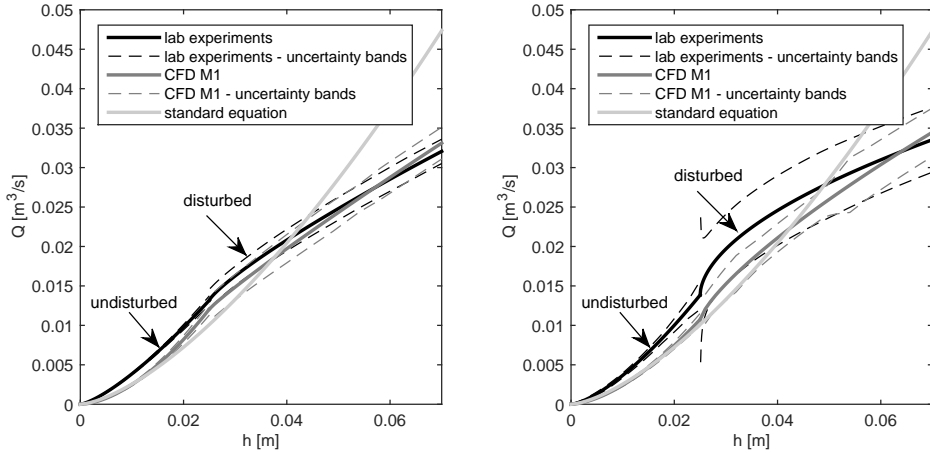


Figure 2.10: Discharge relationships with 2σ uncertainty bands for locations 1 (left) and 3 (right) derived from the lab experiments, the CFD simulations with model M1 and the standard equation. The uncertainty bands in the disturbed regime run to infinity at the start of the regime due to the fitting procedure.

The figures show that the lab experiments (left side) exhibit more outspoken behaviour than the CFD simulations (right side), e.g. the discharge relationships in both flow regimes show more curvature for the lab experiments than for the CFD simulations. As expected from the hydraulic behaviour of the scale model, the discharge relationship for location 1 has smaller uncertainty bands than location 3, and the uncertainty bands for the disturbed regime are larger than for the undisturbed regime. The 2σ uncertainty bands for all locations in the lab experiments are $<9\%$ for the undisturbed regime and $<17\%$ for the disturbed regime. For the CFD simulations all uncertainty bands remain $<9\%$.

For easy comparison the previously displayed discharge relationships for the scale model have been plotted in the same graph together with the standard equation, see figure 2.10. The systematic overestimation in the simulated water levels compared to the lab experiments leads to a consistent underestimation of the flow rate. Differences for location 1 are $<0.002 m^3/s$ ($<27\%$ for undisturbed flow and $<4\%$ for disturbed flow), for location 3 $<0.005 m^3/s$ ($<31\%$ for undisturbed flow and $<10\%$ for disturbed flow). For both locations the uncertainty bands do not overlap in the undisturbed regime, but do in the disturbed regime.

From this it is concluded that unverified CFD simulations are found to be incapable of determining reliable discharge relationships in the undisturbed regime for the scale model. The systematic error in the simulated water levels will have a minor influence on this. A major contribution arises from the grid size because of the low water levels involved, since in the VOF method the water surface can only be distinguished with the resolution of the local grid size. Because the water level and the uncertainty bands increase in the disturbed regime, CFD is found to be able to determine the discharge relationships in the disturbed regime within the uncertainty bands of the lab experiments. As the backwater effect due to the weir chamber geometry becomes dominant in the disturbed regime, it is concluded that the unverified CFD simulations are suitable to determine these discharge relationships for the scale model.

The flow rate estimated through the standard equation (equation 2.1) is less accurate in describing the discharge based on the lab experiments than the flow rate derived from the CFD simulations. For the undisturbed regime differences between the standard equation and the CFD results are $<0.001 \text{ m}^3/\text{s}$ and mostly captured by the uncertainty bands. For the disturbed regime the standard equation is unable to describe the discharge based on the lab experiments. Differences between the flow rate based on the standard equation and the lab experiments of $>0.010 \text{ m}^3/\text{s}$ ($>40\%$) are found. The standard equation is thus not applicable in the disturbed regime.

2.3.2 Field measurements vs CFD (prototype)

A data set with discharge-water level pairs has been derived from the water level measurements in the SST. The data points with 2σ error bars and a fitted relationship are shown in the left side of figure 2.11. In the right side the corresponding results for the CFD simulations with model M2 are displayed for location 7, the actual sensor location. In figure 2.12 the discharge relationships from the field measurements, the CFD simulations and the standard equation are plotted in the same graph for easy comparison.

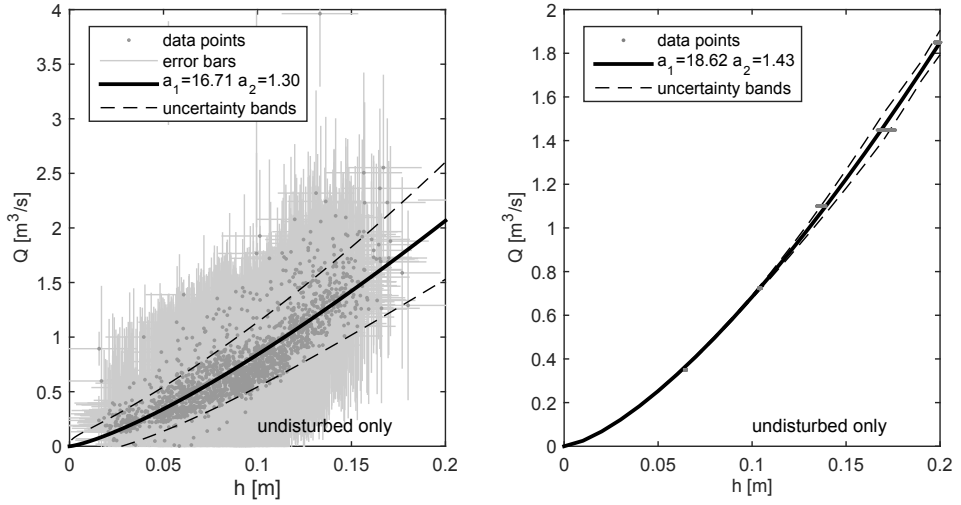


Figure 2.11: Discharge relationships with 2σ uncertainty bands derived from field measurements (left), and CFD simulations with model M2 for location 7 (right). Note the scale difference in the y-axis.

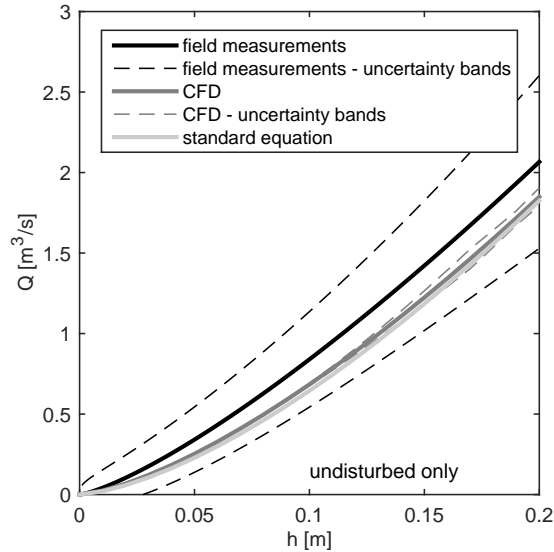


Figure 2.12: Discharge relationships with 2σ uncertainty bands derived from the field measurements, the CFD simulations with model M2 and the standard equation.

From figure 2.11 it is found that the data set does not indicate a flow regime change, which is consistent with the lab experiments since the range of the measured water levels remains within the up-scaled undisturbed regime ($<2.5 \times 8 = 20 \text{ cm}$). Hence only one relationship was fitted. The uncertainty bands for the relationship based on the field measurements are relatively wide due to the natural spread in the derived data points and the quality of the available measurements. This reflects the purpose of weirs in sewer systems: they are meant as control structures (limiting discharges to the surface water while preventing flooding), not measuring devices.

The differences between the discharge relationships for the prototype in figure 2.12 strongly resemble those for the scale model in figure 2.10 for the undisturbed regime. The relationship derived from the CFD simulations almost equals the standard equation, but is lower than the relationship based on the field measurements. Differences with the relationship from the field measurements are $<0.22 \text{ m}^3/\text{s}$ (on average $<25\%$), and easily stay within the field measurements uncertainty bands. From this it is concluded that CFD is suitable to determine discharge relationships for the prototype weir with the reliability needed for practical application. However, for this weir and under these circumstances (only for the undisturbed flow regime due to the restriction on filling of SST only), the added value compared to the standard equation turned out to be low.

2.4 Discussion

2.4.1 Results

For the scale model, the water levels above the weir range from 0 to 2.5 cm in the undisturbed regime and from 2.5 to 6.5 cm in the disturbed regime. That CFD is applicable to derive accurate discharge relationships in the disturbed regime and not in the undisturbed regime at this scale, is partly attributed to the difficulty of modelling thin water layers due to the higher influence of the surface water tension. This is further supported by the result for the prototype. At this 8 times larger scale,

CFD is applicable in the undisturbed regime. For the prototype no measurements were available in the disturbed regime, so for this situation, the applicability of CFD for deriving accurate discharge relationships could not be investigated. Still, as the results indicate that for higher water levels above the weir crest the accuracy of the CFD results improves, it is expected that that CFD is also applicable at prototype size in the disturbed regime.

Apart from the difficulty of modelling thin water layers, the deviation of the derived discharge relationships in the undisturbed regime between the lab experiments and the CFD simulations is partly accounted to the discretization in space and time. Application of two different grids, specialized for the undisturbed and disturbed flow regime (low and high water levels) would probably improve accuracy, since in the VOF method the water surface can only be distinguished with the resolution of the local grid. Refining the grid in the region where the free surface is expected to be, could result in a better approximation of the free surface without affecting the computational cost.

2.4.2 Scientific significance

(He et al., 2011) showed that CFD could be used to optimise the functioning of a storm water settling tank. They validated the results of their CFD simulations through scale model measurements. However, they did not derive discharge relationships. (Lipeme Kouyi et al., 2003; Larrarte, 2006; Mignot et al., 2012) worked on validation of CFD but for different parameters or distinctly different geometries than needed for the derivation of discharge relationships based on level measurements. (Fach et al., 2009; Lipeme Kouyi et al., 2011; Isel et al., 2013, 2014) claim CFD can be applied to derive discharge relationships, but their models are uncalibrated and their results unvalidated. In this study, the applied CFD models are uncalibrated but the simulation results have been validated: water levels are validated for model M1 based on scale model experiments and the derived discharge relationships for models M1 and M2 based on scale model experiments and field measurements respectively. The results agree with literature that CFD is capable of describing the complex hydraulic behaviour occurring in weir chambers with deviating geometry and that the derived discharge relationships in the disturbed regime significantly differ from dis-

charges calculated through the standard equation. This study thus supplies a quantitative support to unvalidated literature results. It confirms that different discharge relationships are needed for different flow conditions and that differentiation in the applicability of the discharge relationships derived through CFD is needed: in the disturbed flow regime the relationships are applicable; in the undisturbed regime it depends on the thickness of the water layer above the weir crest.

2.4.3 Practical significance

The findings of this study form a basis to advance engineering practice in wastewater management. For existing CSO locations it presents an alternative for the weir discharge determinations listed in the introduction. Through CFD simulations, site specific discharge relationships can be applied for existing (or optimised) sensor locations. These could be used for monitoring and modelling purposes. For new CSO locations optimal sensor locations could be determined, accompanied by discharge relationships with known uncertainties in case of backwater effects.

2.5 Conclusions and recommendations

In this chapter the applicability of CFD simulations for deriving reliable discharge relationships for a weir where the weir chamber limits the discharged flow rate is investigated. For that purpose field measurements, lab experiments on a scale model, and simulations with multiple CFD models were available.

Based on the results described the following is concluded:

- Unverified CFD simulations:
 - Can describe the complex hydraulic behaviour occurring in the lab experiments, including a change in flow regime;
 - Can be applied to determine the optimal sensor location based on the local hydraulic conditions;
 - Can be used to derive reliable discharge relationships ($\sim 10\%$ accuracy) in the disturbed regime to be applied with regular water level measurements and accompanying uncertainties;

- Can be used to derive reliable discharge relationships (on average at least ~25% accuracy) in the undisturbed regime at prototype size, to be applied with regular water level measurements and accompanying uncertainties;
- Could not obtain reliable discharge relationships in the undisturbed flow regime at scale model size, characterised by very low water levels, with the applied grid and software;
- The standard weir equation for frontal weirs:
 - Describes the discharge in the undisturbed regime (scale model and prototype size) almost as good as the discharge relationships derived from the CFD simulations;
 - Is shown not to be applicable in the undisturbed regime as no description of the backwater effect is included;
- The results presented in this chapter supply a quantitative support to earlier publications on the applicability of CFD for the derivation of discharge relationships, that were based on unvalidated results.

Further research is recommended on i) the application of two different grids, specialized for low and high water levels (undisturbed and disturbed flow regime), ii) running the same models in different software programs for the undisturbed regime to get more insight on the softwares influence on the results, iii) the uncertainties associated with CFD modelling of low flow rates/water levels over weirs, and iv) the information needed to apply a similar methodology on weirs in weir chambers with multiple in- and outflows.

Finally, it is remarked that performing verified CFD simulations is always preferable to unverified CFD simulations. Use of additional knowledge (measurements or otherwise) on the system's physical behaviour will only benefit the predictive capabilities of the simulations.

Acknowledgements

The author would like to acknowledge the municipality of Eindhoven for their cooperation, the supplied measurements and for additional funding for manufacturing the scale model.

3 Design and performance evaluation of simplified sewer models

3.1 Introduction

Applying real time control (RTC) in urban wastewater management requires model simulations at several stages, from initiation to evaluation. Models support understanding of the functioning of a wastewater system, are applied in the design of the control algorithm and in case of model predictive control also for the implementation of the control itself, and they could be needed in a performance evaluation. Some of these applications require long term simulations and/or scenario analysis.

When control of the entire urban wastewater system is aimed for, integrated models are needed. For integrated models, sub models for sewer systems, wastewater treatment plants (WWTPs) and possibly the receiving waters are coupled into one model, making them extensive and complex. This influences two properties that are of main importance for RTC: the accuracy of the results and the required simulation time. Accurate results are needed to generate confidence in the effect of the proposed RTC strategy and to reach a significant effect when implemented. The simulation time increases with the model size, leading to long simulation times for integrated model simulations. For example, simulating the entire hydrodynamic sewer model for the sewer system of Eindhoven ($\sim 4,000$ *ha* connected area) for a period of 24 hours takes approximately 45 minutes on a regular laptop (4 cores of 2.8 *GHz* each).

This chapter is an adapted version of: Van Daal-Rombouts, P.M.M., Sun, S., Langeveld, J.G., Bertrand-Krajewski, J.-L., Clemens, F.H.L.R., (2016). Design and performance evaluation of a simplified dynamic model for combined sewer overflows in pumped sewer systems. *Journal of Hydrology*, 538:609-624. doi: <http://dx.doi.org/10.1016/j.jhydro1.2016.04.056>.

Combining the long simulation times required for integrated modelling and the need for long term simulations and scenario analysis for the application of RTC in urban wastewater management, the need for rapid simulation is evident.

To speed up simulations, simplified models, also commonly referred to as conceptual or surrogate models, are applied. Simplified models consist in many representations, see e.g. (Motiee et al., 1997; Vaes et al., 1999; Mannina and Viviani, 2010; Coutu et al., 2012; Wolfs and Willems, 2014), but all aim to compress the complexity of the real system in only a few characteristics and/or relationships. To ensure their representativeness, the simplified models are calibrated against field measurements. The model structure and parameter set that lead to the best overall fit with the measurements is accepted as the best simplified model. Attempts to find appropriate calibration algorithms are described in e.g. (Vrugt et al., 2009; Mair et al., 2012; Wolfs et al., 2013; Krebs et al., 2014).

Previous research, see e.g. (Vaes et al., 2001; Kleidorfer et al., 2009; Sun and Bertrand-Krajewski, 2012, 2013a; Dotto et al., 2014; Del Giudice et al., 2015), made clear that the model input can have a major impact on the simplified models performance. When constructing simplified models for real sewer systems, however, usually only a few measurements are available for model calibration. Sewer systems that are not specifically monitored for research purposes will likely have water level measurements at the discharges to the WWTP and surface water and flow measurements if sewage is pumped to the WWTP. No flow measurements are generally available at free flow discharges to the WWTP and at combined sewer overflow (CSO) locations. Simplified models are therefore, in the majority of cases, calibrated based on the available water level measurements. The best performing model is obtained by adjusting model parameters to reproduce the measurements based on criteria such as Nash-Sutcliffe or root mean squared errors (RMSE).

The outputs of a (simplified) sewer model applied in integrated modelling are the discharges to the other sub systems: the WWTP and surface water. Although the quality of the calibration is a measure for the capability of the simplified sewer model to reproduce observations, it does not necessarily imply a sufficiently accurate determination of the discharges. Therefore, in the research presented here, simplified sewer models are calibrated with the established DREAM algorithm (Vrugt et al., 2008, 2009), while the performance is evaluated on the correct determination of the occurrence of CSO events and the best estimation of the total volumes discharged to the surface water.

Three simplified models are used to represent the processes in the sewer systems: i) a rainfall runoff outflow (RRO) model, ii) a static reservoir model (SR) and iii) a dynamic reservoir model (DR). RRO models simulate the surface runoff generation process and the discharges at the outlet of small catchments equipped with sloped sewer systems. Among RRO models, (Sun and Bertrand-Krajewski, 2013b) have demonstrated the effectiveness of the standard linear reservoir model for such cases. However, the simple linear relation between the discharge and the storage in the fictitious reservoir of the model is likely not to be effective for looped sewer systems equipped with pumping stations and CSO structures. Other process descriptions are needed in order to characterize the flow behaviour in these more complicated systems. In this study, a standard RRO model is thus complemented with either the SR model or the more elaborate DR model to represent looped, pumped, sewer systems.

For the derivation of the SR models, geometrical information and pumping station settings are taken from a full hydrodynamic (FH) model, i.e. a 1D-model taking into account hydrodynamic processes in the sewer system. For the DR models additional key relationships between variables are obtained through FH model simulations. In the development of SR and DR models, simplicity was constantly balanced against physical representativeness. Simplicity, and by that reproducibility and applicability in practical RTC situations, was pursued.

A comparison of three simplified models is thus presented: i) a single RRO model, ii) a combination of RRO + SR models and iii) a combination of RRO + DR models for the simulation of CSO events and volumes. Additionally, the performance of the simplified and FH models are compared. This study has been conducted for two sewer catchments in the Netherlands: Loenen and Waalre. Both catchments consist of pumped, combined sewer systems, but differ in size, structure and average ground level slope.

This chapter is organised as follows. In section 3.2 the catchment areas, monitoring data and available FH models are introduced. Here also the simplified models are described in detail as well as the calibration procedure and the performance evaluation method. Results are described in section 3.3 for the calibration of the simplified models, the mutual performance evaluation of the calibrated simplified models and the performance of the calibrated simplified models compared to the uncalibrated FH model. The results are discussed in section 3.4, followed by conclusions and recommendations in section 3.5.

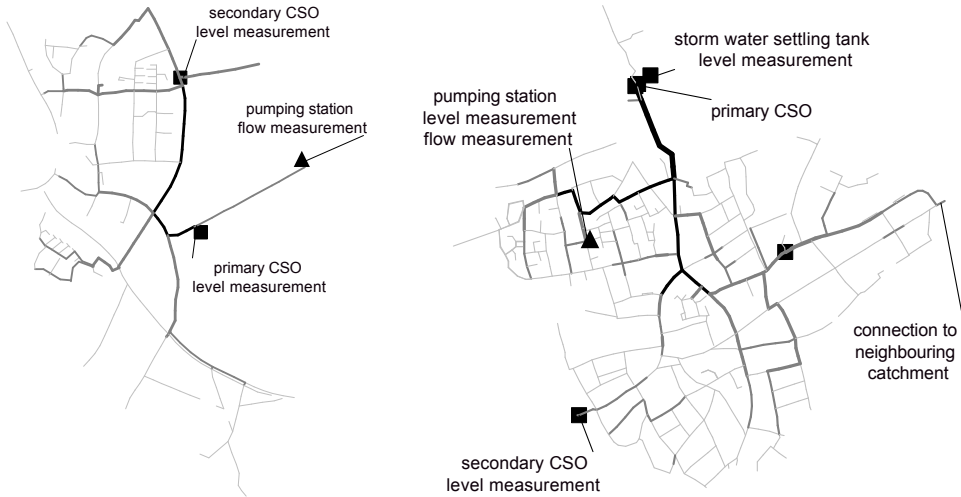


Figure 3.1: Sewer system layout for Loenen (left) and Waalre (right). Monitoring locations and locations of pumping stations and CSOs are indicated. Line colour and width indicate pipe diameter ranges: ≥ 1500 mm (thick black), ≥ 1000 (black), ≥ 600 (thick grey), ≥ 400 (grey) and < 400 mm (light grey).

3.2 Materials and method

3.2.1 Sewer catchments

Two combined sewer systems have been selected to test the simplified models: Loenen and Waalre. Loenen is located in the central east of the Netherlands in a mildly sloping area. This system has a partly looped and partly branched character. It is equipped with one pumping station and two CSOs. One CSO, referred to as primary, is located downstream in the sewer system and discharges much more and more often than the upstream, secondary, CSO. At the location of the pumping station an additional inflow from a small neighbouring sewer system is incorporated. Sewer system characteristics and layout can be found in table 3.1 and figure 3.1 (left).

Waalre is located in the wastewater system of Eindhoven, just south of the Eindhoven. The sewer system is looped with one pumping station, a primary CSO equipped with a settling tank and a secondary CSO that rarely discharges. Additionally, Waalre is connected by a gravity conduit to a neighbouring catchment in the east. Although water can flow both ways, it serves as a discharge for Waalre. Characteristics of the sewer systems are listed in table 3.1, while figure 3.1 (right) displays the sewer system layout.

Table 3.1: Sewer system characteristics for Loenen and Waalre.

property	unit	Loenen	Waalre
number of inhabitants	–	2,100	6,200
contributing area	<i>ha</i>	23.4	52.3
average slope ground level	%	0.91	0.14
static storage volume	$m^3 - mm$	947 - 4.0	2,704 - 5.2
WWF pumping capacity	m^3/h	209	400
number of CSO structures	–	2	2 (incl. 1 SST)
length of conduits	<i>km</i>	12.3	27.6

3.2.2 Monitoring data

For Loenen monitoring data is available at a one-minute interval from June 2001 to January 2002, collected as part of a dedicated research project. Flow measurements are available at the pumping station and an inflow into the pumping station from a neighbouring catchment. Level measurements are available in the pumping chamber and at the CSO locations, as displayed in figure 3.1 (left). Additionally, two rain gauges were installed in the catchment. Due to various reasons no continuous data set is available for the measuring period.

For Waalre monitoring data at the sewer system boundaries is available at a one-minute interval. Flow (Hach, Flo-Tote) is measured at the pumping station. Level measurements (Vega, Vegabar 66) are available in the pumping chamber, inside the settling tank and at the secondary CSO location. The measuring locations are indicated in figure 3.1 (right). Additional one-minute interval rain gauge measurements (Observator, OMC-210) are performed at several locations approximately 10 *km* around Waalre. All measurements are recorded permanently. Data validation was performed applying the algorithms described in (Van Bijnen and Korving, 2008).

Rain radar data with a five-minute interval and pixel size of 1x1 *km* are available from the Royal Netherlands Meteorological Institute. For Waalre the radar data is calibrated against the rain gauge measurements using a procedure based on conditional merging as described in (De Niet et al., 2013). The rain radar calibration was performed only during wet weather days and when the rain gauges functioned in the period of April 2011 to January 2012.

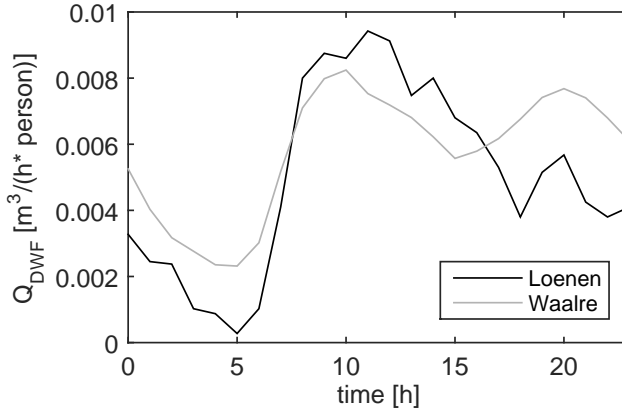


Figure 3.2: Daily DWF profiles per person for Loenen and Waalre.

3.2.2.1 Dry Weather Flow

Daily dry weather flow (DWF) profiles have been derived from the monitoring data for both catchments. For Waalre it was based on the pump flow measurements in 2011. The mean hourly pumped discharge at DWF days was used to represent a typical daily DWF profile. DWF days are defined as having received less than 0.05 mm of precipitation after exponential smoothing (80% accounted to the current day and 20% to the following day) to prevent false detection of DWF days due to the absence of rain gauges inside the catchment. Unrealistic measurements and periods with snowfall have been manually discarded. The DWF profile for Loenen was previously derived using a similar strategy (Langeveld, 2004). The resulting profiles can be found in figure 3.2.

3.2.3 Full hydrodynamic (FH) models

FH models for both sewer catchments are available in InfoWorks ICM (www.innovyze.com). The FH model for Loenen was previously calibrated (Langeveld, 2004), following the procedure described by (Clemens, 2001). The calibration involved a detailed check of the geometrical database and tuning of several parameters to match measured and modelled water levels at up to ten locations. As the calibration resulted in very close resemblance between the modelled and measured water levels (deviations <5 cm), it was concluded that the geometrical database was virtually without errors. The FH model for Waalre was validated following the procedure described in

(Langeveld et al., 2013). It involved the comparison of measured and modelled water levels as a function of time at the three monitoring locations. No parameter optimisation was performed. As mentioned in the report (Liefing, 2012) the measured and modelled water levels resembled one another in general and it was concluded that no large errors in the geometrical database existed. Nevertheless, occasional deviations in measured and modelled water levels of up to 50 *cm* occurred.

The FH models are applied in this study for three purposes: i) properties of the geometrical database and pumping station settings are utilized in the design of the SR and DR models, ii) key relationships between variables are obtained by means of FH model simulations and applied in the DR model, and iii) the performance of the simplified models is compared to the performance of the FH models. For all simulations with the FH models for any of the above purposes, a standard (uncalibrated) parameter set is employed as (Korving and Clemens, 2005) showed that the portability of event specific parameter sets for FH models is low. The main distinction between the calibrated FH model for Loenen and validated FH model for Waalre lies therefore in the trustworthiness of the underlying geometrical database.

The simulations performed with the FH model for the second purpose, application in the design of the DR model, are based on ten years (1955 to 1964) of 15-minute interval rainfall measurements in De Bilt, the Netherlands. This rainfall series is advised for long term rainfall simulations in the Netherlands (RIONED Foundation, 2004). The simulations were executed with a one-minute time step, recording for every time step the volume, water level and flows in all manholes, conduits, pump and CSO chambers, etc. The derivation of the required relationships is described in detail in section 3.2.4.3.

3.2.4 Model structures

The general structure of the three simplified models is shown in figure 3.3. Model M1 includes only a RRO model. Model M2 combines a RRO model and a SR model, while model M3 combines a RRO model and a DR model. Rainfall, DWF and optional additional flows are model inputs, while flows to the surface water (Q_{SW}) and to the WWTP (Q_{WWTP}) are model outputs. In the following sections, all models are explained in more detail.

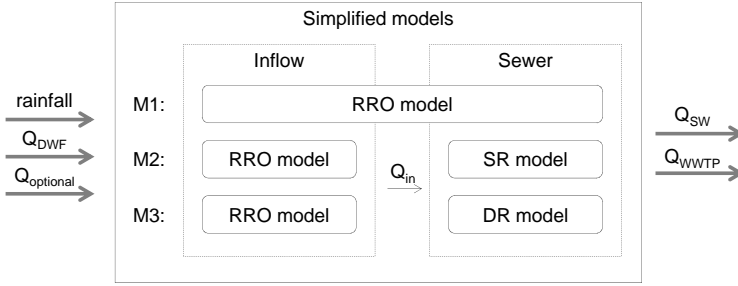


Figure 3.3: The three simplified models M1 to M3 convert the three inputs to two discharges to the surface water (Q_{SW}) and the WWTP (Q_{WWTP}). RRO: rainfall runoff outflow, SR: static reservoir, DR: dynamic reservoir.

3.2.4.1 Rainfall runoff outflow (RRO) model

The standard linear reservoir model is a typical RRO model, see e.g. (Sun and Bertrand-Krajewski, 2013b). It comprises of a rainfall loss model followed by a linear reservoir. The rainfall loss model consists of initial (I_{ini} [mm]) and proportional (P_{cons} [-]) rainfall losses, i.e. depression losses and ratio of contributing and total area. The resulting net rainfall (I_{net} [mm]) occurs with a time lag (T_{lag} [min]) and feeds the linear reservoir with a reservoir constant (K [min]). The outflow of the standard linear reservoir (Q_{out}) is derived from the inputs using:

$$Q_{out}(t) = \exp\left(-\frac{\Delta t}{K}\right) Q_{out}(t - \Delta t) + \left[1 - \exp\left(-\frac{\Delta t}{K}\right)\right] I_{net}(t - T_{lag})A, \quad (3.1)$$

with t the time [min] and A the contributing area [ha]. For more details on the standard linear reservoir model the reader is referred to (Sun and Bertrand-Krajewski, 2013b).

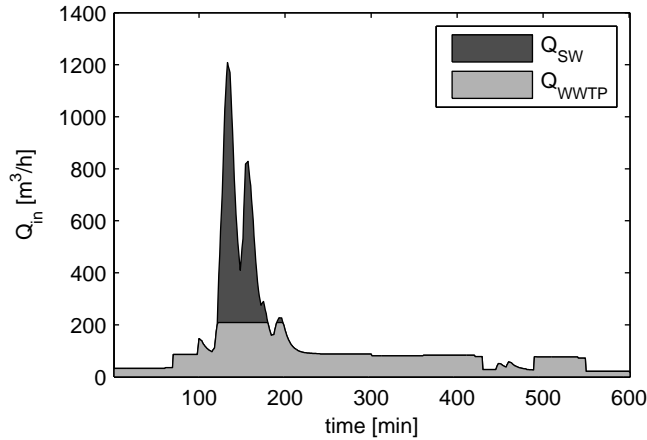


Figure 3.4: The output of the RRO model is split into Q_{SW} and Q_{WWTP} based on the maximum pumping capacity of the catchment ($209 \text{ m}^3/\text{h}$ for Loenen).

To determine the total inflow into the sewer models (Q_{in} in figure 3.3) for models M2 and M3, Q_{DWF} and $Q_{optional}$ are simply added to Q_{out} . For model M1, Q_{out} together with Q_{DWF} and $Q_{optional}$ represent both the surface runoff and the subsequent flow routing within the sewer system. It is split in the two sewer discharges Q_{SW} and Q_{WWTP} on the assumption that as much water is pumped to the WWTP as possible, i.e. all discharges up to the maximum pumping capacity are accounted to Q_{WWTP} as illustrated in figure 3.4 for Loenen. For Waalre, Q_{WWTP} is determined using the same method. From the remainder, the discharge through the connection to the neighbouring catchment (determined from FH model simulations as it is not monitored) is subtracted before accounting it to Q_{SW} .

3.2.4.2 Static reservoir (SR) model

SR Loenen

The SR model aims to represent processes within the sewer system that the basic RRO model cannot explicitly simulate. FH model properties of the geometrical database and pumping station settings are applied in its design. A schematic representation of the SR model for Loenen is shown in figure 3.5. It consists of a single basin for the sewer system which is filled by Q_{in} as described in the previous section. It empties through a pump resulting in Q_{WWTP} , and a single CSO resulting in Q_{SW} .

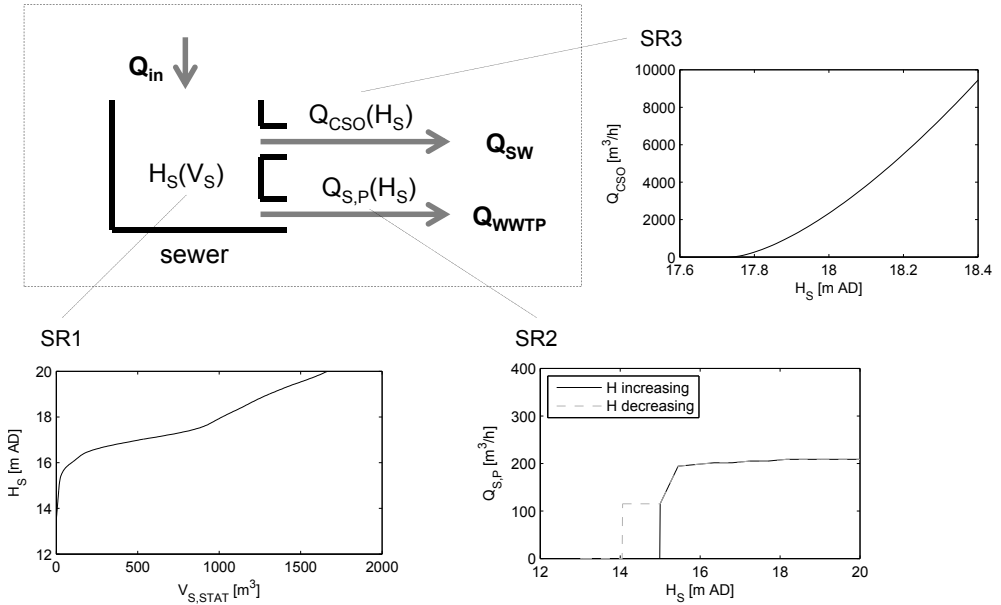


Figure 3.5: Schematic representation of the SR model for Loenen. Applied characteristics or relationships as displayed in graphs SR1 to SR3 are elaborated upon in the main text.

Several characteristics or relationships are applied in the SR model, numbered SR1 to SR3 in figure 3.5. Their representation and derivation were performed as follows:

- SR1** Static storage-level curve. The static storage-level curve is used to convert the sewer volume (V_S) into the water level in the sewer (H_S). It is derived from the geometrical database of the FH model as the cumulative volume of all manholes, conduits, etc. of the sewer system under each possible water level;
- SR2** Discharge through pump. The discharge through the pump ($Q_{S,P}$) is calculated through H_S and the pump characteristic. The pump characteristic is taken from the FH model. The DWF and maximum capacity are 115 and 209 m^3/h respectively. The switch on and off level are 15.00 and 14.05 m above Normal Amsterdam Water Level ($m AD$), respectively;

SR3 Discharge through CSO. The discharge through the CSO (Q_{CSO}) is taken to be only caused by the primary CSO. The discharge is calculated through H_S and the standard weir equations for frontal weirs:

$$Q_{free} = a_1 h^{a_2} \quad (3.2)$$

for free outflow, with flow Q_{free} [m^3/s], h [m] water level above the weir crest, a_1 [$m^{1.5}/s$] taken to be 1.36 times the weir length in meters and a_2 [-] taken to be 1.5. Or

$$Q_{sub} = a_3 h_{DS} \sqrt{2g(h_{US} - h_{DS})} \quad (3.3)$$

for submerged outflow, with flow Q_{sub} [m^3/s], h_{US} and h_{DS} [m] the upstream and downstream water level above the weir crest, a_3 [m] taken to be 0.8 times the weir length [m] and g the standard acceleration due to gravity $9.81 m/s^2$. Submerged outflow is assumed to occur when $2/3 h_{US} < h_{DS}$. For Loenen only free outflow is assumed.

SR Waalre

A schematic representation of the SR model for Waalre is depicted in figure 3.6. It consists of a basin for the sewer system and a basin for the settling tank. The sewer basin is filled by Q_{in} and has three discharges: one through the pump resulting in Q_{WWTP} , one through the connection with the neighbouring catchment and one through a single CSO to the settling tank. The discharge through the CSO fills the settling tank that is emptied either through a pump back into the sewer basin, or through a CSO to the surface water resulting in Q_{SW} .

Again several characteristics or relationships have been applied in the model, numbered SR4 to SR10 in figure 3.6. Their representation and derivation were performed as follows:

SR4 Static storage-level curve sewer. See SR1 with the sewer storage excluding the storage of the settling tank;

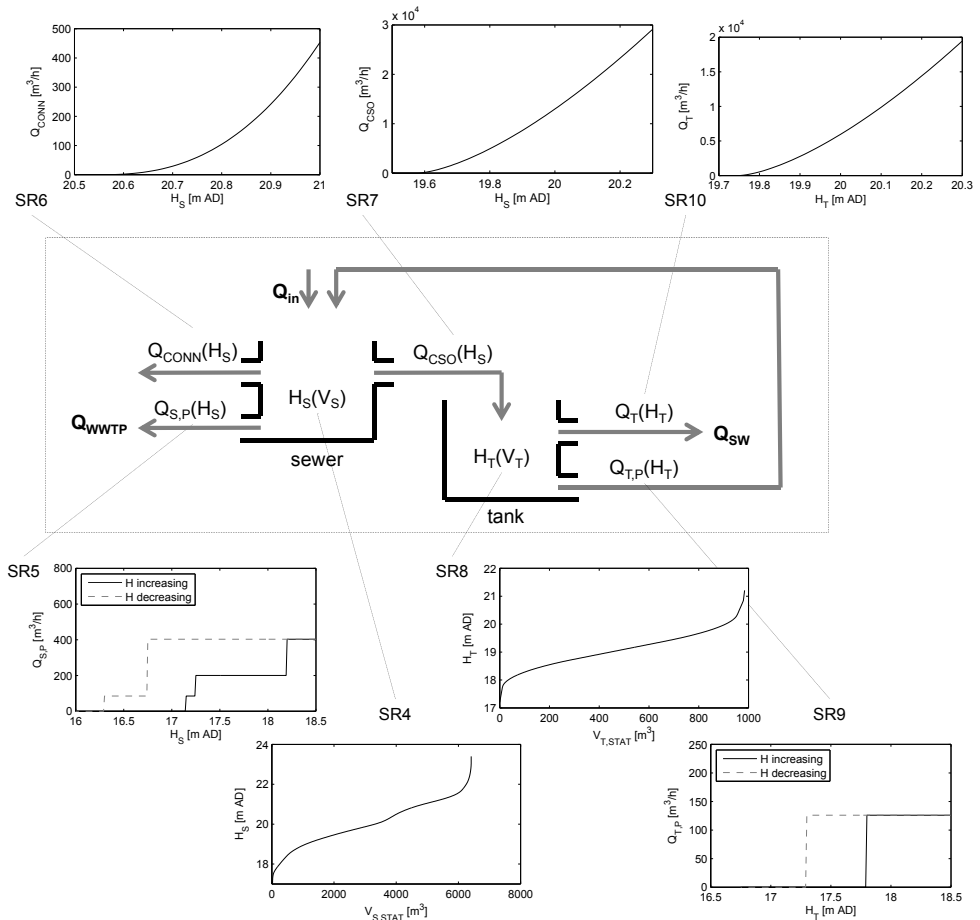


Figure 3.6: Schematic representation of the SR model for Waalre. Applied characteristics or relationships as displayed in graphs SR4 to SR10 are elaborated upon in the main text.

- SR5** Discharge sewer through pump. The discharge through the pump ($Q_{S,P}$) is calculated through the water level in the sewer (H_S) and the pump characteristic. The pump characteristic is derived from analysis of the water level and flow measurements at the pumping station, and (Van Daal-Rombouts, 2012). The DWF and maximum capacity are 85 and 400 m^3/h respectively. The switch on level is 17.15 $m AD$, the switch off level 16.30 $m AD$;
- SR6** Discharge sewer through connection. From simulations with the FH model it was found that water only flows from Waalre to the neighbouring catchment. The discharge through the connection (Q_{CONN}) is calculated through H_S and the standard equation for a free outflow over a V-notch weir,

$$Q = a_4 \tan\left(\frac{\theta}{2}\right) h^{(5/2)} \quad (3.4)$$

to mimic the connecting sewers egg shape. Here Q is the flow [m^3/s], a_4 a constant [$m^{1/2}/s$] taken to be 1.4, θ the notch angle taken to be 67 degree, and h [m] the water level over the weir crest. Free outflow is assumed at all times and the bottom of the notch is taken to be the highest invert of the connecting conduit;

- SR7** Discharge sewer through CSO. The discharge through the CSO (Q_{CSO}) is taken to be caused only by the primary CSO and is calculated through H_S and equations 3.2 and 3.3. Both free and submerged outflow are allowed (only free outflow is displayed);
- SR8** Static storage-level curve settling tank. The static storage-level curve is used to convert the settling tank volume (V_T) into the water level in the tank (H_T). It is derived from the FH model, similar to SR1;
- SR9** Discharge settling tank through pump. The discharge of the settling tank through the pump ($Q_{T,P}$) is based on H_T and the pump characteristic. The pump characteristic was taken from the FH model, where the pumping capacity was adjusted to match the monitoring data;
- SR10** Discharge settling tank. The discharge of the settling tank (Q_T) is calculated through H_T and equation 3.2.

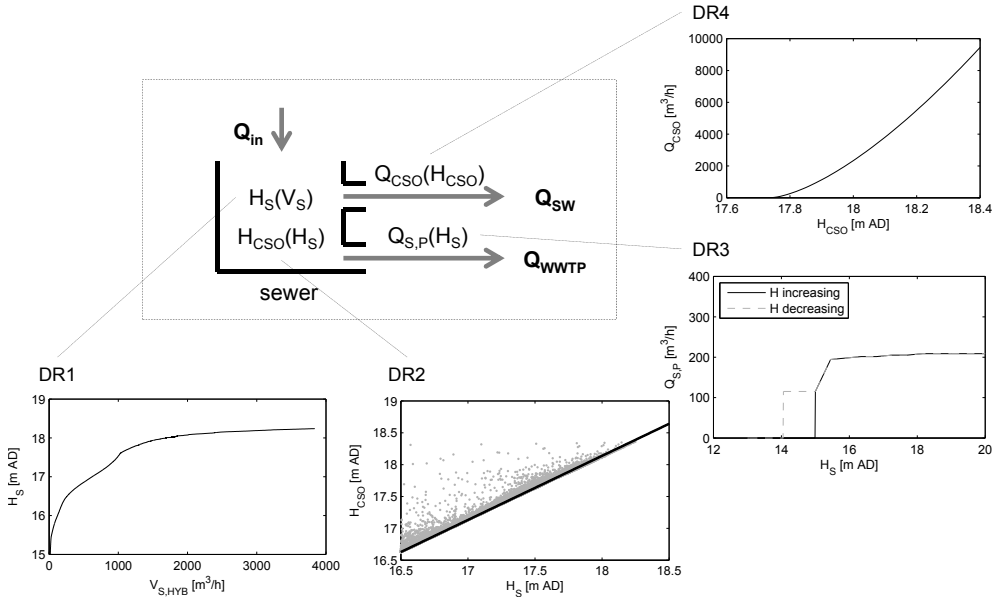


Figure 3.7: Schematic representation of the DR model for Loenen. Applied characteristics or relationships as displayed in graphs DR1 to DR4 are elaborated upon in the main text.

3.2.4.3 Dynamic reservoir (DR) model

DR Loenen

The DR models for the sewer systems are similar to the SR models, but contain additional relationships derived from FH model simulations to better account for the dynamic behaviour of a sewer system. A schematic representation of the DR model for Loenen is shown in figure 3.7 and can be compared to the SR model in figure 3.5. Differences are expressed in the storage-level curve applied (SR1 vs. DR1) and the water level applied in the CSO discharge (DR2 vs. no equivalent in the SR model).

The characteristics or relationships applied in the DR model are numbered DR1 to DR4 in figure 3.7. Their representation and derivation are explained below:

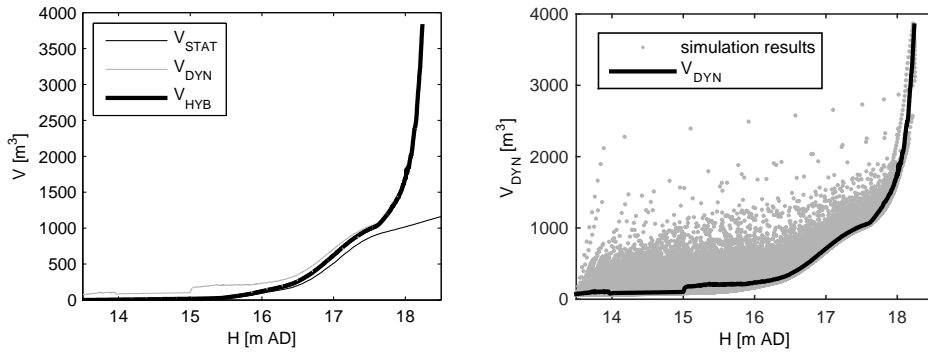


Figure 3.8: Hybrid storage-level curve (left) and derivation of the dynamic storage-level curve from the FH model simulation results (right) for Loenen.

DR1 Hybrid storage-level curve. A so called hybrid storage-level curve is used to convert the sewer volume (V_S) into the water level in the sewer (H_S). The hybrid curve follows the static storage-level curve (see SR1) for low water levels to correctly model DWF circumstances and pumping behaviour, and gradually turns to the dynamic storage-level curve for high water levels (with possibly pressurised flow conditions) to take the dynamic properties of the sewer system under wet weather flow (WWF) conditions and CSO discharges into account. Figure 3.8 (left) displays the static, dynamic, and hybrid storage curves for Loenen.

The dynamic storage-level curve was derived from simulations performed with the FH model as described in section 3.2.3. The resulting water volumes in the entire sewer system (every minute for ten years) were grouped in one-cm intervals of the corresponding water level at the pumping station. The grouped volumes were averaged and smoothed to obtain the dynamic storage-level curve, as displayed in figure 3.8 (right). Note that the dynamic storage-level curve converges towards the static storage-level curve for DWF conditions or low rain intensities as the water level in the sewer system levels off;

DR2 Level at CSO. H_S is converted into the water level at the primary CSO location (H_{CSO}). The relationship is based on FH model simulations, where a linear relation is fitted through the simulated water levels at the pumping station and the CSO location. Only elevated water levels (WWF conditions) are taken into account;

DR3 Discharge through pump. See SR2;

DR4 Discharge through CSO. See SR3, only now H_{CSO} is applied instead of H_S .

DR Waalre

A schematic representation of the DR model for Waalre is shown in figure 3.9 and can be compared to the SR model in figure 3.6. Differences are expressed in the storage-level curve applied (DR5 vs. SR4), the water level applied in the CSO discharge (DR6 vs. no equivalent in the SR model) and the water level applied in and the calculation of the flow through the connection (DR7 vs. no equivalent in SR model, DR9 vs. SR6).

The characteristics or relationships applied in the DR model for Waalre are numbered DR5 to DR13 in figure 3.9. Their representation and derivation are explained as follows:

DR5 Hybrid storage-level curve sewer. A hybrid storage-level curve is used to convert V_S into H_S . The derivation follows DR1. The resulting curves for Waalre are displayed in figure 3.10: the static, dynamic, and hybrid storage curves to the left, and the derivation of the dynamic storage-level curve from the FH model simulation results to the right;

DR6 Level at CSO. Similar to DR2, a relationship has been derived between H_{CSO} and H_S . As Waalre is equipped with the settling tank, two linear segments that connect at the highest weir crest level of the settling tank have been applied. Only elevated water levels (WWF conditions) are taken into account;

DR7 Level at connection. Similar to H_{CSO} in DR6, a relationship between the water level at the connection to the neighbouring catchment (H_{CONN}) and H_S is derived from the FH model simulations. A linear relation has been fitted, taking only elevated water levels (WWF conditions) into account;

DR8 Discharge sewer through pump. See SR5;

DR9 Discharge sewer through connection. The discharge of the sewer through the connection to the neighbouring catchment (Q_{CONN}) is based on H_{CONN} and a relationship derived from the FH model simulations. The simulated water levels at the connection and the corresponding flow through the connection were fitted with a third order polynomial equation. To prevent unrealistic (negative) output a maximum value is set for H_{CONN} ;

DR10 Discharge sewer through CSO. See SR7, where H_{CSO} is applied in the calculation of the discharge from the sewer;

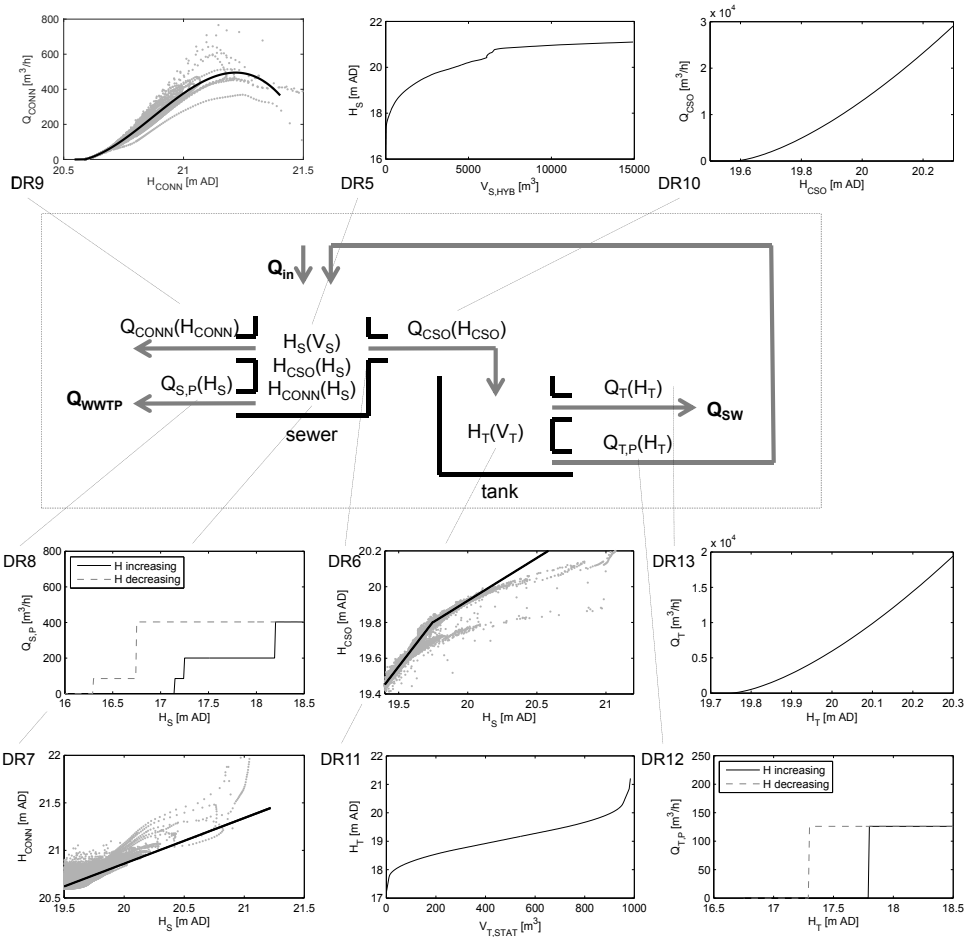


Figure 3.9: Schematic representation of the DR model for Waalre. Applied characteristics or relationships as displayed in graphs DR5 to DR13 are elaborated upon in the main text.

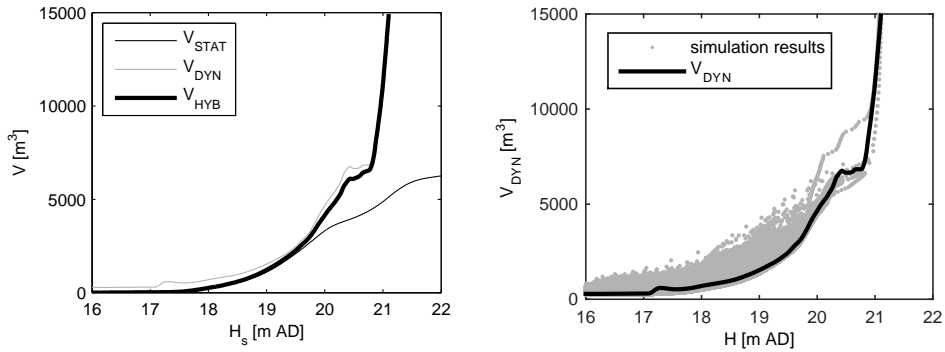


Figure 3.10: Hybrid storage-level curve (left) and derivation of the dynamic storage-level curve from the FH model simulation results (right) for Waalre.

DR11 Static storage-level curve settling tank. See SR8;

DR12 Discharge settling tank through pump. See SR9;

DR13 Discharge settling tank. See SR10.

3.2.5 Calibration procedure

3.2.5.1 DREAM algorithm

Calibration, which adjusts model parameters by minimizing the difference between model outputs and measurements, is an important step before applying simplified models. The research on calibration methods in the area of rainfall-runoff modelling is comprehensive, leading to the application of automatic calibration methods instead of traditional manual calibration mainly based on trial and error approaches. In this study an automatic calibration method (the differential evolution adaptive metropolis (DREAM) method (Vrugt et al., 2008, 2009)) was applied for the calibration of the RRO models.

Table 3.2: Calibration parameters with search range.

parameter	abbreviation	unit	search range
initial rainfall loss	I_{ini}	<i>mm</i>	0 - 4
proportional rainfall loss	P_{cons}	–	0 - 1
lag time	T_{lag}	<i>min</i>	0 - 120
reservoir constant	K	<i>min</i>	0 - 240

The DREAM method is based on the Bayesian theorem, which considers model parameters as probabilistic variables revealing the probabilistic belief on the parameters according to observed model outputs. In the DREAM method the probability distribution function of parameters is derived using an iterative approximation method (the Markov chain Monte Carlo (MCMC) method) coupled with multiple chains in parallel in order to provide a robust exploration of the search space. In addition to an optimal model parameter set, the DREAM method also results in an evaluation of model parameter uncertainty, which provides important information on model reliability. The effectiveness of the DREAM method in water related model calibration has been demonstrated in many previous studies, e.g. (Keating et al., 2010; Leonhardt et al., 2014).

3.2.5.2 Parameter optimisation

The DREAM method is applied to calibrate the parameters of the RRO model to find the minimal difference between the simplified model output and the measurements. Table 3.2 shows the parameters, units and the search range for the calibration procedure. The search range was based on physically plausible boundaries for the parameters.

The algorithm minimises the sum of squared errors (SSE) between the model output and measurements. Water level measurements are applied in the calibration as they are the actual monitoring data available, containing all information on the sewer systems behaviour. For Loenen the water level measurement at the primary CSO location is used to calibrate M2 and M3. For Waalre the water level measurements at the pumping station and inside the settling tank are applied, by minimising the sum of the SSEs for each model output-measurement combination. Only periods with elevated water levels are considered in the calibration, as the RRO model parameters are connected to rainfall only. Since water levels do not have significance in M1, its

calibration is based on the total outflow from the sewer system, i.e. the sum of the measured pump flow and the calculated outflow at the CSO locations (determined with the measured water levels and equation 3.2) for Loenen and Waalre. For Waalre the outflow through the connection with the neighbouring catchment is added. As this flow is not monitored, it is based on FH model simulations for the respective rain events.

The information on which the models are calibrated is similar, especially for the elevated water levels relevant for CSO discharges. M2 and M3 are calibrated on measured water levels at the CSO locations. The discharge to the surface water in M2 and M3 is calculated using the modelled water level and equation 3.2. The same equation with the measured water levels is applied to determine the outflow for the calibration of M1. Additionally, the pumped outflow supplies information during low intensity rainfall, as contained in the level measurements at the pumping station (in case of Waalre) or the primary CSO location (for Loenen) when it is not yet discharging.

The calibration is performed using 10,000 iterations in the DREAM method, as it was found from test runs that the cumulative density functions of the parameters do not change (within the parameter stability) after several thousand iterations. The last 5,000 iterations are used for further analysis: the optimal parameter set and model output are derived, and the model is run with all 5,000 parameter sets to determine the 95% confidence intervals for the water levels and discharges.

3.2.5.3 Events

For each catchment six rain events are available for the parameter optimisation, i.e. they led to a significant rise in water level in the sewer system, with or without discharge to the surface water, no external influences were known and monitoring data was available and judged reliable after data validation. The selected events and their characteristics are summarised in table 3.3.

(Korving and Clemens, 2005) showed that the portability of event specific parameter sets for FH models is low. (Sun and Bertrand-Krajewski, 2012) investigated the impact of calibration data selection on the model performance of regression models. Given the limited data set, full consideration of this aspect is beyond the scope of this paper. It is clear, however, that comparison of the model structures on single event calibration is insufficient. Therefore three scenarios have been explored:

Table 3.3: Selected rain events with key characteristics.

catchment area	event [<i>dd – mm – yyyy</i>]	rainfall depth [<i>mm</i>]	max rain intensity [<i>mm/h</i>]	duration [<i>hh : mm</i>]	discharge to surface water [<i>y/n</i>]
Loenen	30 June 2001	9.9	24.8	06:12	y
	18 July 2001	13.9	25.4	14:36	y
	19 July 2001	12.2	34.0	12:15	n
	23 July 2001	12.3	19.4	07:48	y
	27 August 2001	17.0	24.0	07:45	y
	23 August 2001	7.4	6.0	07:39	n
Waalre	29 April 2011	6.5	5.2	06:20	n
	14 August 2011	27.0	23.4	10:35	y
	18 August 2011	12.0	14.9	07:20	n
	22 August 2011	39.2	68.8	23:04	y
	14 December 2011	15.4	11.9	23:31	y
	16 December 2011	33.4	8.5	22:15	y

1. Calibration of single rain events;
2. Calibration on all events together;
3. Calibration on any set of 3 events and verification with the remaining 3 events.

3.2.6 Performance evaluation

The performance of the calibrated simplified model structures should be evaluated on the capability to correctly represent the sewer systems functioning at the system boundaries. As argued in the introduction this is not obtained by comparing the best fits between the measured and modelled water levels but by comparing the discharges from the system, i.e. to the WWTP and the surface water. As the RRO models are calibrated, i.e. all calibration parameters are related to rainfall, the focus of the performance evaluation will be on the CSO discharges to the surface water. As the discharge to the WWTP is also relevant for integrated studies it will be reported for completeness.

Common sense dictates that the impact of CSO events depends foremost on the occurrence of such events, with the absolute discharged flows of secondary consequence. This is supported by literature stating that impact based RTC can influence the systems performance for small and moderate events, contrary to large events on which it has no influence (Langeveld et al., 2013), and that up to a certain point overflow frequency is a good indicator of receiving water impact (Lau et al., 2002). Therefore the first evaluation criterion for the simplified sewer models is the correct determination of CSO event occurrences. The second evaluation criterion is the correct determination of the total discharged volume.

Based on the monitored water levels at the CSO locations in the sewer systems and settling tank, for each event and catchment the discharge to the surface water (Q_{SW}) is calculated through application of equation 3.2. Additionally the total discharge to the WWTP (Q_{WWTP}) is calculated from the pump flow measurements. For each model structure and scenario, the modelled total discharged volumes (V_{SW} and V_{WWTP}) are determined as the integral of the model outputs Q_{SW} and Q_{WWTP} .

CSO event occurrences are analysed through false positives (FP) and false negatives (FN). A FP is defined as a CSO event occurrence ($V_{SW} > 0$) in the model output but not in the measurements, a FN as a CSO event occurrence in the measurements but not in the model output. For the comparison of discharged volumes, differences in V_{SW} (and V_{WWTP}) between the model output and the measurements are calculated and listed for each event and scenario. Cumulative results for each scenario are determined by taking the root mean squared errors (RMSE) over all events.

For comparison purposes the selected rain events have also been simulated using the FH models. The comparison between simplified models with calibrated inflow parameters and FH models with uncalibrated inflow parameters is relevant since the FH models simulate the sewer systems behaviour in greatest detail and hence are deemed to be most accurate (Meirlaen et al., 2001; Ferreri et al., 2010; Rubinato et al., 2013). This might hold true for calibrated FH models but not for the much more commonly applied uncalibrated models, as proper calibration of FH models is very time consuming and requires a very large monitoring data set.

Finally, the simulation time of the simplified model structures and the FH model will be compared.

3.3 Results

3.3.1 Calibration

As described in the previous section the performance of the simplified model structures will be evaluated based upon the correct determination of CSO occurrences and the total discharge to the surface water. The calibration results, however, provide useful insight into the models functioning. Therefore, a typical calibration result for each catchment will be presented. Nash-Sutcliffe efficiency indexes (NS) (Nash and Sutcliffe, 1970) are supplied for easy comparison of the calibration results. Optimal parameter sets will be given for all events and scenarios.

The results for the individual calibration of rain events 27 August 2001 (Loenen) and 14 August 2011 (Waalre) for all model structures are displayed in figures 3.11 and 3.12 respectively. From top to bottom the applied rainfall is shown, followed by the model results for M1 (based on the total sewer outflow Q_{OUT}), and M2 and M3 (based on the water level in the sewer system H_S and H_{CSO}). For Waalre additional water level measurements in the settling tank were applied (H_T), the results of which have been added to the bottom of figure 3.12. For each model structure the optimal results are displayed together with their 95% confidence bands.

Figures 3.11 and 3.12 show that M2 and M3 are in general well able to describe the sewer systems behaviour: the measurements applied in the calibration are closely followed during the filling of the basins, once they are full and during emptying, resulting in NS values >0.95 for Loenen and >0.75 for Waalre. Small differences occur between these models especially during filling and in the response to temporal changes in the rainfall. M1 can not describe the sewer systems behaviour in detail as it has only the reservoir constant K to account for surface storage and in-sewer storage. The response to rainfall is therefore more smoothed, which is best demonstrated in figure 3.11. NS values <0.4 are found.

For both catchments and all model structures the 95% confidence bands are mostly $<1\%$. Logically, the influence of the (inflow) calibration parameters on water levels in sewer systems is most apparent at the onset of a rain event or during temporal changes, resulting in confidence bands up to 10% for M2 and M3, while they stay $<1\%$ for M1.

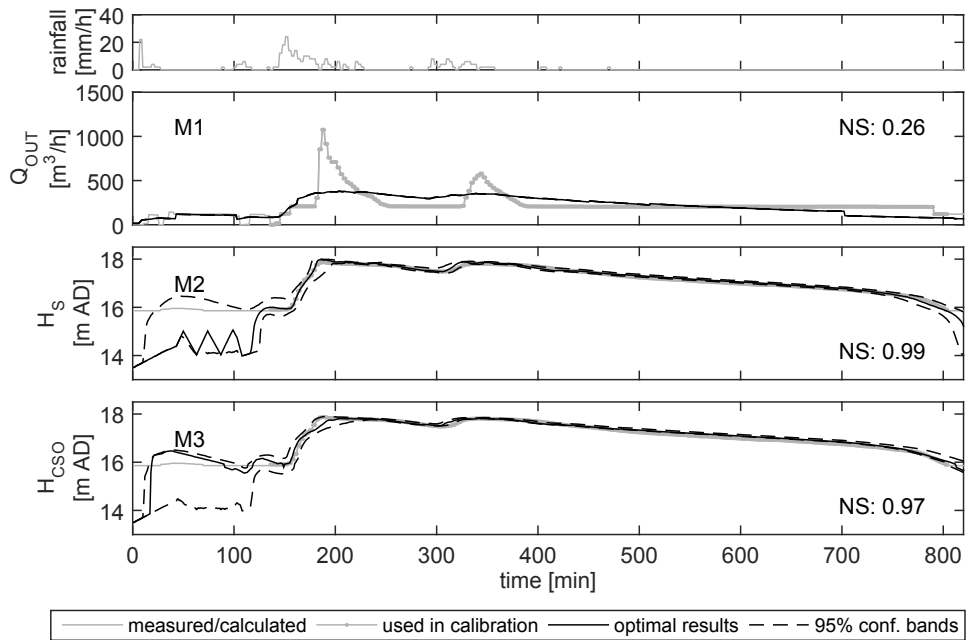


Figure 3.11: Results for the individual calibration of rain event 27 August 2001 for all model structures for Loenen.

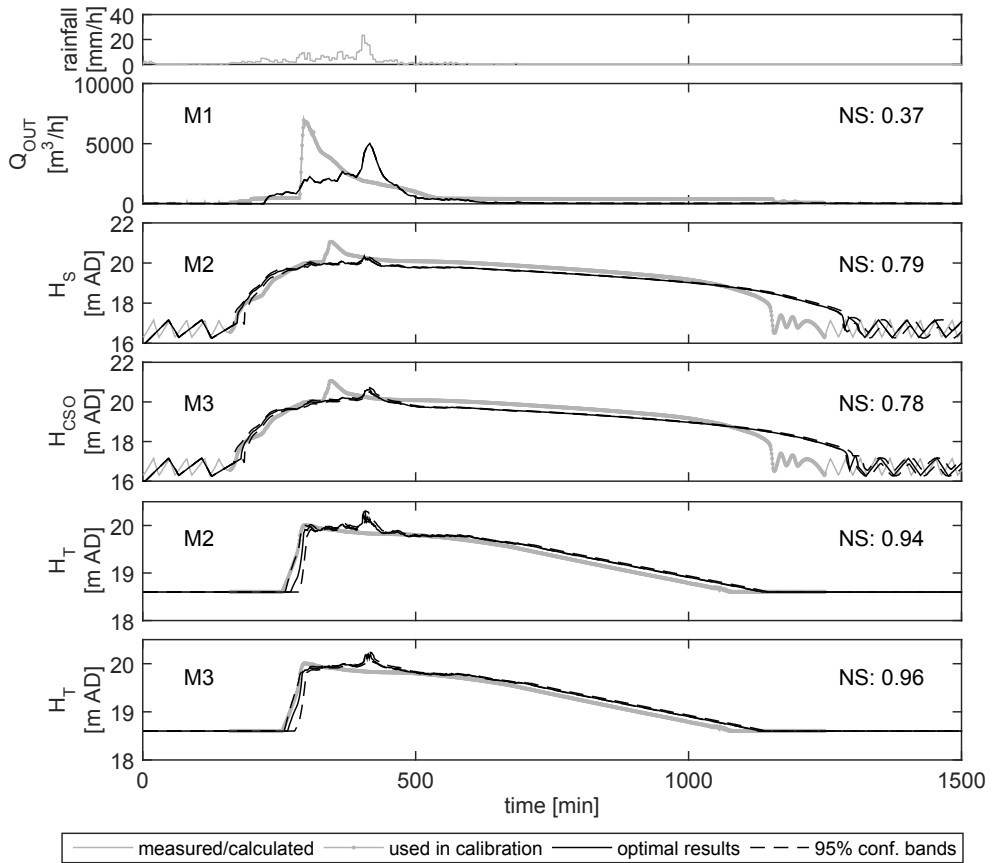


Figure 3.12: Results for the individual calibration of rain event 14 August 2011 for all model structures for Waalre.

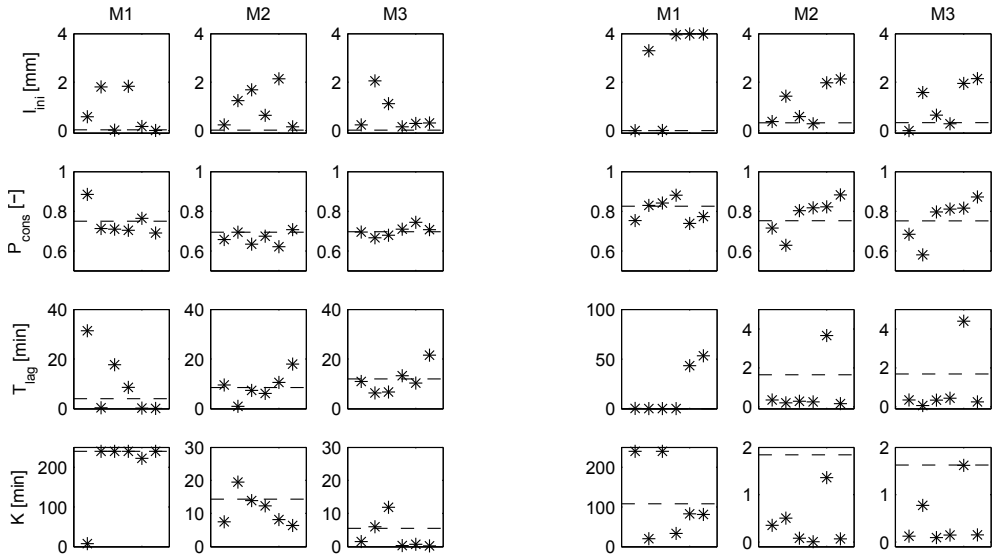


Figure 3.13: Optimal parameter values for scenarios 1 (individual calibrated events (asterisks)) and scenario 2 (all events together (line)) for Loenen (left) and Waalre (right). The horizontal axis presents event numbers. Scales for T_{lag} and K may vary.

For all scenarios (see section 3.2.5.3) for Loenen, NS values for M2 and M3 are > 0.90 . For M1, values differ strongly from -8.52 to 0.44. For Waalre for M2 and M3 in scenario 1, NS values range between 0.61 and 0.96, with one event around zero. In scenario 2 the values drop to 0.5 to 0.6. The NS values for M1 again differ strongly between events and scenarios from -9.42 to 0.82.

Figure 3.13 shows the optimal parameter values for Loenen (left) and Waalre (right) for all model structures. In asterisks the results for scenario 1 (calibration on single rain events) are given, the line indicates the parameter values for scenario 2 (all events together). Results for all twenty possible combinations of three calibration events in scenario 3 can be found in figure 3.14. The optimal parameter values reflect the results for the water levels and NS values: the parameters for M2 and M3 show much resemblance within a catchment, while M1 deviates. Especially the difference in K stands out, as the RRO model in M1 has to account for surface and in-sewer storage, while in M2 and M3 only for the surface storage. The optimal parameter values between scenarios 2 (line in figure 3.13) and 3 (figure 3.14) are consistent, indicating that the exact split in a calibration and verification set does not have a major impact on the outcome.

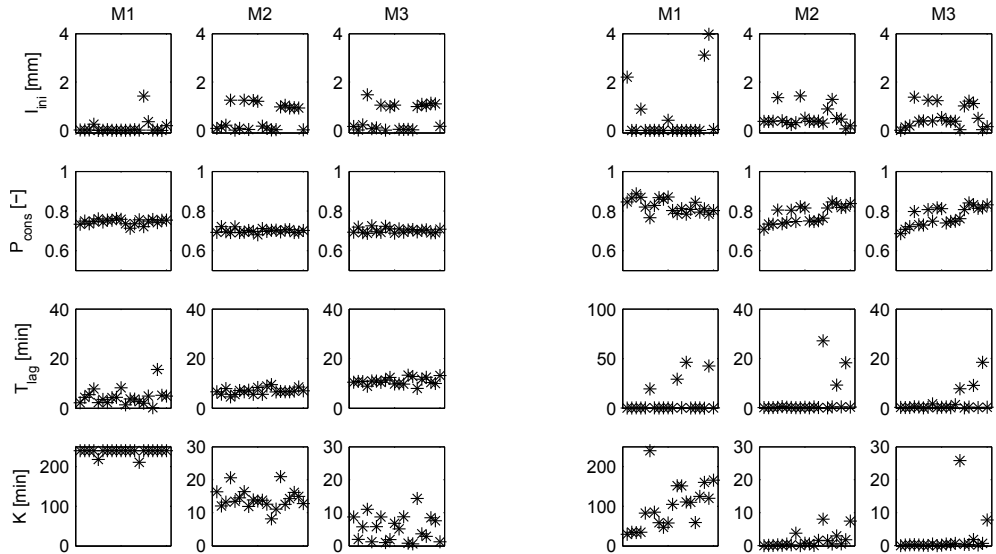


Figure 3.14: Optimal parameter values for scenario 3 for Loenen (left) and Waalre (right). The horizontal axis presents the 20 possible combinations to take 3 events from 6. Scales for T_{lag} and K may vary.

3.3.2 Performance evaluation

3.3.2.1 Model discharge

As the calibration of the simplified models is performed on rainfall related parameters, the focus of the performance evaluation will be on the discharge to the surface water (Q_{SW}) while the discharge to the WWTP (Q_{WWTP}) is included for completeness.

The optimal Q_{SW} and Q_{WWTP} for all model structures for the calibration of the single events of 27 August 2001 (Loenen) and 14 August 2011 (Waalre) are displayed in figures 3.15 and 3.16 as well as the discharges determined from the measurements. The difference between M1 and M2/M3 observed in the calibration results are also clear from these figures: Q_{SW} for M1 tends to be more smoothed because of the higher value for K .

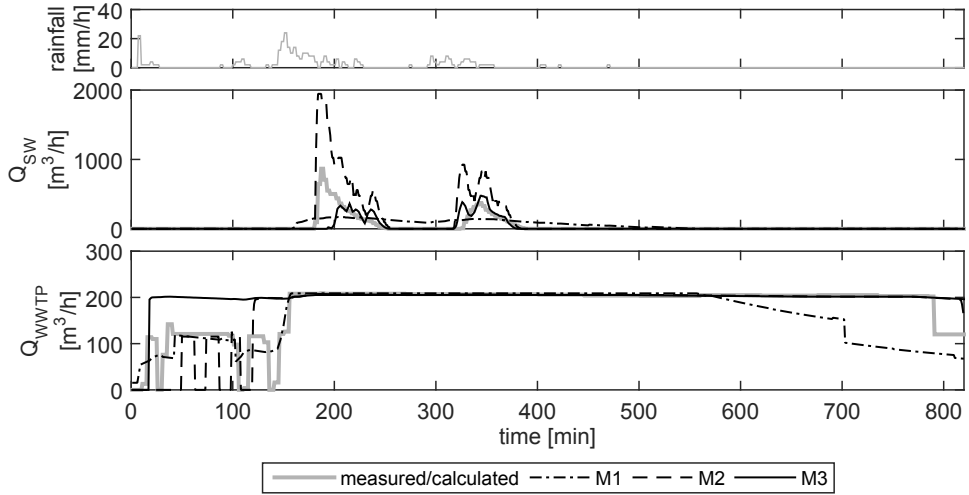


Figure 3.15: Optimal Q_{SW} and Q_{WWTP} for the individually calibrated event of 27 August 2001 for Loenen.

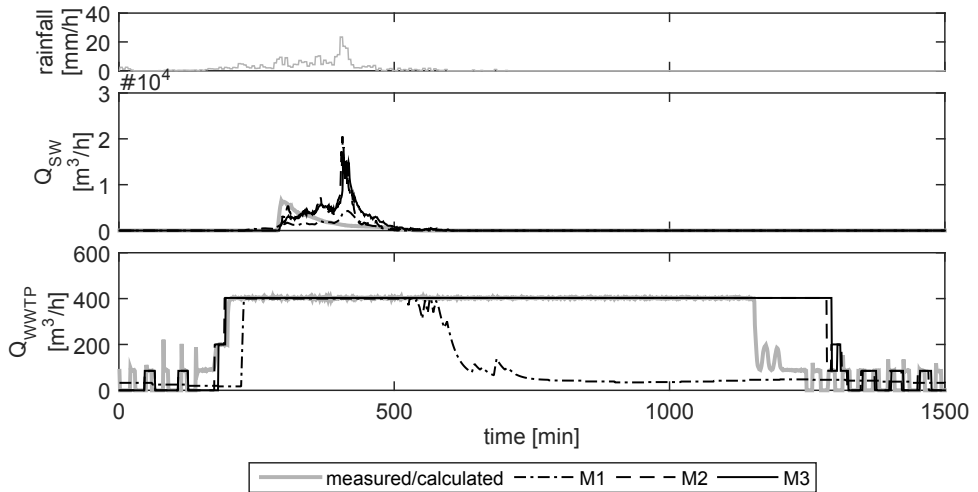


Figure 3.16: Optimal Q_{SW} and Q_{WWTP} for the individually calibrated event of 14 August 2011 for Waalre.

3.3.2.2 Determination of CSO events

FPs and FNs for all events for each model structure and scenario, based on the optimal parameter sets, are given in table 3.4. For scenarios 1 and 2 the total number is reported, for scenario 3 the results have been averaged over all combinations and multiplied by two for easy comparison. Additionally, results for the FH model have been added.

Based on the FPs and FNs in table 3.4, M1 can be immediately discarded for these catchments. For each scenario and catchment two FPs are recorded, the exact number of rain events that did not lead to a CSO event. This is easily explained since a rain event leading to a significant rise in water level in a pumped sewer system will likely contain rain intensities higher than the pumping capacity of the sewer system reserved for WWF (design guideline in the Netherlands: 0.7 mm/h). In M1 all rainfall in excess of this capacity has to be discharged to the surface water, leading to a CSO event. The calibration algorithm unsuccessfully tries to overcome this inadequacy in the model structure by delaying the rainfall (high T_{lag}) and smoothing the response (high K), as can be found from the optimal parameter values in figure 3.13.

For M2 and M3 the results are less conclusive. Single FPs or FNs occur depending on the catchment and scenario applied. The floating point values for scenario 3 for Waalre (due to averaging over all possible combinations) and the optimal parameter values in figure 3.13 further indicate that the inflow parameters are calibrated differently depending on the selection of calibration/verification events. Only for M3 for Loenen no FPs or FNs occur in any scenario signalling that M3, combining the RRO and DR models, is likely the best performing model for Loenen.

3.3.2.3 Determination of discharged volumes

The total volumes discharged to the surface water (V_{SW}) for each model structure and scenarios 1 and 2 are displayed in figure 3.17 for Loenen and 3.18 for Waalre. V_{SW} is the integrated model output Q_{SW} , for which the optimal values and 95% confidence bands are determined as described in section 3.2.5.2. The calculation of the 95% confidence intervals for the measurements is based on a deviation from the discharge determined by the standard weir equation, equation 3.2, of 25%. This percentage is estimated on previous work by (Van Daal-Rombouts et al., 2014) on scale models and (Fach et al., 2009) on computational fluid dynamics. Both studies

indicate deviations between the actual (measured or calculated) CSO discharge and the discharge determined with the standard weir equation of up to 50%. They also indicate that this strongly depends on the water level above the weir crest leading to under and over estimations of the flow. Therefore an intermediate value was selected. For the FH model a deviation of 50% was applied as it is feasible to calibrate FH models up to 5 *cm* difference in water levels combined with equation 3.2.

The cumulative results for V_{SW} and V_{WWTP} , given in table 3.5, were determined by taking the RMSE of the results from the optimal parameter sets over all events. The RMSEs for scenario 3 have been averaged over all possible combinations. RMSEs for the FH model were added as well.

The results for V_{SW} in figures 3.17 and 3.18 and table 3.5 support the preliminary conclusion that M3 outperforms M2 for Loenen. For all scenarios the RMSE and the uncertainty bands for M3 are smaller than for M2. Despite the inability of M1 to correctly determine CSO event occurrences, it outperforms M2 based on V_{WS} . For Waalre the performance of M2 and M3 are similar, corresponding to the determination of the CSO events. Nevertheless, M2 consistently performs better than M3. Similar to Loenen, M1 generally performs well based on V_{SW} . The difference in the performance of M2 and M3 between the catchments is also reflected in the optimal parameter values (figure 3.13). The parameter values for Waalre are close resulting in similar RMSE values in table 3.5, while for Loenen there is more variety between the model structures especially for I_{ini} and K .

For V_{WWTP} the RMSE values in table 3.5 show that model M1 consistently performs worse than M2 and M3 for all scenarios and both catchments. M2 and M3 generally perform on a similar level, which is to be expected as the pumping regime in the SR and DR model structures is the same.

3.3.2.4 Uncalibrated FH models

Finally the performance of the FH models is compared to the performance of the calibrated simplified models. The comparison is made for scenario 2, calibration for all events together, since there a single parameter set is derived for each model structure, similar to the single standard parameter set for the FH model.

Based on the determination of CSO event occurrences (table 3.4) the FH model performs at a similar level as M2 and M3. For Loenen one FP is noted for the FH model, while none for M2 and M3. For Waalre it is reversed.

Table 3.4: FPs and FNs for all 6 events for each model structure and scenario based on the optimal parameter sets. The results for scenario 3 have been averaged over all combinations and multiplied by two for easy comparison.

scenario	1: individual events		2: all events together		3: 3 events calibration, 3 events verification			
	total FP	total FN	total FP	total FN	mean FP	mean FN	mean FP	mean FN
catchment/ model structure								
Loenen								
M1	2	0	2	0	2	0	2	0
M2	1	0	0	0	1	0	1	0
M3	0	0	0	0	0	0	0	0
FH			1	0				
Waalre								
M1	2	0	2	0	2	0	1.9	0
M2	0	1	1	0	0.4	0.2	0.6	0.1
M3	0	1	1	0	0.4	0.2	0.6	0.1
FH			0	0				

Table 3.5: RMSE for V_{SW} and V_{WWTP} for all 6 events for each model structure and scenario (1: individual events, 2: all events together, 3: calibrate and verify on 3 events each) based on the optimal parameters sets.

catchment/ model structure	RMSE [m^3]							
	V_{SW}				V_{WWTP}			
	1	2	3	3	1	2	3	3
			cali- bration	verifi- cation			cali- bration	verifi- cation
Loenen								
M1	112	150	147	178	445	242	248	255
M2	416	197	346	364	67	150	135	158
M3	57	145	94	125	124	143	133	132
FH		661				399		
Waalre								
M1	3,470	2,469	2,448	2,157	3,072	2,075	2,307	2,240
M2	5,202	967	2,593	2,212	422	1,331	995	1,330
M3	5,398	1,480	2,788	2,487	556	1,346	1,027	1,354
FH		2,658				619		

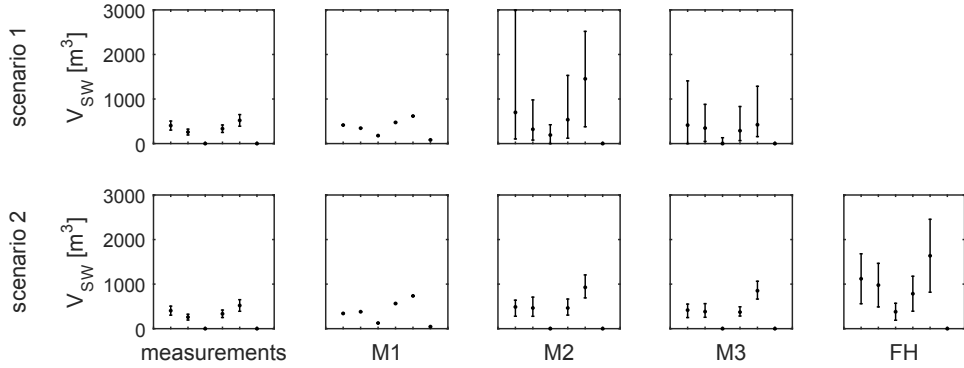


Figure 3.17: V_{SW} with 95% confidence bands for all events and each model structure for Loenen. For scenarios 1 (individual events, top) and 2 (all events together, bottom). The horizontal axis presents event numbers.

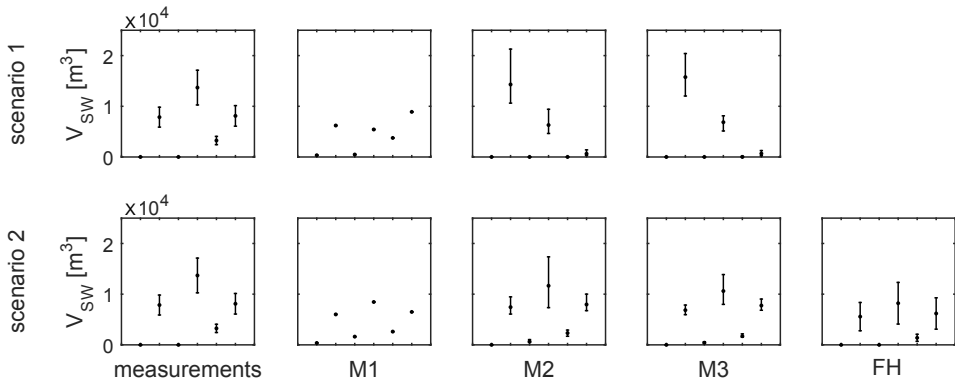


Figure 3.18: V_{SW} with 95% confidence bands for all events and each model structure for Waalre. For scenarios 1 (individual events, top) and 2 (all events together, bottom). The horizontal axis presents event numbers.

Taking the RMSE for V_{SW} (table 3.5) into account, the FH model is easily outperformed by both M2 and M3, while V_{WWTP} is worse for Loenen and better for Waalre.

The simulation time for the FH models takes 1,000 to 5,000 times longer than for M2/M3 or 250,000 to 475,000 times longer than for M1.

From the perspective of both the simulation time and accuracy of results it is concluded that it is better to apply simplified calibrated models in optimisation or RTC studies than uncalibrated FH models.

3.4 Discussion

The difference in performance of M2 and M3 for Loenen and Waalre can be explained by the information available for the simplified model design and calibration as described in sections 3.2.2 and 3.2.3. All information is better known or of higher quality for Loenen: i) the monitoring data for Loenen was gathered for research purposes, while the monitoring campaign for Waalre received less dedicated attention, ii) for Loenen two rain gauges were installed in the catchment itself, while for Waalre no local rain gauges were available, and iii) the geometrical database underlying the FH model for Loenen is better known than for Waalre. The results for the RMSE of V_{SW} indicate that the more detailed model M3, i.e. the RRO model for the runoff combined with the DR model for the sewer system, is favoured when high quality information is available (in this case Loenen), while the less detailed model M2, RRO with SR, suffices when the information is of lower quality (Waalre).

One main source of uncertainty for Waalre likely stems from the calibrated rain radar input. The rainfall in general seems reasonable with NS values in the event calibration of M2 or M3 >0.6 . In detail the rainfall seems off in intensities and/or timing, an example of which can be found in figure 3.16. Judging from the rainfall, the models responses in Q_{SW} are in accordance (main peak in the outflow after main peak in the rainfall). However, in the measurements the main peak in the outflow occurs right at the beginning of the rain event. The other events display a similar mismatch between the rainfall and the outflow. This may also explain the very low values for the parameters T_{lag} and K , see figure 3.13, as the calibration procedure tries to correct the mismatch in the input data.

The NS values reported in section 3.3.1 are based on the calibration parameters for each time step, and the FP/FN in table 3.4 and RMSE in table 3.5 are based on V_{SW} , which is integrated over time. Each presents information on the performance of the model structure. NS indicates the quality of the description of the sewer systems behaviour in general, while the others are specific for CSO discharges. The difference between the best performing model structures based on these criteria, especially for Loenen, is striking. Model M2 and M3 have similar NS values > 0.9 , but M3 is much more accurate based on FP/FN and RMSE. Simplified sewer models are calibrated on measurements, generally only water levels, but used to determine CSO discharges. These results show that care should be taken in choosing performance indicators suitable to the purpose of the model, likely leading to multiple indicators.

3.5 Conclusions and recommendations

This chapter dealt with the design and performance evaluation of a so called dynamic simplified sewer model for the accurate and rapid calculation of sewer system discharges for RTC applications. The dynamic simplified sewer model (M3) consists of a calibrated rainfall runoff outflow (RRO) model and a dynamic reservoir (DR) model for the sewer behaviour. It contains characteristics derived from full hydrodynamic (FH) model simulations to account for the dynamic properties of the sewer system behaviour.

The performance of M3 was tested for two combined, pumped catchments and compared against two other simplified models, M2 (calibrated RRO model with a static reservoir (SR) model) and M1 (calibrated RRO model only), and uncalibrated FH models. The performance was not solely based on the goodness of fit of the calibration but primarily on the correct determination of CSO event occurrences, and secondly on the correct determination of the total discharged volumes to the surface water.

From this research the following conclusions are drawn:

- Model M1 simulates $>100,000$ times faster than the FH model; models M2/M3 are $>1,000$ times faster than the FH model;
- M1 is unsuitable to correctly determine CSO occurrences for pumped catchments. The model structure is unable to retain rain intensities higher than the pumping capacity reserved for WWF, resulting in too many CSO discharges;

- M2 and M3 are able to describe the behaviour of pumped sewer systems;
- In case of detailed and trustworthy information available for the design and calibration of the model (Loenen), M3 easily outperforms M2 based on CSO activity. If the available information is of lower quality (Waalre), M2 consistently performs slightly better indicating that the derivation of the more detailed DR model is not worthwhile;
- M2 and M3 outperform the verified by uncalibrated FH models based on the total discharge to the surface water. In RTC studies the application of suitable calibrated simplified models is therefore preferred over uncalibrated FH models;
- Performance indicators for the selection of the most appropriate model structure should be selected carefully in relation to the modelling objectives, likely leading to multiple indicators, each one providing a specific approach of the models' performances;
- For rainfall driven modelling, trustworthy and local rainfall measurements remain necessary despite the availability of rain radar data to either apply as direct model input or the correction of radar data;

Future research is recommended in the area of statistical substantiation of the results as the available data sets were too limited to allow a statistical analysis of the results themselves. Additionally, the use of continuous data sets instead of the current intermittent ones would be advised to include more information on the conditions prior to events.

Considering the performance of the investigated simplified models for the relatively small sewer catchments Loenen and Waalre, the conversion and performance of the model concept for large sewer catchments, consisting of several sub catchments and multiple important CSO locations, would be a second point of interest for further research.

Acknowledgements

The author would like to acknowledge Innovyze (www.innovyze.com) for kindly supplying a research licence for the use of the software program InfoWorks ICM. Also the author would like to thank the Van Gogh Programme for supplying a Travel Grant to cover travel expenses for the cooperation between TU Delft and INSA Lyon.

4 Empirical influent water quality model

4.1 Introduction

For the development and assessment of integrated real time control (RTC) in urban wastewater systems, integrated models are needed to describe the functioning of the system as a whole and determine the impact of control strategies. For this purpose sub models for sewer systems and wastewater treatment plants (WWTPs) are coupled into one integrated model, possibly supplemented with receiving water models. Difficulties arise as sewer models generally contain only hydraulic parameters, while WWTP models require additional input on water quality parameters for the influent.

In a comprehensive review, (Martin and Vanrolleghem, 2014) discussed the available approaches for generating influent data. The approaches range from i) data driven methods based on creating databases with monitoring and experimental data and derive models using the data, ii) very simple models based on harmonic functions and iii) phenomenological models.

The data driven methods comprise two different approaches. The first method uses pollutant release patterns derived from literature to generate dynamic influent data aggregating the punctual emissions from the database (De Keyser et al., 2010). The second method interpolates available influent data at e.g. a daily timescale to e.g. hourly dynamics (Devisscher et al., 2006).

This chapter is an adapted version of: Langeveld, J.G., Van Daal-Rombouts, P.M.M., Schilperoort, R.P.S., Flameling, T., Nopens, I., Weijers, S.R., (2017). Empirical sewer water quality model for generating influent data for WWTP modelling. *Water*, 9(7):491. doi: <http://dx.doi.org/10.3390/w9070491>.

The simple models based on harmonic functions are very suited for the analyses of dry weather flow (DWF) situations, but less so for wet weather flow (WWF) situations (Martin and Vanrolleghem, 2014).

The phenomenological models are the most detailed influent models, that can give a phenomenological representation of dynamics of WWTP influent, including diurnal patterns, weekend, seasonal and holiday variations as well as rain events (Gernaey et al., 2011; Flores-Alsina et al., 2014; Martin and Vanrolleghem, 2014). Despite being labelled as ‘promising’ (Martin and Vanrolleghem, 2014), today’s phenomenological models, cannot adequately reproduce the dynamics in WWTP influent during wet weather due to a relatively poor representation of the build-up and wash off of urban pollutants. This is also true for the most recently published influent generator by (Talebizadeh et al., 2016), who use a mix of statistical and conceptual modeling techniques for synthetic generation of influent time series.

The limitations associated with the use of influent generators are not surprising given the state of the art knowledge on the physical-chemical, biological and transport processes occurring in sewer systems (Bertrand-Krajewski et al., 1993, 1998; Ashley et al., 1999, 2004; Bertrand-Krajewski, 2007). Especially sediment transport is not very well understood and not very successfully reproduced in deterministic sewer models. This is partly due to the fact that it is currently not possible to get enough data on the initial sewer sediment conditions throughout an entire sewer network. It is interesting to note that the developers of influent generators, showing many similarities with simplified or parsimonious sewer models (Willems, 2006, 2010), are facing the same issues as sewer modelers in the past, i.e. how to incorporate the contribution of in-sewer stocks during storm events to the outflow of sewers via either combined sewer overflow (CSO) or WWTP influent.

In order to overcome the limitations of deterministic sewer models, regression models have been proposed, which are validated against monitoring data. A recent successful example of this approach is given by (Dembélé et al., 2011), who developed an empirical model for storm water total suspended solids event mean concentrations with rainfall depth and antecedent dry weather period as input variables. These empirical relations, that are valid at a CSO or storm sewer outfall, however, are not suitable for

the prediction of WWTP influent quality, as these models do not predict the influent quality during DWF. For WWTP influent modelling, the empirical model described by (Rousseau et al., 2001), relates the influent concentration to the daily flows. A weak point of this approach is the impossibility to account for the dynamics during storm events. This is a major drawback, as storm events typically do not last a full day.

Recent applications of water quality sensors have resulted in the availability of long time series of WWTP influent quantity and quality (Gruber et al., 2004; Schilperoort, 2011). These time series contain a lot of information on the response of the influent quality to storm events and the contribution of in-sewer stocks to WWTP influent (Schilperoort et al., 2012).

In this chapter, time series analysis is used to understand the dynamics of WWF related variations in WWTP influent quality and to relate the variation in influent quality to influent hydraulics. This allowed the development of an empirical model based on understanding of the underlying physical processes.

The chapter is organised as follows. In section 4.2, first the system and available data set of WWTP Eindhoven are described and second the model development and calibration method are presented. The calibration results and the transferability of the concept are discussed in section 4.3, which is concluded with some foreseen applications of the model. Conclusions and recommendations are presented in section 4.4.

4.2 Materials and method

4.2.1 System description: the wastewater system of Eindhoven

The Dommel river is relatively small and sensitive to loadings from CSOs and WWTP effluent. The river flows through the city of Eindhoven (the Netherlands) from the Belgian border (south) into the river Meuse (north). The Dommel receives discharges from the 750,000 population equivalent WWTP of Eindhoven and from over 200 CSOs in ten municipalities. In summer time, the base flow in the river just downstream the WWTP comprises 50% of WWTP effluent, increasing to 90% during small storm events. The Dommel does not yet meet the requirements of the European Union Water Framework Directive (WFD, 2000). The water quality issues to be addressed

are dissolved oxygen depletion, ammonia peaks and seasonal average nutrient concentration levels (Weijers et al., 2012; Benedetti et al., 2013). Earlier research, within the KALLISTO project (Langeveld et al., 2013), has demonstrated that the WWTP effluent is the main source for the toxic ammonia peaks in the Dommel river and that the ammonium peaks in the WWTP effluent can be significantly reduced by applying integrated real time control (RTC): activating in-sewer storage volume to reduce and delay the hydraulic peak loading of the WWTP during storm events was shown to be effective. (Van Daal-Rombouts et al., 2016a) introduced a new RTC concept: the smart buffer, which minimizes the peak load to the biology at WWTP Eindhoven by applying the aforementioned RTC combined with using only one of three primary clarifiers during dry weather and using the other two only during storm events.

The ten municipalities contributing to the WWTP influent are divided over three catchment areas that are very different in size and character, each having a separate inflow to the WWTP, see figures 4.1 and 4.2. Wastewater from the municipality of Eindhoven accounts for approximately 45% (in practice ranging between 14,000 and 17,000 m^3/h) of the hydraulic capacity and is discharged directly to the WWTP. The other nine (much smaller) municipalities are each connected to one of the two wastewater transport sewers, one to the north (Nuenen-Son, 7 *km* in length) and one to the south (Riool Zuid, 31 *km* in length), accounting for respectively <10% (3,000 m^3/h) and 45% (in practice ranging from 14,000 to 15,000 m^3/h) of the hydraulic capacity. An elaborate description of the studied wastewater system can be found in (Schilperoot, 2011).

4.2.2 Monitoring network and data validation

At each of the three inflows into the WWTP (locations ‘A’ in figure 4.2) on-line spectroscopy sensors (s::scan, UV-VIS) have been installed that measure equivalent concentration values of wastewater quality parameters, more specifically total suspended solids, chemical oxygen demand (COD) and filtered COD (dissolved fraction), at a two-minute interval. Ammonium (NH_4 , Hach, Amtax) has been recorded at an interval of five minutes in the Eindhoven Stad and Riool Zuid influent. In addition, flow (Siemens Danfoss, Sitrans FM Magflow) and water levels (Vega, Vegawell) have been registered every minute at these locations. In this study, only monitoring data from the year 2012 has been used.

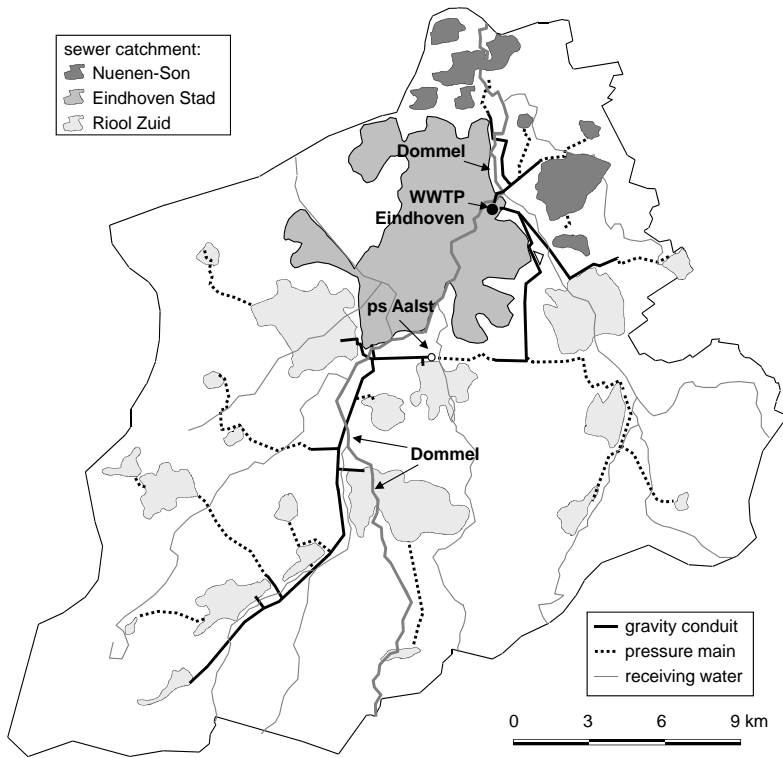


Figure 4.1: Wastewater system of Eindhoven and its receiving streams.

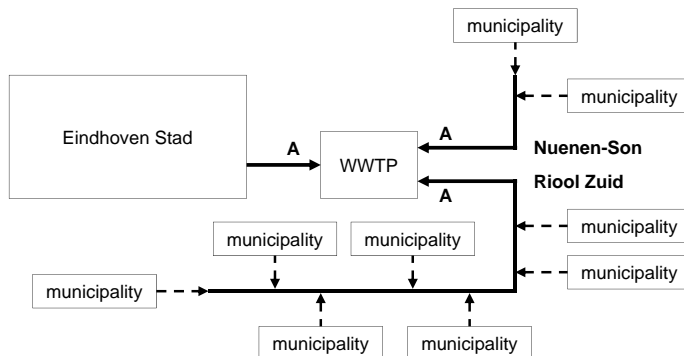


Figure 4.2: Schematic lay out of wastewater system Eindhoven. WWTP influent locations are marked 'A'.

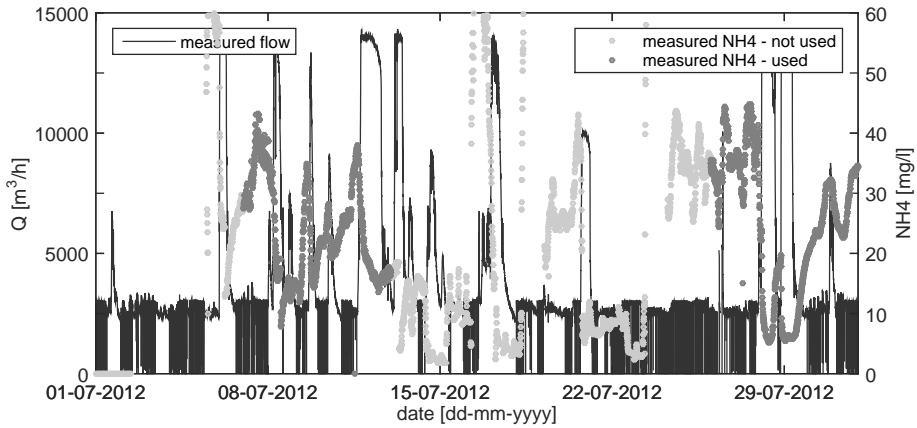


Figure 4.3: Example of the quality evaluation of the monitoring data.

The monitoring data have been validated manually, focusing on obtaining reliable data for calibration of WWF processes. Figure 4.3 shows an example of the data and their evaluation. In this figure, and all other figures in this chapter, the data used for calibration is represented by the dark grey bullets, data not used for calibration with light grey bullets.

After validation, only 38.5% of the data was considered to have an acceptable quality during the conditions required. This percentage of data perceived ‘good enough’ after validation may seem relatively low. During earlier research projects (2007 to 2008) at WWTP Eindhoven on UV-VIS sensors, the percentage of ‘good enough’ data after data validation ranged between 50 and 75%, despite very intensive maintenance and surveillance (Schilperoort, 2011) and without restrictions on the influent conditions. WWTP influent has shown to be a very difficult medium for water quality monitoring.

The data set after validation comprises at least 30 storm events with good data for each calibration performed. In the model calibration, these events, including the antecedent dry day and several following dry days, have been used.

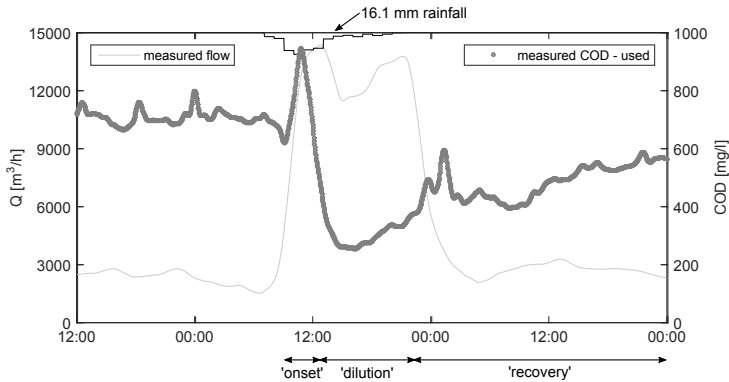


Figure 4.4: WWF dynamics during the stages of a storm event on 12 June 2008 in the influent for Eindhoven Stad.

4.2.3 Data analysis

In earlier work (Schilperoort et al., 2012), a part of this data set has been used to study the dynamics of wastewater composition. This resulted in well described typical diurnal patterns during DWF and typical dynamics during WWF (figure 4.4). For WWF, it has been observed that the concentration levels of the wastewater show a typical pattern during a storm event: a short period called ‘onset’ of the storm event, with an increased concentration level for particulate matter but not for dissolved matter, a longer period called ‘dilution’, where dilution of both dissolved and particulate matter takes place, and ‘recovery’, a period where dissolved and particulate matter gradually return to DWF levels.

4.2.4 Model development

The general idea of the model development is that the measured hydraulic influent data, i.e. flow and water level in the influent pumping station, can be used to make a distinction between the four patterns: DWF, onset of WWF, dilution during WWF and recovery after WWF. Each of these patterns is denoted as a system state, during which a certain relation between flow and concentration level applies. This allows to incorporate the contribution of in-sewer stocks on top of the mixing process between wastewater and storm water. The latter is a common feature of influent models applied to simulate both dry and wet periods, while explicitly accounting for the contribution of in-sewer stocks circumvents the relatively limited knowledge on associated in-sewer processes.

The average dry weather diurnal pattern is the core of the model. As long as the system state is ‘DWF’, the average dry weather diurnal pattern based on monitoring data is used, together with the measured flow data. The average dry weather diurnal pattern has been derived from flow monitoring data by averaging the monitoring data of ten dry days over five-minute intervals with the same time stamp.

During wet weather, the model superimposes a number of processes on the DWF pattern for water quality to mimic onset, dilution and recovery. The type of parameter (NH₄ or COD) and the type of event (small, medium or large) determine which of these processes is to be applied. The type of event is used as characteristic of a storm event, as it was found that the relation between flow and concentration levels differs very much between small, medium and large storm events. The measured hydraulics, in this case the flow and water level in the influent pumping station, are used to determine which of the described processes should be activated in the model, using the scheme in figure 4.5.

As indicated in figure 4.5, two conditions have to be met to change from DWF to WWF. The first is that the upper limit for dry weather conditions (Q_{DWF} , set at the 95-percentile of the flow values collected during dry weather at a specific time stamp) has to be exceeded, the second that the event volume should exceed a certain threshold (V_{Th} set at 5.000 m^3) or the event maximum flow should exceed a certain threshold (Q_{Th1} set at $4.000\text{ m}^3/h$). The second condition is added to exclude apparent events in the data caused by interference of the pump operation due to for example maintenance.

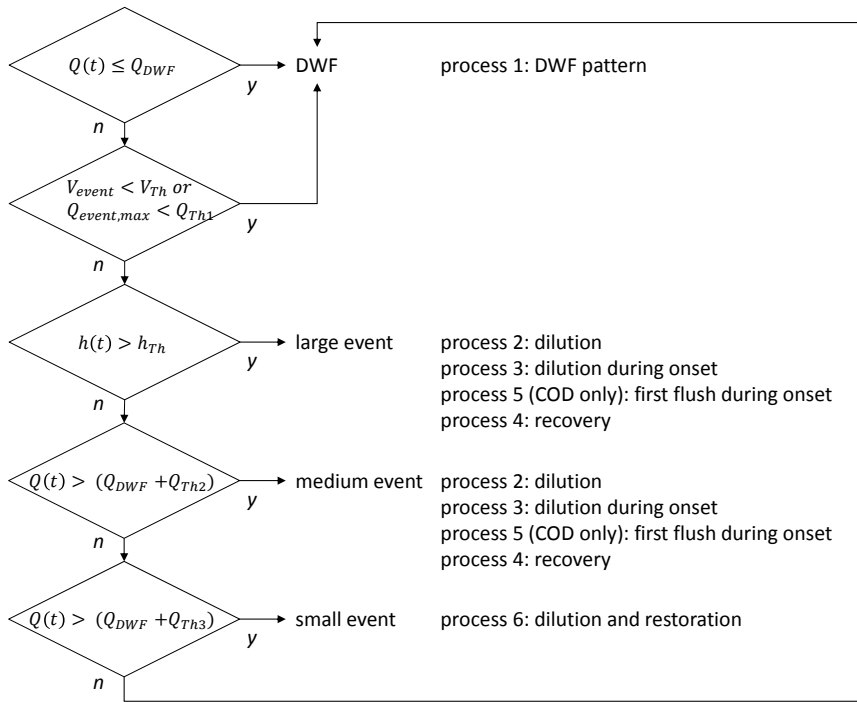


Figure 4.5: Selection of events and water quality processes using information on hydraulics. The thresholds (abbreviated as Th) for Eindhoven Stad are defined as: $h_{Th} = 11.30 \text{ mAD}$, $V_{Th} = 5,000 \text{ m}^3$, $Q_{Th1} = Q_{Th2} = 4,000 \text{ m}^3/\text{h}$, $Q_{Th3} = 500 \text{ m}^3/\text{h}$.

A large storm event is defined as an event for which the water level in the influent chamber rises above a certain threshold value (h_{Th} set at 11.30 *mAD*). This typically only occurs if the sewer system starts filling during storm events exceeding the influent pumping capacity of the WWTP. During medium and small storm events the water level in the influent chamber does not rise above h_{Th} . These events are distinguished by the exceeding the 95-percentile of the DWF flow values with more (medium event) or less (small events) than threshold Q_{Th2} set at 4.000 m^3/h . Medium storm events are typically relatively small, low intensity storm events, where the inflow is less than the available pumping capacity (approximately equal to an interceptor capacity of 0.7 *mm/h* or 7 m^3/ha). Small storm events typically have an inflow less than 0.2 *mm/h* or 2 m^3/ha).

The processes applied in the model are:

Process 1 is the basic process for all parameters. It is the DWF pattern for water quality, derived from high-frequency monitoring data collected during multiple dry weather days through averaging over the same time stamps;

Process 2 mimics dilution and is based on the ratio between the actual flow (Q_{actual}) and the 95-percentile for the flow during DWF at that time of the day at the location of the WWTP inlet works (Q_{DWF}). The wastewater concentration is calculated using

$$C_{WWF}(t) = C_{DWF}(t) \left(a_1 \frac{Q_{DWF}(t)}{Q_{actual}(t)} - a_1 + 1 \right), \quad (4.1)$$

with C_{WWF} the calculated concentration during wet weather, and C_{DWF} the concentration during DWF conditions at that time of the day. The dilution factor a_1 [-] is introduced to allow adjustment to the dilution rate in the calibration procedure. $a_1=1$ indicates that the dilution is exactly inverse to the increase in flow. $a_1<1$ imposes an increase in pollutant loads during the event, which could be necessary to account for pollutant contributions originating from in-sewer stocks. $a_1>1$ imposes a decrease in pollutant loads during the event, which could be expected for a compound where in-sewer stocks are zero and a part of the pollutants would be discharged via a CSO. For low dilution ratios, i.e. $Q_{DWF}(t)/Q_{actual}(t)$ being close to 1, the factor a_1 has a limited influence, for higher dilution ratios, the factor a_1 contributes to a larger extent;

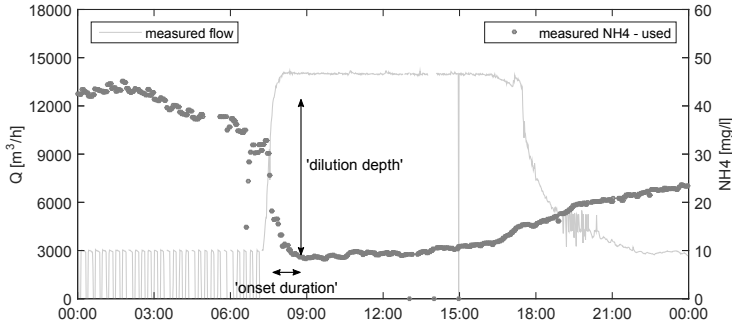


Figure 4.6: Parameters of parabolic function that describes the delayed dilution of the quality parameters compared to the flow.

Process 3 accounts for dilution during the onset of storm events. Process 3 is described by a parabolic function, valid for the period between the start of the storm event and the moment of maximum dilution. The length of this period, the duration of the onset a_3 , is determined during model calibration. This process is necessary to account for the delayed dilution observed in the monitoring data. This is clearly visible in for example figure 4.9. During the first part of the event on 28 July 2012, the influent flow increased rapidly to the maximum flow rate of $14.000 \text{ m}^3/\text{h}$, while the NH_4 concentration gradually reduces to a minimum of 5 mg/l . Using equation 4.1 during the onset of the storm event, would result in an overestimation of the dilution. Instead, during the onset of the storm event the following equation applies:

$$C_{WWF}(t) = C_{DWF}(t) \frac{\text{dilution depth}}{a_2^2} (t - t_{\text{end onset}})^2 - \text{dilution depth} + 1. \quad (4.2)$$

Where a_2 is the duration of the onset stage and *dilution depth* is the minimal ratio $C_{DWF}(t)/C_{WWF}(t)$ during the onset stage of the storm event. Figure 4.6 shows the parameters in the parabolic function of equation 4.2;

Process 4 reproduces restoration, which describes the gradual return from the WWF concentration levels to DWF levels after the storm event. Based on the analysis of the available data set, restoration can be assumed to be a linear process at rate a_3 [$mg/(ls)$] until the concentration returns to the DWF value. During the restoration phase, the concentration is calculated through

$$C_{WWF}(t+1) = C_{WWF}(t)(1 + a_3)dt; \quad (4.3)$$

Process 5 describes a first flush in concentration levels of particulate material, see figure 4.4 for an example for COD, and is thus not valid for soluble substances. This initial peak increases the concentration during the first stage of a storm event, before dilution becomes the dominant process. Process 5 is modelled as a triangle that causes an instant increase of the COD concentration of a_4 [mg/l] at the onset of the event, and decreases with a fixed rate a_5 [$mg/(ls)$];

Process 6 regards dilution and restoration for small events. Process 6 describes the concentration profile as a isosceles triangle, where dilution takes place at a rate a_6 [$mg/(ls)$] during t_6 hours and recovery at the same rate a_6 during the next t_6 hours. In the case of Eindhoven Stad and Riool Zuid a duration of $t_6 = 13$ hours proved to be a good estimate.

4.2.5 Model calibration

In this study the differential evolution adaptive metropolis (DREAM) method (Vrugt et al., 2008, 2009) is applied to calibrate the parameters of the empirical model to find the minimal difference between the model output and the monitoring data. The effectiveness of DREAM in water related model calibration has been demonstrated in many previous studies, e.g. (Keating et al., 2010; Leonhardt et al., 2014).

Table 4.1 shows the model parameters, units and the search range for the calibration procedure. The threshold values for selecting the type of event (h_{Th} , V_{Th} , Q_{Th1} , Q_{Th2} , Q_{Th3} and t_6) have been derived during data analysis prior to the calibration of the model parameters. Consequently, they were not included in the model calibration. Future users of the model on other catchments could include these parameters as part of the model calibration. This may however lead to over parameterisation of the model and hence low parameter identifiability.

Table 4.1: Model parameters, units and search range for the calibration procedure.

model parameter	abbr	unit	search range	parameter
dilution factor	a_1	—	0 - 2	NH4, COD
dilution delay time	a_2	<i>min</i>	0 - 600	NH4, COD
recovery factor	a_3	<i>mg/(ls)</i>	0 - 0.01	NH4, COD
peak first flush concentration	a_4	<i>mg/l</i>	0 - 2,000	COD
recovery factor first flush	a_5	<i>mg/(ls)</i>	0 - 10	COD
recovery factor small events	a_6	<i>mg/(ls)</i>	0 - 0.01	NH4, COD

The calibration is performed using 5,000 iterations in DREAM for the COD model and 2,500 for the NH4 model, as it was found from test runs that the cumulative density functions of the parameters do not change (within the parameter stability) after a few thousands of iterations. The last 50% of the iterations are used for further analysis: the optimal parameter set and model output are derived, and the model is run with all these parameter sets to determine the 95% confidence intervals for the NH4 and COD concentrations.

4.3 Results and discussion

This section first presents an overview of the calibration and model results, and a discussion of their quality based on data from catchment Eindhoven Stad. Second, the transferability of the model concept is discussed using data from catchment Riool Zuid. Finally some foreseen applications of the model will be described.

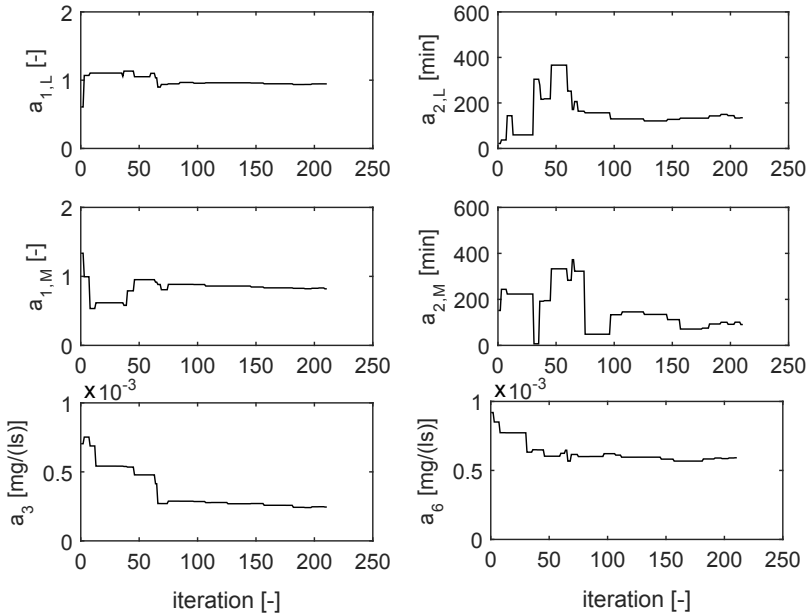


Figure 4.7: Parameter values during the model calibration of NH₄ for Eindhoven Stad. For each iteration, only the first Markov Chain of the parameter set is shown.

4.3.1 Calibration results

The DREAM algorithm has been applied with a total of 5,000 iterations for the COD model and 2,500 for the NH₄ model. The algorithm uses $2N$ Markov Chains, with N being the number of model parameters being evaluated. This resulted in 312 iterations for the COD model and 208 iterations for the NH₄ model. Figure 4.7 shows the variation in model parameter values during the calibration process for the NH₄ model for catchment Eindhoven Stad for the first Markov Chain of each iteration. Parameters concerning medium and large storm events are denoted as M and L respectively. The value of each of the model parameters is relatively stable during the calibration process, showing that the number of iterations was sufficient to converge. The correlation between the model parameters was found to be limited from figure 4.8, showing a high identifiability of the model parameters.

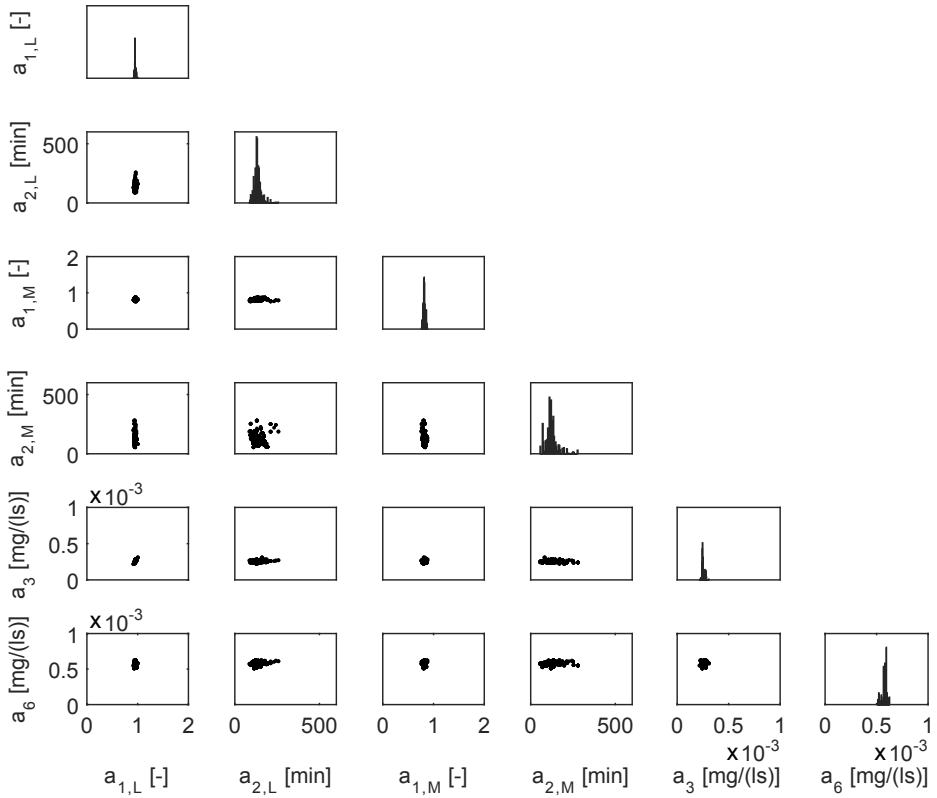


Figure 4.8: Posterior distribution of model parameters a_1 to a_6 for the NH4 model for catchment Eindhoven Stad based on the final 50% of the iterations. The histograms represent the posterior distribution of individual model parameters and the scatter plots represent the relationships for various combinations of parameters.

Table 4.2: Calibrated parameters values for the NH4 and COD model for Eindhoven Stad. Subscript S, M and L denote small, medium and large storm events respectively.

model parameter	abbr	unit	NH4 model	COD model
dilution factor, L	$a_{1,L}$	—	0.95	0.63
dilution delay time, L	$a_{2,L}$	<i>min</i>	123	342
dilution factor, M	$a_{1,M}$	—	0.82	0.47
dilution delay time, M	$a_{2,M}$	<i>min</i>	115	589
recovery factor, M+L	a_3	<i>mg/(ls)</i>	0.00025	0.00014
peak first flush concentration	a_4	<i>mg/l</i>	n.a.	48
recovery factor first flush	a_5	<i>mg/(ls)</i>	n.a.	0.19
recovery factor, S	a_6	<i>mg/(ls)</i>	0.00059	0.00017

The model parameter values are shown in table 4.2 for the NH4 and COD model. For the NH4 model, there is no strong need to distinguish between large and medium storms, as the model parameters are similar. For COD, however, the model parameters differ strongly between large and medium storm events. The values for the dilution factor a_1 for NH4 are below, but close to one, indicating that for NH4 the contribution of in-sewer stocks is relatively limited. For COD, however, the values of a_1 are quite low indicating high peak load factors as a result of WWF. For the maximum dilution ratio observed, i.e. the DWF minimum ($2,100 \text{ m}^3/\text{h}$) divided by the maximum flow ($15,000 \text{ m}^3/\text{h}$) = 0.14, equation 4.1 with $a_1=0.5$ returns $C_{WWF}=0.57C_{DWF}$. As at that moment the flow is 7.1 times higher than Q_{DWF} , the calculated influent load will be 4 times the DWF load. This peak load factor has been observed regularly in monitoring data for this catchment (Schilperoort, 2011).

4.3.2 Model results

Figure 4.9 shows the resulting predicted and measured water quality for NH4 in the WWTP influent for Eindhoven Stad. The results show that the dynamics in the model (solid black line) and the monitoring data (grey dots) show an overall good agreement in terms of dynamics and absolute values during wet weather during the large events of 28 and 29 July. In the monitoring data, dilution starts a little bit earlier than in the model. During the medium event on 31 July, the model fit is less satisfying. During dry weather (25 to 28 July), the daily variation in the measured concentration of NH4 is represented reasonably well by the model; the remaining differences are due to the fact that the DWF dynamics in the model represent the average DWF concentration levels and the actual DWF varies per day. The root mean

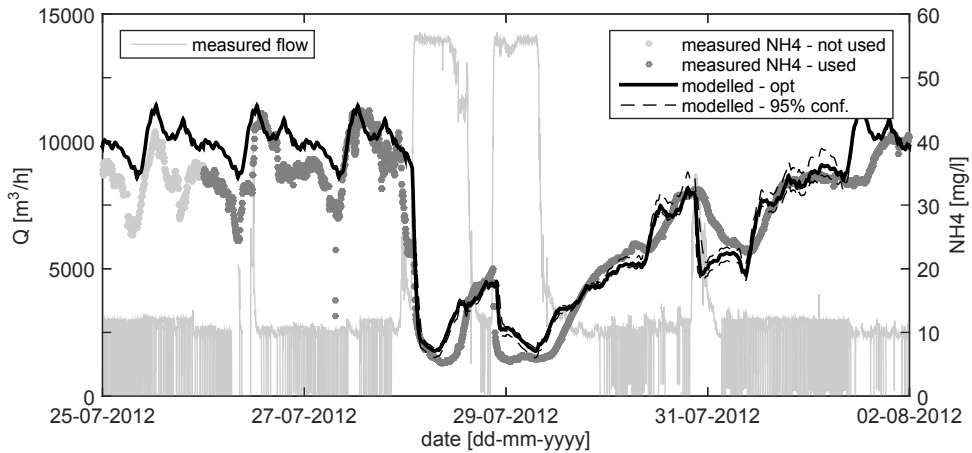


Figure 4.9: Model vs. monitoring data: NH₄ concentration in the WWTP influent for Eindhoven Stad.

squared error (RMSE) for the NH₄ model based on the data used in the calibration is 6.3 mg/l , or nearly 16% related to the mean DWF concentration. Figure 4.10 shows the cumulative density function (CDF) of the model results and the monitoring data for NH₄ and COD. As expected due to the daily variation in DWF concentrations, the high concentration levels (occurring during DWF) are captured less accurately than the low concentration levels (occurring during WWF).

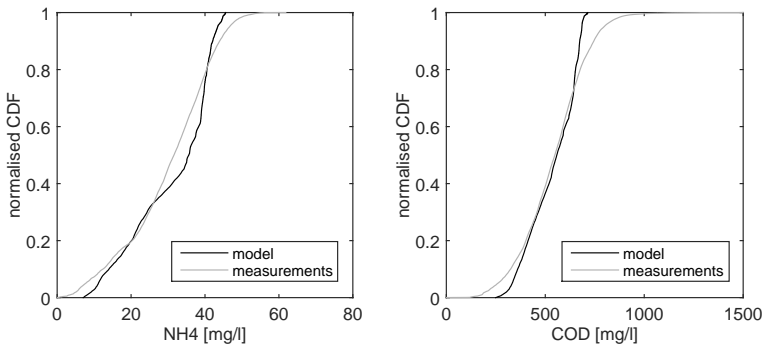


Figure 4.10: Normalised CDF functions of model results and measurements for NH₄ and COD in the WWTP influent for catchment Eindhoven Stad.

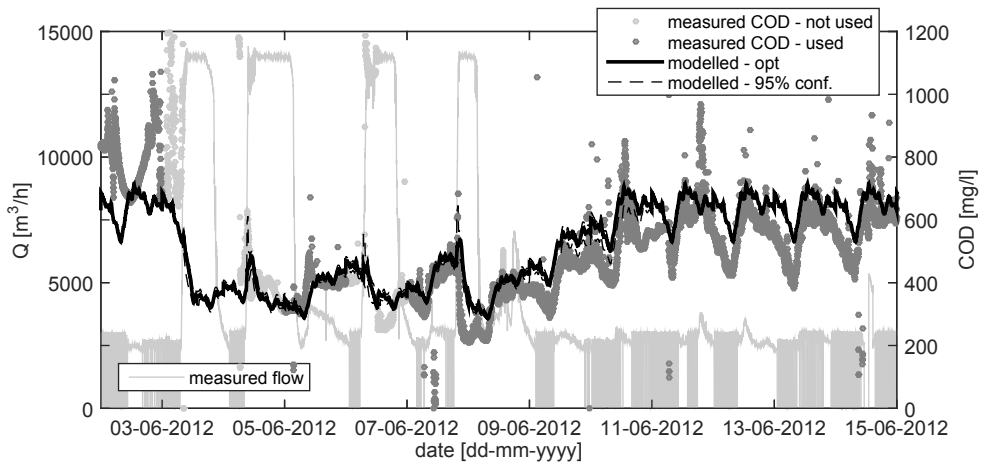


Figure 4.11: Model vs. monitoring data: COD in the WWTP influent for Eindhoven Stad. The small peaks in influent concentration (typically referred to as ‘first flush’) at the beginning of storm events on 4, 6 and 8 June are adequately represented by the model.

The model results for the COD model for Eindhoven Stad are shown in figure 4.11. The COD model also incorporates process 5 describing the peak first flush concentration on 4, 6 and 8 June. As expected, the model fit is not as good as for the NH_4 model. This is partly due to the difference in the quality of the monitoring data, illustrated by the outliers in the monitoring data shown in this figure and partly due to the fact that modelling suspended solids is more difficult than modelling solutes. The RMSE for the COD model based on the data used in the calibration is 109 mg/l , equivalent with 18% of the mean DWF concentration. This RMSE for COD is in relative terms comparable to the RMSE for NH_4 .

The influent model has been developed to deliver input for WWTP models that is reliable enough to assess WWTP performance and to assess the impact of measures, such as RTC in wastewater systems. An earlier version of this influent model has already been used for this purpose in the KALLISTO project at water board De Dommel (Weijers et al., 2012; Langeveld et al., 2013)¹. The RMSE values for NH₄ based on the current influent model just meet the quality requirements for WWTP influent data derived by (Langeveld et al., 2003), while for COD they easily meet these requirements. This shows that the influent model is sufficiently accurate for the described modelling purposes.

4.3.3 Transferability of the concept

The structure of the influent model has been developed for catchment Eindhoven Stad only. The data from the catchment Riool Zuid has been used to verify the concept, using the same routines for calibration. In this respect, it has to be noted that the sub catchments Eindhoven Stad and Riool Zuid are independent catchments, allowing to test the transferability of the concept.

The calibrated model parameters are shown in table 4.3. For Riool Zuid, the model parameters for medium and large storms are very similar for both the NH₄ and COD model, showing that this distinction between large and medium events is not necessary for this catchment. The model parameter values for the dilution factor a_1 for Riool Zuid show a strong similarity with the model parameters for Eindhoven Stad. For NH₄, the dilution during the storm event, calculated by equation 4.1, remains nearly reciprocal to the increase in influent flow during the storm event. This indicates that during the storm event, nearly all nitrogen in the WWTP influent stems from the wastewater, with only very limited contributions from the rainfall runoff and the in-sewer stocks.

¹The influent model described in this chapter was improved with respect to the earlier version on the following aspects: i) the events are defined slightly differently, ii) process 3 was added to the model description to better account for the delayed dilution of the wastewater concentration with respect to the influent flow, and iii) the model parameters were determined through calibration instead of trial and error. All improvements were conducted by the author of this thesis.

Table 4.3: Calibrated parameters values for the NH4 and COD model for Riool Zuid. Subscript S, M and L denote small, medium and large storm events respectively.

model parameter	abbr	unit	NH4 model	COD model
dilution factor, L	$a_{1,L}$	—	0.96	0.49
dilution delay time, L	$a_{2,L}$	<i>min</i>	373	590
dilution factor, M	$a_{1,M}$	—	0.98	0.49
dilution delay time, M	$a_{2,M}$	<i>min</i>	427	548
recovery factor, M+L	a_3	<i>mg/(ls)</i>	0.00033	0.00034
peak first flush concentration	a_4	<i>mg/l</i>	n.a.	60
recovery factor first flush	a_5	<i>mg/(ls)</i>	n.a.	0.06
recovery factor, S	a_6	<i>mg/(ls)</i>	0.00027	0.00002

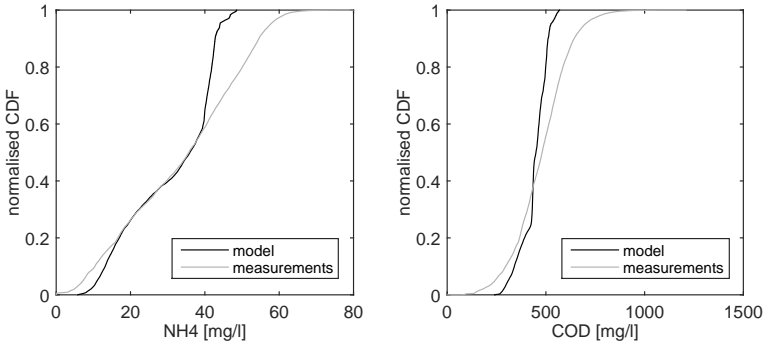


Figure 4.12: Normalised CDF functions of model results and measurements for NH4 and COD in WWTP influent for Riool Zuid.

For COD, the dilution factor $a_1=0.49$ results in COD concentration levels during the high flow period of a storm event of between 250 and 300 *mg/l* and, as a consequence, high influent peak loads. This additional load arriving via the influent at the WWTP during a storm event originates mainly from in-sewer stocks (Schilperoort et al., 2012), given the fairly low COD concentration in Dutch storm water of 61 *mg/l* (Boogaard and Lemmen, 2007).

The overall model performance for Riool Zuid, expressed in terms of RMSE, is comparable with the performance for Eindhoven Stad. The RMSE amounts to 8.9 *mg/l* for NH4, equivalent to 22% of the mean DWF value for the NH4 model and to 126 *mg/l* for COD, equivalent to 25% of the mean DWF value for the COD model. Like for Eindhoven Stad, the cumulative density function for model results and monitoring data show reasonable agreement for both NH4 and COD, see figure 4.12, with once again the biggest differences in the higher (DWF) concentration ranges.

As there was no need to change the model structure, it is concluded that the model is transferable to other catchments, provided that the dynamics during WWF show similar patterns as described in figure 4.4.

Literature confirms these patterns to be fairly general. (Bruns, 1998; De Mulder et al., 2017) defined a number of distinct phases in the influent pollutograph during storm events:

Phase 1 increase of flow rate and subsequently an increase of the load arriving at the WWTP due to the ‘push’ of wastewater with DWF concentration levels. This phase is more distinct if more wastewater is stored downstream in either large interceptor sewers or rising mains;

Phase 2 increased concentration of suspended solids as eroded sewer sediments starts to arrive at the WWTP. These sediments are usually transported with a velocity lower than the fluid velocity (Bertrand-Krajewski et al., 1993);

Phase 3 arrival of diluted wastewater at the WWTP;

Phase 4 return to DWF equilibrium. Equilibrium for dissolved compounds will be reached as soon as all remaining storm runoff has been transported (pumped) towards the WWTP. Reaching equilibrium for suspended solids may take longer since it takes time before all depressions within the sewer system are filled again with sediment.

Phase 1 and phase 2 are both part of the onset of the storm event, phase 3 is similar to the dilution stage, and phase 4 relates closely to the stage of recovery after the storm events. Despite the need of further research on the transferability, the similarities in system dynamics strongly indicate a wider applicability of the model than just Eindhoven Stad and Riool Zuid.

The consistency in the dilution factors for NH₄ and COD for Eindhoven Stad and Riool Zuid (with dilution factors for NH₄ just a little smaller than one, indicating a small contribution of in-sewer stocks and dilution factors for COD around one half, indicating a large contribution of in-sewer stocks) demonstrate that the empirical model is able to capture the contribution of in-sewer stocks during the dilution phase of the event adequately. This is an important benefit of the model compared with influent generators reviewed by (Martin and Vanrolleghem, 2014). The differences in model parameters related to the first flush and recovery after the event seem to be

linked with the differences in layout of the sewer system. Future research is necessary to further elaborate on the relation between parameter values and physical characteristics of the catchment. The amount of in-sewer storage relative to the pumping capacity of the WWTP will likely be related to the length of the recovery period, as these characteristics determine the emptying time of the sewer system, which will be related to the length of the recovery.

The differences in performance between the catchments, although relatively small, can be attributed to the different characteristics of Riool Zuid compared to Eindhoven Stad and possibly also to the limited quality of the sensor data. This is illustrated by figures 4.13 and 4.14. In figure 4.13, the results are shown for Riool Zuid for the week after 16 July 2012 and in figure 4.14 for the first two weeks of December 2012. During the events of 17 and 21 July, the monitoring data show two distinct dilution phases during the events. One dilution phase occurs at the beginning of the storm event and one at the end. This phenomena does not occur during the storm events of 2 and 4 December 2012, but does to a lesser extent on December 10. The Riool Zuid catchment has a very different structure compared to Eindhoven Stad (see figures 4.1 and 4.2). While Eindhoven Stad consists of a gravity system draining to one central point, Riool Zuid has a 31 *km* long transport sewer with a number of sub catchments of various sizes at different distances. It is assumed that the double dip is caused by a difference in transport times for two main areas in this catchment, which causes the concentrations to drop for a second time during a storm event. The double dilution dip is of course driven by rainfall and as a result, the spatial variation in the rainfall is the main explanatory factor for the differences per event. In the model, this effect could be mimicked by dividing Riool Zuid in two catchment basins, with a cut at pumping station Aalst, as indicated in figure 4.1, and to add the transport time in the transport sewer to one of the basins. However, as the error in the model results is relatively small due to the low influent flows, this adjustment was not considered necessary at this moment.

The base line of the model consists of the mean DWF concentration. Data analysis of available routine 24-hour composite samples of the WWTP influent has shown that there is no seasonal trend for NH₄ and COD. Despite the absence of a seasonal trend, the mean DWF concentration varies during the monitoring period. Due to a lack of sampling data, it could not be determined whether changes in this DWF concentration level were due to real changes or due to e.g. a temporary drift of the sensor. Differences in the main DWF concentration levels have been observed for

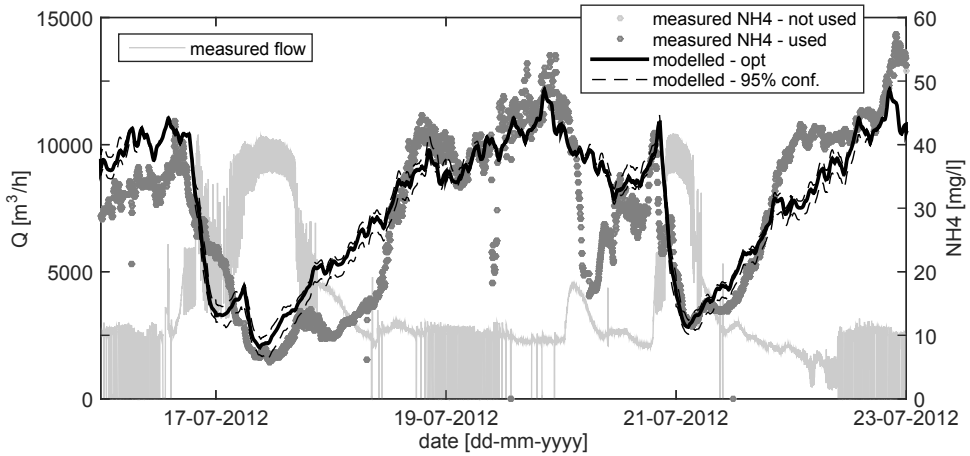


Figure 4.13: Model vs. monitoring data: NH₄ concentration in the WWTP influent for Riool Zuid. ‘Double’ dilution dips occur at 17 July around 12:00 AM, 18 July around 0:00 AM and on 21 July at 2:00 and 12:00 AM.

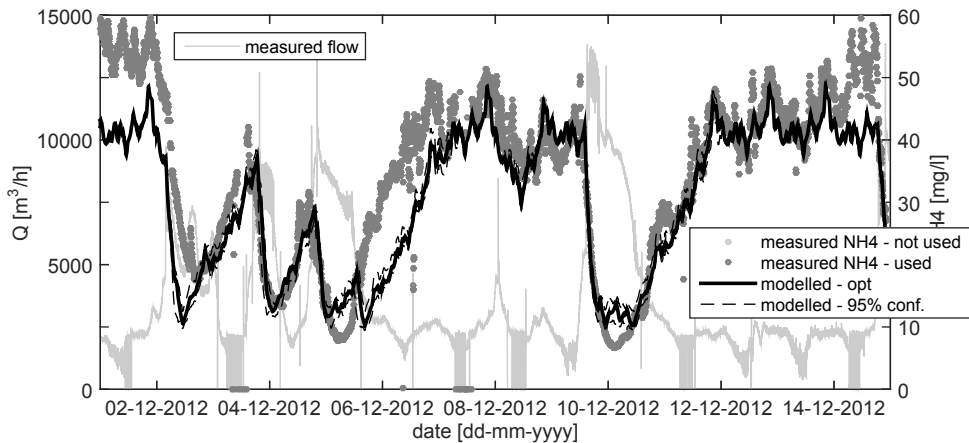


Figure 4.14: Model vs. monitoring data: NH₄ concentration in the WWTP influent for Riool Zuid.

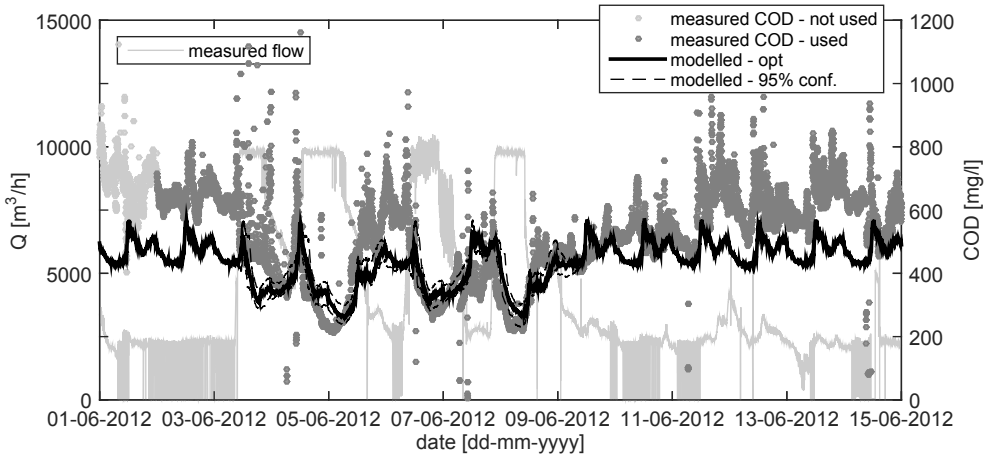


Figure 4.15: Model vs. monitoring data: COD concentration in WWTP influent for Riool Zuid.

NH₄, e.g. compare the concentration levels on 16 July in figure 4.13 (around 40 *mg/l*) and 1 December in figure 4.14 (around 55 *mg/l*). This difference is even bigger for COD, see figure 4.15. The mean DWF, derived from monitoring data, is nearly 500 *mg/l*, while the monitoring data on 2 June are nearly 700 *mg/l*. In this study, the model has been calibrated using the mean DWF derived from all available monitoring data during DWF.

Finally, the results shown in this paper are based on NH₄ and COD only. NH₄ is representative for solutes predominantly originating from the wastewater. COD is representative for parameters with an additional significant contribution from in-sewer stocks, i.e. sediment and biofilm, to the pollutant load in the influent during storm events (Schilperoort et al., 2012). For WWTP modelling also other parameters, such as phosphorous, need to be taken into account. Total phosphorous is known to exert similar behaviour as COD and consequently, the COD model may be used to recalculate the total phosphorous concentration. Ortho-phosphate, on the other hand, is dissolved and behaves in the sewer like NH₄ (Krebs et al., 1999) and consequently, the NH₄ model may be used.

4.3.4 Applications

The influent model as described in this chapter generates influent water quality dynamics using measured influent hydraulics as input. This application has been used in chapter 6 to evaluate the performance of an integrated, impact based RTC strategy in the wastewater system of Eindhoven.

Another application of the influent model is described in (Langeveld et al., 2013), where an earlier version of the influent model has been implemented in an integrated model to generate influent water quality dynamics based on the simulated influent water quantity from a sewer sub model. In this application, a representative DWF curve based on monitoring data has been used. It would also have been possible to use harmonic functions for DWF and to use the influent model to complement the time series with WWF dynamics. In other words, the influent model can be applied on measured or simulated hydraulics and may also be applied in combination with the harmonic functions described in section 4.1. Moreover, as the empirical influent model is developed to adequately mimic WWF dynamics, it might be included in the phenomenological influent pollutant disturbance scenario generator (Flores-Alsina et al., 2014), which is the latest version of the phenomenological model developed by (Gernaey et al., 2011), replacing the relatively weak current sewer model module applied.

The influent model can also be used for surveillance of monitoring equipment at the inlet of the WWTP. E.g. earlier research has shown that the hydraulic monitoring data at WWTP Eindhoven is very reliable with over 99% good data (Schilperoort, 2011). Running the influent model continuously on measured hydraulic data and comparing raw monitoring data of the influent water quality with the simulated influent water quality data would allow early and easy detection of anomalies in the monitoring data. This could be used to alarm operators to check the monitoring equipment. Early detection of problems with sensors will possibly result in a higher yield.

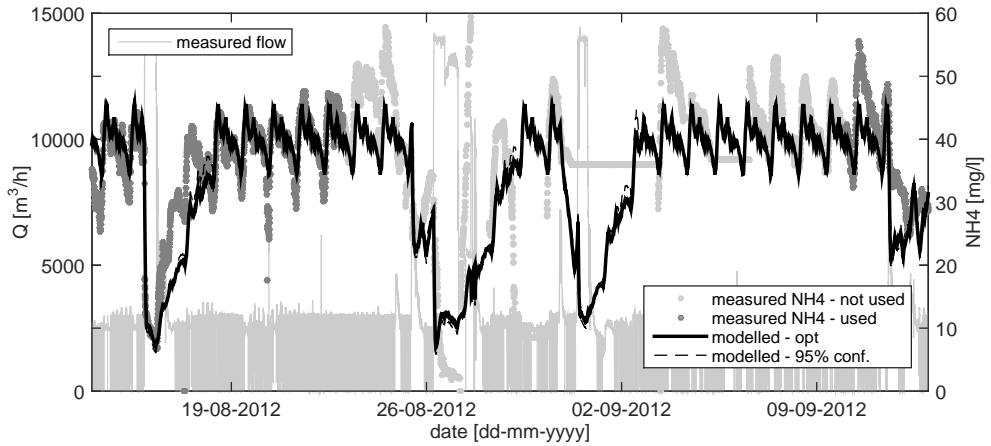


Figure 4.16: Gap filling with the influent model. Example for NH_4 in WWTP influent for Eindhoven Stad.

A final application of the influent model discussed in this paper is gap filling, as attempted by e.g. (De Mulder et al., 2017) to obtain continuous time series as input for modelling purposes. Figure 4.16 shows an example of the application of gap filling. The dots show the measured NH_4 concentration in the influent of WWTP Eindhoven. The dark grey dots are data that could be used e.g. for assessing the performance of the influent model, the light grey dots show data that were rejected during the validation. The black line shows the simulated concentrations by the influent model. By applying gap filling a continuous time series could be generated, where the final time series is composed of the dark grey dots and where these are missing, data are filled in using the influent model results.

For some of the potential applications of the model, such as gap filling or data validation, it is advised to regularly check the absolute value of the sensor data during DWF to ascertain whether changes in the DWF concentration level are due to real changes or due to a sensor drift. In case these are due to e.g. seasonal variation in the influent concentration levels during DWF, this should be accounted for when applying the influent model. The routine 24-hour samples typically available for WWTP influent may be used to check for a seasonal pattern.

4.4 Conclusions and recommendations

Modelling of influent quality is an increasingly important tool to enable WWTP models to optimise the performance of WWTPs during wet weather. The main issue in modelling wastewater quality during storm events is to account for in-sewer stocks, which have a varying contribution to the wastewater quality. Neither traditional sewer water quality models nor the available influent generators are capable of adequately addressing this issue.

The proposed empirical model is founded on a detailed study of the observed water quality and predicts it by combining a number of actual processes, such as DWF, dilution, restoration and first flush. For Eindhoven Stad, the model describes the NH_4 concentration (solute substance) with a RMSE of 6.3 mg/l or 16% related to the mean DWF concentration, for COD (associated with particulate matter) these are 109 mg/l and 18%, respectively.

The model structure has been demonstrated to be transferable to a catchment with different characteristics. Eindhoven Stad is a large catchment with the WWTP located near the centre, Riool Zuid comprises of a long interceptor sewer, which drains the wastewater from seven municipalities with a range of catchment sizes. Due to spatial variation of the rainfall and variation in travel times, ‘double dilution’ dips may occur in the influent coming from Riool Zuid. Despite these different dynamics and characteristics, there was no need to adjust the model structure of the empirical influent model. Future research in catchments in sewer systems with less in-sewer storage volume is needed to further explore the transferability of the model concept.

The model concept facilitates integrated modelling of urban wastewater systems by translating influent hydraulics to influent quality. This is a necessary step in the application and evaluation of integrated RTC in urban wastewater systems. The model concept could also be used to fill gaps in time series for influent water quality and be used for advanced data validation to detect outliers and drift of water quality sensors, as these sensors are still very vulnerable and data quality control remains a difficult issue.

Acknowledgements

This research is funded by KRW-innovation subsidy from AgentschapNL (www.agentschapnl.nl). The Dutch Foundation for Applied Water Research (STOWA) is engaged in this project to communicate and publish the research results.

5 A methodology for the performance evaluation of RTC

5.1 Introduction

An overall conviction that real time control (RTC) has the potential to improve the operation of urban wastewater systems is present in literature, see e.g. (Nelen, 1992; Erbe et al., 2002; Fuchs and Beeneken, 2005; Puig et al., 2009). Closer examination in section 1.2, however, revealed that the effectiveness of RTC in urban wastewater management in practice is not yet established, and that no methodology is available to determine the performance of RTC.

This chapter contributes to the discussion on the effectiveness of RTC in urban wastewater systems in practice and its evaluation. Questions on how to deal with ever changing conditions in real life situations, and the need for and implications of including uncertainty analysis are addressed. It will focus on systems that at least encompass a combined sewer system. ‘Regular’ process control of wastewater treatment plants (WWTPs), such as aeration or return activated sludge control, is considered beyond its scope, as this topic is dealt with intensively in literature (Olsson, 2012; Olsson et al., 2014). On the contrary, integrated control of urban wastewater systems is still considered to be at an early stage of development.

This chapter is an adapted version of: Van Daal-Rombouts, P.M.M., Gruber, G., Langeveld, J.G., Muschalla, D., Clemens, F.H.L.R., (2017). Performance evaluation of real time control in urban wastewater systems in practice: review and perspective. *Environmental Modeling & Software*, 95:90–101. doi: <http://dx.doi.org/10.1016/j.envsoft.2017.06.015>.

This chapter is organised as follows. In section 5.2 a detailed problem statement is presented. Section 5.3 proposes a methodology for the performance evaluation of RTC in practice. This is followed by a case study in section 5.4 to show the impact of the evaluation period and uncertainty analysis on the supposed effectiveness of two RTC scenarios on a simple and easy to understand sewer network. Section 5.5 discusses the results from the case study and the methodology itself. Finally, section 5.6 contains conclusions and recommendations.

5.2 Problem statement

Many developments in RTC in urban wastewater systems reported about in literature have taken place based on modelling exercises, for both hypothetical systems and ‘real-world’ case studies. For example (Schilling et al., 1996) describe an early application of RTC on a sewer system and wastewater treatment plant combined. (Einfalt et al., 2001) introduce the central basin approach, that to date in German speaking countries is viewed as the method to define the optimum controlled state of a system. (Erbe and Schütze, 2005) further integrate the modelling environment and take a quality approach. (Vanrolleghem et al., 2005) deal with the difficulties of preparing an integrated model for RTC application. An investigation into the effect of rainfall forecasting on the runoff and its potential for RTC are described by (Krämer et al., 2007). (Schütze et al., 2008) introduce the German M180 guideline document for the planning of RTC systems in urban drainage catchments. Equipment needed for the implementation of RTC is reviewed by (Campisano et al., 2013) and the effort needed is described by (Beeneken et al., 2013). (Garcia et al., 2015) give an overview of and references for different implementation levels, optimisation strategies and software tools for RTC in urban wastewater systems. Recently, (Garbanini Marcantini et al., 2016) claim intermittent operation of RTC can help determine the impact of RTC more easily and (Löwe et al., 2016) looked into the influence of rainfall forecasting and its uncertainties on RTC strategies.

Simultaneous to these developments, at several locations system-wide RTC has been implemented in practice, for which a non-exhaustive and concise overview will be presented. Unless stated otherwise the main objective of the applied RTC is reduction of combined sewer overflow (CSO) activity, possibly at specific sites. As early as 1994 a model predictive control strategy was prepared for implementation in Seattle (Gelormino and Ricker, 1994). (Fuchs and Beeneken, 2005) describe the process of implementing a rule-based control that includes rainfall forecasts in Vienna. In

Quebec, a model predictive control system based on rain forecasts is executed in a stepwise manner. The first phase is presented in detail in (Pleau et al., 2005), while (Fradet et al., 2011) describe the later phases and the project in a wider scope. The applied model and global control development for Berlin is described in detail in (Pawlowsky-Reusing, 2006). In Copenhagen, RTC is implemented as described in (Grum et al., 2011). It includes risk assessment and flow forecasting. (Hoppe et al., 2011) describe the development of a pollution based RTC strategy for the separate sewer system of Wuppertal. In Wilhelmshaven the aim of the implemented RTC is twofold: CSO reduction and WWTP influent limitation in case of critical situations. (Seggelke et al., 2013) describe the effectiveness based on one year of operation. For Kessel-Lo, (Dirckx et al., 2014) provide details on construction and cost aspects regarding the implemented RTC. A recent application of RTC in the sewer system of Bordeaux is described in Robitaille et al. (2016), including an evaluation over a period of three years.

It is noted that for WWTPs, a benchmark for control strategies has been developed, allowing to test strategies in a general sense in a controlled model environment (Alex et al., 1999). This procedure is very promising for mutually comparing the effectiveness of control strategies at WWTPs, but not to quantify the added value of the control in urban wastewater systems in reality. This is due to for example the propagation of errors between sub systems, the difference between model results and reality and the influence of operational issues.

From the papers that deal with implemented RTC systems, the current practice for a performance evaluation of implemented RTC in the field of urban wastewater management was extracted. First of all, a performance evaluation is not always carried out (or reported). When it is executed, there is no consensus on the procedure. It is generally (with a few exceptions) based on either less than ten storm events or over a period of maximum a few months only. Comparisons are made between the systems functioning with and without RTC based on measurements or modelling results or a mixture of both. Only two publications were found that describe the effectiveness or functioning of existing RTC over periods longer than one year. Second, none of the publications cited report on uncertainties in parameters used for the performance

evaluation, leaving the question on the significance of the effect open. Only (Hoppe and Gruening, 2007) and (Breinholt et al., 2008) make a point for including uncertainty analysis in RTC evaluation, but their call has remained unheard so far. Even (Löwe et al., 2016), who in a modelling exercise do apply uncertainties in the rainfall estimation and use many events from a three year period, still refrain to include uncertainties in the final performance evaluation.

Current practice is thought to originate from the reality of working with actual systems, for customers in a commercial setting, along with an unfounded trust in our ability to understand reality and describe it in models (Harremoës, 2003). Urban wastewater systems are normally not operated for the purpose of research and therefore changes in set points, operation strategy and even infrastructural adaptations are continuously made. In other words, in practical situations one is never certain about the structure and geometry of the whole considered system, although this is desired from a scientific point of view. High quality measurements are hard to obtain in real working conditions, especially simultaneously and for a prolonged period. Generating a data set for a performance evaluation for an prolonged period of time is therefore a technical and organisational feat. Uncertainty analysis is believed to be omitted because in actual systems uncertainties are often not known, it is deemed complicated and time consuming, and the results become more difficult to communicate. Customers add to this by expecting (fast) results and preferring their money well spent, at least on paper.

Omitting uncertainty analysis and too short evaluation periods are the two main deficiencies of current practice in performance evaluation of RTC in urban wastewater management. The first represents a lack of certainty in the significance of the result. An improvement of 10% could easily fall within the measurement or model output uncertainty, thus preventing a firm conclusion on the effectiveness of the imposed RTC system. When comparing measurements with imposed RTC and model results without RTC or vice versa, different sources of uncertainty are involved making uncertainty analysis even more essential and cumbersome. The second deficiency leads to an evaluation based on a limited range of conditions in which urban wastewater systems are operated. E.g. applying only events in summer or winter might influence the RTCs impact on a WWTP functioning considerably. In addition, prolonged wet or dry weather periods could have a significant impact if they are not included in the data set.

To advance the field of RTC in urban wastewater management these two main deficits should be addressed.

Table 5.1: Overview of possible RTC strategies and examples of accompanying goals in urban wastewater management.

strategy	goal (examples)
emission based	hydraulic load reduction (at CSOs or WWTP influent) pollution load reduction (at CSOs, WWTP influent or effluent)
impact based	reduction of toxic discharges mitigation of oxygen depletion reduction of eutrophication reduce hydro morphological impacts
operational optimisation	reduce maintenance needs remove sewer sediments reduce energy needs

5.3 Methodology

Urban wastewater management is a wide research field and each system and each RTC application is unique. It is therefore impossible to supply one ready-made solution for the evaluation of the effectiveness of RTC. However, it is possible to define general steps that should be followed in every evaluation. These steps, with a distinction between data and model driven evaluations, are combined into a methodology which is described in the following sections. A flow chart for the methodology is supplied in figure 5.1.

5.3.1 General

The first step in undertaking any RTC project is defining a clear goal (step 1 in figure 5.1). A clear goal describes the overall end one wants to achieve in as much detail as possible to facilitate objective assessment. In urban wastewater management this would specify where (e.g. WWTP influent), what (e.g. ammonium load), and how it should be optimised (e.g. minimise). It could also contain possible adverse effects that should be avoided (e.g. without increase of CSOs or without causing more frequent flooding). Table 5.1 contains a list of possible goals classified to several RTC strategies.

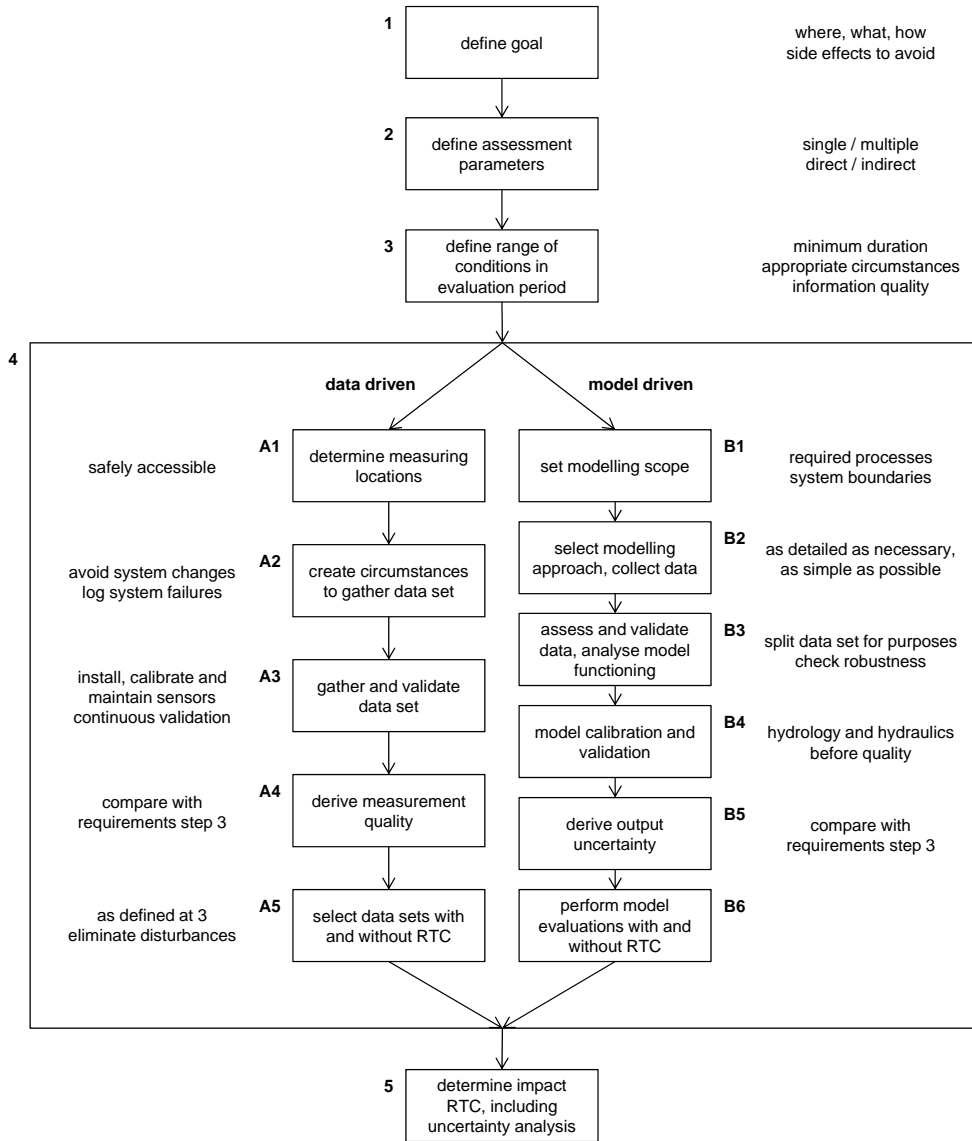


Figure 5.1: Flow chart for the proposed methodology for determining the impact of RTC in practice using a data or model driven approach.

Table 5.2: Examples of RTC goals and possible assessment parameters.

strategy	goal	assessment (examples)	
		(in)direct	parameter
emission based	pollution load reduction (at CSOs)	direct	- pollutant concentrations e.g. COD, TSS, NH4 - discharged volume - frequency and duration
		indirect	- surrogate pollutant concentrations e.g. electric conductivity, turbidity, temperature - visual pollution reports
impact based	prevention of toxic peaks	direct	- river pollutant concentrations e.g. NH4
		indirect	- CSO and/or effluent discharges - surrogate pollutant concentrations at CSOs and/or effluent e.g. electric conductivity, turbidity, temperature
operational optimisation	reduce maintenance needs	direct	- number of maintenance orders - man-hours spent on maintenance
		indirect	- number of pump switches - down time of installations

The second step is to determine an appropriate assessment parameter (step 2) to show whether the goal was reached or not. Several parameters might be interchangeable, multiple parameters could be used and also indirect parameters could help in the assessment. E.g. when aiming to reduce CSO discharges, one could try to determine lower CSO discharge capacities but maybe higher WWTP influent flows contain the same information and are more easily established. Table 5.2 contains examples of RTC goals and possible direct and indirect assessment parameters.

The third step is to determine the range of conditions needed to evaluate the performance of the applied RTC with respect to the goal (step 3). Matters of importance could be whether the interest lies in long or short term effects, anticipated variability in assessment parameters between events, if seasonal influences are expected, and if dry, wet or changing weather conditions are aimed for. From this the minimum duration and appropriate circumstances for the evaluation period can be determined. The evaluation period should naturally at least encompass the phenomenon that is assessed. As general rule of thumb the evaluation period should be quadratic to the return period of the phenomenon. This step also provides details on the required quality of the information on the assessment parameters such as the frequency and allowed uncertainty.

Further information needs and points of interest depend on the application of a data or model driven evaluation (step 4). They are described in the following sections. Both are aimed at acquiring time series for the assessment parameters representative for the systems functioning with and without RTC and with known uncertainty intervals. These can be applied to determine whether the RTC has a significant effect on the systems functioning (step 5) considering the defined goal (step 1). Since step 5 is very dependent on the assessment parameter(s) and evaluation period no further details are supplied. However, in section 5.4 an example is presented where the evaluation is performed for the specified case.

5.3.2 Data driven evaluation

When carrying out a data driven performance evaluation, great care is needed in gathering and selecting the applied data set. The main points of attention will be addressed following the items numbered ‘A’ in step 4 in the flow chart in figure 5.1. First of all (item A1), appropriate measuring locations that provide the information needed within budget should be determined (Thompson et al., 2011). Also the locations should be safely accessible and vandal-proof.

Then, the right circumstances should be created under which to gather the measurements (item A2). Changes to the system other than the implemented RTC should be avoided. If this is not possible, the changes (what, where, when, why, etc.) should be logged and communicated. This also holds for possible system failures (hardware, software, communication, etc.). Investing in a good working relation with operational personnel will pay off in this respect.

Next, the measurements themselves should be performed (item A3). Since a high quality data set is needed, much effort is required. Without going into too much detail, the sensors should be carefully installed, calibrated, maintained, and the measurement data should be adequately stored and regularly validated to ensure a high yield. More information on performing high quality measurements can be found in e.g. (Gruber et al., 2004; Schilperoort, 2011), while e.g. (Van Bijnen and Korving, 2008; Métadier and Bertrand-Krajewski, 2011) deal with validation techniques.

Along with item A3, the achieved measurement frequency and uncertainty should be derived (item A4) and compared to the requirements defined at step 3. If it is insufficient, a return to item A3 is needed to improve the quality of the measurements.

Finally, data sets with and without RTC should be selected (item A5). Here, information from step 3 (conditions needed for evaluation), item A2 (logbooks on circumstances during measuring period) and item A3 (validated data set) converge. It goes without saying that enough validated data under the right circumstances should be available to cover the conditions needed to perform the evaluation for both the situation with and without the investigated RTC active.

Note that existing data could possibly be used, e.g. for the non-controlled situation, in which case the data itself should be scrutinised and meta data on the measurements and system known in detail. While the previous description is meant for gathering a new data set, it could also serve as a guideline for working with existing measurements.

5.3.3 Model driven evaluation

The flowchart in figure 5.1 also shows the methodology for a model driven performance analysis for RTC in practice, step 4 items numbered ‘B’. It is consistent with the modelling practice described in (Muschalla et al., 2009), to which the reader is referred for more details. In this case, the first step (item B1) is to set the scope of the models. System boundaries should be defined that determine which sub systems have to be considered and which relevant processes have to be included.

As a second step, the modelling approach and the models data demand has to be considered (item B2). The modelling approach should be able to meet the requirements from step 3, which means it should be able to model the processes during the appropriate circumstances and deliver the required information. To do so, measurements are required as model input and for model calibration and validation purposes. At this stage, data should be gathered for these purposes and its general adequacy for the tasks evaluated. If no suitable data set is available, the procedure described in the previous section could be adapted for obtaining the necessary measurements.

Next, the data should be validated and assessed (item B3) to see if they meet the conditions set in step 3. Different data sets should be defined that are going to be applied in: i) the model calibration and validation at item B4, ii) the model output uncertainty evaluation at item B5, and iii) the simulations for the performance evaluation at item B6. Again, further monitoring might be necessary. Also the models functioning has to be analysed. Preliminary simulations should be checked with respect to the functioning of (possible) sub models and interfaces, and the robustness of the model output due to uncertainty in the model inputs and parameters.

To ensure the model output is representative for the investigated system the model should be calibrated (identification of the model parameters) and validated (checking the predictive capacity of the derived parameter set) (item B4). If applicable, first the hydrologic and hydraulic properties should be calibrated, followed by a calibration of any quality properties. Logically, the calibration should include the relevant processes. If, for example, high frequency output will be analysed the calibration can't be performed on daily averaged values, or WWTP models should be calibrated for wet weather situations if the response to rain events is relevant.

Based on the prepared model, the uncertainty in the output assessment parameter(s) should be derived (item B5) and compared to the requirements from step 3. For this purpose, simulations with measured input should be performed and the output should be compared to corresponding measurements for the assessment parameter(s). If the output uncertainty is too large, the previous steps need to be retraced to improve the quality of the output.

The final model specific step (item B6) is to perform model simulations with the selected data with and without RTC applied.

Similar to the measurements, also existing models might be used. In this case items B1 to B6 could be followed to check the fitness of the model for the purpose of RTC performance evaluation.

Table 5.3: Characteristics of the sewer network with basins 1 to 3 representing actual catchments and basin 4 a hypothetical transport sewer. The conversion from m^3 to mm is based on the total connected area draining to the sewer systems of the respective catchments. For basin 4 the summed connected area from basins 1 to 3 was applied.

basin	inhabitants	connected area	static storage		pump capacity
			network	tank	
	[–]	[ha]	[m^3] - [mm]	[m^3] - [mm]	[m^3/h] - [mm/h]
1	1,845	10.2	800 - 7.8	n.a.	93.6 - 0.92
2	9,526	88.4	5,747 - 6.5	230 - 0.3	1,101.6 - 1.25
3	2,318	19	861 - 4.5	586 - 3.1	140.4 - 0.74
4	n.a.	n.a.	1,176 - 1.0	n.a.	1,100.0 - 0.94

5.4 Case study

A performance analysis for two RTC scenarios is shown through a case study. The impact of the evaluation period and uncertainty analysis on the effectiveness of the RTC scenarios is investigated. The case study is based on a selection of the wastewater system of Eindhoven, the Netherlands, see (Schilperoort, 2011) for a detailed description. Three sewer catchments were selected and supplemented with a hypothetical transport sewer to a WWTP as boundary condition for explanatory purposes.

5.4.1 System characteristics

The investigated network consists of three combined sewer catchments located to the southeast of Eindhoven: Duizel (1), Eersel (2) and Riethoven (3), see figure 5.2. A fourth basin is added that represents a hypothetical transport sewer to a WWTP. These three catchments were selected to create a realistic but simple case study, i.e. limited in size and no influences from other sewer systems.

The sewers consist of combined gravity systems with several mm in-sewer storage and limited emptying capacity through pumps (typically $<1 mm/h$). Excess wastewater during heavy rainfall is discharged to the surface water through CSOs. Contrary to Duizel, the sewer systems of Eersel and Riethoven are equipped with storm water settling tanks (SSTs) that serve as additional storage prior to discharge to the surface water. An additional CSO without storage is available for the hypothetical transport sewer. The network characteristics are given in table 5.3.

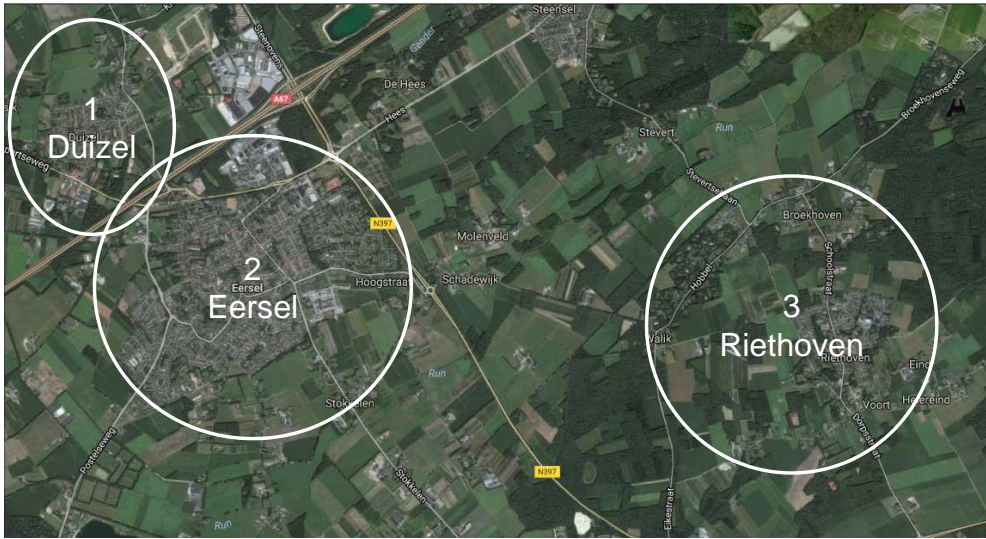


Figure 5.2: Geographical location of the sewer catchments, located to the southeast of Eindhoven, as applied in the simplified sewer model (source: google maps).

Table 5.4: Rainfall characteristics for catchment 1, which is similar to other catchments. The event volume >5 mm is selected as a measure for events that are relevant for CSO discharges based on the in-sewer storage in table 5.3.

year	total annual rainfall [mm]	number of events [–]	number of events with total rainfall volume > 5 mm [–]
2011	748	226	45
2012	826	266	50
2013	699	216	41

5.4.2 Measurements

Radar rainfall measurements for the Netherlands with a 1×1 km resolution are performed at a five-minute interval by the Royal Netherlands Meteorological Institute. For each catchment, the radar measurements for the years 2011 to 2013 were applied. Table 5.4 summarises some rainfall characteristics for catchment 1, which is very similar to the characteristics for the other catchments. Compared to the mean annual rainfall in the Netherlands (~ 800 mm), especially 2013 was a relatively dry year. In 2013 also fewer events occurred that could have led to CSO activity.

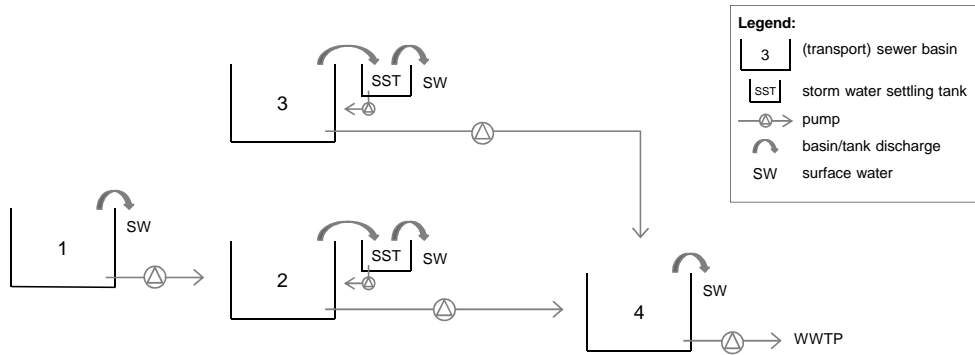


Figure 5.3: Overview of the simplified sewer model.

At the pumping stations of catchments 1 to 3 water flows (Hach, Flo-Tote) are registered at a one-minute interval as part of daily operation.

5.4.3 Model

A simplified model for the sewer network, an overview of which is shown in figure 5.3, is built in Matlab[®] to simulate the water flows in the sewer network with a one-minute interval. The model consists of one lumped basin per catchment and converts sewer inflows (dry weather flow (DWF), runoff, pump discharges from other basins), via the basin volume, into outflows (pump and CSO discharges). Basin 4 represents a transport sewer and only receives inflow from basins 2 and 3.

Regarding the inflows, diurnal DWF profiles with a water consumption per inhabitant have been generated from the flow measurements at the pumping stations following the procedure described in (Van Daal-Rombouts et al., 2016b). Runoff is calculated from the rainfall series following the Dutch guidelines through the NWRW-model that takes into account evaporation, initial losses, infiltration (Horton approach) and routing delays (linear reservoir). For more information see (Van Luijtelaaar and Rebergen, 1997).

The outflows are based on the filling degree (FD) of the basins, which is the current volume in the basin divided by the static storage volume of the represented sewer network. Pumps switch on at 2% FD with a linearly increasing capacity until the maximum is reached at 5% FD. For decreasing FDs the pumps remain at their current capacity until the systems are empty. CSOs immediately discharge all water volume above 100% FD. If multiple CSOs exist in the sewer network, they are lumped into one in the simplified model.

SSTs are modelled as separate basins located between a CSO and the surface water. Similar to the CSOs they immediately discharge all water volume in the SST above 100% FD. Filled SSTs are emptied into the corresponding sewer basin in ten hours after the FD in the affected basin falls below 50%.

The simplified model structure applied is similar to the models M2 and M3 in chapter 3, but not the same. The runoff model applied here was selected to agree with the Dutch standards. The runoff model applied in chapter 3 was selected based on international standards. Also for this research some further simplifications were made, such as not applying storage-level curves in the basins, as water levels are not relevant for the case study and the conversion from water volume to water levels would slow down the simulations.

5.4.4 Uncertainty analysis

Uncertainties are included through a forward uncertainty analysis, executed through Monte Carlo simulations. 1,000 replicates are simulated and ranked after which the median value (50%) and upper (95%) and lower (5%) boundaries are extracted. Uncertainties in the basin volumes (including dynamic storage) and maximum pump capacities are taken into account according to a normal distribution with 95% confidence intervals of 20 and 10% above and below the mean, respectively. No correlation between the uncertainties of the parameters and catchments are assumed. The sampled uncertainties have, however, been kept the same between RTC scenarios to compare their results. The confidence intervals and number of parameters were selected at the lower end of the representative scale so that the uncertainty in the model output remains as limited as possible.

No uncertainties in the runoff were taken into account, although it is noted that large uncertainties arise from the rainfall and subsequent conversion to runoff. For the sake of the example however, the interest lies in the effect of the RTC on the sewer system functioning (and in this case sewer model functioning) given a specific runoff. This situation reflects practical situations where the runoff is not exactly known, but does not change. Furthermore, the proposed RTC in no way affects the runoff and makes use of hydraulic input only, by-passing uncertainties in the hydrological models. Both present further reason to exclude runoff uncertainties. This does not imply that whatever runoff can be applied. It should be representative for the actual rainfall and contain enough variation to account for the conditions in which the RTC should be functioning. In this example, it is deemed that the first condition is sufficiently covered by taking an established runoff model as described in the previous section. The second condition will be elaborated upon in the results and discussion sections.

Following the same reasoning, also no uncertainties are taken into account for the DWF. The representativeness is covered by applying calibrated DWF profiles. However, no variation during the year is present. As the DWF accounts for an equivalent of only several *mm* runoff per day and expected variations are <50%, this is not deemed to influence the results.

5.4.5 RTC scenarios

Two rule-based RTC scenarios have been implemented. Both scenarios are based on expert judgement, i.e. no optimisation of the rules was performed. Also no predictive control was applied.

CSO reduction (RTC CSO)

This RTC aims to reduce CSO activity (number of events and total discharged volumes). The following rules have been implemented:

1. *if* the filling degree (FD) of any basin >80% *then* pump at maximum capacity;
2. *if* the FD of an upstream basin < FD of a downstream basin *then* limit the maximum pump capacity of the upstream basin to 85%.

Maximum WWTP inflow reduction (RTC WWTP)

This RTC aims to limit the maximum discharge to the WWTP (pumped discharge of basin 4) without increasing CSO activity. The following rules have been implemented:

1. *if* the filling degree (FD) of basin 4 $< 80\%$ *then* limit the maximum pump capacity of basin 4 from 1,100 to $825 \text{ m}^3/\text{h}$;
2. *if* the FD of any basin $> 80\%$ *then* pump the respective basin at maximum capacity;
3. *if* the FD of an upstream basin $<$ FD of a downstream basin *then* limit the maximum pump capacity of the upstream basin to 75%.

5.4.6 Results

Before looking into the impact of the RTC scenarios on the systems functioning, first the representativeness of the model results for the uncontrolled scenario (from here on referred to as ‘reference scenario’) was checked. For this purpose, the average number of CSO events per year (~ 10), the total volume discharged through CSOs relative to the total inflow ($\sim 3\%$) and the percentage of time the pump capacities surpassed 25% of the maximum capacity ($< 10\%$) were calculated for the median model result. All characteristics match with normal behaviour for sewer systems in flat areas that contain large in-sewer storage volumes and are emptied through pumps discharging to a WWTP, see e.g. (Korving, 2004). Therefore, the model is found to represent the sewer systems functioning accurately enough for the purpose of this example.

5.4.6.1 RTC CSO

The impact of the RTC CSO scenario compared to the reference scenario, for the individual basins for the entire simulation period (2011 to 2013) and the separate years, is displayed in figure 5.4. Hardly any difference can be found for the number of CSO events and total CSO volume. For both parameters, for every basin and for all displayed periods, overlap between the confidence bands of the scenarios occurs. The median values do show change. For basins 1 to 3 the total CSO volume increases by 0 to 3.8% without changing the number of events. Because of this, less water is transported to basin 4 where all CSO events (and thus all CSO volume) are prevented in case of the RTC CSO scenario. Looking at the total network, the median number of CSO events decreases by 17% and the total CSO volume by 5%. Due to the wide confidence bands this change is not significant.

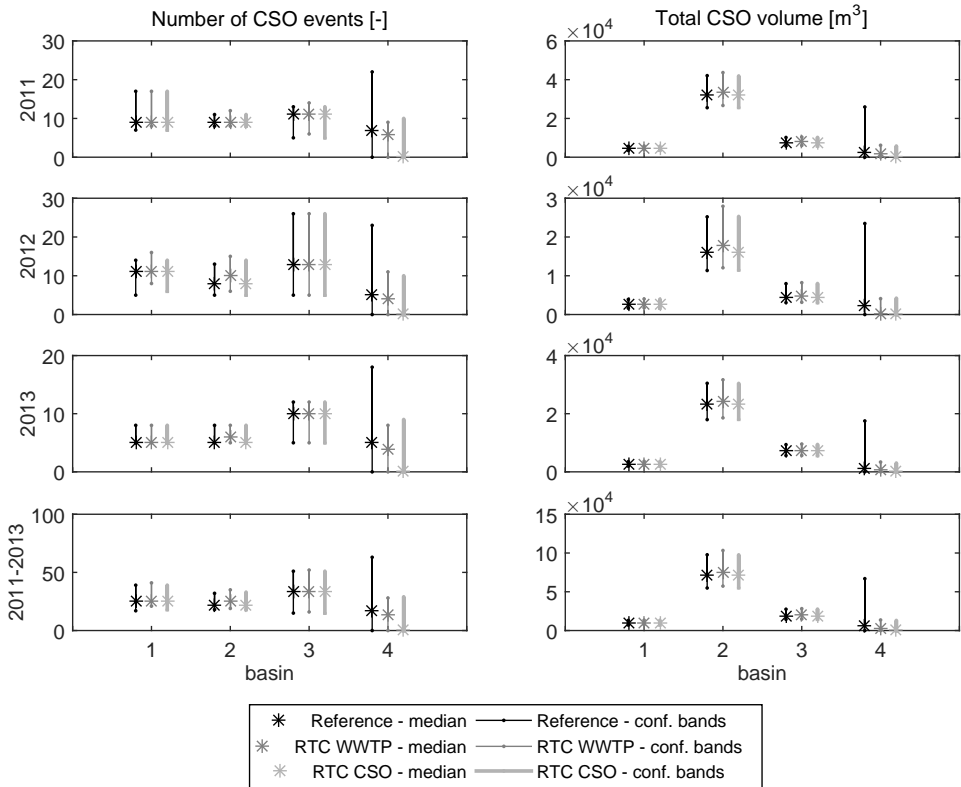


Figure 5.4: Number of CSO events (left) and total CSO volume (right) for each basin. From top to bottom first all years are displayed separately, followed by all years combined. In the graphs the results for the reference scenario and each of the two RTC scenarios are shown. Note the changing scales on the y-axis.

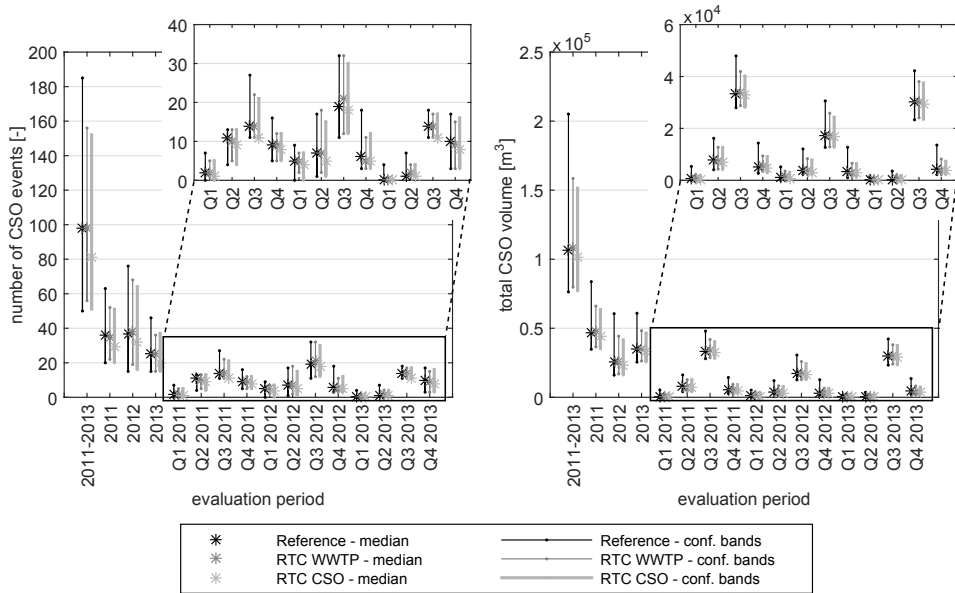


Figure 5.5: Number of CSO events (left) and total CSO volume (right) for all basins summed for simulations with the reference scenario and with each of the two RTC scenarios. On the horizontal axis different evaluation periods are given from all years together via separate years to separate quarters.

The uncertainties in both number of CSO events and CSO volume are much larger for basin 4 in the reference situation than in the controlled situations. This is because in the controlled situations the outflow of basins 1 to 3 is limited regardless to the sampled uncertainty in the pump capacity, reducing the inflow of basin 4. This cumulative effect leads to much smaller confidence bands in the investigated parameters in the controlled scenarios.

Figure 5.5 displays the same parameters, but now for the total system (sum of individual basins) and with more differentiation in the assessment periods. When comparing the effectiveness of RTC within one period (e.g. 2011 or Q3 2013 with and without control), as one could do for a model driven evaluation, the same results are found as previously described: the median values change (a decrease for the total number of events of 0 to 29%, and a decrease for the total CSO volume of 0 to 8%) but the confidence bands overlap for every period.

When comparing scenarios over different periods (e.g. 2011 for the reference situation with 2012 for RTC CSO, or Q2 2012 with Q3 2012), as one would do for a data driven evaluation, different results are found. Now the confidence bands sometimes do not overlap (e.g. Q2 and Q3 2011), indicating a significant influence from the applied RTC. The median values for comparison between adjacent quarterly periods, however, change between an improvement and a deterioration (100% improvement to 1000% deterioration for the total number of events, and 100% improvement to >1000% deterioration for the total CSO volume). When comparing full adjacent years only, the median still changes sharply (a decrease in the total number of events of 11 and 46%, and for the total CSO volume a decrease of 50 and an increase of 32%) and the confidence bands overlap again, so no definitive effect can be established anymore.

Finally, it is remarked that the influence of the annual rainfall and the number of events with a significant volume on the CSO activity, see table 5.4, is ambiguous. Both reflect the mean number of CSO events in a year (2012 highest, 2013 lowest), but for the total CSO volume this is opposite (2012 lowest, 2013 highest). This is to be expected as CSO activity is governed by more extreme rain events.

5.4.6.2 RTC WWTP

The impact of the RTC WWTP scenario on the pump capacity of the individual basins, for the entire simulation period (2011 to 2013) compared to the reference scenario, is displayed in figure 5.6. It contains the final 20% of the cumulative density functions (CDFs) of the pump capacity normalised to the maximum capacity. I.e. each pump capacity time series is ranked, normalised and the final 20% is displayed. The control clearly changes parts of the CDFs, but the confidence bands overlap everywhere for basins 1 and 3. For basins 2 and 4, that receive inflow from upstream basins, significant changes are found. Looking at median values for the discharge to the WWTP (basin 4), the RTC WWTP scenario decreases the duration of pumping at >0.9 times the norm capacity by 89%, at the cost of an increase of 31% pumping at >0.67 times the norm capacity. A decrease of the highest pump capacities is expected to be accompanied by an increase in lower capacities as the total discharge to the WWTP should stay approximately the same.

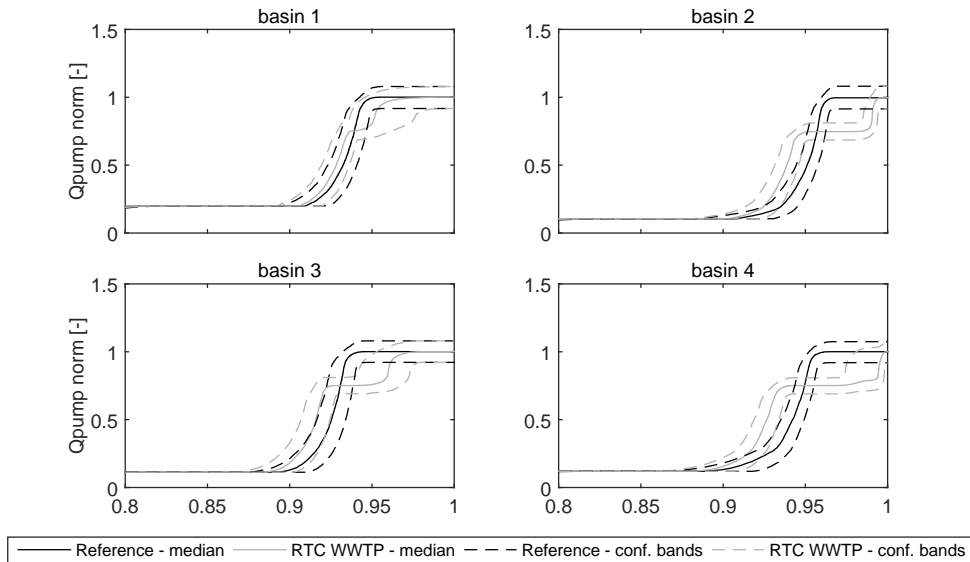


Figure 5.6: Pump capacity normalised to its maximum capacity for each basin for all years for simulations with the reference scenario and the RTC WWTP scenario. Normalised pump capacities of 1.1 are a result of the application of 10% uncertainty intervals in the Monte Carlo simulations.

The RTC WWTP scenario was restricted to induce no negative side effects on the CSO operation. As can be found from figures 5.4 and 5.5 there is no indication of a significant negative effect on either the number of CSO events or the total CSO volume when compared to the reference scenario. The median number of CSO events for the entire period and total system stays the same, while the total CSO volume increases by an insignificant 1%.

In figure 5.7 the results for the discharge to the WWTP (basin 4) are displayed in more detail. It shows the percentage of time the normalised pump capacity is >0.67 (left) and >0.90 (right) with distinction in the evaluation period. Similar to the results for RTC CSO in figure 5.5, the results differ between evaluation periods. In this case, however, when comparing within one period the impact of the RTC WWTP scenario with respect to the reference scenario is significant for all evaluation

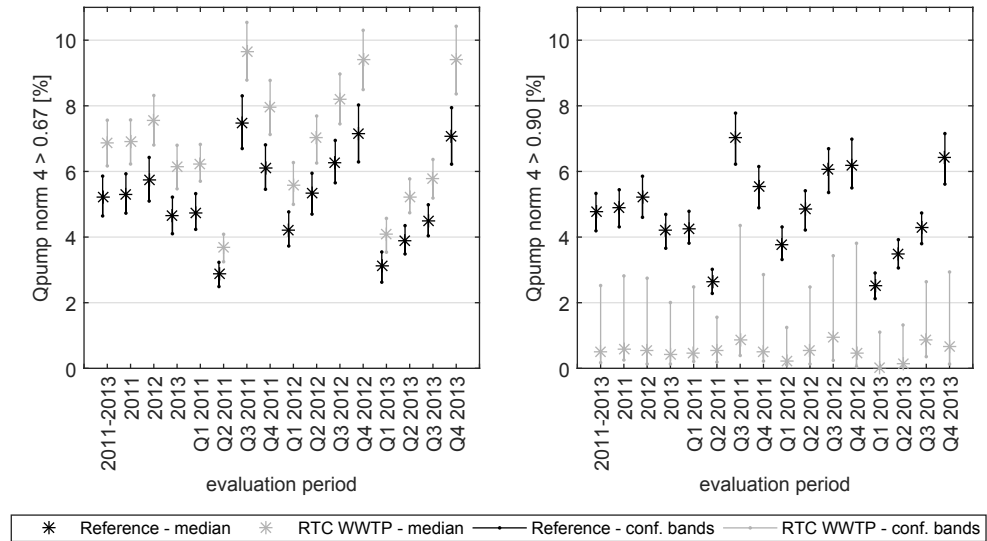


Figure 5.7: Percentage of time the pump capacity normalised to the maximum capacity of the WWTP (basin 4) is >0.67 (left) and >0.90 (right) for simulations with the reference scenario and the RTC WWTP scenario. On the horizontal axis different evaluation periods are given from all years together via separate years to separate quarters.

periods examined: the RTC WWTP scenario decreases the duration of pumping at >0.90 times the norm capacity by 80 to 100%. When comparing between adjacent quarterly periods, RTC WWTP in all cases decreases the duration of the maximum pump capacity for the median value. The range of the decrease of the duration of the maximum pump capacity widens to 67 to 100% and in some cases the improvement is not significant anymore (see e.g. Q2 and Q3 2011).

5.5 Discussion

5.5.1 Case study results

The case study presents a clear illustration of several aspects related to the evaluation of the effectiveness of RTC in practice:

- The susceptibility for RTC and its effectiveness is very much dependent on the goal that is aimed for. In the case study a reduction in CSO activity (events or volume) could hardly be achieved even looking at the median values only. Contrary to the RTC CSO scenario, the RTC WWTP scenario showed great potential in reducing the WWTP influent with significant differences between the reference and controlled situation. The RTC WWTP scenario focussed on reduction of influent flows (quantity). Reducing peak influent flows also reduces peak loads to the biological treatment of the WWTP, thereby also improving the treatment performance (quality) (Langeveld et al., 2002).
- The evaluation period was shown to influence the outcome of an evaluation of the effectiveness of RTC to a very large extent, due to the variability in rainfall. Comparing between the same period (for a model driven evaluation) results differ between no effect and 30% reduction for the RTC CSO scenario. Comparing adjacent years (for a data driven evaluation) the results for the RTC CSO scenario differ up to 30% for the number of CSO events and up to 80% (spanning both reduction and increase) for total CSO volume. For the RTC WWTP scenario the influence of the evaluation period is smaller, but still the outcome differs up to 33% when comparing adjacent quarterly periods. This asks for a careful consideration of the selected evaluation period when determining the effectiveness of RTC. Especially in case of CSO related parameters, which depend on less often occurring rain events, an evaluation period lasting at least the square of the return period should be applied.
- For many evaluation periods in the example, the median values do respond to the imposed RTC scenarios and often in the desired way. Without uncertainty analysis it would have been credible to present these results as the effect of the imposed RTC. However, especially for the RTC CSO scenario, the uncertainty analysis reveals that the uncertainty bands are up to an order of magnitude larger than the effect itself. This shows the particular importance of including uncertainty analysis in any RTC evaluation.

In the case study it was decided to include the minimum number of parameters to describe the systems functioning, as well as limited uncertainty intervals for these parameters. In this way the resulting model output uncertainty was as limited as possible. Still, the output uncertainty was largely dominant over the effect of one of the control scenarios. Including more sources of uncertainty, in the model input through for example the rainfall or connected area, or by applying a more elaborate model structure and thus more parameters, leads to even larger output uncertainties. This could result in the situation that no significant effect of any RTC scenario could be determined. To prevent this situation, thorough calibration and verification of the applied models is necessary, or a data driven evaluation should be adopted. In the next section this will be discussed further.

5.5.2 Methodology

For the final performance evaluation, it is not important if a data or model driven approach is taken. Both approaches have advantages and disadvantages, as listed in table 5.5, and for each situation a well-founded choice should be made and communicated.

Executing a performance analysis following the proposed methodology will take considerable effort. Gathering of measurements and preparation of models to the required standards, as mentioned in section 5.3.2 and 5.3.3, is challenging. Nevertheless, to quantify the effect of RTC, the use of sufficient quantity and quality measurements and models is necessary. Part of these tasks should already have been performed when designing and implementing the RTC. Careful planning before implementation of the RTC and choosing the appropriate approach (data or model driven) will result in a minimal additional effort required. From a scientific point of view, an evaluation should aim at quantifying the effect or RTC measures. In a commercial setting, the willingness of a client to invest in a quantitative evaluation will be closely related to the gains the RTC is supposed to provide. If substantial investments in for example the treatment process depend on the performance of an implemented RTC strategy, the additional required effort will not be problematic. The practical applicability and consequences of the methodology have been investigated for an implemented RTC scheme in the wastewater system of Eindhoven and are described in the next chapter.

Table 5.5: Advantages and disadvantages of a performance evaluation with the assessment through measurements or models.

assessment	(dis) advantages	examples
data driven	advantages	<ul style="list-style-type: none"> - measurements contain information on the true functioning of the system that a model can never achieve - smaller uncertainty bands because errors are not propagated through models - operators usually have insight in measurements needed for an evaluation, which could enlarge the acceptance of the implemented RTC
	disadvantages	<ul style="list-style-type: none"> - difficulty of obtaining high quality, simultaneous measurements at relevant locations - two evaluation periods are needed (with and without RTC) with representative and comparable conditions
model driven	advantages	<ul style="list-style-type: none"> - assessment possible based on parameters that are difficult to measure due to practical constraints - possibly clear comparison is feasible between scenarios based on only one evaluation period (see next point)
	disadvantages	<ul style="list-style-type: none"> - transferability of parameters sets between events was shown to be low by e.g. (Korving and Clemens, 2005). Applying RTC may require a new calibration and corresponding measurements for those parts of the model influenced by the control - large uncertainty bands because errors are propagated through models and additional errors associated with parameter identification - measurements are needed for the preparation of the models and to determine the uncertainties, which could possibly also be applied in the evaluation directly

The case study highlighted the problem of determining a significant effect for RTC when small improvements are aimed for. One way to overcome this is the application of high accuracy measurements so that the uncertainty bands are strongly reduced. In a hypothetical experiment, the RTC CSO scenario for the case study can be shown to significantly cause a reduction in CSO volume for basin 4. This entails taking the median values from the simulated results and assuming these are measurements with corresponding uncertainty bands. The uncertainties were based on the paper by (Campisano et al., 2013) and were taken to be 1% for flow measurements in filled pipes (applied for the pump capacities) and 5% for flow measurements in partly filled pipes (applied for CSO discharges). As these percentages are deemed optimistic by the author and a high yield for (simultaneous) measurements remains problematic, high accuracy and robust sensors are called for.

The RTC scenarios in the case study focus on reducing water quantity discharges. The methodology, however, is not restricted to quantity oriented performance evaluations. Also RTC aimed at objectives such as pollution or energy reduction could be evaluated using the same methodology.

Finally, the proposed methodology can also be applied for determining the expected effectiveness of a designed RTC strategy if historic measurements are available. The outcome could help decide if the RTC should be implemented or redesigned. It would also provide valuable information for the actual performance evaluation such as an estimate on the expected effect and the accuracy needed to significantly determine it, the locations for which information is needed, whether the available meta information on the system is satisfactory and if the conditions needed for the evaluation are adequate.

5.6 Conclusions and recommendations

This chapter dealt with the performance evaluation of RTC in practice in urban wastewater systems that at least encompass a combined sewer system. A review of literature on this topic demonstrated a lack of consensus on how to do this. In the procedures described two main deficiencies were identified: omitting uncertainty analysis and applying too limited evaluation periods. A general methodology was proposed to evaluate the performance of RTC that is either data or model driven and takes into account these deficiencies. What approach should be applied is case dependent. It is up to the engineer or researcher to choose the most appropriate approach and communicate the motivation for this choice.

A performance analysis of two RTC scenarios was shown through a case study for a combined sewer system with limited discharge capacity to a WWTP. It was demonstrated that the susceptibility of a case for the successful application of RTC and the possibility to determine a significant effect is very much dependent on the goal. It also clearly illustrated the need for taking uncertainties into account and that careful consideration in the selected evaluation period is required.

When RTC aims for small improvements, small uncertainty bands are needed to be able to determine a significant effect. To this end, sensors that are more robust and high accuracy than the ones now available are necessary. Also dedicated attention is required to ensure sensor output reaches its full potential.

Although some RTC systems should have been operational for over a decade, no publications were found that deal with the functioning and effectiveness of these systems after several years. It would be of great benefit for the field of urban wastewater management if these experiences would be shared.

6 Application of the methodology on the wastewater system of Eindhoven

6.1 Introduction

Although real time control (RTC) has been implemented in urban wastewater systems in practice at multiple locations, the effectiveness of the applied control has not yet been established as argued in sections 1.2 and 5.2. Additionally, no uniform methodology was found for the performance evaluation of RTC in wastewater systems for case studies. Therefore, in the previous chapter a methodology was proposed for this purpose, in which the evaluation period is considered and uncertainties are taken into account. This chapters deals with the practical application of the methodology on a case: the wastewater system of Eindhoven, where two impact based RTC scenarios were designed, implemented and evaluated.

As described in section 1.4, the wastewater system of Eindhoven is characterised by a densely populated area that poses a large stress on the local receiving waters, consisting of small lowland rivers and creeks, through wastewater treatment plant (WWTP) effluent and numerous combined sewer overflows (CSOs). The ecological water quality is affected by dissolved oxygen (DO) depletion and ammonium (NH₄) peaks. Previous research by (Langeveld et al., 2013) has shown the WWTP to be an important source for both NH₄ peaks and DO depletion and that application of integrated, impact based RTC could help mitigate these problems.

This chapter is an adapted version of: Van Daal-Rombouts, P.M.M., Benedetti, L., De Jonge, J., Weijers, S.R., Langeveld, J.G., (*submitted*). Performance evaluation of a smart buffer control at a wastewater treatment plant. *Water Research*.

Table 6.1: List of abbreviations.

abbrev.	explanation
BS	booster pumping station between PCs and activated sludge tanks
CSO	combined sewer overflow
DO	dissolved oxygen
DWF	dry weather flow
EFF	effluent
ES	catchment Eindhoven Stad
INF	influent
H	water level
m_{AD}	Normal Amsterdam Water Level
MG	mixing gutter after influent pumping station
NH ₄	ammonium
NS	catchment Nuenen-Son
PC	primary clarifier
Q	flow
Q_{BIO}	total flow to the activated sludge tanks
Q_{BIOmax}	maximum current hydraulic capacity of the activated sludge tanks
Q_{ES}	influent flow from catchment ES
Q_{INF}	total influent flow from all three catchments
Q_{INFmax}	maximum current total influent capacity from all three catchments
Q_{NS}	influent flow from catchment NS
Q_{RZ}	influent flow from catchment RZ
Q_{SST}	flow towards the SST
RMSE	root mean squared error
RTC	real time control
RZ	catchment Riool Zuid
SST	storm water settling tank
WWF	wet weather flow
WWTP	wastewater treatment plant

The implemented, complementary controls aim at improving the use of the available tanks at the WWTP and storage volume in the contributing catchments:

- Storm Tank Control. Optimises the operation of the WWTP storm water settling tank (SST) with respect to the contributing catchments to reduce unnecessary discharges of the SST and subsequent DO depletion;
- Primary Clarifier Control. Optimises the operation of the primary clarifiers (PCs) and influent pumping station to reduce peak loading of the activated sludge tanks and subsequent NH₄ peaks.

This chapter is organised as follows. Table 6.1 contains a list of abbreviations applied in this chapter. Section 6.2 recaps the main features of the wastewater system, and introduces the WWTP, RTC scenarios and the methods applied in the performance evaluation. Section 6.3 describes the results of the performance evaluation, which is followed by a discussion on the results in section 6.4. Finally, conclusions are presented in section 6.5. Supplementary material on the implementation of the RTC scenarios can be found in appendix D.

6.2 Materials and method

6.2.1 The wastewater system of Eindhoven

The wastewater system of Eindhoven is displayed in figure 6.1 and consists of a WWTP, three combined sewer catchments and the river Dommel as receiving surface water for the WWTP effluent and approximately 200 CSOs.

Sewer catchment Eindhoven Stad (ES) serves the city of Eindhoven and contributes approximately 45% to the total influent of the WWTP. Sewer catchment Riool Zuid (RZ) serves seven municipalities south of Eindhoven through a 31 *km* transport sewer and also contributes approximately 45% to the WWTP influent. Sewer catchment Nuenen-Son (NS) is located to the northeast of Eindhoven and represents less than 10% of the influent; in terms of optimisation of the wastewater system NS is considered insignificant. As the WWTP is located in Eindhoven, with a connected area of

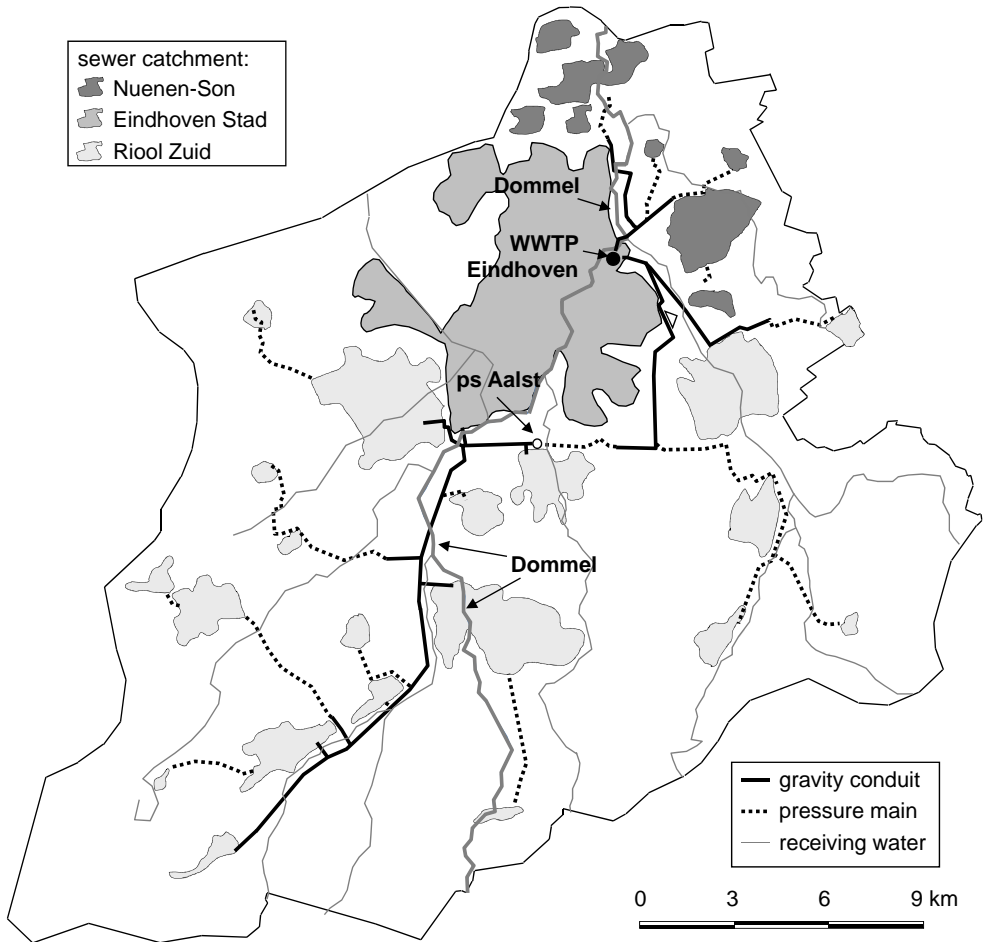


Figure 6.1: Overview of the wastewater system of Eindhoven. Figure adapted from (Schilperoort, 2011).

approximately 2000 *ha* and which' sewer consists of one looped gravity system, the functioning of ES is strongly influenced by the operation of the influent pumping station. This influence is much less significant for RZ due to the transport sewer, where pumping station Aalst acts as a barrier and several municipal sewer systems are connected through pumps. In the transport sewer between the WWTP and pumping station Aalst approximately 10,000 m^3 idle storage is available.

The receiving waters consist of a network of small lowland rivers that eventually combine into the river Dommel which originates in Belgium and flows northward into the river Meuse. In dry summer periods the WWTP effluent can constitute up to 50% of the rivers base flow, under storm conditions this increases to 90%.

6.2.2 WWTP Eindhoven

A schematic overview of the WWTP of Eindhoven is displayed in figure 6.2. The WWTP has a capacity of 750,000 population equivalent and a maximum hydraulic capacity of 35,000 m^3/h . It generally consists of an influent pumping station with a pumping chamber for each catchment and three identical treatment lines. Each treatment line has a maximum hydraulic capacity of 8,750 m^3/h and consists of one PC, an activated sludge tank and four secondary clarifiers. In between the PCs and the activated sludge tanks the water is mixed at a booster pumping station (BS). To bypass the treatment lines in case of high inflows, a storm water settling tank (SST) is available to store and eventually discharge partly settled wastewater.

6.2.2.1 Measurements

Quantity and quality measurements are performed at the WWTP as part of daily operation. For this study only a small number of measurements is used as indicated in figure 6.2:

- Influent flows (Siemens Danfoss, Sitrans FM Magflow) from the catchments and flows to the activated sludge tanks (derived from revolutions Archimedian screws). At 6 April 2016 an additional flow (derived from revolutions Archimedian screws) to the SST became available;
- Water levels in the influent chambers and the SST (Vega, Vegawell);

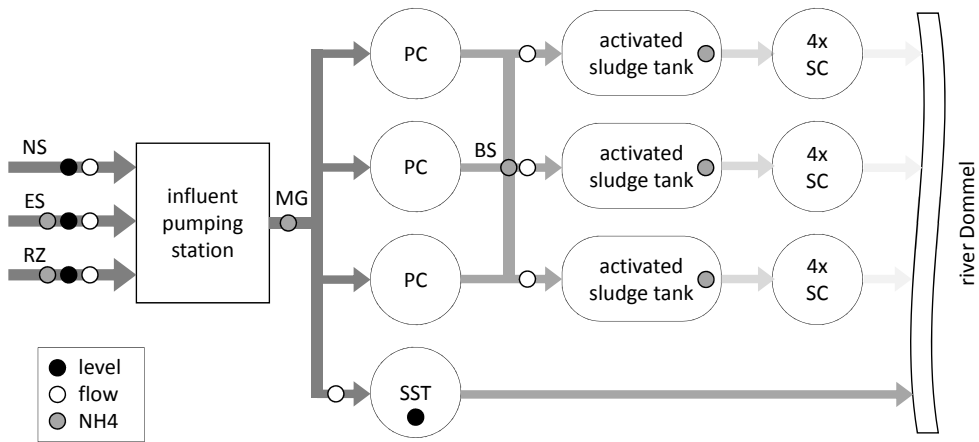


Figure 6.2: Schematic overview of WWTP Eindhoven. Relevant measuring locations are indicated by dots. The NH₄ measurement at the booster pumping station measures the mixed flow to the activated sludge tanks.

- NH₄ concentrations (Hach, Amtax) in the influent flows of ES and RZ, in the mixing gutter before the PCs (referred to as MG), in the flow towards the booster station (BS) and in each activated sludge tank.

All flow and water level measurements are near continuously available in the WWTP SCADA control system. The NH₄ measurements are performed every five minutes.

Water levels (Vega, Vegabar 66) at all CSOs in the contributing sewer catchments are measured at a one-minute time step. These measurements are sent to a central database every 24 hours, making them available for system analysis but not for active control.

Data handling

The monitoring data applied in this study shows deficiencies. To be able to apply the data in direct analysis and as input for WWTP model simulations, these deficiencies were remedied. For this purpose, all data was post processed to generate a uniform time axis with a one-minute time step and missing individual data points were filled through linear interpolation. Additional processing was performed for the flow and NH₄ measurements as described below.

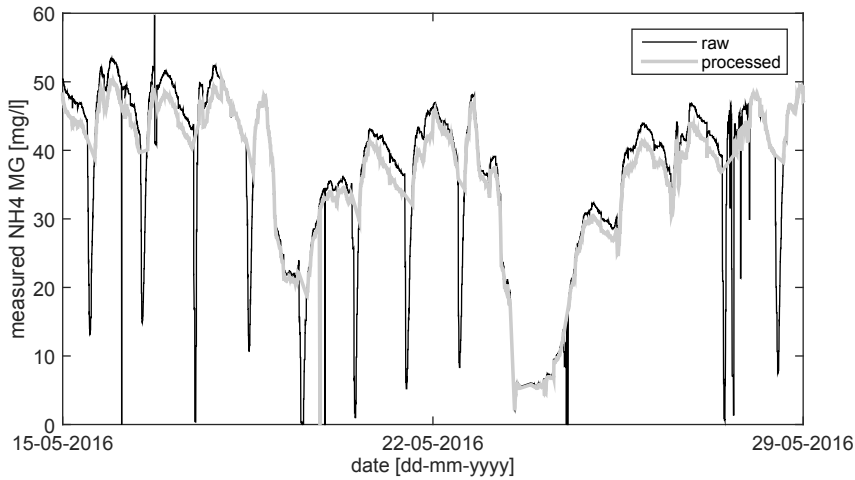


Figure 6.3: Example of the impact of the applied corrections to the measured NH4 concentrations at location MG.

Communication errors lead to two and five hours of missing data on 19 and 23 May 2016 respectively. As this occurred during two large rain events, the WWTP was at its maximum intake before and after the communication error. The missing flow values were filled by the linear interpolation between the last and first available measurements.

For the NH4 measurements, no additional corrections were made for locations ES and RZ as only selected periods have been applied. For locations MG and BS, the analysers experienced problems with an automatic cleaning and calibration procedure. The resulting repetitive drops in the registered data series were removed.

The NH4 sensors at locations MG and BS are redundant as they are separated by a PC only, introducing a time shift but having little influence on the NH4 concentration (correlation factor $R^2 = 0.79$ over a period of 5.5 months). Using the measurements at BS, six periods of missing data or general sensor failure at location MG were filled or replaced with time shifted data. Finally, drift in the NH4 measurements at location MG was corrected to a daily average of 45 mg/l based on 24-hour composite samples at the same location. Figure 6.3 displays an example of the raw and processed NH4 measurement series for location MG.

6.2.2.2 WWTP model

The WWTP is modelled with the WEST simulator (www.mikepoweredbydhi.com) using a modified activated sludge model No. 2D bio kinetic model (Gernaey and Jørgensen, 2004). A specific secondary settling model developed to cope with wet weather conditions (sludge buffering and peaks of effluent solids) was applied (Benedetti et al., 2011).

The available monitoring and process control data allowed a thorough calibration combined with an analysis of the required model structure. The model is calibrated on data from 2010 by adjusting the bio kinetic model parameters as little as possible, while paying more attention to the quality of data and information on system characteristics and operation.

It is considered beyond the scope of this paper to go into detail on the model setup and calibration. More details can be found in (Amerlinck, 2015). The model verification is described in section 6.2.4.3.

6.2.2.3 Standard control

In the standard WWTP control the SST is operated during all storm events as intended in its design: the total influent is split equally over three treatment lines and one water line. From an integrated point of view many of these SST discharges are deemed (partly) unnecessary as there is no threat of discharges from the CSOs in the contributing catchments, as shown in figure 6.4. Furthermore, if SST discharges are necessary, the SST is operated well below its maximum capacity (not shown in figure), possibly causing needless CSO discharges. As the CSOs are generally not equipped with settling tanks, discharges from the SST are preferred to minimise pollution to the receiving water.

The standard control for the PCs operates all three PCs (total volume 26,250 m^3) alike and continuously. During dry weather flow (DWF) conditions the tanks are filled with raw sewage and have a hydraulic retention time of four hours, which reduces to one hour for maximum influent flows. At the onset of a rain event the stored concentrated sewage is transported at wet weather flow (WWF) rate to the activated sludge tanks. The resulting peak load to the aeration tanks contributes to NH_4 peaks in the WWTP effluent. In figure 6.5 some examples are shown where clear NH_4 peaks were measured in the activated sludge tanks during rain events following DWF conditions on 1 and 15 November 2013 and 21 March 2014.

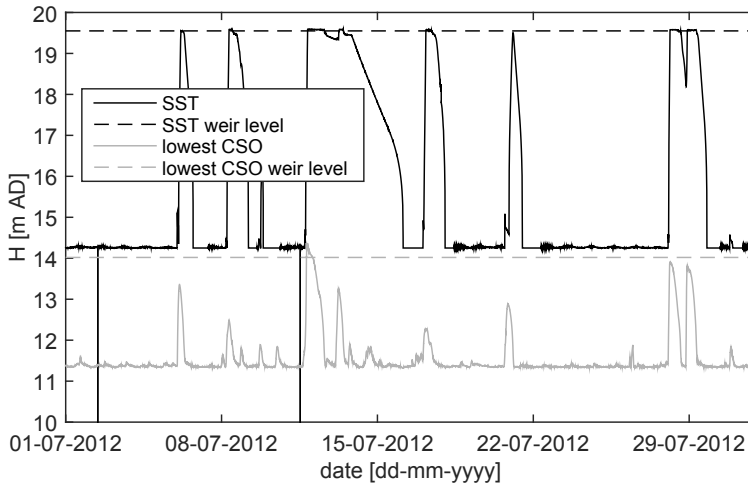


Figure 6.4: Example of the water level in the SST with the SST weir level and the water level at the CSO location with the lowest weir level for July 2012.

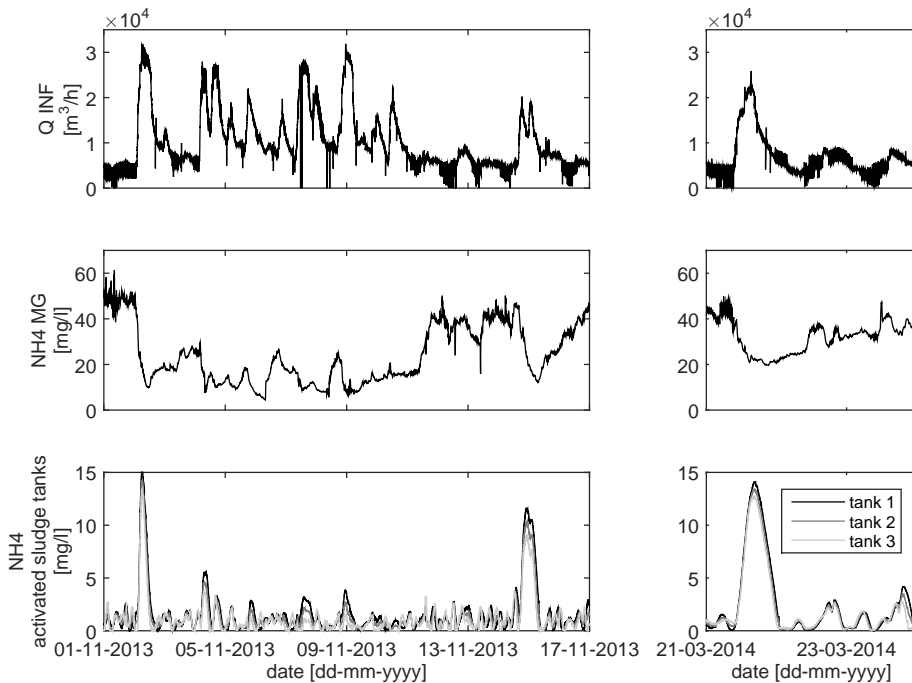


Figure 6.5: Example of NH4 peaks in the activated sludge tanks.

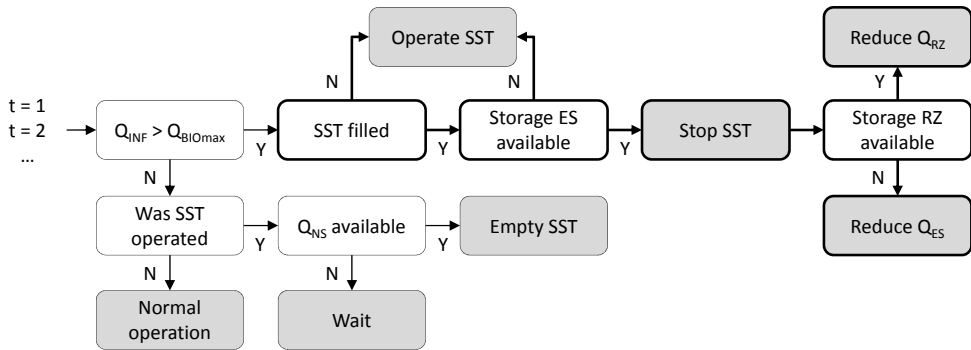


Figure 6.6: Flow diagram of SST operation with the Storm Tank Control. Flow is followed for every time step in WWTP SCADA control system. Thick black lines indicate changes with respect to the standard control.

6.2.3 Storm Tank Control

6.2.3.1 Aim

The Storm Tank Control aims to optimise the operation of the SST with respect to the sewer catchments to i) reduce unnecessary SST discharges and subsequent DO depletion in the receiving waters and ii) utilise the SST to its full capacity when discharges are necessary for minimisation of CSO discharges. At the same time an increase in the number of CSO events in the catchments should be avoided.

6.2.3.2 Design

The Storm Tank Control incorporates the functioning of the contributing sewer catchments ES and RZ into the operation of the SST through the water level measurements in the respective influent chambers. A flow diagram of the Storm Tank Control is displayed in figure 6.6, where thick black lines indicate changes with respect to the standard control. The SST is operated when the total influent flow (Q_{INF}) surpasses the current maximum flow to the activated sludge tanks (Q_{BIOmax}) under the condition that it may only discharge if the CSOs of ES are prone to spill. Nevertheless, the SST is allowed to fill independent of the water level in ES to make use of the storage capacity of the tank.

Storage in the catchments is activated if the water level in ES remains below a certain threshold by reducing the influent flow from either ES or RZ, where RZ is reduced whenever possible to use the available idle storage. Once the water level in ES rises above the threshold, the SST is operated at its maximum allowed capacity to favour SST discharges over regular CSO discharges. As soon as the water level in ES falls below the threshold, the SST is taken out of operation reducing the duration of SST discharges. The SST emptying procedure was not changed; it is emptied back into the influent chamber of NS once influent capacity for NS (Q_{NS}) is available.

6.2.3.3 Evaluation

The Storm Tank Control is evaluated based on measurements following the methodology depicted in the flow chart in 5.1. Two data sets representative for the SST functioning with the Storm Tank Control and the standard control were selected. The most important criterion for the evaluation periods is that the full range of inflow conditions is present in which the SST could logically be operated, where the main differentiation arises from the catchments from which the majority of the flow is originating. To representatively assess the water levels and flow capacities minimum requirements for the availability and quality of the measurements were set: the measuring interval should not exceed 2 minutes and uncertainties should not exceed 5 cm or 5% (1σ) from the current actual value respectively. The rather loose uncertainties arise from the need to mainly follow the dynamics of the measurements rather than knowing the absolute value.

Following the volume based approach of the control the assessment parameters applied are the number of SST fills and discharges, the total discharged volume, discharge duration, the event mean total influent flow during a discharge and the event mean discharged flow. No water quality parameters were taken into account. Quality oriented parameters have no added value over volume oriented parameters, as the control does not target the treatment process. Additionally, CSO events from catchment ES are applied to evaluate possible side effects.

All applied parameters are available as part of daily operation at the WWTP, or can easily be derived from them. The measurements are processed at a one-minute time step, satisfying the demand. The accuracy of the flow measurements is $< 1\%$ as described in (Schilperoort, 2011). The maximum uncertainty of the water level measurements is estimated to be 3 cm based on the difference between redundant measurements in the influent line. Both remain within the limits set.

Table 6.2: Statistics on the rainfall characteristics in the evaluation periods for the Storm Tank Control. Events with a rainfall depth >7 mm are deemed interesting for the SST operation as this equals the Dutch design in-sewer storage capacity for combined sewer systems.

evaluation period	months	rainfall depth		events >7 mm		average event rainfall depth >7 mm
	[#]	[mm]	[mm/year]	[#]	[#/year]	[mm]
reference	35	2262	776	94	32	14.1
controlled	10.5	585	669	24	27	12.7

The evaluation period for the standard control (reference period) ranges from January 2012 to November 2014. The period for the Storm Tank Control (controlled period) runs from December 2014 to 15 October 2015. In these periods, to the authors knowledge, no significant changes in the catchments, at the WWTP or in the operation occurred other than the Storm Tank Control. Regarding the inflow conditions 131 events occurred in which the SST could have been operated for the reference period and 35 with the Storm Tank Control activated. For the standard control 43 events occurred with inflow mainly originating from ES, for 8 events from RZ only and for 47 events from ES and RZ. For the Storm Tank Control this occurred for 3, 3 and 17 events respectively. As multiple events are available for each situation, these evaluation periods are deemed sufficient to evaluate the performance.

Additional to the events, rainfall statistics on the evaluation periods derived from a Royal Netherlands Meteorological Institute hourly precipitation measurement at Eindhoven airport are presented in table 6.2. The controlled period was a little dryer in all respects than the reference period.

The final evaluation step is described in section 6.3.1.

6.2.4 Primary Clarifier Control

6.2.4.1 Aim

The aim of the Primary Clarifier Control is to optimise the operation of the PCs to reduce peak loading of the activated sludge tanks and subsequently reduce NH_4 peaks in the WWTP effluent. For this purpose, the influent pumping station settings were adjusted as well to better utilise the in-sewer storage capacity. The Storm Tank Control is incorporated in the Primary Clarifier Control.

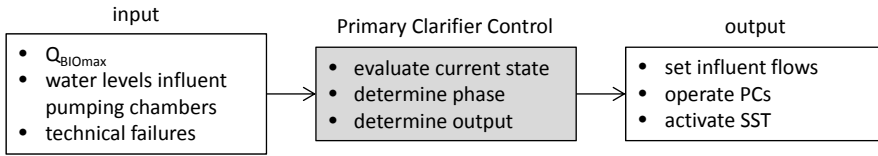


Figure 6.7: Schematic overview of the Primary Clarifier Control.

6.2.4.2 Design

The Primary Clarifier Control, schematically displayed in figure 6.7, operates the influent pumping stations and PCs based on the maximum current activated sludge capacity (Q_{BIOmax}) and the water levels in the pumping chambers, as a measure for the available storage capacity in the catchments. It consists of four phases depending on the inflow conditions: 0 - DWF, 1 - start WWF, 2 - WWF and 3 - limited WWF. The hydraulic capacity at which the WWTP is operated differs for each phase and can only (but not necessarily) reach its maximum in phase 2. This allows for wastewater storage in the catchments, where storage in RZ is favoured over ES whenever possible. An additional phase 4 was introduced as fall back scenario. It is applied automatically in case of technical failures, or manually if desired by the operators. The Storm Tank Control is embedded in the Primary Clarifier Control in phases 1, 2 and 4. Due to the combined constraints of the controls, the SST can fill but not discharge in phase 1. In phases 2 and 4 the SST can fill and discharge.

An example of the operation of the Primary Clarifier Control in case of a spatially uniform, strong rain event is presented in figure 6.8. During DWF only one PC is operational. At the onset of WWF, the control switches to phase 1 where the SST is filled and an additional PC is operated. The influent from RZ is reduced to activate the available storage and allow additional influent flow from ES. As the catchments gradually fill, phase 2 is activated: the influent is maximised, all PC are operational and the SST discharges. Once the influent flows have largely reduced at the end of the rain event, the control switches to phase 3: one PC is taken out of operation and the SST is not allowed to be activated. This phase continues until DWF is reached or a return to phase 2 is necessary.

As during phase 0 only one PC is operated, the storage of concentrated sewage in the PCs is reduced to a third of the standard control. The PCs are dynamically operated such that they contain as diluted sewage as possible given the hydraulic conditions. To further reduce the peak load when PCs are added, they are partly emptied during DWF.

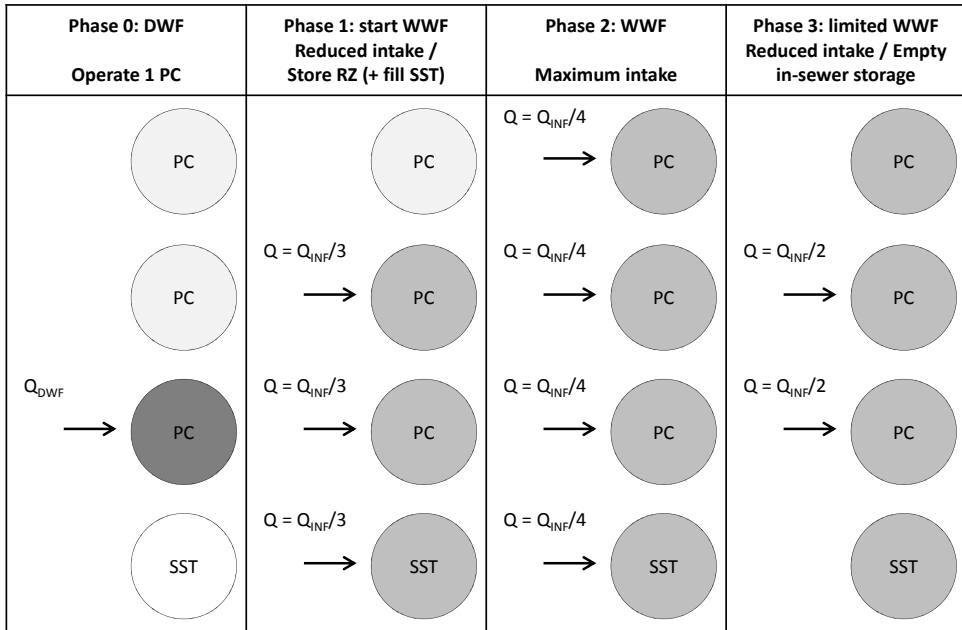


Figure 6.8: Example of the operation of the Primary Clarifier Control in case of a spatially uniform, strong rain event.

Prior to the detailed design and implementation of the Primary Clarifier Control a field test was executed to investigate the impact of applying only one PC instead of three during DWF. No adverse effects on the removal efficiency were found. Appendix E contains a brief description of the field test and its results.

6.2.4.3 Evaluation

The evaluation of the Primary Clarifier Control is based on WWTP model simulations following the flow chart in figure 5.1. An evaluation based on measurements is not possible due to simultaneous optimisation and testing of WWTP controls and maintenance of WWTP components during the evaluation period that could all influence the NH₄ effluent concentrations.

The demands on the evaluation period for the Primary Clarifier Control mainly go into the range of inflow conditions, as for the evaluation of the Storm Tank Control. Several small (control remains in phase 3 without influent flow limitation), medium (control remains in phase 3 with influent flow limitation) and large events (control switches to phase 2) are required to get sufficient insight in the controls performance.

The preparation of the input data sets for the WWTP model and verification of the WWTP model itself will be described in the following sections. The final evaluation step will be described in section 6.3.2.

Preparation of data sets

Data for the evaluation is available between 15 March and 22 November 2016 with the exception of June. In June numerous problems occurred in the wastewater system due to excessive rainfall such as river flooding, extended negative overflows and technical failures at the WWTP. The control was switched to the fall back scenario, making the period unsuitable for the evaluation. In the remaining months 16 small, 14 medium and 15 large events occurred which is deemed sufficient for the performance evaluation. The effect of the absence of winter months will be discussed in section 6.4.

For the performance evaluation of the Primary Clarifier Control two mutually comparable data sets are needed as WWTP model input: one with the standard control and one with the Primary Clarifier Control. Figure 6.9 contains a chart that describes the steps taken in deriving these data sets.

From the measured influent flows and water levels in the influent chambers with the Primary Clarifier Control activated, the flows and water levels that would have occurred with the standard control have been derived. For this purpose, first the discharge from the catchments is derived from the current flow and change in water level in the influent chambers using static storage curves for the respective catchment. From this discharge and the constraints for the standard control (limiting the maximum intake only), the corresponding influent flows and water levels were deduced. The conversion was checked through comparing the total influent volume in an event, deviations being $< 1\%$ for all events.

An influent model was derived for NH_4 that relates the variation in influent quality to influent hydraulics. The model first distinguishes different types of events and then imposes relationships between quantity and quality on a dry weather NH_4 concentration based on these events. It results in a time series containing both DWF and WWF in the WWTP influent. More details on the influent model can be found in chapter 4. The applied NH_4 influent concentrations were deduced using this model, the influent hydraulics and the measured NH_4 concentration at location MG. The resulting NH_4 concentrations were corrected to preserve the mass balance based on the measured and deduced NH_4 loads. Corrections between -20 and $+20\%$ have been applied.

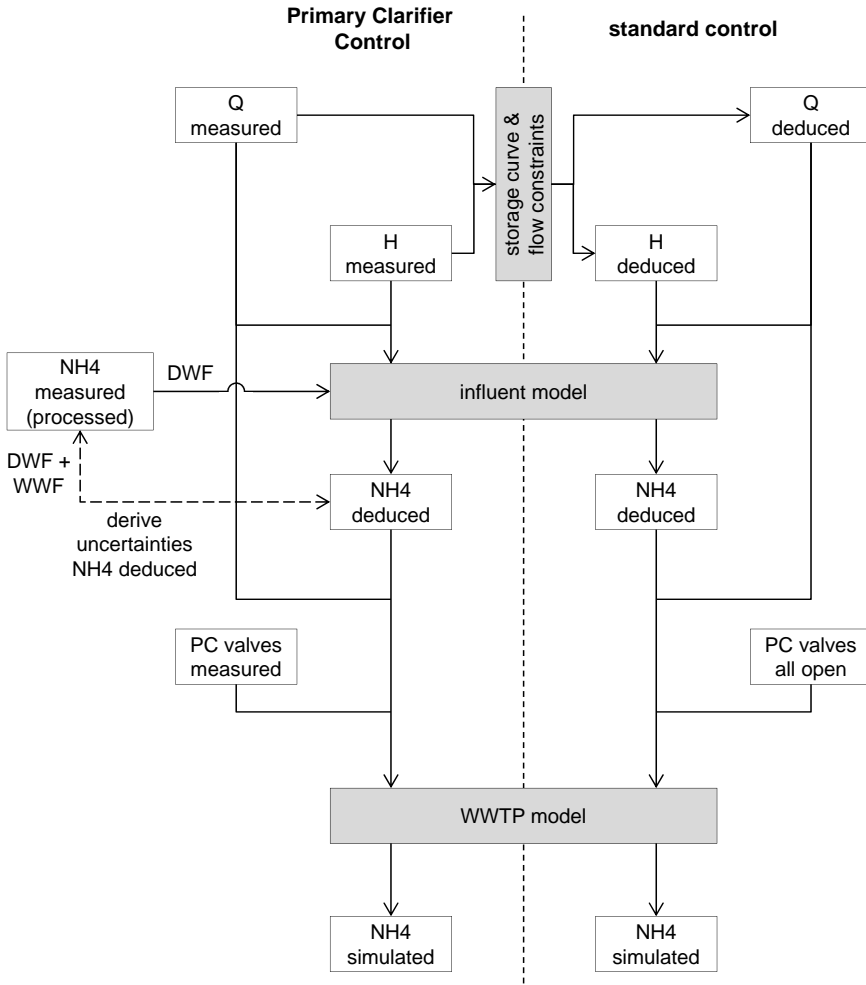


Figure 6.9: Chart that describes the steps taken in the derivation of the data sets for the evaluation of the Primary Clarifier Control.

Uncertainties in the input data set for the WWTP model are largely dominated by the uncertainties in the deduced NH_4 . The applied uncertainty is derived from the deduced NH_4 concentration for the Primary Clarifier Control and the measured NH_4 concentration. The root mean squared error (RMSE) between the two series equals 5.2 mg/l and is taken as half the (1σ) uncertainty band.

Additional inputs to the WWTP model are the measured temperature in the activated sludge tanks and in case of the Primary Clarifier Control, the measured status of the valves to operate the PCs.

WWTP model verification

The WWTP model has been verified with respect to the simulated NH_4 concentrations. For this purpose, seven periods, containing DWF and WWF situations in all seasons in the years 2012 to 2014, were simulated and compared to measured NH_4 concentrations. The NH_4 model input uncertainty is derived from the measured NH_4 concentration at location MG and the average grab sample concentration. The RMSE between the two series equals 3.6 mg/l and is taken as half the (1σ) uncertainty band. The (1σ) uncertainty in the measurements was taken to be 5%, since little deviation was found between the measurements in the three tanks.

A representative example of the simulated and measured NH_4 concentration in one of the activated sludge tanks is given in figure 6.10. The simulated WWF NH_4 peaks are nicely captured. For almost all events the modelled and measured uncertainty bands overlap, over- and underestimations of the peak height occur and the rising and falling slopes have the same angle. This indicates that the model contains no systematic errors with respect to the NH_4 peaks originating from WWF. As these are aimed at in the Primary Clarifier Control, the WWTP model is found to be applicable in the performance evaluation of the Primary Clarifier Control.

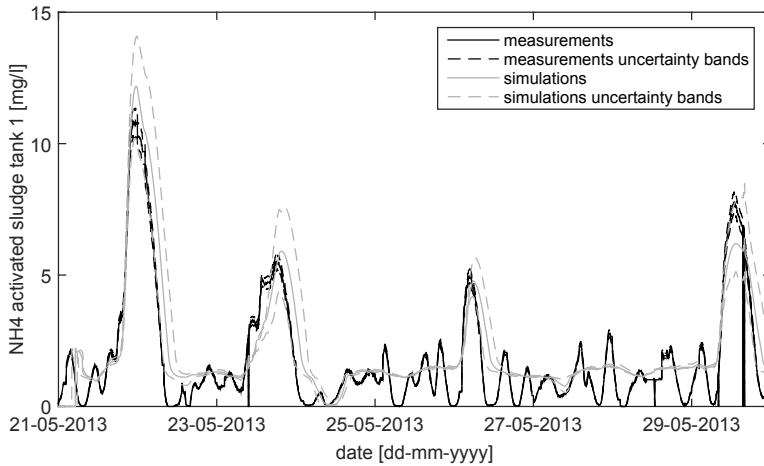


Figure 6.10: Example of the measured and simulated NH_4 concentration for the WWTP model verification.

6.3 Results

6.3.1 Storm Tank Control

A typical example of the functioning of the SST in the standard control is given in figure 6.11. In the top graph the influent flows are presented and in the bottom graph the corresponding water levels in the influent pumping chambers and the SST are given. Once the SST is full, its discharge is added to the middle graph. The SST discharges between 9:00-11:00h and 14:00-17:00h due to renewed inflow from RZ. Following the Storm Tank Control the final part of the first and the entire second SST discharge would have been unnecessary as the water level in ES falls below the threshold for CSO spills which is set at 13.30 *mAD*.

An example of SST operation with the Storm Tank Control is given in figure 6.12. The SST fills between 19.30-23:00h. Once it is full, the water level in the pumping chamber of ES is checked. As it is below the threshold, the SST is taken out of operation by matching the total influent flow and the total flow to the activated sludge tanks through reduction of the influent flow for RZ.

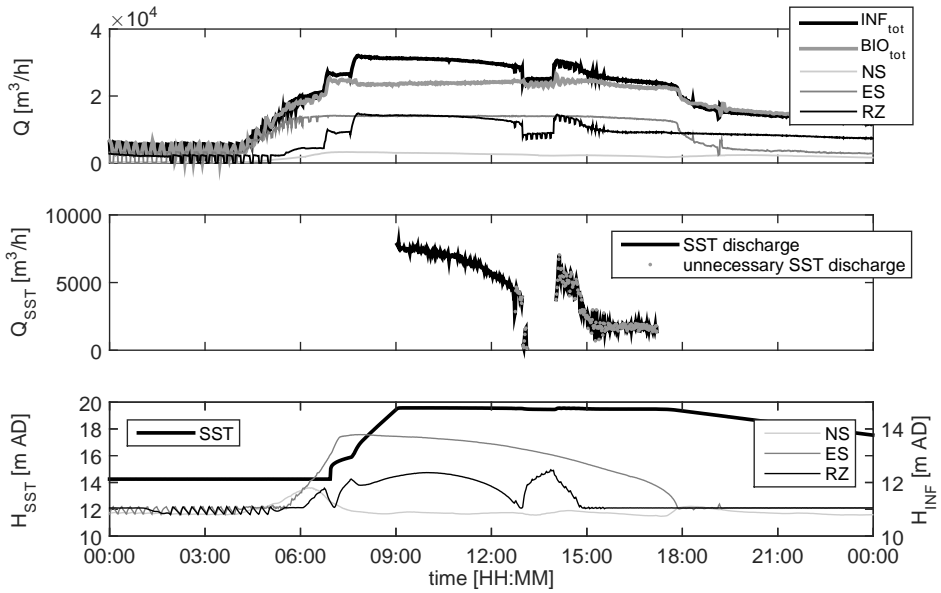


Figure 6.11: Example of the SST operation at 8 September 2013 in the standard control. All SST discharges from approximately 13:00h onwards are deemed unnecessary. The SST is empty at 14.25 *mAD* and full at 19.48 *mAD*.

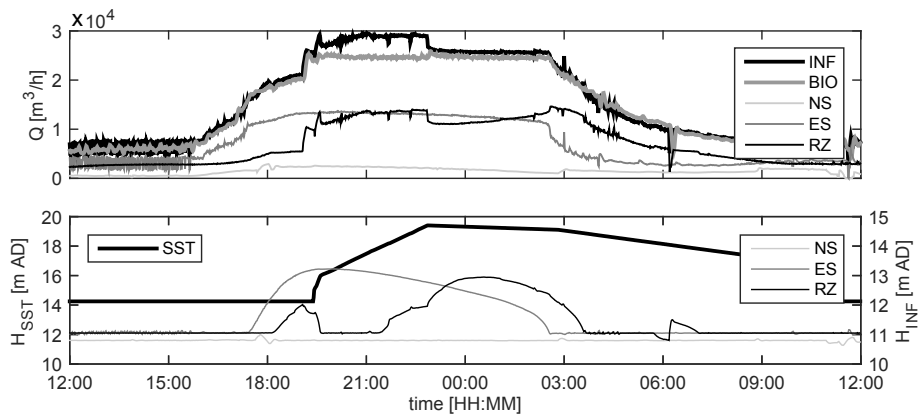
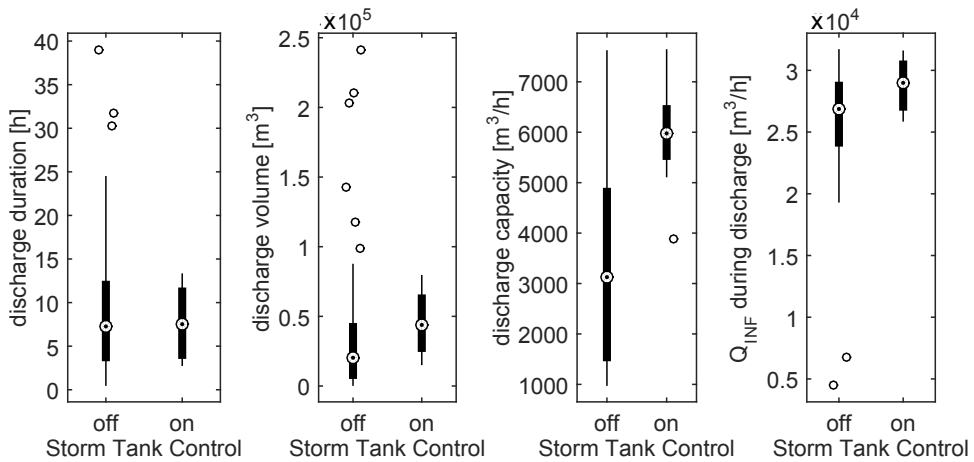


Figure 6.12: Example of the SST operation with the Storm Tank Control at 28 and 29 January 2015. The SST is filled and taken out of operation once it is full and storage is available in both ES and RZ. The SST is empty at 14.25 *mAD* and full at 19.48 *mAD*.

Table 6.3: Statistics for SST discharges with the Storm Tank Control and standard control.

statistic	standard control	Storm Tank Control
number of months data	35	10.5
number of fills	93	28
number of discharges	59	10

**Figure 6.13:** Boxplots for several assessment parameters for SST discharges for all events with the Storm Tank Control and standard control. The discharge capacity and total influent flow are event mean values.

In table 6.3 and figure 6.13 several statistics for SST discharges derived from the measurements are summarized for the Storm Tank Control and standard control. Relative to the number of months data available, the number of times the SST fills is equal for both situations. The number of discharges, however, is reduced 44% by the Storm Tank Control. This is much more than the 16% that could be expected based on the lower number of rain events with more than 7 mm rainfall depth. It agrees with the first aim of the Storm Tank Control: reducing the number of discharges. For the duration of a SST discharge (4%) no significant change was found, although fewer outliers with long durations are present.

The second aim was to utilise the SST to its full capacity when discharges are necessary. The median discharged volume (116%) and median event mean discharged flow (91%) are significantly higher for the Storm Tank Control than for the standard control as can be found from figure 6.13, even though the average event volume is lower in the period for the Storm Tank Control. When the SST is discharging, it is thus operated closer to its maximum capacity than with the standard control. For the median event mean total influent flow during SST discharges a smaller but still significant difference was found (8%).

From the data an estimate for the total reduction in discharged SST volume by the Storm Tank Control can be derived. This is based on the number of times the SST filled with the Storm Tank Control, the ratio of the number of discharges and fills for the standard control and the event mean discharged volume for the standard control. The SST could have discharged 685,000 m^3 in the period the Storm Tank Control was active while it discharged only 459,000 m^3 . This amounts to an estimated 33% reduction in discharged volume.

It was found that the SST with the new control only discharges when necessary based on possible CSO discharges. Also no apparent negative effect on the number of CSO discharges was found.

6.3.2 Primary Clarifier Control

The functioning of the Primary Clarifier Control and its influence on the effluent NH_4 concentration is demonstrated in figure 6.14 (black lines) that successively shows the influent flow, influent NH_4 concentration, effluent NH_4 concentration and phase of the control. Most of the time the Primary Clarifier Control is operating in phase 0 (DWF mode) with only one PC activated. As the influent flow increases the control switches to phase 1 to activate an additional PC. For the first two events the total inflow remains limited and the control switches to phase 3, avoiding changes in PC operation, to gradually treat all wastewater. The final event displayed requires all PC to be operated in phase 2.

Comparing the Primary Clarifier Control with the standard control in figure 6.14 (grey lines), the Primary Clarifier Control limits and/or delays the influent flow. Therefore, at high influent flows the wastewater is more diluted in case of the Primary Clarifier Control. Together with buffering less concentrated sewage in the PCs the influence on the NH_4 peaks in the effluent is evident.

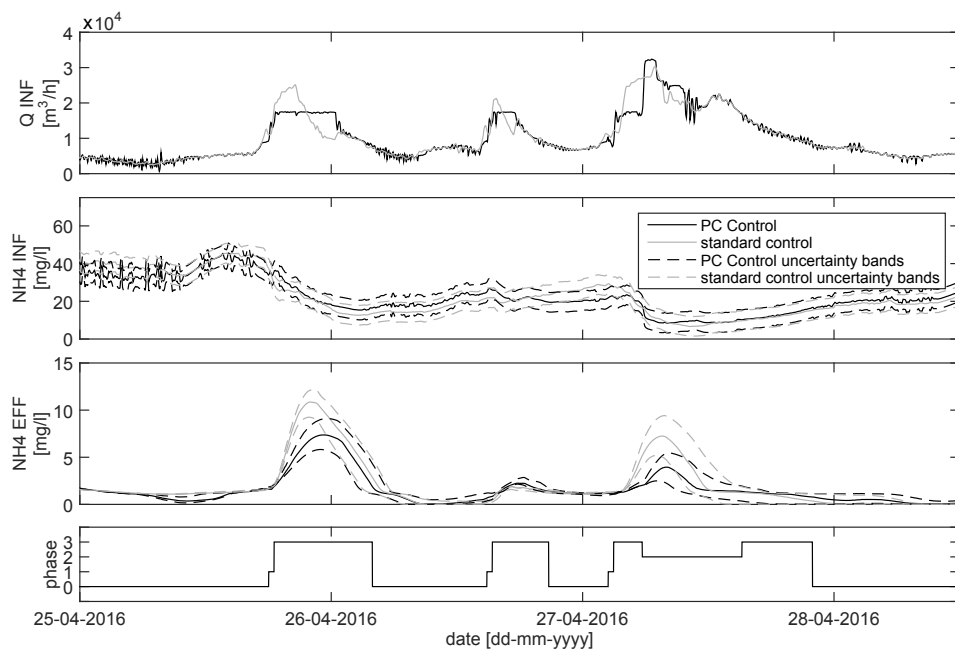


Figure 6.14: Example of functioning and effect of the Primary Clarifier Control on the NH_4 effluent concentration for two medium and one large events compared to the standard control.

Looking at the entire evaluation period, the Primary Clarifier Control has resided in phases 0, 1, 2, 3 and 4 for 86, 1, 3, 7 and 3% of the time, respectively. This means the WWTP can be operated with only one PC for 86% of the time and for at least 94% of the time a reduced number of PCs is sufficient. Besides reducing storage of undiluted sewage in the primary clarifiers, this presents operational gains with respect to maintenance, personnel and ultimately costs.

In the analysis of all events, it was found that in some cases the events, or a time span just before them, were clearly treated differently by the influent model. These events were excluded from the final analysis for which a total of 10 small, 10 medium and 11 large events remained. Figure 6.15 contains plots for all the remaining events with the NH_4 effluent maximum peak height on the vertical axis and the total event WWF load on the horizontal axis. Mean values are represented by asterisks and the upper and lower limits by the uncertainty bands. The total event WWF load equals the total event load minus the event 95% DWF load.

Positive, neutral or negative performance for the Primary Clarifier Control compared to the standard control was determined based on the plots in figure 6.15. In a comparison based on mean values, neutral performance is assigned if the differences are less than 15%. Positive performance is assigned, if the difference is at least 15% with the Primary Clarifier Control being lower and negative performance is assigned otherwise. The results have been summarised in table 6.4, where an additional distinction between event sizes was made. For small events the overall performance of the Primary Clarifier Control is slightly negative, while for medium events the performance is slightly positive. For large events, however, the performance is distinctly positive. This is also reflected in the mean change over the small, medium or large events. On average an improvement of 11% is found for the maximum NH_4 concentration and 4% for the total NH_4 event load. For large events the improvement increases to 19 and 20% respectively.

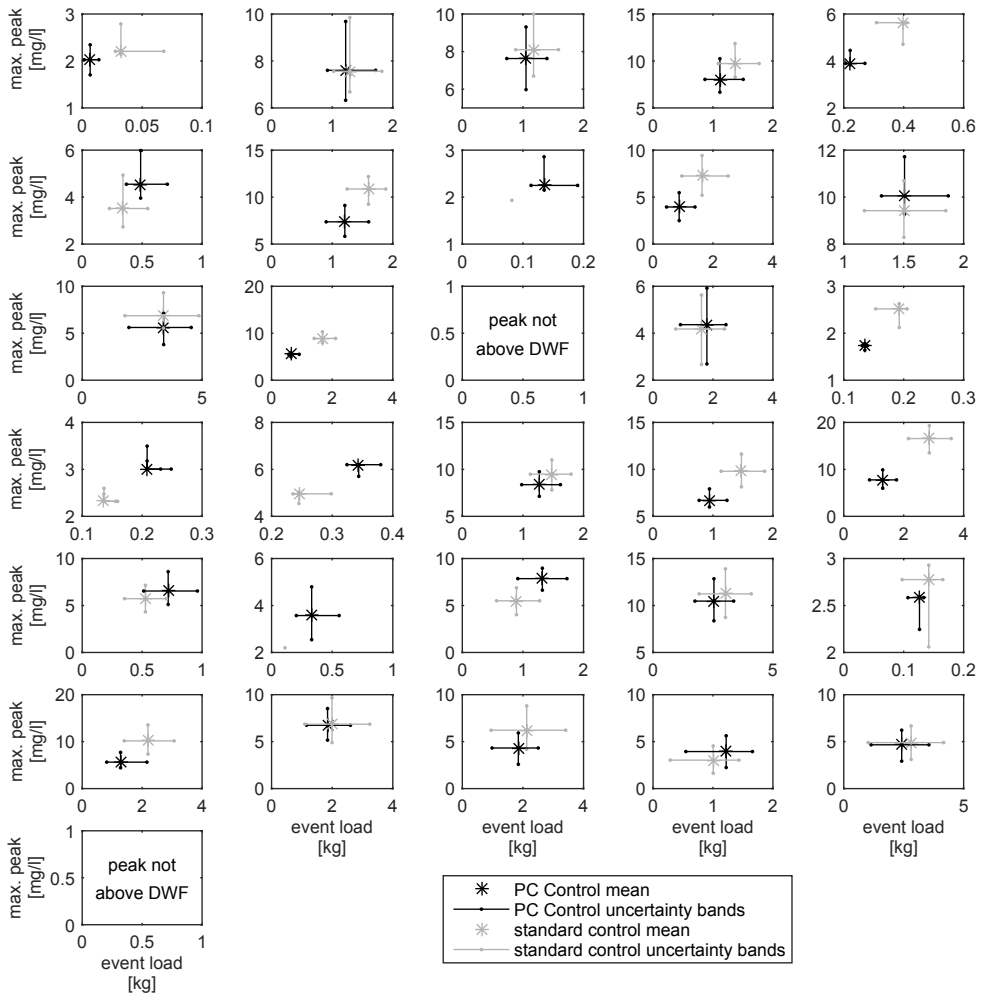


Figure 6.15: Performance of the Primary Clarifier Control compared to the standard control based on the maximum NH₄ effluent concentration and total event WWF load for all events. Scales on both axes vary.

Table 6.4: Summarised performance of the Primary Clarifier Control compared to the standard control.

*Caused by one event where the maximum concentration does not surpass the 95% DWF concentration, otherwise the value would be -8%.

event size	mean values			significant change			mean change for all events based on mean values	
	pos. [#]	neutr. [#]	neg. [#]	pos. [#]	neutr. [#]	neg. [#]	max. peak [%]	event load [%]
small	3	2	5	3	3	4	4	22*
medium	4	3	3	2	7	1	-8	2
large	7	3	1	4	7	0	-19	-20
all	14	8	9	9	17	5	-11	-4

To determine the significant performance of the Primary Clarifier Control, the uncertainty bands need to be taken into account. This was done through imagining an ellipse through the uncertainty bands in figure 6.15 and assessing the overlap of the ellipses. If they overlap, neutral performance was assigned. If there is no overlap, the performance was positive if the ellipse for the Primary Clarifier Control was to the lower left (lower peak and/or lower load) of the ellipse for the standard control, otherwise negative performance was assigned. The results are also summarised in table 6.4. Including uncertainty analysis results in more events begin marked as neutral. The overall conclusions, however, remain the same: the performance of the Primary Clarifier Control is significantly better than the standard control for large events.

The Primary Clarifier Control specifically aims at reducing the NH₄ peaks in the WWTP effluent during storm events. The impact of the control on total effluent loads for standard effluent parameters, such as total phosphate and total nitrogen, is summarised in table 6.5 for the entire evaluation period. Overall, the control results in a decrease of the NH₄ load in the effluent, a smaller increase in the nitrate load in the effluent and overall a decrease in the total nitrogen load. In addition, the total phosphorous load in the effluent also decreases, showing that the bio-P removal also benefits from decreasing the influent peak loads.

Table 6.5: Comparison between the average daily loads for several water quality parameters in the WWTP effluent over the evaluation period based on simulations with the Primary Clarifier Control compared and the standard control.

parameter	average pollutant load over evaluation period [kg/d]	
	standard control	Primary Clarifier Control
NOx	713.9	728.1
NH4	258.8	232.5
Ntot	1,165.1	1,139.0
Ptot	127.6	114.9
CODtot	4,925.2	4,640.7

6.4 Discussion

Determining the performance of the two implemented RTC strategies, taking into account representative evaluation periods and relevant uncertainties, was shown to be possible. To the authors knowledge it is the first time that RTC is demonstrated to have a significant positive effect for a real world case. For the Storm Tank Control, with the evaluation based on operational quantity parameters only, this was fairly straightforward. For the Primary Clarifier Control, involving quality parameters and model simulations, the evaluation was much more complex. More detailed consideration and planning at the start of the implementation project, taking the evaluation into account, could have made the evaluation easier. For example, the impact of making simultaneous changes in the WWTP operation could have been more explicitly considered and possibly dealt with differently. In addition, a tailor made monitoring setup for the evaluation would have included an on-line NH4 measurement in the effluent.

Some further remarks considering the performance evaluation of the Primary Clarifier Control:

- An influent model was applied to achieve comparable input data sets for the WWTP model. While analysing the results almost one third of the events were discarded because the influent model had clearly treated the two sets differently. To determine the impact of the discarded events, they were evaluated nevertheless. The results were found to be very similar, with a bias favouring the Primary Clarifier Control;

- The WWTP has been operated at a reduced capacity since June. Because of this, the activated sludge tanks have not been loaded up to their design capacity. Higher loads to the activated sludge tanks lead to higher effluent peaks. As the Primary Clarifier Control aims to reduce the effluent peaks, lower loading of the activated sludge tanks decreases the opportunity for reduction and thus decreasing its apparent performance. As still a significant positive effect is found, the performance of the Primary Clarifier Control is expected to improve when the maximum capacity of the WWTP is restored;
- The evaluation period does not contain any winter months. However, the decrease of peak loads to the activated sludge tanks due to the applied Primary Clarifier Control is independent from temperature. In addition, as in winter the wastewater temperature is lower, the efficiency of the WWTP is lower due to slower conversion processes. Consequently, it can be expected that the Primary Clarifier Control will even be more advantageous in winter than in summer time, as the capacity of the WWTP to deal with influent peak decreases with temperature. As such, the results presented in this paper, which do not contain a winter period, will underestimate the effect Primary Clarifier Control may have on an annual basis. The absence of winter months in the evaluation period therefore do not hamper the validity of the performance analysis results, but renders these on the safe side;
- The performance of the Primary Clarifier Control for small events deviates from the overall performance. This is partly caused by an artefact in the WWTP model that results in temporary NH_4 peaks to the activated sludge tanks when additional, partly empty, PC are added. This artefact is most relevant for small events, when the NH_4 concentration in the influent remains relatively high. It has little influence on the overall performance of the control;
- The PC control is meant to reduce NH_4 peaks in the WWTP effluent that cause negative impacts in the receiving surface water. These are mainly problematic for high peaks and high loads that occur for large events. As the Primary Clarifier Control clearly positively influences the WWTP functioning during large events, without serious deterioration during small and medium events, it is concluded the Control functions as intended.

6.5 Conclusions

Two integrated, impact based controls at WWTP Eindhoven were described and evaluated. Both aim to improve the use of the available tanks at the WWTP and storage in the contributing catchments. For the first time, to the authors' knowledge, it is demonstrated that a significant improvement can be achieved through the application of RTC in practice, taking into account uncertainties and applying a relevant evaluation period.

The Storm Tank Control aims to reduce the SST discharges, causing DO depletion in the receiving waters. Based on measurements it was shown that the Storm Tank Control significantly improves the SST operation compared to the standard control. For the evaluation period, the number of discharges is reduced by 44% and the discharged volume by an estimated 33%. The control had no negative impact on CSO discharges from the contributing catchments.

The Primary Clarifier Control aims to reduce peak loading of the activated sludge tanks, which cause NH₄ peaks in the WWTP effluent and receiving waters. Based on model simulations it was shown that the Primary Clarifier Control significantly improves the NH₄ effluent quality compared to the standard control. The maximum event NH₄ concentration in the evaluation period for large events, that cause most acute problems, is reduced 19% on average while the load reduced 20%. For medium and small events, a smaller positive and slightly negative impact is found respectively. Side effects of the Primary Clarifier Control are operational gains as the WWTP has been operated with a reduced number of PCs for 94% of the time.

Acknowledgements

The author would like to acknowledge the indispensable contribution of numerous employees of water board De Dommel in the control design and during the implementation and testing of the controls.

7 Concluding remarks

This thesis deals with real time control (RTC) in urban wastewater systems as a means to adapt the wastewater systems functioning to changing conditions. The main research question was: How can the effectiveness of RTC in urban wastewater systems be determined? The sub questions go into the tools needed for an evaluation, the key elements of an evaluation methodology and the applicability of such a methodology in practice. In the following section the main answers are summarised. In section 7.2 recommendations for further research and application of the results are presented.

7.1 Results summary

The mind map displaying the main features associated with RTC from the introduction is displayed once more in figure 7.1. The main features added to in this thesis are:

- Enhancing the models that describe the interactions at the sewer system boundaries, chapters 2 to 4;
- Proposing a methodology for the performance evaluation of RTC, chapter 5;
- Applying the methodology on the wastewater system of Eindhoven, chapter 6.

The applicability of unverified computational fluid dynamics (CFD) simulations for the derivation of accurate weir discharge relationships was researched for weirs where the weir chamber geometry has a dominant influence on the hydraulic behaviour. For this purpose a unique set of scale model measurements, field measurements and CFD simulations was gathered. It was found that unverified CFD simulations are able to describe the complex hydraulic behaviour occurring in the lab experiments, including a change in flow regime: in the undisturbed flow regime the weir chamber has no

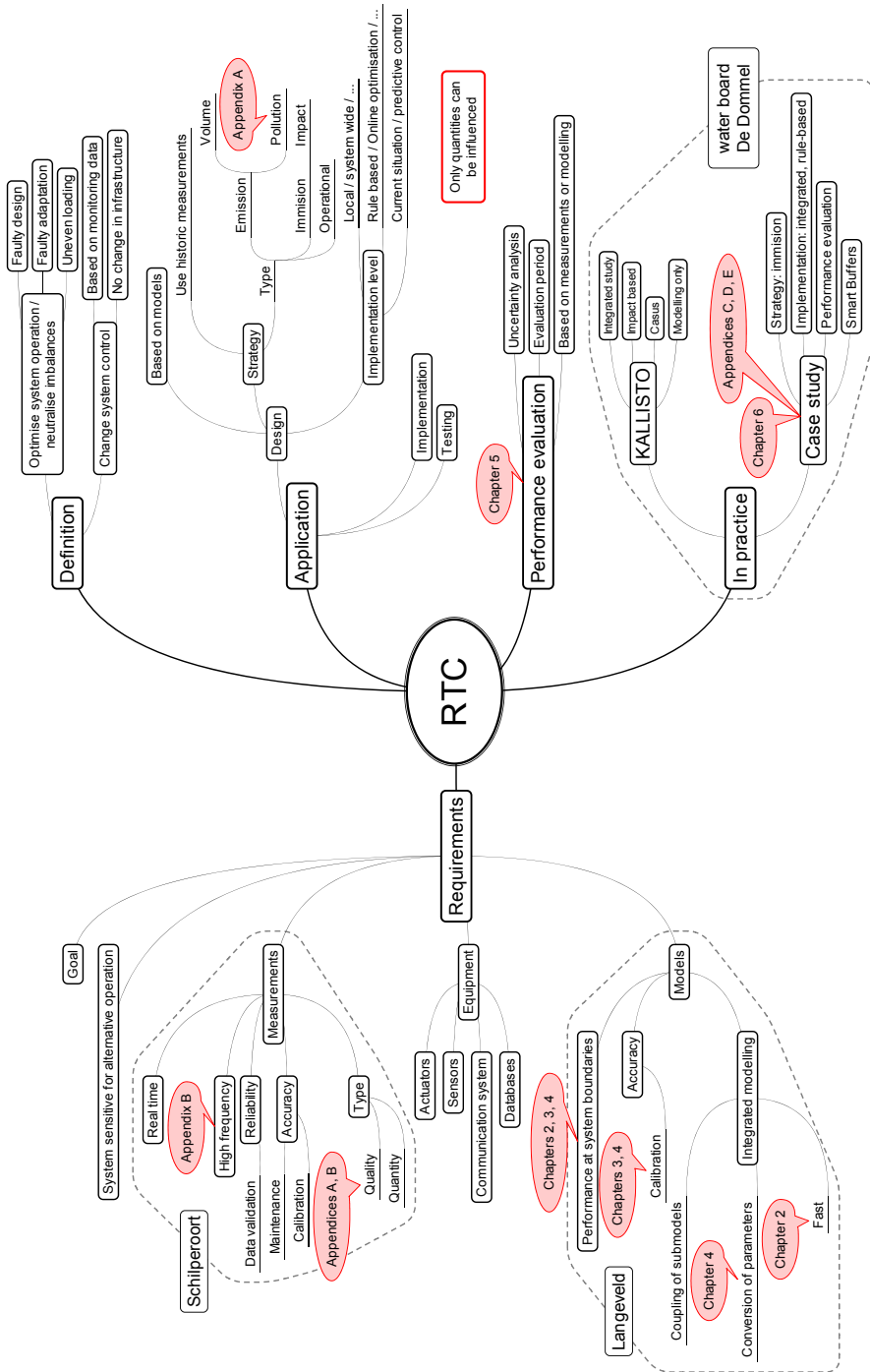


Figure 7.1: Mind map displaying the main features of RTC. Call out balloons point out to which features this thesis contributes.

influence, in the disturbed flow regime backwater effects occur due to the weir chamber geometry. Discharge relationships derived from unverified CFD simulations in the undisturbed flow regime perform at a similar level to the standard discharge equation for frontal weirs. In the disturbed regime the derived discharge relationships are $\sim 10\%$ accurate, which is sufficient to be applied with regular water level measurements, while the standard equation was shown to be inapplicable. Furthermore, the simulations can be applied to determine the optimal water level measurement location based on the local hydraulic conditions.

The design of simplified sewer models, applied for their short simulation times, and their capacity to accurately determine CSO activity was investigated. The design of a 'static' and a 'dynamic' simplified sewer model were described in detail. The performance of the calibrated simplified models were compared mutually, with a runoff only model and with uncalibrated full hydrodynamic models for two sewer catchments. The evaluation was based on the accurate determination of CSO events (occurrence and total volume) and the quality of the model calibration. It was found that the static and dynamic simplified sewer models, contrary to runoff only models, are able to describe the behaviour of pumped sewer systems. The dynamic model outperforms the static model when high quality information is available for the design and calibration of the model, otherwise the static model suffices. The calibrated static and dynamic simplified sewer models both outperform the uncalibrated full hydrodynamic models based on the CSO activity. As the simplified models are also $>1,000$ times faster, the application of appropriate, calibrated simplified models in RTC studies is preferred over uncalibrated full hydrodynamic models. Finally, it was found that performance indicators should be selected carefully in relation to the modelling objectives, likely leading to multiple performance indicators.

Finally, an empirical model for WWTP influent quality was derived and assessed. The model predicts the influent quality in dry and wet weather conditions based on the influent hydraulics and combines a number of processes, such as dry weather flow, dilution, restoration and first flush. It describes the ammonium concentration (solute substance) with a root mean squared error of 6.3 mg/l or 16% related to the mean dry weather flow concentration, and 109 mg/l and 18% for the chemical oxygen demand concentration (particulate matter). The transferability of the model concept was demonstrated for a sewer catchment with different characteristics, which resulted in root mean squared errors of $<25\%$ of the mean dry weather flow concentrations for ammonium and chemical oxygen demand.

A methodology for the performance evaluation of RTC in urban wastewater systems is proposed, that explicitly includes uncertainty analysis and selecting an appropriate evaluation period. It can be applied using measurements or models. In a case study for a simplified sewer network it was demonstrated that the successful application of RTC and the possibility to determine a significant effect is very much dependent on the goal of the control. It clearly illustrates the need for uncertainties analysis, since the uncertainty bands are up to an order of magnitude larger than the effect itself. Finally, it was shown that careful consideration of the evaluation period is required as the effect of the control differed up to 80% spanning both positive and negative impacts depending on the period applied.

The applicability of the proposed methodology was demonstrated for two integrated, impact based controls that were implemented at the WWTP of Eindhoven. For the first time, it was demonstrated that a significant improvement can be achieved through the application of RTC in practice. For the Storm Tank Control measurements were applied in the evaluation. The control reduced the number of discharges of the storm water settling tank by 44% and the discharged volume by an estimated 33%. The control had no negative impact on CSO discharges from the contributing sewer catchments. For the Primary Clarifier Control the evaluation was performed through simulations. It reduces the maximum event ammonium concentration in the effluent for large events by on average 19%, while the load reduces 20% on average. For medium and small events, a smaller positive and slightly negative impact is found respectively. Due to the Primary Clarifier Control the WWTP has been operated with a reduced number of primary clarifiers for 94% of the time.

7.2 Recommendations

Throughout this thesis measurements have been applied to understand the system functioning, for direct analysis, as model input, for model calibration, and for application in RTC. However, in many cases this required much effort, in some cases to the extent that the research was hampered. Strikingly, quantity and quality measurements used for daily operation are consistently good. It is thus possible to achieve a high yield, but due to lack of attention in the monitoring chain (manufacturers, suppliers, operators and end users) they are not obtained. Especially for application in

RTC, the availability of on-line, accurate, high frequency measurements is essential. This requires long-term investments in qualified personnel with the sole focus on monitoring, and the development of high-accuracy and robust sensors. Also more service oriented agreements between costumers and suppliers, such as to pay for equipment only after three months of high quality data is achieved, would provide incentive for suppliers to invest in good advise and cooperation.

Any application of RTC should start with a thorough investigation of the functioning of the system under consideration based on measurements or calibrated and verified models. Scrutinising the functioning of a system in reality pretty much always provides unexpected insight, whether on the system as a whole or on key structures in the system. The case applied in chapter 2 alone shows that such structures are not necessarily logical from a hydraulic point of view and that differences between the designed and as-build structures can be significant. When RTC is implemented, the system functioning should be repeatedly checked. Individual structures in a wastewater systems are continuously adapted, (un)intentionally influencing the functioning of the system and thereby the impact of the control.

The case study for RTC evaluation in chapter 5 and the application of the methodology in chapter 6 demonstrate that many opportunities for RTC in urban wastewater systems can be found in limiting discharges to the WWTP. This contradicts the usual RTC aim of CSO reduction. The case study even showed the very limited gain possible through such controls. Returning to the RTC landscape from the introduction, repeated in figure 7.2, most applications of RTC are found for the little effective volume based control strategies. Impact based control and especially quality based control have received markedly less attention. Another task for the scientific community is to shift its attention to explore this landscape more equally. Examples of relevant questions are: how can quality and impact based control be implemented, what additional information is needed, is it possible to acquire this information or are further developments of measurements and/or models necessary, does it result in additional benefits? Some explorations in the field of quality measurements can be found in appendices A and B, but much more work is required.

		implementation level				
		local	system wide – one optimal set	system wide – choose between sets	model predictive control	...
strategy ↓	volume based		Nelen, 1992		Puig et al., 2009	
	quality based			Hoppe et al., 2011		
	impact based			Seggelke et al., 2013		
	...		Erbe et al., 2002			

Figure 7.2: Landscape for RTC in wastewater systems, based on different strategies and implementation levels.

In this thesis the positive effect of two RTC scenarios is demonstrated, confirming the conviction of the scientific community in the abilities of RTC for at least one case study. Taking another look at the RTC landscape, it now is possible to quantify the benefits associated with a certain location in the landscape. The ideal of selecting the location in the landscape for a certain case based on the benefits and demands for that location becomes feasible. However, a thorough exploration of all possible locations will likely take too much effort. Further research should be dedicated to develop a guideline or tool, similar to the PASST planning tool that scans the suitability for control of a case (Schütze et al., 2008), that indicates likely suitable locations in the landscape for a specific case.

The work presented in this thesis supports the entire RTC chain: from initiation to design, implementation and evaluation. The RTC landscape, figure 7.2, can serve as a framework to support the discussion at the initiation of RTC in urban wastewater management. It can help select the appropriate strategy and implementation level for a specific case. Application of the methodology in chapter 5 in the design phase will provide an estimate on the benefits the control is likely to achieve. This is necessary input for the decision to implement or further improve the control. Simultaneously, the steps in the methodology give valuable information for the implementation and ultimately the evaluation of the control. It for example highlights if the models and

measurements are adequate for the task. If not, this is detected at an early stage and the results so far provide information for the requirements to remedy the deficits. Naturally, the methodology supports the performance evaluation of the control ultimately implemented. Sharing of short and long-term performance evaluations and experiences with operational RTC are needed for the further development of RTC in urban wastewater systems.

Concerning the wastewater system of Eindhoven, the controls that are now implemented have been classified as integrated and impact based. However, both could be taken a step further. The controls are integrated in the sense that they are designed using knowledge on the functioning of the entire urban wastewater system and use measurements representative for the functioning of the sewer system and WWTP. Still, only measurements and actuators at the WWTP are applied. In terms of integration, the incorporation of measurements in the sewer and transport systems, inclusion of the control stations in the southern transport sewer and inclusion of the river diversion works in the control algorithm will likely have additional benefits for the systems performance. The impact based control strategy is similarly based on the application of system knowledge in the control design. Active incorporation of the river status through (quality) measurements will provide additional valuable information that could lead to further optimisation of the systems functioning.

Bibliography

- Alex, J., Beteau, J., Copp, J., Hellinga, C., Jeppsson, U., Marsili-Libelli, S., Pons, M., Spanjers, H., and Vanhooren, H. (1999). Benchmark for evaluating control strategies in wastewater treatment plants. In *Proceedings of European Control Conference ECC'99*, pages 1–6, Karlsruhe.
- Amerlinck, Y. (2015). *Model refinements in view of wastewater treatment plant optimization: improving the balance in sub-model detail*. PhD thesis, Ghent University.
- Ashley, R., Balades, J.-D., Bertrand-Krajewski, J.-L., Brombach, H., and Butler, D. (2004). *Solids in Sewers*. IWA.
- Ashley, R., Hvitved-Jacobsen, T., and Bertrand-Krajewski, J.-L. (1999). Quo vadis sewer process modelling? *Water Science & Technology*, 39(9):9–22.
- Azimi, A. and Rajaratnam, N. (2009). Discharge Characteristics of Weirs of Finite Crest Length. *Journal of Hydraulic Engineering*, 135(12):1081–1085.
- Beeneken, T., Erbe, V., Messmer, A., Reder, C., Rohlfing, R., Scheer, M., Schütze, M., Schumacher, B., Weilandt, M., and Weyand, M. (2013). Real time control (RTC) of urban drainage systems A discussion of the additional efforts compared to conventionally operated systems. *Urban Water Journal*, 10(5):293–299.
- Benedetti, L., Langeveld, J., Van Nieuwenhuijzen, A., De Jonge, J., De Klein, J., Flameling, T., Nopens, I., Van Zanten, O., and Weijers, S. (2013). Cost-effective solutions for water quality improvement in the Dommel River supported by sewer-WWTP-river integrated modelling. *Water Science & Technology*, 68(5):965–73.
- Benedetti, L., Nyerup Nielsen, C., and Thirsing, C. (2011). Modelling for integrated sewer-WWTP operation with ATS in Copenhagen. In *Proceedings of the 12th Nordic Wastewater Conference*, Helsinki.

- Bertrand-Krajewski, J.-L. (2004). TSS concentration in sewers estimated from turbidity measurements by means of linear regression accounting for uncertainties in both variables. *Water Science & Technology*, 50(11):81–88.
- Bertrand-Krajewski, J.-L. (2007). Stormwater pollutant loads modelling: Epistemological aspects and case studies on the influence of field data sets on calibration and verification. *Water Science and Technology*, 55(4):1–17.
- Bertrand-Krajewski, J.-L., Briat, P., and Scrivener, O. (1993). Sewer sediment production and transport modelling: A literature review. *Journal of Hydraulic Research*, 31(4):435–460.
- Bertrand-Krajewski, J.-L., Chebbo, G., and Saget, A. (1998). Distribution of pollutant mass vs volume in stormwater discharges and the first flush phenomenon. *Water Research*, 32(8):2341–2356.
- Bettez, J., Townsend, R., and Comeau, A. (2001). Scale model testing and calibration of City of Ottawa sewer weirs. *Canadian Journal of Civil Engineering*, 28(4):627–639.
- Blumensaat, F., Stauer, P., Heusch, S., Reußner, F., Schütze, M., Seiffert, S., Gruber, G., Zawilski, M., and Rieckermann, J. (2012). Water quality-based assessment of urban drainage impacts in Europe - where do we stand today? *Water Science & Technology*, 66(2):304–313.
- Boogaard, F. and Lemmen, G. (2007). STOWA Storm water Database: The facts about the quality of storm water runoff - De feiten over de kwaliteit van afstromend regenwater. Technical report, STOWA 2007-21.
- Bos, R. and Kruger-Van der Griendt, M. (2007). Overstortkalibratie in Petten. *Rivieringswetenschap*, 7(27):116–137.
- Breinholt, A., Santacoloma, P., Mikkelsen, P., Madsen, H., and Grum, M. (2008). Evaluation framework for control of integrated urban drainage systems. In *Proceedings of ICUD11*, pages 1–12, Edinburgh.
- Brombach, H. and Weiss, G. (2005). A new overflow measurement device. In *Proceedings of ICUD10*, number August, pages 1–8, Copenhagen.
- Bruns, J. (1998). *Dynamische Koppelung von Regenwasserbehandlung und Abwasserreinigung bei Mischwasserzuzfluss*. PhD thesis, Stuttgart University.
- Butler, D. and Davies, J. (2004). *Urban Drainage*. Number 1.

- Campisano, A., Cabot Ple, J., Muschalla, D., Pleau, M., and Vanrolleghem, P. (2013). Potential and limitations of modern equipment for real time control of urban wastewater systems. *Urban Water Journal*, (February 2014):1–12.
- Campisano, A., Creaco, E., and Modica, C. (2009). P controller calibration for the real time control of moveable weirs in (proportional) sewer channels. *Water Science & Technology*, 59(11):2237–44.
- Clemens, F. (2001). *Hydrodynamic models in urban drainage: application and calibration*. PhD thesis, TU Delft.
- Coutu, S., Del Giudice, D., Rossi, L., and Barry, D. (2012). Parsimonious hydrological modeling of urban sewer and river catchments. *Journal of Hydrology*, 464-465:477–484.
- De Keyser, W., Gevaert, V., Verdonck, F., De Baets, B., and Benedetti, L. (2010). An emission time series generator for pollutant release modelling in urban areas. *Environmental Modelling & Software*, 25(4):554–561.
- De Mulder, C., Flameling, T., Langeveld, J., Amerlinck, Y., Weijers, S., and Nopens, I. (2017). Automating the raw data to model input process using flexible open source tools. In *Frontiers International Conference on Wastewater TreatMent*, pages 1–5, Palermo.
- De Niet, A., De Jonge, J., Korving, H., Langeveld, J., and Van Nieuwenhuijzen, A. (2013). Het beste van twee werelden, correctie van neerslagradar op basis van grondstations voor toepassing in stedelijk gebied. *H2O online*, (April):1–5.
- Del Giudice, D., Reichert, P., Bareš, V., Albert, C., and Rieckermann, J. (2015). Model bias and complexity Understanding the effects of structural deficits and input errors on runoff predictions. *Environmental Modelling & Software*, 64:205–214.
- Deltares (2016). Wave-Height-meter.
- Dembélé, A., Bertrand-Krajewski, J.-L., Becouze, C., and Barillon, B. (2011). A new empirical model for stormwater TSS event mean concentrations (EMCs). *Water Science & Technology*, 64(9):1926–34.
- Devisscher, M., Ciacci, G., Fé, L., Benedetti, L., Bixio, D., Thoeye, C., De Gueldre, G., Marsili-Libelli, S., and Vanrolleghem, P. (2006). Estimating costs and benefits of advanced control for wastewater treatment plants - the MAgIC methodology. *Water Science & Technology*, 53(4-5):215–223.

- Dirckx, G., Schütze, M., Kroll, S., Thoeye, C., De Gueldre, G., and Van De Steene, B. (2011). Cost-efficiency of RTC for CSO impact mitigation. *Urban Water Journal*, 8(January 2015):367–377.
- Dirckx, G., Van Assel, J., and Weemaes, M. (2014). Real Time Control from desk study to full implementation. In *Proceedings of ICUD13*, number September, pages 1–8, Sarawak.
- Dotto, C., Kleidorfer, M., Deletic, A., Rauch, W., and McCarthy, D. (2014). Impacts of measured data uncertainty on urban stormwater models. *Journal of Hydrology*, 508:28–42.
- Einfalt, T., Pape, E.-M., and Hatzfeld, F. (2001). Güteorientiertes Nachweisverfahren für gesteuerte Mischwasserentlastungen - Quality-oriented test methods for controlled stormwater structures in combined sewers. *Korrespondenz Abwasser*, 3:1–7.
- Erbe, V., Risholt, L., Schilling, W., and Londong, J. (2002). Integrated modelling for analysis and optimisation of wastewater systems - the Odenthal case. *Urban Water*, 4(1):63–71.
- Erbe, V. and Schütze, M. (2005). An integrated modelling concept for immission-based management of sewer system, wastewater treatment plant and river. *Water Science & Technology*, 52(5):95–103.
- Fach, S., Sitzenfrei, R., and Rauch, W. (2009). Determining the spill flow discharge of combined sewer overflows using rating curves based on computational fluid dynamics instead of the standard weir equation. *Water Science & Technology*, 60(12):3035–43.
- Ferreri, G., Freni, G., and Tomaselli, P. (2010). Ability of Preissmann slot scheme to simulate smooth pressurisation transient in sewers. *Water Science & Technology*, 62(8):1848–1858.
- Flores-Alsina, X., Saagi, R., Lindblom, E., Thirsing, C., Thornberg, D., Gernaey, K., and Jeppsson, U. (2014). Calibration and validation of a phenomenological influent pollutant disturbance scenario generator using full-scale data. *Water Research*, 51:172–185.

- Fradet, O., Pleau, M., and Marcoux, C. (2011). Reducing CSOs and giving the river back to the public: innovative combined sewer overflow control and riverbanks restoration of the St. Charles River in Quebec City. *Water Science & Technology*, 63(2):331–8.
- Fuchs, L. and Beeneken, T. (2005). Development and implementation of a real-time control strategy for the sewer system of the city of Vienna. *Water Science & Technology*, 52(5):187–194.
- Garbanini Marcantini, L., Schegg, S., Mischler, B., Hesse, K., Gresch, M., and Rieckermann, J. (2016). Ein hierarchischer Regelungsalgorithmus zur praxistauglichen Abflussregelung von Entwässerungsnetzen. In *AquaUrbanica*, pages 1–8, Tigi-Kaltbad.
- Garcia, L., Barreiro-Gomez, J., Escobar, E., Tellez, D., Quijano, N., and Ocampo-Martinez, C. (2015). Modeling and real-time control of urban drainage systems: A review. *Advances in Water Resources*, 85(18):120–132.
- Gelormino, M. and Ricker, N. (1994). Model-predictive control of a combined sewer system. *International Journal of Control*, 59(3):793–816.
- Gernaey, K., Flores-Alsina, X., Rosen, C., Benedetti, L., and Jeppsson, U. (2011). Dynamic influent pollutant disturbance scenario generation using a phenomenological modelling approach. *Environmental Modelling & Software*, 26(11):1255–1267.
- Gernaey, K. and Jørgensen, S. (2004). Benchmarking combined biological phosphorus and nitrogen removal wastewater treatment processes. *Control Engineering Practice*, 12(3):357–373.
- Göbel, P., Dierkes, C., and Coldewey, W. (2007). Storm water runoff concentration matrix for urban areas. *Journal of Contaminant Hydrology*, 91(1-2):26–42.
- Gruber, G., Winkler, S., and Pressl, A. (2004). Quantification of pollution loads from CSOs into surface water bodies by means of online techniques. *Water Science & Technology*, 50(11):73–80.
- Grum, M., Thornberg, D., Christensen, M., Shididi, S., and Thirsing, C. (2011). Full-scale real time control demonstration project in copenhagen’s largest urban drainage catchments. In *Proceedings of ICUD12*, pages 1–7, Porto Alegre.
- Harremoës, P. (2002). Integrated urban drainage, status and perspectives. *Water Science & Technology*, 45(3):1–10.

- Harremoës, P. (2003). Ethical aspects of scientific incertitude in environmental analysis and decision making. *Journal of Cleaner Production*, 11(7):705–712.
- He, C., Marsalek, J., Rochfort, Q., and Krishnappan, B. (2006). Case Study: Refinement of Hydraulic Operation of a Complex CSO Storage/Treatment Facility by Numerical and Physical Modeling. *Journal of Hydraulic Engineering*, 132(2):131–139.
- He, J., Valeo, C., Chu, A., and Neumann, N. (2011). Prediction of event-based stormwater runoff quantity and quality by ANNs developed using PMI-based input selection. *Journal of Hydrology*, 400(1-2):10–23.
- Heller, V. (2011). Scale effects in physical hydraulic engineering models. *Journal of Hydraulic Research*, 49(3):293–306.
- Hirt, C. and Nichols, B. (1981). Volume of fluid (VOF) method for the dynamics of free boundaries. *Journal of Computational Physics*, 39(1):201–225.
- Hoppe, H. and Gruening, H. (2007). Significance of uncertainties in the input data used in the integrated design of wastewater systems. In *Proceedings of Novatech*, pages 1607–1614.
- Hoppe, H., Messmann, S., Giga, A., and Gruening, H. (2011). A real-time control strategy for separation of highly polluted storm water based on UVVis online measurements from theory to operation. *Water Science & Technology*, 63(10):2287–2293.
- Hoseini, S. (2014). Experimental investigation of flow over a triangular broad-crested weir. *ISH Journal of Hydraulic Engineering*, 20(2):230–237.
- IPCC (2014). Climate Change 2014: Synthesis Report. Technical report, IPCC, Geneva, Switzerland.
- Isel, S., Dufresne, M., Bardiaux, J., Fischer, M., and Vazquez, J. (2013). Computational fluid dynamics based assessment of discharge-water depth relationships for combined sewer overflows. *Urban Water Journal*, 11(8):631–640.
- Isel, S., Dufresne, M., Fischer, M., and Vazquez, J. (2014). Assessment of the overflow discharge in complex CSO chambers with water level measurements - On-site validation of a CFD-based methodology. *Flow Measurement and Instrumentation*, 35:39–43.

- Joannis, C., Ruban, G., Gromaire, M.-C., Chebbo, G., and Bertrand-Krajewski, J.-L. (2008). Reproducibility and uncertainty of wastewater turbidity measurements. *Water Science & Technology*, 57(10):1667–73.
- Johnson, M. (2000). Discharge coefficient analysis for flat-topped and sharp-crested weirs. *Irrigation Science*, 19(3):133–137.
- Keating, E., Doherty, J., Vrugt, J., and Kang, Q. (2010). Optimization and uncertainty assessment of strongly nonlinear groundwater models with high parameter dimensionality. *Water Resources Research*, 46(10):1–18.
- Kleidorfer, M., Möderl, M., Fach, S., and Rauch, W. (2009). Optimization of measurement campaigns for calibration of a conceptual sewer model. *Water Science & Technology*, 59(8):1523–30.
- KNMI (2015). KNMI'14 climate scenarios for the Netherlands. Technical report.
- Korving, H. (2004). *Probabilistic assessment of the performance of combined sewer systems*. PhD thesis, TU Delft.
- Korving, H. and Clemens, F. (2005). Impact of dimension uncertainty and model calibration on sewer system assessment. *Water Science & Technology*, 52(5):35–42.
- Krämer, S., Fuchs, L., and Verworn, H.-R. (2007). Aspects of Radar Rainfall Forecasts and their Effectiveness for Real Time Control - The Example of the Sewer System of the City of Vienna. *Water Practice & Technology*, 2(2):42–49.
- Krebs, G., Kokkonen, T., Valtanen, M., Setälä, H., and Koivusalo, H. (2014). Spatial resolution considerations for urban hydrological modelling. *Journal of Hydrology*, 512:482–497.
- Krebs, P., Merkel, K., and Kühn, V. (1999). Dynamic changes in wastewater composition during rain runoff. In *Proceedings of ICUD8*, pages 920–927, Sydney.
- Lacour, C., Joannis, C., Schütze, M., and Chebbo, G. (2011). Efficiency of a turbidity-based, real-time control strategy applied to a retention tank: a simulation study. *Water Science & Technology*, 64(7):1533–1539.
- Lacour, C. and Schütze, M. (2011). Real-time control of sewer systems using turbidity measurements. *Water Science & Technology*, 63(11):2628.
- Langeveld, J. (2004). *Interactions within wastewater systems*. PhD thesis, TU Delft.

- Langeveld, J., Benedetti, L., De Klein, J., Nopens, I., Amerlinck, Y., Van Nieuwenhuijzen, A., Flameling, T., Van Zanten, O., and Weijers, S. (2013). Impact-based integrated real-time control for improvement of the Dommel River water quality. *Urban Water Journal*, 10(5):312–329.
- Langeveld, J., Clemens, F., and Van der Graaf, J. (2002). Increasing wastewater system performance - The importance of interactions between sewerage and wastewater treatment. *Water Science and Technology*, 45(3):45–52.
- Langeveld, J., Clemens, F., and Van der Graaf, J. (2003). Interactions within the wastewater system: requirements for sewer processes modelling. *Water Science & Technology*, 47(4):101–8.
- Langeveld, J., Schilperoort, R., and Weijers, S. (2012). Climate change and urban wastewater infrastructure: there is more to explore. *Journal of Hydrology*.
- Langeveld, J., Veldkamp, R., and Clemens, F. (2005). Suspended solids transport: An analysis based on turbidity measurements and event based fully calibrated hydrodynamic models. *Water Science & Technology*, 52(3):93–101.
- Larrarte, F. (2006). Velocity fields within sewers: An experimental study. *Flow Measurement and Instrumentation*, 17(5):282–290.
- Lau, J., Butler, D., and Schütze, M. (2002). Is combined sewer overflow spill frequency/volume a good indicator of receiving water quality impact? *Urban Water*, 4(2):181–189.
- Leonhardt, G., Sun, S., Rauch, W., and Bertrand-Krajewski, J.-L. (2014). Comparison of two model based approaches for areal rainfall estimation in urban hydrology. *Journal of Hydrology*, 511:880–890.
- Lepot, M., Aubin, J.-B., and Bertrand-Krajewski, J.-L. (2013). Accuracy of different sensors for the estimation of pollutant concentrations (total suspended solids, total and dissolved chemical oxygen demand) in wastewater and stormwater. *Water Science & Technology*, 68(2):462–471.
- Lepot, M., Momplot, A., Lipeme Kouyi, G., and Bertrand-Krajewski, J.-L. (2014). Rhodamine WT tracer experiments to check flow measurements in sewers. *Flow Measurement and Instrumentation*, 40:28–38.
- Liefting, H. (2012). Toetsing rioolmodel Waalre. Technical Report 6 september, Royal Haskoning DHV; Witteveen+Bos.

- Lijklema, L., Tyson, J., and Lesouef, A. (1993). Interactions between sewers treatment plants and receiving waters in urban areas: A summary of the INTERURBA '92 workshop conclusions. *Water Science & Technology*, 27(12):1–29.
- Lipeme Kouyi, G., Bret, P., Didier, J.-M., Chocat, B., and Billat, C. (2011). The use of CFD modelling to optimise measurement of overflow rates in a downstream-controlled dual-overflow structure. *Water Science & Technology*, 64(2):521–527.
- Lipeme Kouyi, G., Vazquez, J., and Poulet, J. (2003). 3D free surface measurement and numerical modelling of flows in storm overflows. *Flow Measurement and Instrumentation*, 14(3):79–87.
- Lombard, V., Toloméo, S., Bertrand-Krajewski, J.-L., Debray, R., Comte, C., and De Bénédictis, J. (2010). Design and operation of pollutant loads monitoring stations for an integrated approach of sewer systems. In *Proceedings of Novatech*, pages 1–10, Lyon.
- Löwe, R., Vezzaro, L., Mikkelsen, P., Grum, M., and Madsen, H. (2016). Probabilistic runoff volume forecasting in risk-based optimization for RTC of urban drainage systems. *Environmental Modelling & Software*, 80:143–158.
- Mair, M., Kleidorfer, M., and Rauch, W. (2012). Performance of auto-calibration algorithms in the field of urban drainage modelling. In *Proceedings of UDM9*, pages 1–10, Belgrade.
- Mannina, G. and Viviani, G. (2010). An urban drainage stormwater quality model: Model development and uncertainty quantification. *Journal of Hydrology*, 381(3–4):248–265.
- Martin, C. and Vanrolleghem, P. (2014). Analysing, completing, and generating influent data for WWTP modelling: A critical review. *Environmental Modelling & Software*, 60:188–201.
- Meirlaen, J., Huyghebaert, B., Sforzi, F., Benedetti, L., and Vanrolleghem, P. (2001). Fast, simultaneous simulation of the integrated urban wastewater system using mechanistic surrogate models. *Water Science & Technology*, 43(7):301–309.
- Métadier, M. and Bertrand-Krajewski, J.-L. (2011). From mess to mass: a methodology for calculating storm event pollutant loads with their uncertainties, from continuous raw data time series. *Water Science & Technology*, 63(3):369–376.

- Métadier, M. and Bertrand-Krajewski, J.-L. (2012). The use of long-term on-line turbidity measurements for the calculation of urban stormwater pollutant concentrations, loads, pollutographs and intra-event fluxes. *Water Research*, 46(20):6836–6856.
- Mignot, E., Bonakdari, H., Knothe, P., Lipeme Kouyi, G., Bessette, A., Riviere, N., and Bertrand-Krajewski, J.-L. (2012). Experiments and 3D simulations of flow structures in junctions and their influence on location of flowmeters. *Water Science & Technology*, 66(6):1325–1332.
- Motiee, H., Chocat, B., and Blanpain, O. (1997). A storage model for the simulation of the hydraulic behaviour of drainage networks. *Water Science & Technology*, 36(8-9):57–63.
- Mourad, M., Bertrand-Krajewski, J.-L., and Chebbo, G. (2006). Design of a retention tank: comparison of stormwater quality models with various levels of complexity. *Water Science & Technology*, 54(6-7):231.
- Muschalla, D., Schütze, M., Schroeder, K., Bach, M., Blumensaat, F., Gruber, G., Klepizewski, K., Pabst, M., Pressl, A., Schindler, N., Solvi, A. M., and Wiese, J. (2009). The HSG procedure for modelling integrated urban wastewater systems. *Water Science & Technology*, 60(8):2065–2075.
- Nash, J. and Sutcliffe, J. (1970). River flow forecasting through conceptual models: Part I - A discussion of principles. *Journal of Hydrology*, 10:282–290.
- Nelen, F. (1992). *Optimized control of urban drainage systems*. PhD thesis, TU Delft.
- Olsson, G. (2012). ICA and me - A subjective review. *Water Research*, 46(6):1585–1624.
- Olsson, G., Carlsson, B., Comas, J., Copp, J., Gernaey, K., Ingildsen, P., Jeppsson, U., Kim, C., Rieger, L., Rodríguez-Roda, I., Steyer, J.-P., Takács, I., Vanrolleghem, P., Vargas, A., Yuan, Z., and Åmand, L. (2014). Instrumentation, control and automation in wastewater - From London 1973 to Narbonne 2013. *Water Science and Technology*, 69(7):1373–1385.
- Pawłowsky-Reusing, E. (2006). Integrated Sewage Management - Final Report. Technical Report January, KompetenzZentrum Wasser Berlin gGmbH.
- Pleau, M., Colas, H., Lavalée, P., Pelletier, G., and Bonin, R. (2005). Global optimal real-time control of the Quebec urban drainage system. *Environmental Modelling & Software*, 20:401–413.

- Puig, V., Cembrano, G., Romera, J., Quevedo, J., Aznar, B., Ramon, G., and Cabot, J. (2009). Predictive optimal control of sewer networks using CORAL tool: Application to Riera Blanca catchment in Barcelona. *Water Science & Technology*, 60(4):869–878.
- RIONED Foundation (2004). Module C2100: Rioleringsberekeningen, hydraulisch functioneren (in Dutch). In *Leidraad Riolering*, pages 1–100.
- RIONED Foundation (2016). Het nut van stedelijk waterbeheer.
- Risholt, L., Schilling, W., Erbe, V., and Alex, J. (2002). Pollution based real time control of wastewater systems. *Water Science & Technology*, 45(3):219–28.
- Robitaille, L., Komorowski, F., Fortier, V., Chadoutaud, E., and Rousseau, J.-P. (2016). Gestion Dynamique des RUTP du bassin versant Louis Fargue à Bordeaux: en route vers une seconde phase de déploiement. In *Proceedings of Novatech*, pages 1–6.
- Rousseau, D., Verdonck, F., Moerman, O., Carrette, R., Thoeye, C., Meirlaen, J., and Vanrolleghem, P. (2001). Development of a risk assessment based technique for design/retrofitting of WWTPs. *Water Science & Technology*, 43(7):287–294.
- Ruban, G., Joannis, C., Zug, C., Blanchet, F., and Cohan-Solal, F. (2002). Evaluation of Discharges by CSO's from Water Depth Measurements: Case Study of a Frontal Weir with Varying Crest Elevation and Backwater Effect. In *Proceedings of ICUD9*, Oregon.
- Rubinato, M., Shucksmith, J., Saul, A., and Shepherd, W. (2013). Comparison between InfoWorks hydraulic results and a physical model of an Urban drainage system. *Water Science & Technology*, 68(2):372–379.
- Schellart, A., Buijs, F., Tait, S., and Ashley, R. (2008). Estimation of uncertainty in long term combined sewer sediment behaviour predictions, a UK case study. *Water Science and Technology*, 57(9):1405–1411.
- Schilling, W. (1989). *Real-Time control of urban drainage systems - The state of the art*. Number April 1989. IAWPRC Task Group on Real-Time Control of Drainage Systems.
- Schilling, W., Andersson, B., Nyberg, U., Aspegren, H., Rauch, W., and Harremoës, P. (1996). Real time control of wastewater systems. *Journal of Hydraulic Research*, 34(6):785–797.

- Schilperoort, R. (2011). *Monitoring as a tool for the assessment of wastewater quality dynamics*. PhD thesis, TU Delft.
- Schilperoort, R., Dirksen, J., Langeveld, J., and Clemens, F. (2012). Assessing characteristic time and space scales of in-sewer processes by analysis of one year of continuous in-sewer monitoring data. *Water Science & Technology*, 66(8):1614–1620.
- Schütze, M., Campisano, A., Colas, H., Schilling, W., and Vanrolleghem, P. (2004). Real time control of urban wastewater systems - where do we stand today? *Journal of Hydrology*, 299(3-4):335–348.
- Schütze, M., Erbe, V., Haas, U., Scheer, M., and Weyand, M. (2008). Sewer system real-time control supported by the M180 guideline document. *Urban Water Journal*, 5(1):67–76.
- Seggelke, K., Löwe, R., Beeneken, T., and Fuchs, L. (2013). Implementation of an integrated real-time control system of sewer system and waste water treatment plant in the city of Wilhelmshaven. *Urban Water Journal*, 10(5):330–341.
- Soulis, K. and Dercas, N. (2012). Field Calibration of Weirs Using Partial Volumetric Flow Measurements. *Journal of Irrigation and Drainage Engineering*, 138(May):481–484.
- Sun, S. and Bertrand-Krajewski, J.-L. (2012). On calibration data selection: The case of stormwater quality regression models. *Environmental Modelling & Software*, 35:61–73.
- Sun, S. and Bertrand-Krajewski, J.-L. (2013a). Input variable selection and calibration data selection for storm water quality regression models. *Water Science & Technology*, 68(1):50–58.
- Sun, S. and Bertrand-Krajewski, J.-L. (2013b). Separately accounting for uncertainties in rainfall and runoff: Calibration of event based conceptual hydrological models in small urban catchments using Bayesian method. *Water Resources Research*, 49:1–14.
- Talebizadeh, M., Belia, E., and Vanrolleghem, P. (2016). Influent generator for probabilistic modeling of nutrient removal wastewater treatment plants. *Environmental Modelling & Software*, 77:32–49.

- Thompson, K., Vamvakieridou-Lyroudia, L., Kapelan, Z., and Savic, D. (2011). Optimal macro-location methods for sensor placement in urban water systems. Technical Report August.
- Tyson, J., Guarino, C., Best, H., and Tanaka, K. (1993). Management and institutional aspects. *Water Science and Technology*, 27(12):159–172.
- Vaes, G., Berlamont, J., and Bermont, J. (1999). Emission predictions with a multi-linear reservoir model. *Water Science & Technology*, 39(2):9–16.
- Vaes, G., Willems, P., and Berlamont, J. (2001). Rainfall input requirements for hydrological calculations. *Urban Water*, 3(1-2):107–112.
- Van Bijnen, M. and Korving, H. (2008). Application and results of automatic validation of sewer monitoring data. In *Proceedings of ICUD11*, pages 1–10, Edinburgh.
- Van Daal-Rombouts, P. (2012). Personal communication.
- Van Daal-Rombouts, P., De Jonge, J., Langeveld, J., and Clemens, F. (2016a). Integrated real time control of influent pumping station and primary settling tank at WWTP Eindhoven. In *Proceedings of SPN8*, pages 282–285, Rotterdam.
- Van Daal-Rombouts, P., Sun, S., Langeveld, J., Bertrand-Krajewski, J.-L., and Clemens, F. (2016b). Design and performance evaluation of a simplified dynamic model for combined sewer overflows in pumped sewer systems. *Journal of Hydrology*, 538:609–624.
- Van Daal-Rombouts, P., Tralli, A., Verhaart, F., Langeveld, J., and Clemens, F. (2014). Applicability of CFD modelling in determining accurate weir discharge - water level relationships. In *Proceedings of ICUD13*, pages 1–8, Sarawak.
- Van Luijtelaar, H. and Rebergen, E. (1997). Guidelines for hydrodynamic calculations on urban drainage in the Netherlands: Backgrounds and examples. *Water Science & Technology*, 36(8-9):253–258.
- Van Zon, H. (1986). *Een zeer onfrisse geschiedenis. Studies over niet-industriële vervuiling in Nederland, 1850-1920*. PhD thesis, University of Groningen.
- Vanrolleghem, P., Benedetti, L., and Meirlaen, J. (2005). Modelling and real-time control of the integrated urban wastewater system. *Environmental Modelling & Software*, 20(4):427–442.

- Veldkamp, R., Henckens, G., Langeveld, J., and Clemens, F. (2002). Field data on time and space scales of transport processes in sewer systems. In *Proceedings of ICUD9*, pages 1–15, Portland.
- Vezzaro, L., Christensen, M., Thirsing, C., Grum, M., and Mikkelsen, P. (2014). Water quality-based real time control of integrated urban drainage systems: A preliminary study from Copenhagen, Denmark. *Procedia Engineering*, 70:1707–1716.
- Vrugt, J., Ter Braak, C., Clark, M., Hyman, J., and Robinson, B. (2008). Treatment of input uncertainty in hydrologic modeling: Doing hydrology backward with Markov chain Monte Carlo simulation. *Water Resources Research*, 44:1–15.
- Vrugt, J., Ter Braak, C., Gupta, H., and Robinson, B. (2009). Equifinality of formal (DREAM) and informal (GLUE) Bayesian approaches in hydrologic modeling? *Stochastic Environmental Research and Risk Assessment*, 23:1011–1026.
- Weijers, S., De Jonge, J., Van Zanten, O., Benedetti, L., and Langeveld, J. (2012). KALLISTO: cost effective and integrated optimization of the urban wastewater system Eindhoven. *Water Practice & Technology*, 7(2).
- Weyand, M. (2002). Real-time control in combined sewer systems in Germany - some case studies. *Urban Water*, 4:347–354.
- WFD (2000). The EU Water Framework Directive.
- Willems, P. (2006). Random number generator or sewer water quality model? *Water Science & Technology*, 54(6-7):387–394.
- Willems, P. (2010). Parsimonious model for combined sewer overflow pollution. *Journal of Environmental Engineering*, (March):316–325.
- Wolfs, V., Villazon, M., and Willems, P. (2013). Development of a semi-automated model identification and calibration tool for conceptual modelling of sewer systems. *Water Science & Technology*, 68(1):167–175.
- Wolfs, V. and Willems, P. (2014). Development of discharge-stage curves affected by hysteresis using time varying models, model trees and neural networks. *Environmental Modelling & Software*, 55:107–119.
- Zabel, T., Milne, I., and McKay, G. (2001). Approaches adopted by the European Union and selected Member States for the control of urban pollution. *Urban Water*, 3(1-2):25–32.

- Zhao, C., Zhu, D., and Rajaratnam, N. (2008). Computational and Experimental Study of Surcharged Flow at a 90 Combining Sewer Junction. *Journal of Hydraulic Engineering*, 134(6):688–700.

A CSO pollution analysis

Introduction

Water quality measurements in sewer systems have been a research topic of interest for several years. Recently the need for in-sewer water quality measurements has increased following regulations such as the WFD, focussing on the quality of water bodies. Wastewater management is therefore changing from emission reduction to impact management (Blumensaat et al., 2012; Weijers et al., 2012). A similar shift of focus is taking place in the application of real time control (RTC) as one of the means for improving the performance of the available infrastructure and hence the wastewater system. In RTC the focus is shifting from 1) volume based RTC (minimising overflow volumes by maximising the utilisation of the storage capacity), via 2) emission based RTC (minimising emission by redirecting flows to the least polluted outflow), to 3) impact based RTC (minimising impact by redirecting flows to the least sensitive receiving water), see e.g. (Erbe et al., 2002; Fuchs and Beeneken, 2005; Vanrolleghem et al., 2005; Lacour and Schütze, 2011).

The potential of RTC for adapting the performance of wastewater system infrastructure essentially depends on three factors. For these, respectively: 1) availability of idle system capacity in time and space, and the possibility to activate this unused system capacity, 2) the differences in pollutant levels between discharge locations and 3) the differences in vulnerability of receiving waters for discharges from wastewater systems.

This is an adapted version of: Van Daal-Rombouts, P.M.M., Schilperoort, R.P.S., Langeveld, J.G., Clemens, F.H.L.R., (2013). CSO pollution analysis based on conductivity and turbidity measurements and implications for application of RTC. In *Proceedings of Novatech2013*. Lyon, France.

For emission and impact based RTC pollution estimates have been used, e.g. storm sewer outfall discharges are typically less polluted than wastewater treatment plant (WWTP) effluent, which in turn is less polluted than combined sewer overflow (CSO) discharges. No distinction is made in the pollution level of different CSOs. Incorporating this would be a significant step forward in the development of RTC: RTC based on quality measurements. However, this requires more reliable and robust measurements on the quality of CSO discharges.

Early work on continuous, in-sewer water quality measurements, see e.g. (Krebs et al., 1999; Veldkamp et al., 2002; Bertrand-Krajewski, 2004; Langeveld et al., 2005; Schellart et al., 2008), focussed on turbidity (TU) and conductivity (EC). These parameters are relatively easy to measure, which is an advantage in the hostile environment of a sewer system. Later on, technologic improvements made the application of more complicated sensors such as spectrometers feasible, allowing continuous monitoring of, for example, total suspended solids (TSS) and soluble chemical oxygen demand (COD_f) (Langergraber et al. 2003).

Nevertheless, measuring pollution directly through parameters like TSS and COD_f is not only more expensive but also requires more expertise and time investment to get reliable results (Schilperoort, 2011). Attention is thus turning back to the more easily measurable parameters, which could serve as surrogate measurements for the more complex direct parameters: (Lepot et al., 2013) have shown that the uncertainties in TU measurements are smaller than in TSS, and (Métadier and Bertrand-Krajewski, 2012) have shown that TU measurements can be correlated to the concentration of TSS. (Lombard et al., 2010) have shown that combining TU and EC measurements gives a good indication of the constituents of wastewater.

The objective of this research is to demonstrate the applicability of and need for surrogate sensors as robust sensors for water quality based RTC. Almost 1.5 years of level, TU and EC measurements at several CSO locations in Eindhoven (the Netherlands) have been analysed to show the suitability of these measurements for determining the most polluted CSO locations. The importance of these results for wastewater system optimisation through quality based RTC is highlighted.

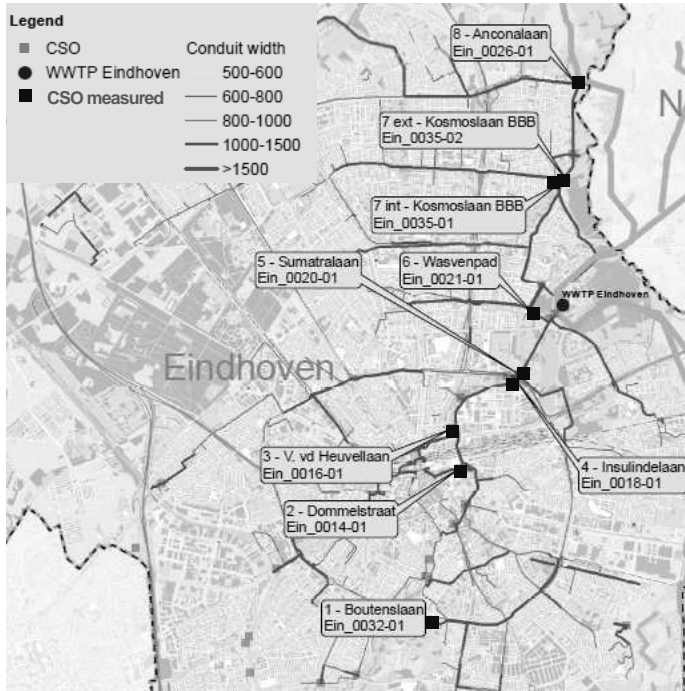


Figure A.1: Measurement locations at seven CSOs, the internal and external weir of a storm water settling tank and the WWTP influent of Eindhoven, the Netherlands.

Materials and method

Area, measurements and sensors

The sewer system under investigation is located in the south of the Netherlands and collects the wastewater from Eindhoven. It consists of approximately 800 km combined and 350 km separate sewer system, 2000 ha of impermeable area, 280,000 population equivalent and has an average gradient of approximately 1:400. Measurements are performed at seven CSO locations, the internal and external weir of a storm water settling tank, and the WWTP influent. A geographical overview of the locations and names can be found in figure A.1.

At each location water level, TU and EC measurements are performed every minute. The following sensors are used: SOLITAX t-line sc (Hach Lange) for TU, 3798-S sc (Hach Lange) for EC and VEGABAR 66 (Vega) for the water level. Additional hourly values of the precipitation depth at Eindhoven Airport from the Royal Netherlands Meteorological Institute (station 370, just outside of Eindhoven) are used.

The quality sensors at the CSO locations and the storm water settling tank are installed approximately 30 to 50 *cm* under the weir height, to ensure measuring of CSO discharges rather than inceptor flows. As a result of this set-up no measurements are registered during dry weather flow with sensor outputs of approximately $-125 \mu\text{S}/\text{cm}$ and 0 *FNU*. At the WWTP continuous measuring series are available.

Data validation and event selection

The measuring period used for this research runs from 1 July 2011 to 15 October 2012. The EC and TU sensors at the CSO locations have been installed during the first month of this period. The EC sensors have only been operational since January 2012. The level sensors have been installed at an earlier date. EC and TU sensors at the WWTP influent have been installed in May 2012.

The quality of all data has been assessed through manual validation and expert judgement. The level measurements show no drift, rise and fall in correspondence to rainfall, and the behaviour during CSO events is as expected. The quality of the EC and TU measurements is assessed for each CSO event individually, since no measurements during dry weather periods are available. The data is evaluated on availability (at least half of the measurements during a CSO event should be available), reasonable values, and the dynamics of the measurement series before, during and after the CSO event.

Of in total 118 recorded CSO events, EC measurements have been accepted for 36% of the events, for TU 91% is accepted. If only CSO events from January 2012 onwards are taken into account (total of 61 CSO events) the accepted percentage for EC rises to 59%, which is still much lower than for TU. This is due to more missing values in the EC than in the TU measurement series.

To determine the most polluted CSO locations, a limited number of events have been selected for analysis from the validated data set. Only events that have caused spills at a minimum of four CSO locations and for which accepted measurements are available for EC and/or TU, have been taken into account. A total of 13 events is selected.

Surrogate event mean concentration and surrogate pollution load

EC and TU both give an indication of the constituents of wastewater. EC is a measure for the dilution of wastewater, since the conductivity of rainwater is lower than that of raw wastewater (Göbel et al., 2007). TU gives an indication of the amount of suspended sediment in the wastewater. Combining these parameters therefore leads to a parameter that includes both phenomena, and thus characterises how polluted the wastewater is (Lombard et al., 2010; Lepot et al., 2013).

Based on the validated data the surrogate event mean concentration (sEMC) is calculated, following e.g. (Mourad et al., 2006). The sEMC is defined as the product of the average values of EC and TU during a CSO event. Please note that the pollution sEMC is a relative measure indicating the quality of the water. The surrogate pollution load (sPL) is calculated through multiplication of the sEMC with the overflow volume.

The overflow volume of a CSO event is estimated from the level measurements. The volume Q [m^3/s] is calculated through $Q = 1.7mbh^{3/2}$, with m [-] an empirical constant taken to be 0.8 for all locations, b [m] the length of the weir and h [m] the water level above the weir crest. This equation is only valid under free outflow conditions. In determining the overflow volume this is assumed for all events and locations. The uncertainty in the overflow volume and its consequences for the results are discussed at the end of the results section.

Results and discussion

Description of EC and TU behaviour

Figure A.2 shows typical EC and TU measurements for WWTP influent. The EC measurements clearly respond to rainfall on 5, 15 and 20 May: the values show a sharp decrease caused by the dilution of the wastewater transported to the WWTP, followed by a gradual return to average dry weather flow values of approximately 800 to 1100 $\mu S/cm$. The EC values do not respond to the rainfall on 9 May. This may be due to the local character of rainfall combined with the low spatial density of the rainfall measurements (one location just outside of Eindhoven).

The TU measurements show a less evident response to rainfall than the EC measurements. Only after rainfall on 15 May a clear increase in TU is recorded. Rainfall on 5 and 20 May, in both cases leading to a strong decrease of EC, leads only to a small increase in TU. Average TU dry weather flow values range between approximately 50 to 200 *FNU*.

In figure A.3 EC and TU measurements during a CSO event are depicted. Please note that that the EC and TU sensors are only operational when the level surpasses the installation level of the sensor. As for the measurements at the WWTP influent, see figure A.2, the EC values decrease due to the dilution of the wastewater followed by a gradual return to dry weather flow values. At the CSO locations, however, only a certain time window is captured (where the dilution of the wastewater is just at its end) resulting in a smaller changes in EC.

The TU measurements show a general decline during the CSO event. When the water level is close to the CSO level, increases in TU are registered. This is most likely due to changes in the hydraulic conditions, leading to an increase in sheer stress and thus an increase in re-suspension of sediment. When the water level is close to the installation height of the sensor, at the start and end of the measurements, a few outliers are recorded.

sEMC and sPL

Average EC and TU values, overflow volumes, the sEMC and sPL have been calculated for 13 events as described in the previous section. The results are presented in tables A.1 and A.2.

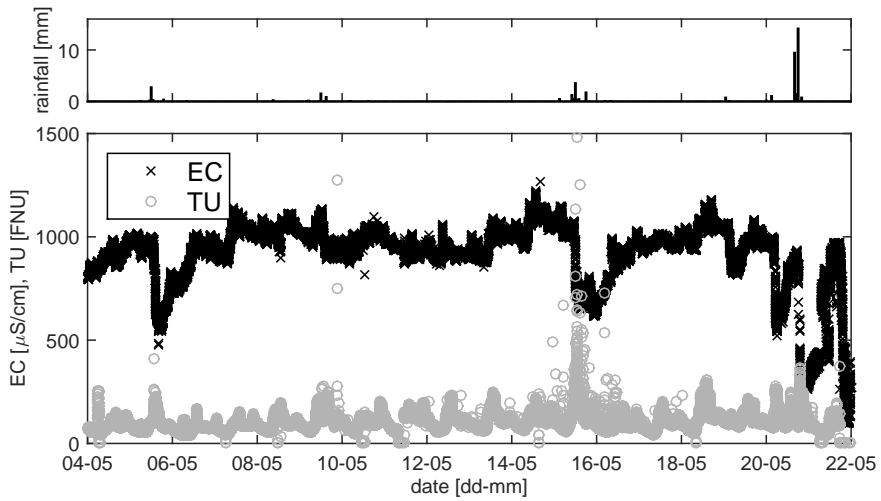


Figure A.2: Example of typical EC and TU measurements. Please note sensor failure from 20 May onwards. WWTP influent, May 2012.

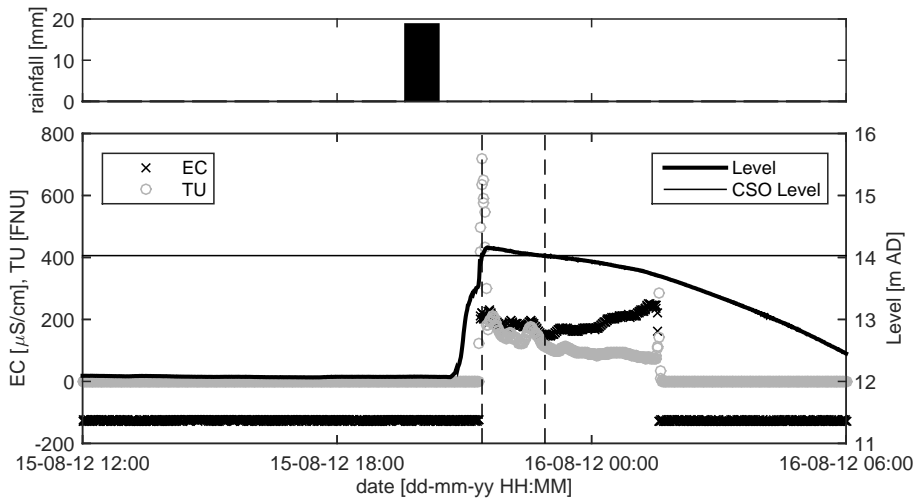


Figure A.3: Example of typical EC and TU measurements during a CSO. Location 4 - Insulindelaan, 15 and 16 August 2012.

Table A.1: Average EC [$\mu S/cm$] and TU [FNU] values, CSO volume [m^3], sEMC and sPL for each event and CSO location. ‘X’ and ‘-’ mark no CSO event and no data available or data rejected, respectively, part I.

loc	EC	TU	volume	sEMC	sPL	EC	TU	volume	sEMC	sPL
14 August 2011						23 August 2011				
1	-	235	1.1E+4	-	-	-	253	1.7E+4	-	-
2	-	34	5.0E+3	-	-	-	65	1.3E+4	-	-
3	-	71	3.4E+4	-	-	-	131	5.8E+4	-	-
4	-	41	2.1E+4	-	-	197	73	6.3E+4	1.4E+4	9.0E+8
5	-	38	1.4E+4	-	-	-	75	2.7E+4	-	-
6	X	X	X	X	X	326	53	2.2E+4	1.7E+4	3.8E+8
7 int	-	73	7.2E+4	-	-	-	77	9.2E+4	-	-
7 ext	-	24	4.7E+4	-	-	102	50	7.1E+4	5.1E+3	3.6E+8
8	-	80	0.0E+0	-	-	-	63	0.0E+0	-	-
14 December 2011						16 December 2011				
1	-	190	1.8E+3	-	-	-	114	4.1E+3	-	-
2	-	54	6.5E+2	-	-	-	41	2.9E+3	-	-
3	-	125	3.6E+3	-	-	-	74	1.0E+4	-	-
4	-	79	2.3E+3	-	-	-	50	8.8E+3	-	-
5	-	62	6.7E+1	-	-	-	34	2.0E+3	-	-
6	-	43	1.8E+3	-	-	-	35	8.5E+3	-	-
7 int	-	-	2.8E+4	-	-	-	-	6.0E+4	-	-
7 ext	-	34	3.2E+4	-	-	-	28	8.4E+4	-	-
8	X	X	X	X	X	X	X	X	X	X
3 January 2012						5 January 2012				
1	183	87	5.0E+2	1.6E+4	7.9E+6	X	X	X	X	X
2	-	93	1.7E+1	-	-	X	X	X	X	X
3	-	153	1.3E+3	-	-	-	77	3.6E+2	-	-
4	-	106	3.7E+2	-	-	116	55	3.2E+2	6.3E+3	2.0E+6
5	X	X	X	X	X	X	X	-	X	-
6	-	85	2.1E+1	-	-	-	41	4.0E+2	-	-
7 int	-	50	1.2E+4	-	-	-	73	2.2E+4	-	-
7 ext	X	X	X	X	X	-	34	2.0E+4	-	-
8	X	X	X	X	X	X	X	X	X	X
19 January 2012						4 June 2012				
1	321	48	4.8E+2	1.5E+4	7.4E+6	270	89	9.2E+2	2.4E+4	2.2E+7
2	124	-	5.2E+2	-	-	X	X	X	X	X
3	131	111	5.8E+3	1.4E+4	8.4E+7	X	X	X	X	X
4	118	68	5.9E+3	8.0E+3	4.7E+7	148	58	2.8E+3	8.6E+3	2.4E+7
5	-	52	9.4E+2	-	-	164	39	3.1E+1	6.4E+3	2.0E+5
6	115	60	5.1E+3	6.9E+3	3.5E+7	222	39	2.0E+3	8.6E+3	1.7E+7
7 int	-	55	5.3E+4	-	-	158	70	5.5E+4	1.1E+4	6.1E+8
7 ext	-	34	5.1E+4	-	-	163	40	3.5E+4	6.6E+3	2.3E+8
8	X	X	X	X	X	-	24	2.2E+3	-	-

Table A.2: Average EC [$\mu S/cm$] and TU [FNU] values, CSO volume [m^3], sEMC and sPL for each event and CSO location. ‘X’ and ‘-’ mark no CSO event and no data available or data rejected, respectively, part II.

loc	EC	TU	volume	sEMC	sPL	EC	TU	volume	sEMC	sPL
11 July 2012						15 August 2012				
1	-	230	6.4E+3	-	-	X	X	X	X	X
2	212	30	6.1E+3	6.3E+3	3.9E+7	198	145	4.7E+2	2.9E+4	1.3E+7
3	153	100	1.5E+4	1.5E+4	2.2E+8	X	X	X	X	X
4	123	84	1.1E+4	1.0E+4	1.1E+8	184	182	5.7E+2	3.4E+4	1.9E+7
5	134	59	1.9E+3	8.0E+3	1.5E+7	X	X	X	X	X
6	137	41	9.2E+3	5.6E+3	5.1E+7	273	106	9.9E+2	2.9E+4	2.8E+7
7 int	-	93	7.7E+4	-	-	-	-	3.5E+4	-	-
7 ext	109	30	6.8E+4	3.3E+3	2.3E+8	181	72	2.4E+4	1.3E+4	3.1E+8
8	-	51	9.8E+3	-	-	X	X	X	X	X
26 August 2012						24 September 2012				
1	274	57	3.9E+2	1.6E+4	6.1E+6	-	245	5.6E+3	-	-
2	-	-	9.0E+2	-	-	-	60	4.3E+2	-	-
3	-	68	3.7E+3	-	-	-	72	3.8E+3	-	-
4	131	52	3.6E+3	6.8E+3	2.5E+7	161	64	3.7E+3	1.0E+4	3.7E+7
5	145	39	4.9E+2	5.7E+3	2.8E+6	-	68	2.4E+2	-	-
6	163	45	5.6E+3	7.2E+3	4.1E+7	155	69	1.8E+3	1.1E+4	1.9E+7
7 int	-	-	7.4E+4	-	-	-	218	4.1E+4	-	-
7 ext	129	27	5.2E+4	3.5E+3	1.8E+8	163	39	2.5E+4	6.4E+3	1.6E+8
8	-	51	7.7E+3	-	-	X	X	X	X	X
3 October 2012										
1	374	93	7.0E+2	3.5E+4	2.4E+7					
2	-	73	3.5E+2	-	-					
3	-	123	2.6E+3	-	-					
4	131	73	9.7E+2	9.5E+3	9.2E+6					
5	X	X	X	X	X					
6	158	56	4.0E+2	8.8E+3	3.5E+6					
7 int	-	114	5.5E+4	-	-					
7 ext	156	41	2.9E+4	6.3E+3	1.8E+8					
8	X	X	X	X	X					

From the results a strong variability for the average EC and TU values between locations and CSO events can be found. However, looking at the highest/lowest average values for EC and TU a pattern emerges. The highest values for EC are consistently measured at location 1 - Boutenslaan. There is no location that consistently has the lowest EC values. For TU locations 1 - Boutenslaan and 3 - V. vd Heuvellaan have the highest values. Lowest values for TU are measured at location 7 ext - Kosmoslaan BBB.

Consistent with the results for EC and TU, location 1 - Boutenslaan has the highest sEMC and location 7 ext - Kosmoslaan BBB the lowest. More specifically, both locations have the highest/lowest sEMC for all measured events. Still it should be noted that only one event has sEMC values for both locations 1 - Boutenslaan and 3 - V. vd Heuvellaan, that has the second highest pollution level values.

From maintenance it is known that the sewer system near location 1 - Boutenslaan is relatively heavily polluted. This CSO is located in a catchment that is connected to the main sewer system via an internal weir and vortex flow regulator before which sedimentation takes place. The high sEMC found, indicate that this sediment could re-suspend during heavy rainfall and is emitted in case of a CSO event.

That location 7 ext - Kosmoslaan BBB has a lower sEMC than location 7 int - Kosmoslaan BBB as well as the overall lowest sEMC, confirms the supposed functioning of the storm water settling tank. This is further supported by the results for TU and EC: location 7 ext - Kosmoslaan BBB has the lowest values for TU (sediments settle in the tank and are not emitted to the receiving water), but not for EC (for which settling has no effect).

Looking at the sPL discharged from a CSO instead of the sEMC of the overflow water, a more diffuse picture arises. This is caused by the large differences in overflow volumes between locations and events. No location is consistently discharging the lowest sPL. Location 7 ext - Kosmoslaan BBB is discharging the highest sPL for most events, but also the lowest in one occasion. That location 7 ext - Kosmoslaan BBB discharges the highest sPL despite having the lowest sEMC, indicates that the storm water settling tank is positioned at the CSO where it is most effective.

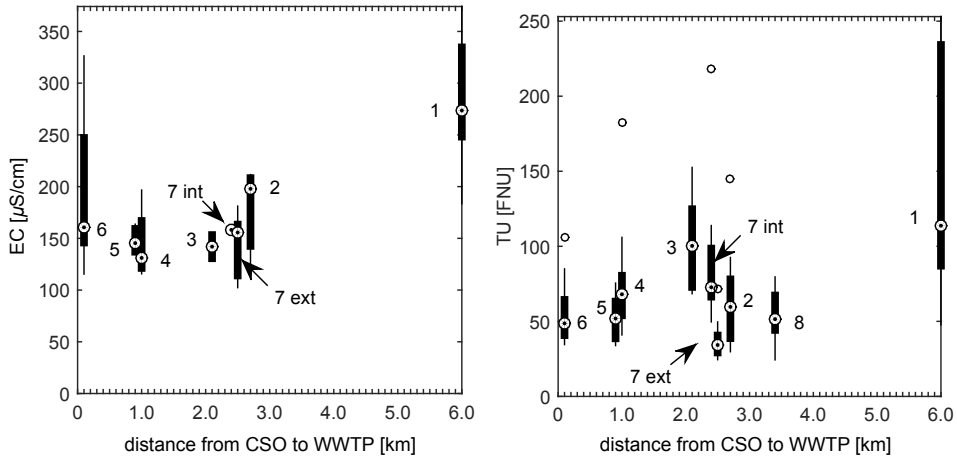


Figure A.4: Boxplots for the EC (left) and TU (right) as a function of distance between the CSO and WWTP. Locations are indicated by their number.

Influence of location

Figure A.4 displays boxplots for EC (left) and TU (right) for all available events as a function of the distance of the CSO with respect to the WWTP. This distance is measured, following the dominant water flow through the sewer system. No indication is found that the location of the CSO is dominant in either parameter. For EC the dilution in the sewer system seems rather uniform with the exception of location 1 - Boutenslaan, TU shows larger differences over the locations and is therefore likely to be determined by local conditions.

RTC potential and water quality measurements

Applying (knowledge based on) quality measurements at CSO locations can have a large impact on the optimal control of wastewater systems. This is found from figure A.5, displaying boxplots of sEMC and sPL for all locations.

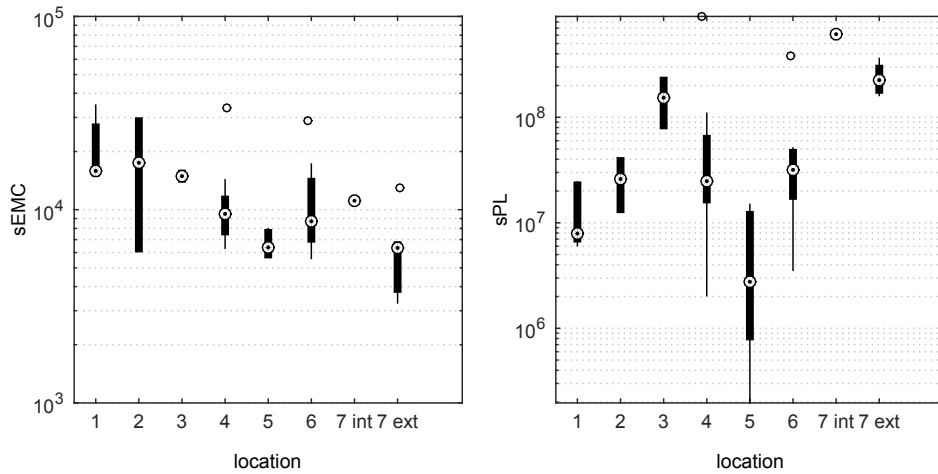


Figure A.5: Boxplots for the sEMC (left) and sPL (right) for each location. No values are available for location 8 - Anconalaan.

Based on the sEMC (left), locations 1 - Boutenslaan and 2 - Dommelstraat would be the first to turn attention to when minimising the impact of the sewer system on the receiving water. Locations 5 - Sumatrалаan and 7 - Kosmoslaan would be last. Based on the sPL (right), locations 3 - V. vd Heuvellaan and 7 - Kosmoslaan would by far be the first places to reduce the impact, while locations 1 - Boutenslaan and 5 - Sumatrалаan would be last. The difference between both parameters is the incorporation of the overflow volume in the sPL, while this is irrelevant for the sEMC.

With RTC it is possible to divert flows and therefore change to some extent the overflow location. If the minimisation of the impact on the receiving water based on the sPL were to be considered, the optimisation would to a large extent be dominated by the overflow volume. The clear difference in sEMC between the locations would have only a minor influence. If only the sEMC was to be considered very different choices would be made.

Discussion

The measuring period available for the analysis contains a limited number of events only. Not all selected events lead to CSO events at all locations, and not all CSO events have been registered properly. The analysis is thus based on an incomplete data set. However the results for the sEMC are consistent between events and locations, and are in line with theoretical expectations and practical evidence. This suggests that the method and outcome are valid. A longer and more complete data set is necessary to perform a more statistically solid analysis.

For determining the sPL, the overflow volumes have been calculated from level measurements. These calculations are based on an empirical formula, which should be calibrated for local conditions. It is known from (Bos and Kruger-Van der Griendt, 2007) that errors in the order of 30% are not uncommon. The CSO locations described in this paper have not been calibrated and the associated errors have not explicitly been taken into account. This will be looked into in further research. It has been checked, however, that the presented conclusions still hold when incorporating a 50% error in the calculated volumes.

Another point of interest for a more thorough investigation is the quality assessment of the data. Ideally the data is validated automatically with standard routines, leading to reproducible results. In the case of measurements at the CSO locations it is difficult to implement such routines, since no continuous time series are available. More attention is needed for this. The quality assessment in this study is based on manual validation and expert judgement. The reproducibility has been tested by having two people perform the assessment independently. They agreed in 92% of the events, the remaining events have been discussed and decided upon.

For this study only EC, TU and level measurements have been available at the CSO locations. The results for the sEMC and sPL based on these measurements are promising. However, additional measurements (from short campaigns), are needed to quantify how polluted a CSO location actually is. These additional measurements could be grab samples to calibrate the EC and TU sensors, or direct high frequency measurements (e.g. TSS) to derive relations between the direct parameter and EC and/or TU. Ideally these measurements should be performed at every location.

Conclusion

In this study it is shown that EC and TU measurements can serve as surrogate measurements in determining the (relative) pollution of a CSO location. The sEMC, defined as the product of EC and TU, has been determined for different locations and events. The results are consistent between locations and events, and locations with the highest/lowest sEMC are in line with theoretical expectations and practical evidence. The sPL, defined as the sEMC multiplied by the overflow volume, is a less strong indicator for the measure of pollution of a CSO location.

EC and TU values have been analysed with respect to the distance between the CSO location to the WWTP. No indication is found that the location of the CSO with respect to the WWTP is of importance for the EC or TU values of a CSO.

Comparison of the sEMC and sPL at the CSO locations, shows that water quality measurements can have a significant impact on the optimal control of a wastewater system. Clear differences in sEMC and sPL between CSO locations were established. This provides evidence for quality based RTC potential in the Eindhoven area.

sEMC and sPL are relative measures. Additional measurements are needed to quantify the amount of pollution.

B Data requirements for quality based RTC

Introduction

In wastewater management, real time control (RTC) is generally considered as one means for improving the performance of the available infrastructure and hence the wastewater system. Essentially, the potential of RTC for adapting this performance depends on three factors, each leading to its own RTC strategy:

- Available idle system capacity → volume based RTC;
- Differences in pollution levels between discharge locations → quality based RTC;
- Differences in vulnerability of the receiving water → impact based RTC.

The development of a RTC strategy requires information, ideally derived from monitoring data, on the characteristics and dynamics of a wastewater system. Once implemented, RTC requires actual data on the systems performance and status of relevant parameters. For volume based RTC level measurements, possibly supplemented with flow measurements, suffice. For quality based RTC, measurements on pollution levels of the wastewater are necessary as well. Impact based RTC has an additional need for measurements in the receiving water, see figure B.1. More information on RTC and developments in the field can be found in (Schütze et al., 2004; Olsson, 2012).

This is an adapted version of: Van Daal-Rombouts, P.M.M., Langeveld, J.G., Clemens, F.H.L.R., (2013). Requirements for quality of monitoring data for water quality based RTC. In *Proceedings of SPN7*. Sheffield, UK.

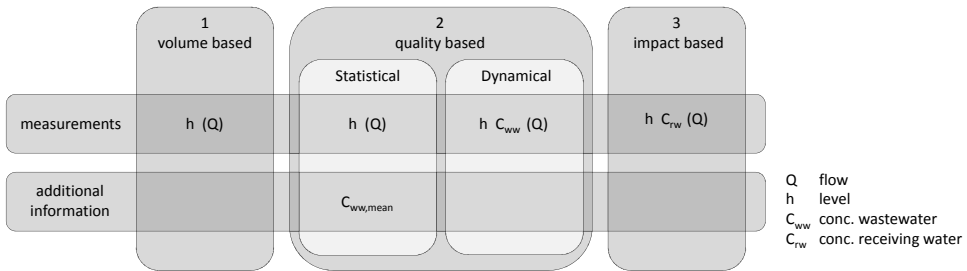


Figure B.1: RTC strategies with required measurements.

A water quality based RTC strategy can be based on historical information on concentration levels, observed under a range of conditions at different locations. With this information, it is possible to derive a ‘Statistical’ RTC strategy, prioritising discharges at the least polluted location (e.g. storm sewer overflows, combined sewer overflows (CSOs) or wastewater treatment plant (WWTP) effluent). A more sophisticated ‘Dynamical’ RTC strategy would base its control on actual information on water quality. For the first strategy, statistical information from previous measurements suffices, whereas for the second strategy, real time measurements are required.

Both water quality based RTC strategies set very different requirements for the water quality data in terms of accuracy, reliability and availability, and hence the sensor performance and data acquisition. (Métadier and Bertrand-Krajewski, 2011) have developed a framework to assess the data quality as part of the post processing. (Campisano et al., 2013) give an overview of the potential and limitations of modern equipment. Still not much is known on the demands on the data required for the application of RTC in wastewater systems.

Analysis of conductivity (EC) and turbidity (TU) measurements in Eindhoven, the Netherlands, show their potential to serve as robust (surrogate) quality measurements for application in quality based RTC, see appendix A. The research presented here analyses the same data set to determine:

- The minimum requirements for (surrogate) quality measurements for application in different water quality based RTC strategies;
- Whether EC and TU measurements can be used for quality based RTC, and at which strategic level.

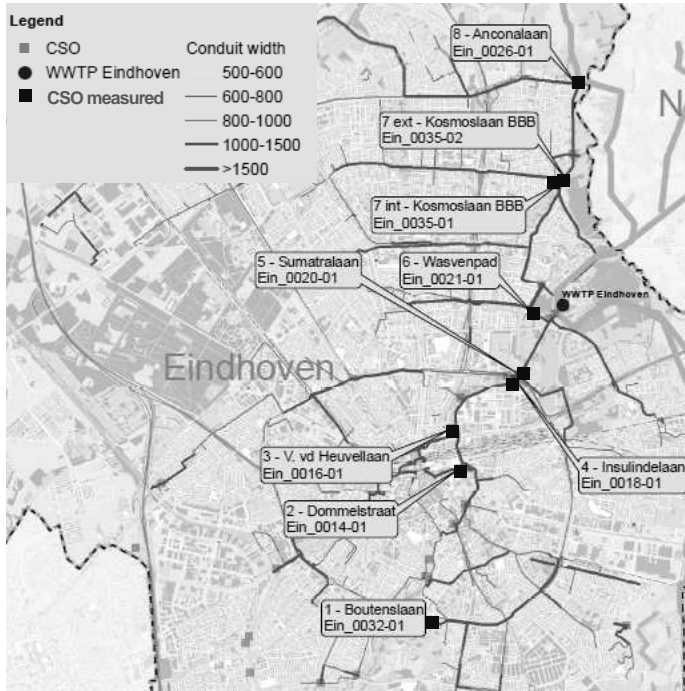


Figure B.2: Measurement locations at seven CSOs, the internal and external weir of a storm water settling tank and the WWTP influent of Eindhoven, the Netherlands.

Materials and method

Area, measurements and sensors

The sewer system under investigation is located in the south of the Netherlands and collects wastewater from the city Eindhoven. It consists of approximately 800 km combined and 350 km separate sewer system, 2000 ha of impermeable area, 280,000 population equivalent and has an average gradient of approximately 1:400. Measurements are performed at seven CSO locations, the internal and external weir of a storm water settling tank, and the WWTP influent. A geographical overview of the locations and names can be found in figure B.2. All measurements are carried out by and stored at water board De Dommel.

At each location water level [mAD], TU [FNU] and EC [$\mu S/cm$] measurements are performed, with a frequency of 1/minute. The following sensors are used: SOLITAX t-line sc (Hach Lange) for TU, 3798-S sc (Hach Lange) for EC and VEGABAR 66 (Vega) for the water level. Additional hourly values of the precipitation depth from the Royal Netherlands Meteorological Institute at Eindhoven Airport (station 370, just outside of Eindhoven) are used. The quality sensors are installed approximately 30 to 50 cm under the weir level, to ensure measuring CSO discharges rather than inceptor flows.

The measuring period used for this research runs from 1 July 2011 to 10 February 2013. The EC and TU sensors at the CSO locations have been installed during the first month of this period. The EC sensors have only been operational since January 2012. The level sensors have been installed at an earlier date. The EC and TU sensors at the WWTP influent have been installed in May 2012.

Demands on data quality

The quality based RTC strategies Statistical (based on historic measurements) and Dynamical (based on real time measurements) set very different demands on the water quality data in terms of accuracy, availability of accepted data, and measuring frequency.

Accuracy

The measurement accuracy describes the ability of the measured value to correctly represent the actual value of the measured parameter. This is reflected in the measurement error of the sensor. From literature a relative measurement error for in-situ TU measurements is found to be 5% (4σ , (Joannis et al., 2008)). For EC measurements the relative measurement error is taken to be 1% from the sensor manual. The measurement accuracy is fixed in the research presented here.

Availability of accepted data

The availability of accepted data in the measurements series depends on the overall measuring set-up, e.g. the sensor choice and performance, installation, maintenance, and data acquisition performance. The availability of accepted data of the measurement series is checked in the data validation process.

The data validation has been performed through a combination of automated and manual checks, and are labelled accordingly. Before the validation procedure single missing values in the measurement series have been filled with the previous value, as these are the result of an artefact in the database. The measurement series have been checked automatically for non-numerical values, values out of bounds, too little variation, outliers, step trends and linear trends. The level measurements have been checked additionally for correlation with rainfall, and the quality measurements at the CSO locations have been checked for correlation with the level measurements. Additional manual validation was required, due to difficulties with the automated detection of outliers and step trends, and periods of sensor malfunctioning. Finally, when the measurement series are deemed reliable for less than five consecutive minutes, the measurements in this period have been rejected as well.

Measuring frequency

The required measuring frequency depends on the information need on the measured processes. To determine the minimum measuring frequency the impact of a reduced measuring frequency will be investigated, where a frequency of 1/minute is assumed to be the highest practically feasible frequency. The impact of a reduced measuring frequency is determined by comparing properties of the original one-minute measurement series, with properties of this series where measurements have been left out to generate a lower measuring frequency.

For Statistical quality based RTC there should be significant differences in the quality of the wastewater at different discharge locations. This will be investigated by determining the event mean concentrations (EMC) from the TU measurements for different frequencies, at all CSO locations for all CSO events. The EMC is defined as the mean of the TU measurements over the duration of the CSO event.

In a Dynamical quality based RTC strategy, the real time changes in the parameters are relevant as well. This will be determined using the EC and TU measurements at the WWTP. Qualitatively the following properties have been looked at:

- The fastest process in the measurement series, which is found from the slope between local maximum and minimum values in the measurement series:

$$\frac{x(t_{local\ max}) - x(t_{local\ min})}{t_{local\ max} - t_{local\ min}};$$

- The fastest changes in the measurement series, which are found from the slopes at time t_i : $\frac{x(t_{i+1}) - x(t_{i-1})}{t_{i+1} - t_{i-1}}$.

To quantify the impact, the missing values in the generated measurement series with a lower frequency have been filled in to match the 1/minute frequency of the original series by interpolation. Here the following properties have been looked at:

- The root mean squared error (RMSE) of the differences between the original and interpolated values is calculated and compared to the mean error of the original series;
- The percentage of interpolated measurements where the difference between the original and the interpolated measurement is larger than the error in the original measurement (percentage information loss, PIL).

Results and discussion

Availability of accepted data

Validation

The data validation resulted in 63% accepted measurements for EC and 50% for TU for the WWTP influent, and on average 36% accepted measurements for EC, 95% for TU and 88% for the level measurements at the CSO locations. All analysis described in this paper are based on accepted data only. Due to the low acceptance rate of the EC measurements at the CSO locations, these measurements are discarded from further analysis.

The acceptance rate of the measurements is as low as 50%. In case of quality based RTC with a Statistical strategy this does not have to be a problem. It depends on the available measuring period and the representativeness of the measurements for that period. For a Dynamical strategy the acceptance rate is dependent on the rejection cause. Rejection of individual measurements are no problem as long as a certain minimum measuring frequency remains available. In this case large gaps in the series occur, that make the acceptance rate inadequate. Furthermore, the validation should be (almost) real time. Faulty measurements should be detected within the time scales of the dynamics of the processes involved.

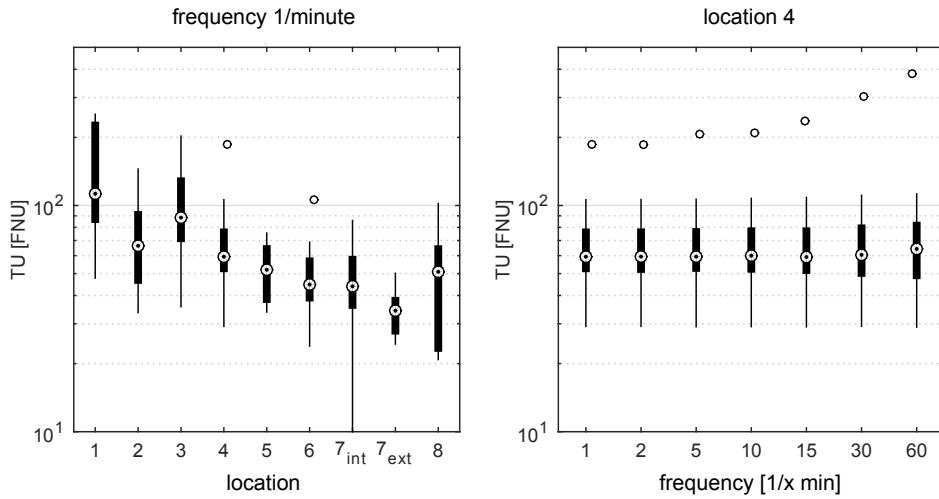


Figure B.3: Boxplots of EMCs for TU measurements. Left: for each CSO location for all CSO events at a 1/minute frequency. Right: for all frequencies for location 4.

Event selection

For the analysis of the measurements at CSO locations only selected CSO events are taken into account. Events are selected by the following rules: measurements display a reliable pattern, a CSO event takes at least 30 *min*, at least 95% of the level and 75% of the TU measurements during a CSO event are accepted. This resulted in the selection of on average 77% of the CSO events.

Measuring frequency

Statistical

The EMCs for the TU measurements show significant deviations at the different CSO locations, as can be found from figure B.3 (left, accuracy is approximately 5 FNU). The right hand side of this figure shows a representative example of the influence of the measuring frequency on the EMCs for location 4. The measuring frequency does not have a significant influence.

For the application of Statistical quality based RTC, the TU measurements at the CSO locations are suitable, based on figure B.3. Since the measuring frequency does not have much influence on the EMCs, a frequency of 1/10-15 minutes is appropriate. Higher frequencies do not contain more information, lower frequencies could result in CSO events not being measured.

Table B.1: RMSE (mean of all values) and PIL (percentage of all values) of the interpolated measurements for different measuring frequencies for EC and TU at the WWTP. The mean error in the original measurements is $9.2 \mu S/cm$ for EC and $5.4 FNU$ for TU.

frequency [$1/x \text{ min}$]	RMSE		PIL	
	EC [$\mu S/cm$]	TU [FNU]	EC [%]	TU [%]
2	7.0	3.5	10.5	7.5
5	7.9	5.0	13.5	12.3
10	10.2	6.7	20.5	18.2
15	12.2	8.6	27.2	24.0
30	15.4	12.7	36.8	32.8
60	21.1	17.3	48.9	43.8

Dynamical

In figure B.4 the fastest processes (top, slope between local minima and maxima) and fastest changes (bottom, slope at one point) in the TU measurements at the WWTP are shown for different measuring frequencies. Please note that only the ranked 100 steepest slopes for each individual frequency are shown. Similar results have been found for the EC measurements at the WWTP (not shown here).

The figure shows the large influence of the measuring frequency on the registration of the dynamics of the measurements. The steepest slopes that are registered decrease significantly with a lower measuring frequency. Differences between measuring frequencies of 1/minute or 1/2 minutes fall within the uncertainty of the measurements, frequencies of 1/5 minutes or lower result in a loss of information on the dynamics present in the time series. Please note that lowering the frequency results in a smaller uncertainty in the calculated slopes.

To quantify these observations, table B.1 shows the RMSE and the PIL for different measuring frequencies for measurements at the WWTP. The RMSE of the difference between the interpolated and original measurements, is related to the mean error in the original measurements ($9.2 \mu S/cm$ for EC and $5.4 FNU$ for TU).

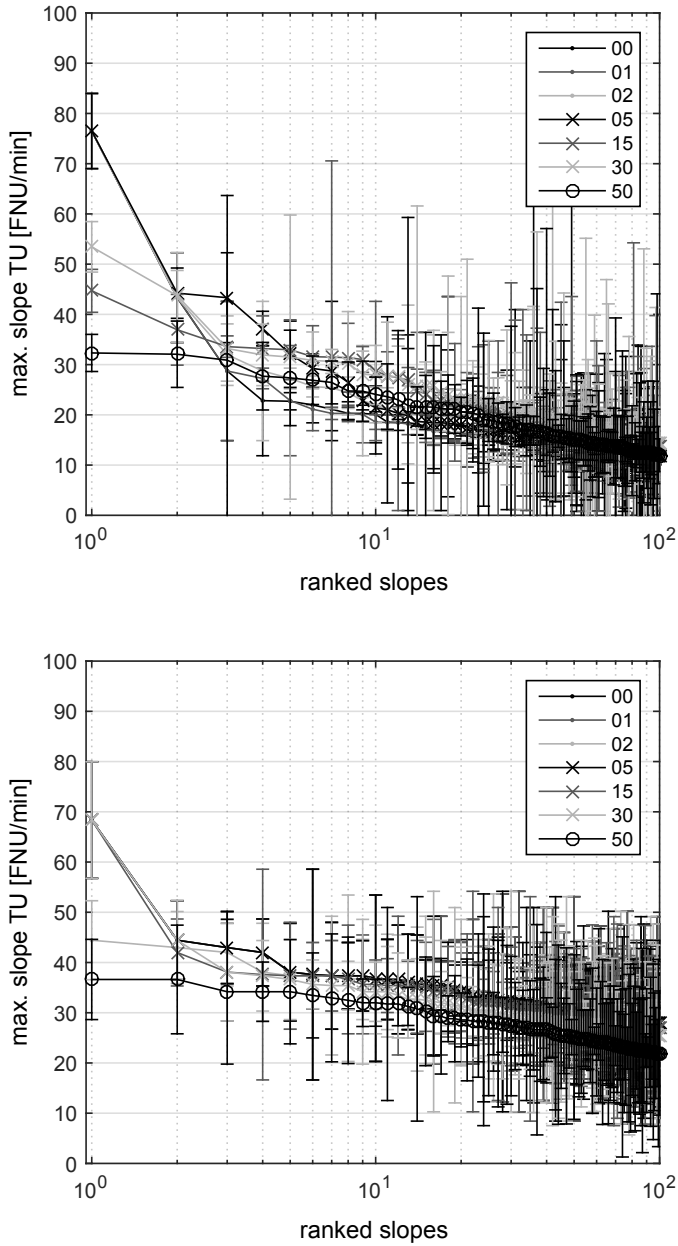


Figure B.4: Sorted 100 largest slopes in TU measurements at the WWTP for different frequencies. Top: slope based on local maximum and minimum values. Bottom: slope based on individual points.

The RMSE surpasses the mean error for both EC and TU at a measuring frequency between 1/5 and 1/10 minutes, indicating that a measuring frequency lower than 1/5 minutes results in a reduced registration of the fast dynamic processes. The PIL gradually increases for lower measuring frequencies. Even a frequency of 1/2 minutes causes 7.5% (TU) to 10.5% (EC) of the interpolated values to differ more than the measurement error from the original measurements. This stresses the importance of high frequency measurements when interested in the dynamics of quality processes.

Both the qualitative and quantitative analysis of the EC and TU measurements show that the minimum measuring frequency is 1/5 minutes, to correctly follow the dynamics of the parameters.

Discussion

The research presented here is aimed at finding the minimum requirements for quality measurements when applying quality based RTC strategies. Measuring at a higher frequency than necessary is recommended, since data storage is no longer an issue and it makes losing some measurements in communication or validation less problematic.

The required measuring frequency investigated here is based on the dynamics of the measured parameters involved, combined with the accuracy of the measurements. Another relevant timescale is the time it takes for a RTC measure to take effect. Measuring much more often than this control time leads to a more uncertain determination of the slopes, see figure B.4, and thus less certain information on the processes to base the RTC action on. It can therefore be argued that the appropriate measuring frequency depends on both the parameter dynamics and the necessary accuracy in the RTC actions. Further research should be directed at this topic.

The data validation of the measurement series has taken much time and had to be performed in part manually, resulting in rejection rates of up to 50% at the WWTP. This is mainly caused by congestion of the bypass installation the sensors are installed in. The low acceptance rate for the EC measurements at the CSO locations is due to a mismatch in the EC values of the wastewater and the measuring range of the sensor. As pointed out, both the manual validation as the high rejection rate are not acceptable for Dynamical quality based RTC. Apart from further automation of the data validation and raising the percentage of accepted data, a sound RTC backup strategy should be implemented in case of sensor malfunctioning or communication problems (Campisano et al., 2013). Depending on the situation this backup strategy could be based on Statistical quality based RTC or volume based RTC.

The accuracy for the EC measurements has been based on the sensor manual, as unlike for TU no research on the in-situ accuracy has been found in literature. Since the measuring principle of the EC sensor is straight forward, the in-situ accuracy has been taken equal to the manufacturers specification. Additional tests should be performed to conform this assumption.

Conclusion

When applying quality based RTC, demands should be set on the quality parameters that serve as input. These demands depend on the implemented strategy. Here a Statistical (based on historic measurements) and a Dynamical (based on real time measurements) strategy are investigated. The quality of the measurements is described by the accuracy, availability of accepted data and the measuring frequency.

The accuracy of the measurements has been fixed during the investigation and is taken into account in the determination of the minimum measuring frequency. The required availability of accepted data of the measurement series for a Statistical strategy depends on the representativeness and length of the measuring period. For a Dynamical strategy the necessary availability of accepted data is dependent again on the minimum measuring frequency and large gaps are not acceptable at all. For the Statistical strategy a measuring frequency of 1/10-15 minutes would suffice, for Dynamical quality based RTC the measuring frequency should be at least 1/5 minutes to follow the dynamic processes involved. A measuring frequency of 1/minute is recommended to obtain redundancy.

The data set analysed in this research is suitable for the application of quality based RTC based on the Statistical strategy. For the Dynamical strategy the accuracy and measuring frequency are suitable, but the availability of accepted data is insufficient.

C Description of the monitoring network in the wastewater system of Eindhoven

This appendix provides a concise overview of the monitoring network of water board De Dommel for the wastewater system of Eindhoven between 2010 and 2016 in tables and figures.

The tables contain the location name or code, together with the measured parameter and unit, the measuring interval in minutes, the start (and if applicable end) date and the location coordinates. No information is supplied about the network before 2010. A start date of 1 January 2010 therefore indicates the sensor was operational before this date. If the sensors were operational at 31 December 2016 no end date is supplied. No judgement on the data quality or (continuous) availability is given.

Tables are supplied for:

- WWTP Eindhoven water quality - influent, table C.1;
- WWTP Eindhoven water quality - other, table C.2;
- Rainfall, table C.3;
- River Dommel water quantity, table C.4;
- River Dommel water quality, table C.5;
- Municipality Eindhoven CSO water quality, table C.6;
- Municipality Eindhoven CSO water levels, table C.7;
- Municipality Bergeijk CSO water levels, table C.8;
- Municipality Eersel CSO water levels, table C.9;
- Municipality Heeze CSO water levels, table C.10;

- Municipality Nuenen CSO water levels, table C.11;
- Municipality Son en Breugel CSO water levels, table C.12;
- Municipality Valkenswaard CSO water levels, table C.13;
- Municipality Veldhoven CSO water levels, table C.14;
- Municipality Waalre CSO water levels, table C.15;

No locations for the water level measurements in the sewer systems of the municipality of Geldrop are supplied. The municipality itself performs measurements at most CSO locations, instead of the water board. The measurements therefore are not part of the monitoring network described.

Two figures are supplied to give a visual overview of the network. Figure C.1 indicates the water quality sensor locations at the WWTP in a schematic representation of the plant. Figure C.2 displays all other sensor locations.

Regular operational parameters for water quantity at the WWTP and in the transport sewers (at the municipalities pumping stations, and the control stations and pumping station Aalst in Riool Zuid) are not included as these are continuously available.

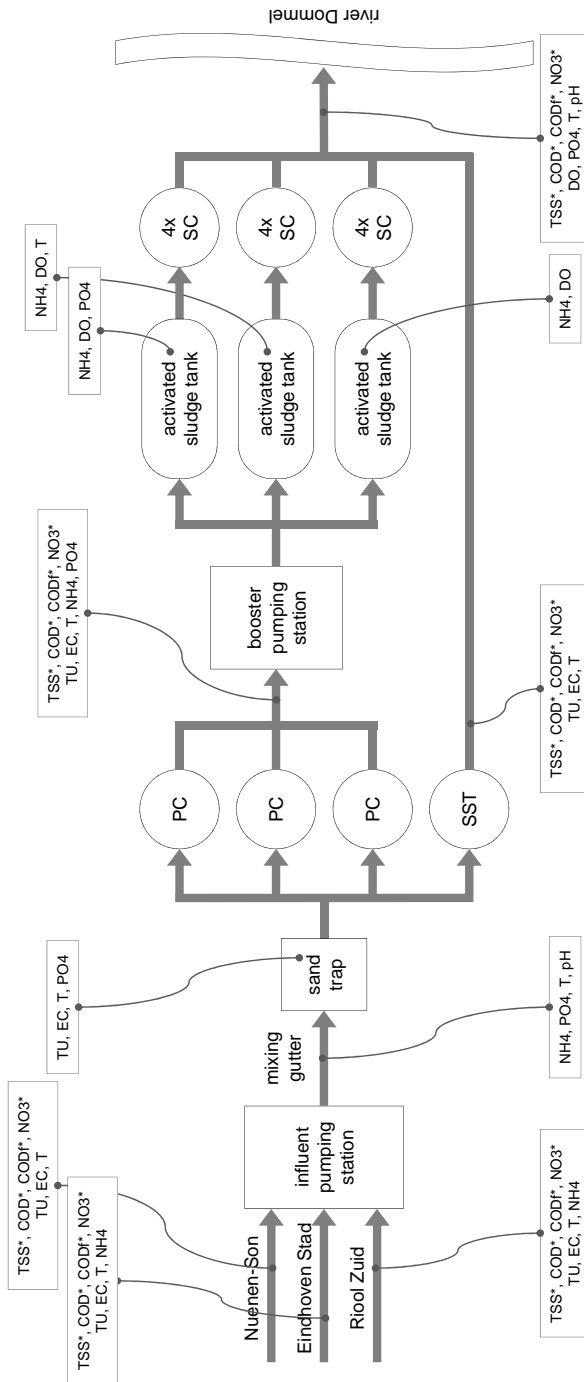
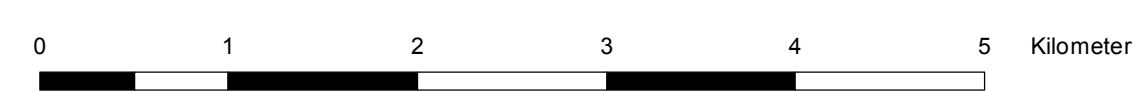
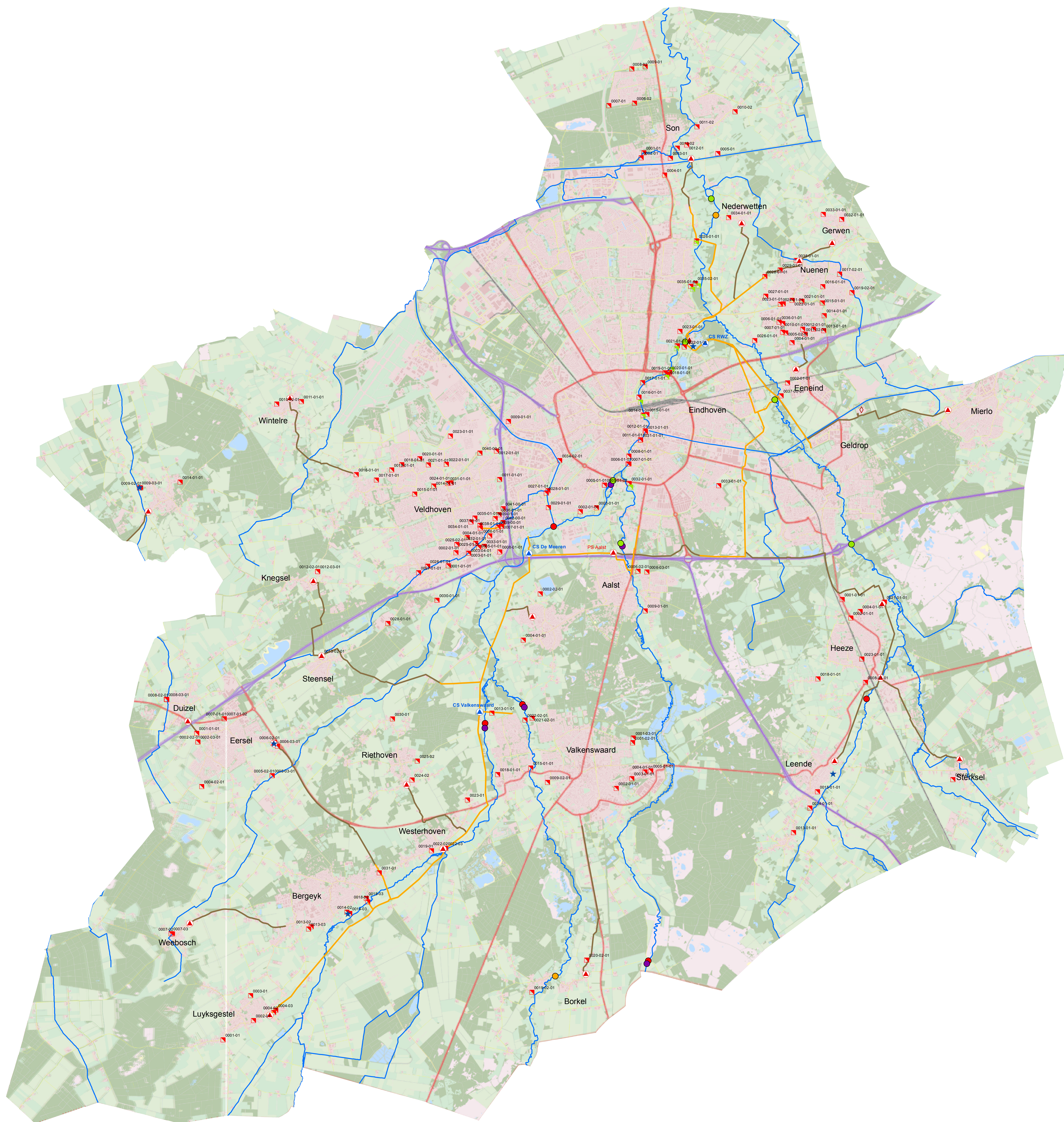


Figure C.1: Schematic overview of WWTP Eindhoven. The water quality monitoring locations as specified in tables C.1 and C.2 are indicated. Parameters marked with an asterisk are equivalent measurements.

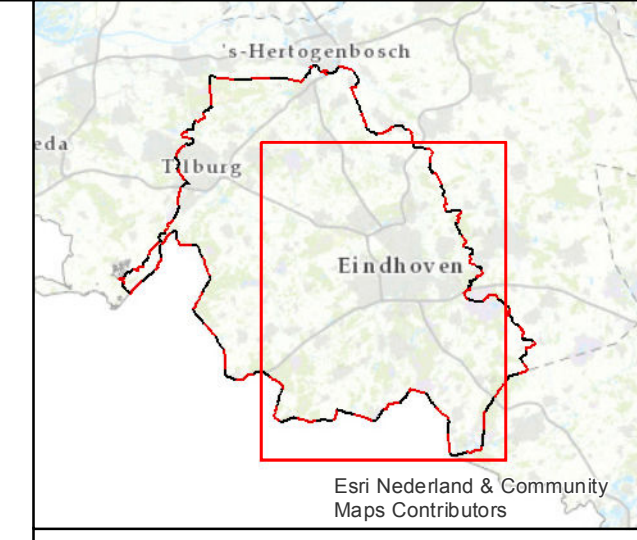


Monitoring network

Polaris

Legenda

- | | | | |
|---|--|---|--|
| <ul style="list-style-type: none"> ♦ WWTP Eindhoven ♦ Sludge treatment Mierlo ♦ Sludge treatment Mierlo ★ Precipitation | <ul style="list-style-type: none"> ▲ Control station ▲ Control station ▲ Pumping station ▲ Pumping station ▲ Sewer water level ▲ Sewer water level ▲ Sewer quality ▲ TU + EC | <ul style="list-style-type: none"> ● River quantity ● NH4 + pH ● DO + T ● River quality ● Q + v ● H | <ul style="list-style-type: none"> — Gravity conduit — Gravity conduit — Pressure main — Pressure main — Watercourse — Watercourse |
|---|--|---|--|



Monitoring network

Polaris

Auteur: Vakgroep GIV
 Datum: 7-3-2017
 Kaartnummer: 1702-1112
 Referentie: P039803
 Schaal: 1:40.000



Table C.1: WWTP Eindhoven water quality for the influent. As the monitoring locations are indicated in figure C.1 no coordinates are supplied. Parameters marked with an asterisk are equivalent measurements.

location	param.	unit	interval [min]	start date	end date
Nuenen-Son	COD*	mg/l	2	01-01-2010	31-05-2015
Nuenen-Son	CODf*	mg/l	2	01-01-2010	31-05-2015
Nuenen-Son	EC	$\mu S/cm$	1	23-09-2014	
Nuenen-Son	NO3*	mg/l	2	01-01-2010	16-10-2012
Nuenen-Son	T	$^{\circ}C$	1	23-07-2015	
Nuenen-Son	TSS*	mg/l	2	01-01-2010	31-05-2015
Nuenen-Son	TU	FNU	1	23-09-2014	
Eindhoven Stad	COD*	mg/l	2	01-01-2010	31-05-2015
Eindhoven Stad	CODf*	mg/l	2	01-01-2010	31-05-2015
Eindhoven Stad	EC	$\mu S/cm$	1	17-08-2012	
Eindhoven Stad	NH4	mg/l	5	14-09-2010	01-01-2016
Eindhoven Stad	NO3*	mg/l	2	01-01-2010	31-05-2015
Eindhoven Stad	T	$^{\circ}C$	1	23-07-2015	
Eindhoven Stad	TSS*	mg/l	2	01-01-2010	31-05-2015
Eindhoven Stad	TU	FNU	1	17-08-2012	
Riool Zuid	COD*	mg/l	2	01-01-2010	31-05-2015
Riool Zuid	CODf*	mg/l	2	01-01-2010	31-05-2015
Riool Zuid	EC	$\mu S/cm$	1	12-09-2014	
Riool Zuid	NH4	mg/l	5	01-01-2012	01-12-2015
Riool Zuid	NO3*	mg/l	2	01-01-2010	31-05-2015
Riool Zuid	T	$^{\circ}C$	1	23-07-2015	
Riool Zuid	TSS*	mg/l	2	01-01-2010	31-05-2015
Riool Zuid	TU	FNU	1	12-09-2014	
Mixing gutter	NH4	mg/l	5	09-03-2016	
Mixing gutter	pH	–	1	14-12-2015	
Mixing gutter	PO4	mg/l	5	03-07-2013	
Mixing gutter	T	$^{\circ}C$	1	14-12-2015	

Table C.2: WWTP Eindhoven water quality for other locations than the influent. As the monitoring locations are indicated in figure C.1 no coordinates are supplied. Parameters marked with an asterisk are equivalent measurements.

location	param.	unit	interval [min]	start date	end date
Sand trap	EC	$\mu S/cm$	1	15-12-2015	
Sand trap	PO4	mg/l	5	03-07-2013	
Sand trap	T	$^{\circ}C$	1	10-02-2016	
Sand trap	TU	FNU	1	17-02-2016	
Booster station	COD*	mg/l	2	24-05-2012	26-05-2015
Booster station	CODf*	mg/l	2	24-05-2012	26-05-2015
Booster station	EC	$\mu S/cm$	1	17-02-2016	
Booster station	NH4	mg/l	5	01-01-2010	
Booster station	NO3*	mg/l	2	24-05-2012	26-05-2015
Booster station	PO4	mg/l	5	01-01-2010	
Booster station	T	$^{\circ}C$	1	17-02-2016	
Booster station	TSS*	mg/l	2	23-03-2016	26-05-2015
Booster station	TU	FNU	1	24-05-2012	
Activated sludge tank 1	DO	mg/l	1	01-01-2010	
Activated sludge tank 1	NH4	mg/l	5	01-01-2010	
Activated sludge tank 1	PO4	mg/l	1	27-04-2010	
Activated sludge tank 2	DO	mg/l	1	01-01-2010	
Activated sludge tank 2	NH4	mg/l	5	01-01-2010	
Activated sludge tank 2	T	$^{\circ}C$	1	01-01-2010	
Activated sludge tank 3	DO	mg/l	1	01-01-2010	
Activated sludge tank 3	NH4	mg/l	5	01-01-2010	
Storm water tank	COD*	mg/l	2	10-09-2011	09-11-2014
Storm water tank	CODf*	mg/l	2	10-09-2011	09-11-2014
Storm water tank	EC	$\mu S/cm$	1	11-03-2016	
Storm water tank	NO3*	mg/l	2	10-09-2011	09-11-2014
Storm water tank	T	$^{\circ}C$	1	11-03-2016	
Storm water tank	TSS*	mg/l	2	10-09-2011	09-11-2014
Storm water tank	TU	FNU	1	18-02-2016	
Effluent	COD*	mg/l	2	29-09-2011	26-09-2014
Effluent	CODf*	mg/l	2	29-09-2011	26-09-2014
Effluent	DO	mg/l	1	01-01-2010	
Effluent	NO3*	mg/l	2	29-09-2011	26-09-2014
Effluent	pH	–	1	17-02-2016	
Effluent	PO4	mg/l	1	01-01-2010	
Effluent	T	$^{\circ}C$	1	01-01-2010	
Effluent	TSS*	mg/l	2	29-09-2011	26-09-2014

Table C.3: Rainfall.

location	param.	unit	interval [min]	start date	end date	x-coord.	y-coord.
WWTP	rainfall	mm	1	22-11-2010		163171	385547
Vessem	rainfall	mm	1	19-11-2010		147527	381558
Eersel	rainfall	mm	1	26-01-2011		151326	374319
Leende	rainfall	mm	1	01-04-2010		167127	373464
Bergeijk	rainfall	mm	1	01-04-2010		153407	369507

Table C.4: River Dommel water quantity.

location	param.	unit	interval [min]	start date	end date	x-coord.	y-coord.
0023	H	<i>mAD</i>	10	01-01-2010		159228	380447
0026	H	<i>mAD</i>	10	01-01-2010		165478	384031
0044	H	<i>mAD</i>	10	01-01-2010		163688	389713
0045	H	<i>mAD</i>	10	01-10-2010		158350	375425
0045	Q	m^3/s	10	01-10-2010		158350	375425
0045	v	<i>m/s</i>	10	01-10-2010		158350	375425
0053	H	<i>mAD</i>	10	01-01-2010		161903	368178
0053	Q	m^3/s	10	01-01-2010		161903	368178
0053	v	<i>m/s</i>	10	01-01-2010		161903	368178
0073	H	<i>mAD</i>	10	01-07-2011		162950	385665
0085	H	<i>mAD</i>	10	01-01-2010		157290	374890
0085	Q	m^3/s	10	01-01-2010		157290	374890
0085	v	<i>m/s</i>	10	01-01-2010		157290	374890
0089	H	<i>mAD</i>	10	01-01-2010		168077	375579
0091	H	<i>mAD</i>	10	01-01-2010		161125	379975
0091	Q	m^3/s	10	01-01-2010		161125	379975
0091	v	<i>m/s</i>	10	01-01-2010		161125	379975
0121	H	<i>mAD</i>	10	01-07-2010		160981	397374
0121	Q	m^3/s	10	01-01-2010		160981	397374
0121	v	<i>m/s</i>	10	01-01-2010		160981	397374
0124	H	<i>mAD</i>	10	01-01-2010		160905	381750
0124	Q	m^3/s	10	01-01-2010		160905	381750
0124	v	<i>m/s</i>	10	01-01-2010		160905	381750

Table C.5: River Dommel water quality.

location	param.	unit	interval [min]	start date	end date	x-coord.	y-coord.
0015	NH4	mg/l	1	24-03-2014		163814	389244
0015	pH	–	1	30-06-2014		163814	389244
0016	NH4	mg/l	1	27-03-2014		162947	385654
0016	pH	–	1	12-04-2016		162947	385654
0017	NH4	mg/l	1	01-04-2010		159273	367743
0017	pH	–	1	27-06-2014		159273	367743
0026	DO	mg/l	10	01-01-2010	16-10-2015	165478	384031
0026	T	°C	10	01-01-2010	16-10-2015	165478	384031
0044	DO	mg/l	10	01-11-2009	08-12-2014	163688	389713
0044	T	°C	10	01-11-2009	08-12-2014	163688	389713
0073	DO	mg/l	10	01-11-2009		162950	385665
0073	T	°C	10	01-11-2009		162950	385665
0091	DO	mg/l	10	01-07-2009		161125	379975
0091	T	°C	10	01-07-2009		161125	379975
0121	DO	mg/l	10	01-10-2010		160981	397374
0121	T	°C	10	01-10-2010		160981	397374
0124	DO	mg/l	10	01-10-2010		160905	381750
0124	T	°C	10	01-10-2010		160905	381750
0168	EGV	mS/cm	10	01-04-2011		167650	379950
0168	DO	mg/l	10	01-04-2011		167650	379950
0168	T	°C	10	01-04-2011		167650	379950
0188	EGV	mS/cm	10	09-07-2012		158570	366890
0188	DO	mg/l	10	09-07-2012		158570	366890
0188	T	°C	10	09-07-2012		158570	366890
0189	EGV	mS/cm	10	09-07-2012		152628	399334
0189	DO	mg/l	10	09-07-2012		152628	399334
0189	T	°C	10	09-07-2012		152628	399334
0190	EGV	mS/cm	10	09-07-2012		150731	401224
0190	DO	mg/l	10	09-07-2012		150731	401224
0190	T	°C	10	09-07-2012		150731	401224
0201	EGV	mS/cm	10	22-10-2012		152037	403856
0201	DO	mg/l	10	22-10-2012		152037	403856
0201	T	°C	10	22-10-2012		152037	403856

Table C.6: Municipality Eindhoven CSO water quality.

location	param.	unit	interval [min]	start date	end date	x-coord.	y-coord.
0014-01-01	TU	<i>FNU</i>	1	01-04-2010	12-07-2016	161758	383608
0014-01-01	EC	$\mu S/cm$	1	01-04-2010	12-07-2016	161758	383608
0016-01-01	TU	<i>FNU</i>	1	01-04-2010	12-07-2016	161643	384116
0016-01-01	EC	$\mu S/cm$	1	01-04-2010	12-07-2016	161643	384116
0018-01-01	TU	<i>FNU</i>	1	01-04-2010	12-07-2016	162455	384755
0018-01-01	EC	$\mu S/cm$	1	01-04-2010	12-07-2016	162455	384755
0020-01-01	TU	<i>FNU</i>	1	12-07-2011	25-01-2016	162508	384811
0020-01-01	EC	$\mu S/cm$	1	12-07-2011	25-01-2016	162508	384811
0021-01-01	TU	<i>FNU</i>	1	01-04-2010	12-07-2016	162722	385562
0021-01-01	EC	$\mu S/cm$	1	01-04-2010	12-07-2016	162722	385562
0026-01-01	TU	<i>FNU</i>	1	01-04-2010	13-07-2016	163266	388524
0026-01-01	EC	$\mu S/cm$	1	01-04-2010	13-07-2016	163266	388524
0032-01-01	TU	<i>FNU</i>	1	01-04-2010	12-07-2016	161364	381670
0032-01-01	EC	$\mu S/cm$	1	01-04-2010	12-07-2016	161364	381670
0035-01-01	TU	<i>FNU</i>	1	01-04-2010	29-09-2016	163103	387241
0035-01-01	EC	$\mu S/cm$	1	01-04-2010	29-09-2016	163103	387241
0035-02-01	TU	<i>FNU</i>	1	01-04-2010	29-09-2016	163232	387333
0035-02-01	EC	$\mu S/cm$	1	01-04-2010	29-09-2016	163232	387333

Table C.7: Municipality Eindhoven CSO water levels.

location	param.	unit	interval [min]	start date	end date	x-coord.	y-coord.
0002-01-01	H	<i>mAD</i>	1	18-11-2010		159977	380875
0003-01-01	H	<i>mAD</i>	1	28-10-2010		160437	380985
0005-01-01	H	<i>mAD</i>	1	04-11-2010		160666	381625
0005-01-02	H	<i>mAD</i>	1	19-04-2016		160666	381625
0006-01-01	H	<i>mAD</i>	1	04-11-2010		161328	382225
0007-01-01	H	<i>mAD</i>	1	09-11-2010		161358	382223
0008-01-01	H	<i>mAD</i>	1	04-11-2010		161355	382449
0009-01-01	H	<i>mAD</i>	1	01-11-2010		157945	383425
0011-01-01	H	<i>mAD</i>	1	04-11-2010		161687	382907
0012-01-01	H	<i>mAD</i>	1	08-11-2010		161815	383160
0013-01-01	H	<i>mAD</i>	1	25-11-2010		161825	383123
0014-01-01	H	<i>mAD</i>	1	08-11-2010		161758	383608
0015-01-01	H	<i>mAD</i>	1	08-11-2010		161864	383616
0016-01-01	H	<i>mAD</i>	1	07-12-2010		161643	384116
0017-01-01	H	<i>mAD</i>	1	07-12-2010		161741	384521
0018-01-01	H	<i>mAD</i>	1	17-11-2010		162455	384755
0019-01-01	H	<i>mAD</i>	1	08-11-2010		162371	384794
0020-01-01	H	<i>mAD</i>	1	23-11-2010		162508	384811
0021-01-01	H	<i>mAD</i>	1	23-11-2010		162722	385562
0022-01-01	H	<i>mAD</i>	1	09-11-2010		162919	385531
0023-01-01	H	<i>mAD</i>	1	18-11-2010		162801	385967
0026-01-01	H	<i>mAD</i>	1	29-11-2010		163266	388524
0027-01-01	H	<i>mAD</i>	1	22-11-2010		159064	381466
0028-01-01	H	<i>mAD</i>	1	22-11-2010		159021	381397
0029-01-01	H	<i>mAD</i>	1	22-11-2010		159078	380991
0031-01-01	H	<i>mAD</i>	1	23-11-2010		161677	382902
0032-01-01	H	<i>mAD</i>	1	13-12-2010		161364	381670
0033-01-01	H	<i>mAD</i>	1	23-11-2010		163893	381604
0034-02-01	H	<i>mAD</i>	1	08-12-2010		159396	382321
0035-01-01	H	<i>mAD</i>	1	14-12-2010		163103	387241
0035-02-01	H	<i>mAD</i>	1	11-12-2010		163232	387333

Table C.8: Municipality Bergeijk CSO water levels.

location	param.	unit	interval [min]	start date	end date	x-coord.	y-coord.
0001-01	H	<i>mAD</i>	1	22-09-2011		149882	365948
0002-01	H	<i>mAD</i>	1	22-01-2011		150743	366492
0003-01	H	<i>mAD</i>	1	12-01-2011		150660	367191
0004-02	H	<i>mAD</i>	1	20-09-2011		151308	366719
0004-03	H	<i>mAD</i>	1	20-09-2011		151370	366779
0007-02	H	<i>mAD</i>	1	14-05-2012		148452	368941
0007-03	H	<i>mAD</i>	1	22-09-2011		148410	368947
0013-02	H	<i>mAD</i>	1	14-05-2012		152371	369142
0013-03	H	<i>mAD</i>	1	12-01-2011		152302	369078
0014-02	H	<i>mAD</i>	1	12-01-2011		153384	369556
0014-03	H	<i>mAD</i>	1	21-03-2011		153462	369519
0018-02	H	<i>mAD</i>	1	12-01-2011		153970	369850
0018-03	H	<i>mAD</i>	1	14-05-2012		153929	369946
0019-01	H	<i>mAD</i>	1	14-05-2012		155771	371292
0022-02	H	<i>mAD</i>	1	14-05-2012		156172	371360
0022-03	H	<i>mAD</i>	1	13-01-2012		156172	371360
0023-01	H	<i>mAD</i>	1	14-05-2012		156793	372725
0024-02	H	<i>mAD</i>	1	14-05-2012		155227	373288
0025-02	H	<i>mAD</i>	1	14-05-2012		155375	373823
0030-01	H	<i>mAD</i>	1	14-05-2012		154672	375019
0031-01	H	<i>mAD</i>	1	03-09-2012		154298	370665

Table C.9: Municipality Eersel CSO water levels.

location	param.	unit	interval [min]	start date	end date	x-coord.	y-coord.
0001-01-01	H	<i>mAD</i>	1	14-05-2012		149135	374611
0002-02-01	H	<i>mAD</i>	1	19-09-2011		149172	374364
0002-03-01	H	<i>mAD</i>	1	14-05-2012		149172	374364
0004-02-01	H	<i>mAD</i>	1	11-01-2011		149279	373105
0005-02-01	H	<i>mAD</i>	1	14-05-2012		151271	373413
0005-03-01	H	<i>mAD</i>	1	14-05-2012		151271	373413
0006-02-01	H	<i>mAD</i>	1	12-01-2011		151329	374351
0006-03-01	H	<i>mAD</i>	1	25-01-2011		151422	374247
0007-01-01	H	<i>mAD</i>	1	12-01-2011		149916	375026
0007-01-02	H	<i>mAD</i>	1	12-01-2011		149916	375026
0008-02-01	H	<i>mAD</i>	1	14-05-2012		148289	375561
0008-03-01	H	<i>mAD</i>	1	14-05-2012		148279	375574
0009-02-01	H	<i>mAD</i>	1	14-05-2012		147553	381548
0009-03-01	H	<i>mAD</i>	1	17-01-2011		147520	381552
0010-02-01	H	<i>mAD</i>	1	17-01-2011		151399	383916
0011-01-01	H	<i>mAD</i>	1	17-01-2011		152093	383987
0012-02-01	H	<i>mAD</i>	1	14-01-2011		152559	379183
0012-03-01	H	<i>mAD</i>	1	14-01-2011		152559	379183
0013-02-01	H	<i>mAD</i>	1	14-05-2012		152669	376801
0014-01-01	H	<i>mAD</i>	1	01-02-2011		148668	381710

Table C.10: Municipality Heeze CSO water levels.

location	param.	unit	interval [min]	start date	end date	x-coord.	y-coord.
0001-01-01	H	<i>mAD</i>	1	11-25-2016		167382	378391
0002-01-01	H	<i>mAD</i>	1	11-23-2016		167630	377869
0004-01-01	H	<i>mAD</i>	1	11-23-2016		167890	378048
0008-01-01	H	<i>mAD</i>	1	11-23-2016		168042	376044
0013-01-01	H	<i>mAD</i>	1	11-23-2016		166006	371804
0014-01-01	H	<i>mAD</i>	1	11-23-2016		166472	372500
0015-01-01	H	<i>mAD</i>	1	11-23-2016		166689	372956
0018-01-01	H	<i>mAD</i>	1	11-23-2016		166696	376151
0021-01-01	H	<i>mAD</i>	1	11-24-2016		168577	378313
0023-01-01	H	<i>mAD</i>	1	11-24-2016		167941	376707
0024-01-01	H	<i>mAD</i>	1	11-24-2016		170512	373302

Table C.11: Municipality Nuenen CSO water levels.

location	param.	unit	interval [min]	start date	end date	x-coord.	y-coord.
0002-01-01	H	<i>mAD</i>	1	06-01-2011		165836	384513
0004-01-01	H	<i>mAD</i>	1	29-12-2010		165968	385652
0005-02-01	H	<i>mAD</i>	1	04-01-2011		165782	385929
0006-01-01	H	<i>mAD</i>	1	01-02-2011		165703	386189
0007-01-01	H	<i>mAD</i>	1	30-12-2010		165694	385950
0010-01-01	H	<i>mAD</i>	1	01-12-2010		166264	386032
0011-02-01	H	<i>mAD</i>	1	14-06-2011		166335	385886
0012-01-01	H	<i>mAD</i>	1	12-04-2010		166571	386029
0013-01-01	H	<i>mAD</i>	1	30-12-2010		166864	385986
0014-01-01	H	<i>mAD</i>	1	03-01-2011		166877	386419
0015-01-01	H	<i>mAD</i>	1	22-12-2010		166823	386772
0016-01-01	H	<i>mAD</i>	1	30-12-2010		166834	387233
0017-02-01	H	<i>mAD</i>	1	06-01-2011		167306	387587
0019-02-01	H	<i>mAD</i>	1	29-12-2010		167659	387063
0021-01-01	H	<i>mAD</i>	1	04-01-2011	11-03-2015	166243	386824
0022-01-01	H	<i>mAD</i>	1	15-12-2010	11-03-2015	165970	386846
0023-01-01	H	<i>mAD</i>	1	15-12-2010	10-23-2012	165715	386749
0024-01-01	H	<i>mAD</i>	1	15-12-2010	11-04-2015	165634	386736
0026-01-01	H	<i>mAD</i>	1	02-01-2011		164912	385713
0027-01-01	H	<i>mAD</i>	1	04-01-2011	03-20-2013	165221	386961
0028-01-01	H	<i>mAD</i>	1	15-12-2010	08-20-2014	165197	387519
0029-01-01	H	<i>mAD</i>	1	15-12-2010	06-11-2012	165627	387704
0032-01-01	H	<i>mAD</i>	1	18-05-2011		167372	389131
0033-01-01	H	<i>mAD</i>	1	09-07-2011		166849	389271
0034-01-01	H	<i>mAD</i>	1	03-01-2011		164170	389188
0035-01-01	H	<i>mAD</i>	1	01-04-2010		166082	387973
0036-01-01	H	<i>mAD</i>	1	03-06-2012		165601	386227
0037-00-01	H	<i>mAD</i>	1	03-06-2012		165654	384150

Table C.12: Municipality Son en Breugel CSO water levels.

location	param.	unit	interval [min]	start date	end date	x-coord.	y-coord.
0001-01	H	<i>mAD</i>	1	22-09-2011		161773	391012
0002-01	H	<i>mAD</i>	1	22-09-2011		161704	390870
0003-01	H	<i>mAD</i>	1	27-01-2011		162529	390868
0004-01	H	<i>mAD</i>	1	22-09-2011		162366	390383
0005-01	H	<i>mAD</i>	1	22-09-2011		163865	390993
0006-02	H	<i>mAD</i>	1	22-09-2011		161514	392415
0007-01	H	<i>mAD</i>	1	22-09-2011		160784	392352
0008-02	H	<i>mAD</i>	1	22-09-2011		161438	393383
0009-01	H	<i>mAD</i>	1	22-09-2011		161816	393456
0010-02	H	<i>mAD</i>	1	22-09-2011		164355	392174
0011-02	H	<i>mAD</i>	1	22-06-2011		163277	391753
0012-01	H	<i>mAD</i>	1	27-01-2011		162987	391241
0013-02	H	<i>mAD</i>	1	22-09-2011		162721	391149

Table C.13: Municipality Valkenswaard CSO water levels.

location	param.	unit	interval [min]	start date	end date	x-coord.	y-coord.
0001-02-01	H	<i>mAD</i>	1	10-08-2011		161460	374341
0001-03-01	H	<i>mAD</i>	1	11-08-2011		161474	374475
0002-01-01	H	<i>mAD</i>	1	20-09-2011		160995	373050
0003-01-01	H	<i>mAD</i>	1	10-08-2011		161435	373327
0004-01-01	H	<i>mAD</i>	1	10-08-2011	23-10-2013	161806	373520
0005-01-01	H	<i>mAD</i>	1	10-08-2011		161973	373548
0009-02-01	H	<i>mAD</i>	1	17-08-2011		159055	373222
0013-01-01	H	<i>mAD</i>	1	19-08-2011		157479	375182
0015-01-01	H	<i>mAD</i>	1	11-08-2011		158580	373626
0018-01-01	H	<i>mAD</i>	1	11-08-2011		157641	373448
0019-02-01	H	<i>mAD</i>	1	11-08-2011		158613	367291
0020-02-01	H	<i>mAD</i>	1	11-08-2011		160154	368203
0021-02-01	H	<i>mAD</i>	1	05-03-2013		158621	375040
0022-02-01	H	<i>mAD</i>	1	05-03-2013		158416	374980

Table C.14: Municipality Veldhoven CSO water levels.

location	param.	unit	interval [min]	start date	end date	x-coord.	y-coord.
0001-01-01	H	<i>mAD</i>	1	15-09-2010		156245	379343
0002-01-01	H	<i>mAD</i>	1	15-09-2010		156463	379718
0003-01-01	H	<i>mAD</i>	1	22-09-2011		156824	379699
0003-04-01	H	<i>mAD</i>	1	12-11-2015		156824	379699
0004-01-01	H	<i>mAD</i>	1	13-09-2010		156785	380141
0005-01-01	H	<i>mAD</i>	1	20-09-2010	11-23-2011	157111	379868
0006-01-01	H	<i>mAD</i>	1	21-09-2010		157419	380191
0007-01-01	H	<i>mAD</i>	1	07-10-2010		157751	380465
0008-01-01	H	<i>mAD</i>	1	20-09-2010		157704	379737
0009-01-01	H	<i>mAD</i>	1	20-09-2010		157573	380679
0011-01-01	H	<i>mAD</i>	1	21-09-2010		157701	381780
0012-01-01	H	<i>mAD</i>	1	21-09-2010	04-18-2016	157610	382590
0014-01-01	H	<i>mAD</i>	1	27-10-2010		155836	381600
0015-01-01	H	<i>mAD</i>	1	16-09-2010		155300	381371
0016-01-01	H	<i>mAD</i>	1	23-09-2010		153646	381917
0017-01-01	H	<i>mAD</i>	1	15-09-2010		154216	381768
0018-01-01	H	<i>mAD</i>	1	23-09-2010		154936	382200
0019-01-01	H	<i>mAD</i>	1	28-09-2010		154649	382054
0020-01-01	H	<i>mAD</i>	1	15-09-2010		155445	382371
0021-01-01	H	<i>mAD</i>	1	30-09-2010		155685	382193
0022-01-01	H	<i>mAD</i>	1	15-09-2010		156191	382212
0023-01-01	H	<i>mAD</i>	1	27-07-2010		156309	383007
0024-01-01	H	<i>mAD</i>	1	01-10-2010		156324	381689
0025-01-01	H	<i>mAD</i>	1	28-10-2010		156491	379944
0025-02-01	H	<i>mAD</i>	1	15-11-2010		156491	379944
0026-01-01	H	<i>mAD</i>	1	06-10-2010		155664	379328
0027-01-01	H	<i>mAD</i>	1	23-09-2010		155409	379148
0028-01-01	H	<i>mAD</i>	1	11-02-2003		154540	377709
0030-01-01	H	<i>mAD</i>	1	05-10-2010		155931	378366
0031-01-01	H	<i>mAD</i>	1	23-09-2010		156233	381674
0032-01-01	H	<i>mAD</i>	1	06-10-2010	11-04-2015	157020	379979
0033-01-01	H	<i>mAD</i>	1	11-10-2010		157261	379894
0034-01-01	H	<i>mAD</i>	1	15-11-2010		156891	380582
0035-01-01	H	<i>mAD</i>	1	21-10-2010		156999	380695
0036-01-01	H	<i>mAD</i>	1	21-10-2010		157683	380784
0037-01-01	H	<i>mAD</i>	1	22-10-2010		157145	380487
0038-01-01	H	<i>mAD</i>	1	03-11-2010		157158	380411
0039-00-01	H	<i>mAD</i>	1	25-04-2012	01-11-2014	157660	380433
0040-00-01	H	<i>mAD</i>	1	25-04-2012	01-30-2014	157143	382530
0041-00-01	H	<i>mAD</i>	1	25-04-2012	03-12-2014	157798	380954
0042-00-01	H	<i>mAD</i>	1	23-04-2012	03-12-2014	157793	380566

Table C.15: Municipality Waalre CSO water levels.

location	param.	unit	interval [min]	start date	end date	x-coord.	y-coord.
0002-02-01	H	<i>mAD</i>	1	06-02-2011		158848	378554
0004-01-01	H	<i>mAD</i>	1	02-02-2011		158367	377243
0006-02-01	H	<i>mAD</i>	1	06-02-2011		161614	379188
0006-03-01	H	<i>mAD</i>	1	04-02-2011		161860	379170
0009-01-01	H	<i>mAD</i>	1	04-02-2011		161816	378071

D Implementation of Smart Buffer controls

This appendix contains details on the implementation of two Smart Buffer controls in the wastewater system of Eindhoven. It supplements the design and performance evaluation of the Storm Tank Control and Primary Clarifier Control described in chapter 6.

Storm Tank Control

The Storm Tank Control was first implemented off-line. Several historical data sets with measured influent flows and water levels, representing a range of rainfall distributions over the catchments, were tested to ensure proper translation of the design into software. The tests revealed an implementation error that could have led to the Archimedian screws filling the storm water settling tank (SST) running dry, which was easily resolved. The control was taken into operation without problems at the end of November 2014.

A screenshot of the implemented control is shown in figure D.1. Colours indicate the current operation and how it arrived there. Additionally, the most important set points calculated by the control and the current water levels in the influent chambers are displayed.

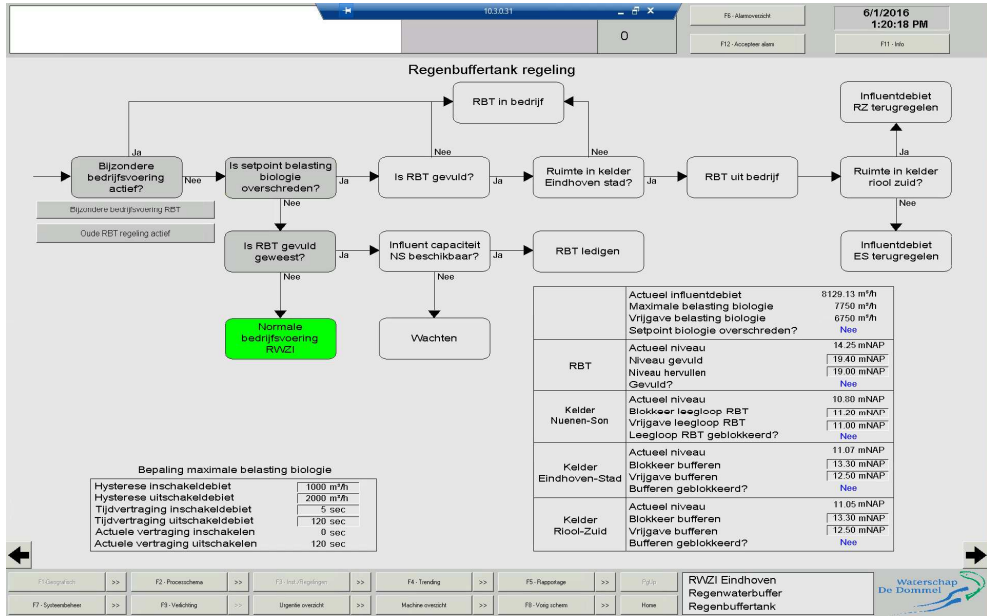


Figure D.1: Screenshot of the implementation of the Storm Tank Control in the SCADA system.

Primary Clarifier Control

To make the Primary Clarifier Control practically feasible, the primary clarifiers (PCs) were equipped with controllable valves as shown in figure D.2. The control was implemented at the end of November 2015 in the SCADA system, a screenshot of which is shown in figure D.3. Colours indicate which phase and PCs are active and if a transition to a new phase is being prepared. Additionally, the most important set points calculated by the control and the current flows and water levels in the influent chambers are displayed. By clicking on a phase a pop-up window appears that details the constraints for switching to another phase. The windows are displayed in figure D.4.



Figure D.2: Picture of the controllable valves to dynamically operate the PCs in the Primary Clarifier Control.

6/1/2016 1:21:39 PM 55

6/1/2016 1:21:39 PM

VBT Regeling

	DWA	start RWA	RWA	einde RWA	Nood- / Storingsfase
	0	1	2	3	4
Q _{bio_grens}	8750	17500	21000	17500	21000
Q _{bio_grens} + Q _{RBT}	8750	26250	29750	17500	29750
Q _{NS} beschikbaar	max 3200	max 3200	max 3200	max 3200	max 3200
Q _{ES} beschikbaar	max 20100	max 21192	max 24692	max 12442	max 24692
Q _{RZ} beschikbaar	max 15000	max 2700	max 16000	max 16000	max 16000
Q _{VBT1}	0	0	max 7000	0	max 7000
Q _{VBT2}	0	max 8750	max 7000	max 8750	max 7000
Q _{VBT3}	max 8750	max 8750	max 7000	max 8750	max 7000
Q _{RBT}	0	max 8750	max 7000	0	max 7000

1104QC01 Instellingen VBT Regeling

omschrijving	actuele waarde	instelling
Tijd tot volgende fasebepaling	0 sec	60 sec
Influentdebiet verlaging door TG	5250 m ³ /h	
Influentdebiet verlaging door VBT	0 m ³ /h	
Influentdebiet verlagen met (Actueel = totale verlaging)	5250 m ³ /h	0 m ³ /h
Influentdebieten	NS: 580 m ³ /h ES: 3278 m ³ /h RZ: 4479 m ³ /h TOT: 8336 m ³ /h	
Ontvangkelder niveau's	NS: 10.94 mNAP ES: 11.07 mNAP RZ: 11.09 mNAP	
VBT gebruikt tijdens DWA bedrijf (Let op verdunningswaterafsluters)		VBT1 VBT3
Huidige status RBT regeling		RBT niet actief

Noodbedrijf

F1: Overzicht >> F2: Proceschema >> F3: Inst./Regelgen >> F4: Trending >> F5: Rapportage >> F6: Pagina >> F7: Systembeheer >> F8: Velding >> Urgente overzichts >> Meelees overzichts >> F9: Vraag stellen >> Home

RWZI Eindhoven Ontvangst Influentgemaal

Waterschap De Dommel

Figure D.3: Screenshot of the implementation of the Primary Clarifier Control in the SCADA system.

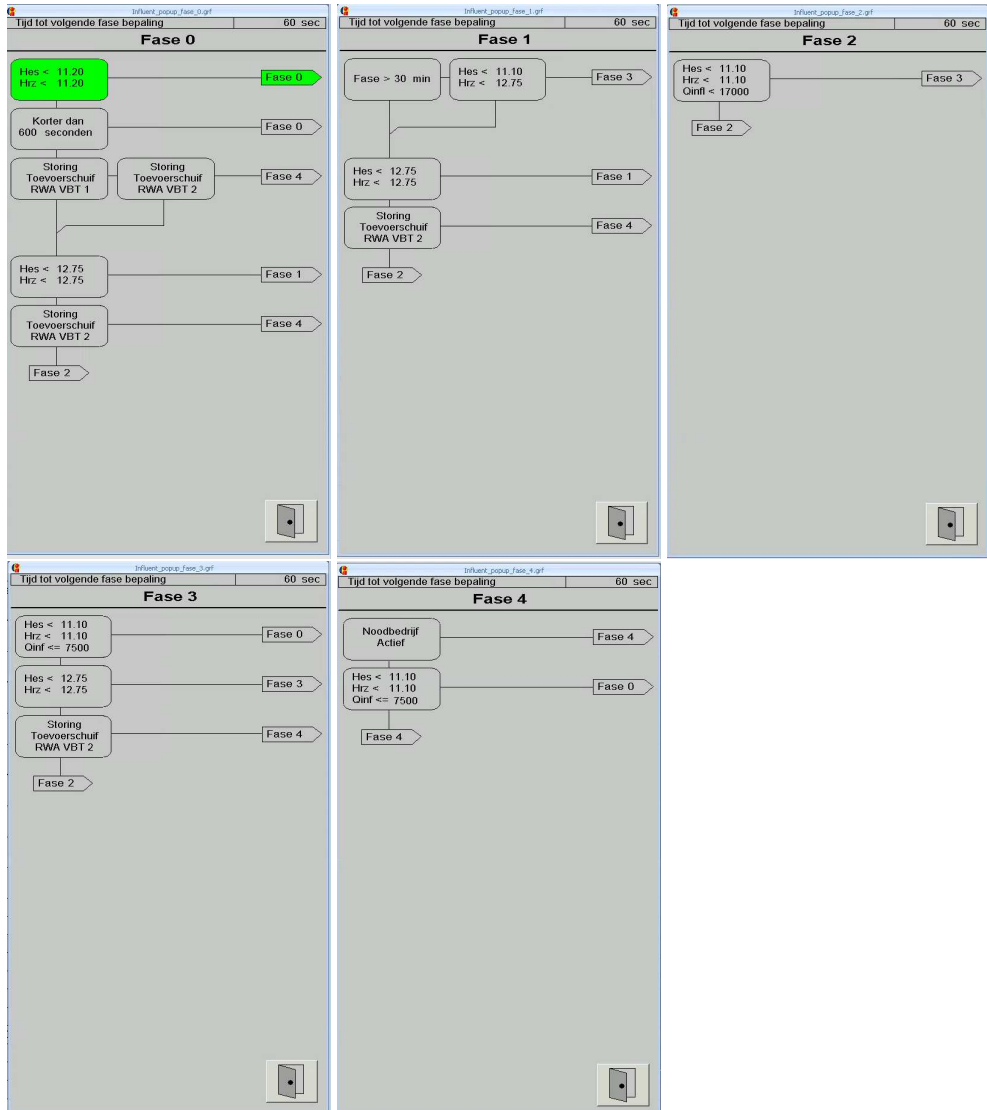


Figure D.4: Pop-up windows that contain constraints for switching to another phase. Windows appear by clicking on a phase in figure D.3.

It was not possible to test the implementation of the Primary Clarifier Control design off-line, due to the complex network of controls for individual components of the WWTP and interactions between them. Therefore, the Primary Clarifier Control and the conversion from design to software had to be tested simultaneously in the field. For that purpose the control was switched on during working hours only. The test period lasted from the end of November 2015 until halfway March 2016. It was laborious due to the weather dependency, making it impossible to ‘rerun’ the same event. In some cases, safety features had to be sidestepped to simulate certain behaviour for proper testing.

During the test period several issues were discovered and resolved: e.g. at maximum flows two of the three valves to close of the PCs turned out to be too low, on opening the PC valves to allow higher influent flows the higher flow capacities could be reached before the valves were opened completely, and there turned out to be a contradiction in the changes made to the influent pumping station control and a previously implemented control to prevent blockage of the grates.

Due to observations on the stability of the control in the test period, the Primary Clarifier Control was simplified to make better use of the WWTPs original stable operation at the expense of some optimal buffering in the catchments.

E Primary clarifier field test

Prior to the detailed design and implementation of the Primary Clarifier Control at wastewater treatment plant (WWTP) Eindhoven, see chapter 6, a field test was executed to investigate the impact of applying only one primary clarifier (PC) instead of three during dry weather flow (DWF) conditions. For this purpose the WWTP was temporarily modified to treat all wastewater under DWF conditions using only one PC.

The PC influent and PC effluent constituents were intensively monitored by automated, volume proportional, 24-hour grab sampling. The samples were analysed following standard lab-procedures for total P, total COD, BOD₅, TSS, NH₄ and Nkj. The monitoring period with only one PC spans a total of 18 days spread over 3 periods: 24 and 25 June, 10 to 23 July and 13 to 18 August 2013. The removal efficiency during this period is summarised in table E.1.

The removal efficiency is compared to the reference situation with three PCs. The reference period runs from January 2011 to May 2013. The removal efficiency is based on automated, volume proportional, 24-hour grab samples that are performed for regulatory purposes 60 times per year. Only DWF days were considered, where a DWF day is defined as receiving less than 120,000 m^3 influent per day for the current and the two previous days. The removal efficiency during this period is summarised in table E.2.

Comparing the removal efficiencies in tables E.1 and E.2 no significant differences can be found. Based on this, it was concluded that during DWF conditions there is no adverse effect in applying only one instead of three PCs.

Table E.1: Removal efficiency primary clarification during DWF conditions with one PC.

removal efficiency	P _{tot} [%]	COD _{tot} [%]	BOD ₅ [%]	TSS [%]	NH ₄ [%]	N _{kj} [%]
average	12	27	23	54	-2	3
minimal	0	17	-1	33	-10	-30
maximal	33	49	44	71	4	12
standard deviation	10	7	11	8	4	9

Table E.2: Removal efficiency primary clarification during DWF conditions with three PCs.

removal efficiency	P _{tot} [%]	COD _{tot} [%]	BOD ₅ [%]	TSS [%]	NH ₄ [%]	N _{kj} [%]
average	15	28	29	54	n.a.	8
minimal	-2	1	7	18	n.a.	-1
maximal	31	56	51	89	n.a.	23
standard deviation	8	10	10	10	n.a.	4

List of publications

Peer-reviewed journal articles

- Van Daal-Rombouts, P.M.M., Sun, S., Langeveld, J.G., Bertrand-Krajewski, J.-L., Clemens, F.H.L.R., (2016). Design and performance evaluation of a simplified dynamic model for combined sewer overflows in pumped sewer systems. *Journal of Hydrology*, 538:609-624. doi: <http://dx.doi.org/10.1016/j.jhydrol.2016.04.056>.
- Van Daal-Rombouts, P.M.M., Gruber, G., Langeveld, J.G., Muschalla, D., Clemens, F.H.L.R., (2017). Performance evaluation of real time control in urban wastewater systems in practice: review and perspective. *Environmental Modeling & Software*, 95:90-101. doi: <http://dx.doi.org/10.1016/j.envsoft.2017.06.015>.
- Langeveld, J.G., Van Daal-Rombouts, P.M.M., Schilperoort, R.P.S., Flameling, T., Nopens, I., Weijers, S.R., (2017). Empirical sewer water quality model for generating influent data for WWTP modelling. *Water*, 9(7):491. doi: <http://dx.doi.org/10.3390/w9070491>.
- Van Daal-Rombouts, P.M.M., Tralli, A., Verhaart, F., Langeveld, J.G., Clemens, F.H.L.R., (*submitted*). Validation of computational fluid dynamics for deriving weir discharge relationships with scale model experiments and prototype measurements. *Flow Measurement & Instrumentation*.
- Van Daal-Rombouts, P.M.M., Benedetti, L., De Jonge, J., Weijers, S.R., Langeveld, J.G., (*submitted*). Performance evaluation of a smart buffer control at a wastewater treatment plant. *Water Research*.

Conference papers

- Van Daal-Rombouts, P.M.M., De Jonge, J., Langeveld, J.G., Clemens, F.H.L.R., (2016). Integrated real time control of influent pumping station and primary settling tank at WWTP Eindhoven. In *Proceedings of SPN8*. Rotterdam, the Netherlands.
- Van Daal-Rombouts, P.M.M., Tralli, A., Verhaart, F., Langeveld, J.G., Clemens, F.H.L.R., (2014). Applicability of CFD modelling in determining accurate weir discharge-water level relationships. In *Proceedings of ICUD13*. Sarawak, Malaysia.
- Langeveld, J.G., Schilperoort, R.P.S., Van Daal-Rombouts, P.M.M., Benedetti, L., Amerlinck, Y., De Jonge, J., Flameling, T., Nopens, I., Weijers, S.R., (2014). A New Empirical Sewer Water Quality Model for the Prediction of WWTP Influent Quality. In *Proceedings of ICUD13*. Sarawak, Malaysia.
- Van Daal-Rombouts, P.M.M., Langeveld, J.G., Clemens, F.H.L.R., (2013). Requirements for quality of monitoring data for water quality based RTC. In *Proceedings of SPN7*. Sheffield, UK.
- Van Daal-Rombouts, P.M.M., Schilperoort, R.P.S., Langeveld, J.G., Clemens, F.H.L.R., (2013). CSO pollution analysis based on conductivity and turbidity measurements and implications for application of RTC. In *Proceedings of Novatech2013*. Lyon, France.
- Van Daal-Rombouts, P.M.M., Langeveld, J.G., Clemens, F.H.L.R., (2012). Water quality based RTC using UV/VIS sensors. In *Proceedings of UDM9*. Belgrade, Serbia.

Workshop contributions

- Van Daal-Rombouts, P.M.M., Langeveld, J.G., Clemens, F.H.L.R., (2015). Integrated real time control of SST operation at WWTP Eindhoven: design and gain. *European Junior Scientist Workshop 22*. Chichilianne, France.
- Van Daal-Rombouts, P.M.M., Langeveld, J.G., Clemens, F.H.L.R., (2013). Determining the transition between DWF and WWF based on water quality measurements. *European Junior Scientist Workshop 20*. Graz, Austria.

National publications

- Van Daal-Rombouts, P.M.M., (2014). Promotieonderzoek naar sturing in het afvalwatersysteem. *RIONEDnieuws*, March 2014.
- Schilperoort, R.P.S., Van Daal-Rombouts, P.M.M., Langeveld, J.G., Van Dijk, P., Renkens, G., Van Nieuwenhuijzen, A., (2013). Troebelheid en geleidbaarheid als indicatorparameters voor de mate van verontreiniging van influent en overstortwater. *Vakblad Riolerings*, 19:13-15.
- Van Daal-Rombouts, P.M.M., Clemens, F.H.L.R., Ten Veldhuis, J.A.E., Pothof, I.W.M., Langeveld, J.G., (2012). Congresverslag Urban Drainage Modelling 9 te Belgrado. *WT-Afvalwater*, 12:326-331.
- Rombouts P., Korving H., Liefing E., Langeveld J., (2010). Standaard uitwisselingsformaat voor storingen in afvalwatersystemen (suf-sas) - ontwikkeling en toetsing van de systematiek. *WT Afvalwater*, 6:159-174.

About the author

Petra van Daal-Rombouts was born on 19 June 1982 in Waalwijk, the Netherlands, and grew up in Kaatsheuvel. She obtained her secondary school gymnasium diploma from the Dr. Mollercollege in Waalwijk in 2000. She started the study Applied Physics at University of Technology Eindhoven and received her M.Sc. degree (ir.) in 2007 on a master thesis called ‘Superparamagnetic bead rotation for biosensor applications’. During her studies she worked as a student assistant in student participation and in guiding secondary school students in research projects. After her graduation, Petra worked for one year at a foundation to promote technology for children up to 14 years old.

Since 2008 Petra is employed at consultancy firm Witteveen+Bos. She started as engineer in the field of urban drainage, specialising in measuring in wastewater and modelling and calibration of sewer systems. From 2012 onwards, she was allowed to dedicate most of her time to pursuing her PhD in the section Sanitary Engineering at Delft University of Technology. Part of this work was performed during a posting of one day/week at water board De Dommel. The results of this research are founding this thesis.

Meanwhile, Petra has resumed her consultancy work at Witteveen+Bos.